

# UC Merced

## UC Merced Electronic Theses and Dissertations

### Title

Nfkbid-driven B cell and antibody responses against T. gondii

### Permalink

<https://escholarship.org/uc/item/9235g8w9>

### Author

Souza, Scott Philip

### Publication Date

2021

### Copyright Information

This work is made available under the terms of a Creative Commons Attribution License, available at <https://creativecommons.org/licenses/by/4.0/>

Peer reviewed|Thesis/dissertation

UNIVERSITY OF CALIFORNIA,  
MERCED

*Nfkbid*-driven B cell and antibody responses to *T. gondii*

By

**Scott P Souza**

A dissertation in partial fulfillment of the requirements for the degree  
of

Doctor of Philosophy

in

Quantitative and Systems Biology

Committee in charge  
Professor Juris Grasis, Chair  
Professor Anna Beaudin  
Professor Chris Amemiya  
Professor Nicole Baumgarth  
Professor Kirk Jensen, Advisor

Portions of Chapter 2 © 2018 Splitt, et al.  
PD-L1, TIM-3, and CTLA-4 Blockade Fails To Promote Resistance to Secondary  
Infection with Virulent Strains of *Toxoplasma gondii*  
©2018 American Society for Microbiology. All Rights Reserved.

All other chapters  
© Copyright  
Scott P Souza, 2021  
All rights reserved.

The dissertation of Scott Souza is approved by:

---

Juris Grasis, Chair

Date

---

Chris Amemiya

Date

---

Nicole Baumgarth

Date

---

Anna Beaudin

Date

---

Kirk Jensen, Research Mentor

Date

University of California, Merced  
2021

## **0.1 Dedication**

I want to dedicate this work to my amazing wife and parents. This has been one long strange trip. I love you all deeply and words can not truly capture my appreciation for your support and companionship throughout this journey. Thank you.

# Contents

0.1	Dedication . . . . .	iv
0.2	List of Figures . . . . .	viii
0.3	Abbreviations . . . . .	xi
0.4	Acknowledgments . . . . .	xiii
0.5	Curriculum Vita . . . . .	xiv
0.6	Abstract . . . . .	xviii
<b>1</b>	<b>Introduction</b>	<b>1</b>
1.1	Toxoplasmosis . . . . .	1
1.2	Host factors mediating immunity to parasites . . . . .	2
1.3	Genetic mapping of correlates of immunity to parasitic infections . . . . .	5
1.4	Regulation of NF- $\kappa$ B and its effect on immune development and activation . . . . .	6
1.5	The role of B cells in immunity to <i>T. gondii</i> . . . . .	8
1.6	Layering immunity to <i>T. gondii</i> , roles for CD8 T cells and B cells in protective immunity against <i>T. gondii</i> . . . . .	9
<b>2</b>	<b>T cell checkpoint therapy does not promote resistance to secondary infection by high virulence strains of <i>T. gondii</i></b>	<b>12</b>
2.1	Introduction . . . . .	12
2.2	Methods . . . . .	15
2.2.1	Parasite strains and cells. . . . .	15
2.2.2	Mice and ethics statements. . . . .	15
2.2.3	Primary infection and serotyping. . . . .	15
2.2.4	Secondary infections and bioluminescence imaging. . . . .	16
2.2.5	Cell isolation, flow cytometry, and in vitro recall infections. . . . .	16
2.2.6	Neutralization and T cell depletion . . . . .	18
2.3	Results . . . . .	19

2.3.1	Cellular responses are required in a mouse model of <i>T. gondii</i> secondary infection. . . . .	19
2.3.2	Diverse <i>T. gondii</i> strains rapidly induce T cell dysfunction within susceptible mice. . . . .	20
2.3.3	Checkpoint blockade fails to promote survival against atypical <i>T. gondii</i> strains . . . . .	22
2.4	Discussion . . . . .	25
<b>3</b>	<b><i>Nfkbid</i> is required for immunity and antibody responses to <i>T. gondii</i></b>	<b>28</b>
3.1	Introduction . . . . .	28
3.2	Methods . . . . .	31
3.2.1	Ethics Statement . . . . .	31
3.2.2	Parasite strains and cell lines . . . . .	31
3.2.3	Mice . . . . .	32
3.2.4	Parasite infections . . . . .	32
3.2.5	Blood plasma isolation and assessment of seroconversion . . . . .	32
3.2.6	Brain superinfection assays . . . . .	33
3.2.7	Genetic linkage analysis . . . . .	33
3.2.8	Cell isolation, in vitro recall infections, and FACS analysis . . . . .	34
3.2.9	Parasite neutralization assay . . . . .	36
3.2.10	SDS-PAGE and immunoblotting for parasite lysate antigen . . . . .	36
3.2.11	RNA isolation and sequencing . . . . .	37
3.2.12	Gene expression analysis and data availability . . . . .	37
3.2.13	LPS-stimulation of enriched B cells and quantitative PCR . . . . .	38
3.2.14	PerC adoptive transfers and IgH allotype chimeric mouse generation . . . . .	38
3.2.15	Bone marrow chimeric mice generation . . . . .	38
3.2.16	ELISA . . . . .	39
3.2.17	RNA Structure Prediction . . . . .	39
3.2.18	Statistics . . . . .	39
3.3	Results . . . . .	40
3.3.1	Non-MHC loci control resistance to secondary infection with <i>Toxoplasma gondii</i> . . . . .	40
3.3.2	Genetic mapping reveals four loci that correlate with immunity to <i>Toxoplasma gondii</i> . . . . .	42
3.3.3	<i>Nfkbid</i> on chromosome 7 is required for immunity and the generation of <i>Toxoplasma gondii</i> -specific antibodies . . . . .	46

3.3.4	Defective B-1 and B-2 responses underlie <i>bumble</i> 's defect in immunity . . . . .	52
3.3.5	Evidence for enhanced B-1 and B-2 cell activation in resistant A/J mice . . . . .	59
3.3.6	B-1 cells in resistant A/J mice have enhanced germline transcription of <i>Ighg</i> constant regions, class-switch recombination and different activation profiles . . . . .	66
3.3.7	Gene dosage of <i>Nfkbid</i> impacts parasite-specific IgG1 and plasmablast differentiation . . . . .	71
3.4	Discussion . . . . .	77
<b>4</b>	<b>GPI reactivity from anti-<i>T. gondii</i> antibodies</b>	<b>80</b>
4.1	Introduction . . . . .	80
4.2	Methods . . . . .	82
4.2.1	Ethics Statement . . . . .	82
4.2.2	Parasite strains and cell lines . . . . .	83
4.2.3	Mice . . . . .	83
4.2.4	Parasite infections . . . . .	83
4.2.5	Blood plasma isolation and assessment of seroconversion .	83
4.2.6	Generation of <i>T. gondii</i> lysate and PI-PLC cleavage of <i>T. gondii</i> lysate . . . . .	84
4.2.7	SDS-PAGE and immunoblotting for parasite lysate antigen	84
4.3	Results . . . . .	85
4.3.1	Non-protein antigens (GIPL) are targets of durable B cell populations . . . . .	85
4.3.2	Intact GPI anchors are required for antibody recognition of <i>T. gondii</i> GPI-anchored surface antigens . . . . .	87
4.4	Discussion . . . . .	90
<b>5</b>	<b>Conclusion: Layered cellular and humoral responses are required for maximal immunity to <i>T. gondii</i></b>	<b>92</b>
5.0.1	Contributions to the field . . . . .	92
5.0.2	Future Directions . . . . .	96
5.0.3	Summary . . . . .	98
<b>6</b>	<b>Appendix tables</b>	<b>102</b>

## 0.2 List of Figures

1.1	IFN $\gamma$ -mediated immunity to <i>T. gondii</i> . . . . .	5
1.2	Humoral immunity to <i>T. gondii</i> . . . . .	10
2.1	CD8 and CD4 T cells are required for immunity in a mouse model of <i>T. gondii</i> secondary infection. . . . .	19
2.2	Diverse <i>T. gondii</i> strains induce differential T cell responses and levels of exhaustion. . . . .	21
2.3	Neutralization with CTLA-4-, TIM-3-, and/or PD-L1-blocking antibodies fails to rescue C57BL/6J mice following challenge with virulent <i>T. gondii</i> strains. . . . .	24
3.1	MHC and non-MHC alleles promote immunity to virulent <i>T. gondii</i> strains in A/J mice. . . . .	41
3.2	Genetic mapping reveals <i>Nfkbid</i> four loci associated with secondary infection immunity. . . . .	44
3.3	<i>Nfkbid</i> -null mice are susceptible to secondary infection but not primary infection. . . . .	47
3.4	<i>Bumble</i> mice have intact T cell responses during secondary infection. . . . .	48
3.5	<i>Nfkbid</i> is required for humoral responses to <i>T. gondii</i> . . . . .	50
3.6	PerC transfer into <i>Nfkbid</i> -null mice delays time to death. . . . .	53
3.7	High avidity <i>T. gondii</i> -specific antibodies are B-2 derived. . . . .	54
3.8	Validating PerC reconstitutions by serum IgM ELISAs and flow cytometry, and survival of muMT mice. . . . .	56
3.9	Susceptibility of irradiated mice to type III primary infections and vaccination. . . . .	58
3.10	Bone marrow chimeras reveal B-1 cells are required for complete immunity after vaccination. . . . .	59
3.11	Immunity in A/J mice correlates with enhanced class-switching in memory B-2 cells and increased serum reactivity to parasite lysate antigen. . . . .	61
3.12	Evidence for enhanced B-1 cell activation in resistant A/J mice. . . . .	63
3.13	CD8 T cell IFN $\gamma$ frequencies are increased in resistant A/J mice. . . . .	65
3.14	B-1 cells express <i>Ighg</i> transcripts in the peritoneal cavity but only express IgG antibody protein in the spleen during <i>T. gondii</i> infection. . . . .	68
3.15	Genes uniquely induced in B-1b cells on day 5 of secondary infection in resistant A/J mice. . . . .	70

3.16	Resistance to <i>T. gondii</i> is correlated with reduced mRNA transcript levels of <i>Nfkbid</i> . . . . .	73
3.17	Gene dosage of <i>Nfkbid</i> influences class-switching to IgG1 and plasmablast differentiation. . . . .	75
3.18	<i>Nfkbid</i> <sup>+/-</sup> mice do not have a survival advantage against <i>T. gondii</i>	76
4.1	Model of GPI anchors, a widely conserved structure and immunogenic target . . . . .	82
4.2	Immunity to <i>T. gondii</i> is correlated with antibody responses to GIPL	86
4.3	Mode of action for the cleavage of GPI-anchored proteins by PI-PLC $\gamma$ . . . . .	88
4.4	Intact GPI moieties are required for antibody reactivity to GPI-linked proteins . . . . .	89
5.1	<i>Nfkbid</i> -driven immunity to <i>T. gondii</i> . . . . .	100

# List of Tables

3.1	Polymorphic genes identified by Quantitative Trait Loci analysis. .	45
6.1	Genes identified by QTL analysis . . . . .	106
6.2	<b>List of bone marrow chimeras generated in this paper</b> . . . . .	107
6.3	<b>Antibodies</b> . . . . .	107
6.4	<b>Blocking Reagents</b> . . . . .	109
6.5	<b>Commercial Products</b> . . . . .	110
6.6	<b>qPCR probes and reagents</b> . . . . .	110
6.7	<b>Chemicals and reagents</b> . . . . .	111
6.8	<b>Experimental Models: Parasite strains</b> . . . . .	111
6.9	<b>Experimental Models: Plasmid</b> . . . . .	112
6.10	<b>Experimental Models: Cell Lines</b> . . . . .	112
6.11	<b>Experimental Models: Organisms/strains</b> . . . . .	112
6.12	<b>Experimental Models: Recombinant Inbred Panel</b> . . . . .	113
6.13	<b>Deposited Data</b> . . . . .	114
6.14	<b>Software</b> . . . . .	114
6.15	<b>Instruments</b> . . . . .	114

### 0.3 Abbreviations

ACK: Ammonium chloride-potassium  
ANOVA: Analysis of variance  
B-1: B-1 B cells  
B-2: Conventional “B-2” B cells  
BCR: B cell receptor  
BM: bone marrow  
CD4: CD4 T cell  
CD8: CD8 T cell  
CTLA-4: cytotoxic T-lymphocyte-associated protein 4  
DEG: Differentially expressed gene  
ELISA: Enzyme-linked immunosorbent assay  
F1: First filial generation  
FACS: Fluorescence-activated cell sorting  
FBS: Fetal bovine serum  
FO: Follicular B cells  
GIPL: Glycoinositolphospholipid  
GPI: Glycosylphosphatidylinositol  
GZB: Granzyme B  
i.c.: intracellular  
i.p.: intraperitoneal  
IFN $\gamma$ : interferon gamma  
IgD: immunoglobulin D  
IgG: immunoglobulin G  
IgM: immunoglobulin M  
IL-2: interleukin-2  
IRG: Immunity-related GTPases  
MZ: Marginal Zone B Cells  
NF- $\kappa$ B: Nuclear factor kappa-light-chain-enhancer of activated B cells  
PC: Plasma cells  
PB: Plasmablasts  
PD-1: programmed cell death protein 1  
PD-L1: programmed cell death protein ligand 1  
PEC: Peritoneal Exudate Cells  
PerC: Peritoneal Cavity  
PV: Parasitophorous vacuole  
PVM: Parasitophorous vacuole membrane

QTL: Quantitative trait loci  
r.o.: retro-orbital  
Tfh: T follicular helper cells  
*T. gondii*: *Toxoplasma gondii*  
TgIST: *T. gondii* inhibitor of STAT1 transcriptional activity  
TIM-3: T cell immunoglobulin and mucin domain-containing-3  
TLR: Toll like receptor  
TNF: Tumor necrosis factor  
Treg: T regulatory cell  
WT: wildtype

## 0.4 Acknowledgments

The insight, support, and work of several brilliant scientists have enabled the research presented within this dissertation.

I want to thank Dr. Jensen for mentoring me over this last half decade. I have never felt like I didn't have your 100% support. I appreciate you as a mentor and a human being, and I am thankful for all the opportunities you have enabled me to attain. Stay fresh.

I am grateful to my thesis committee members: Dr. Chris Amemiya, Dr. Nicole Baumgarth, Dr. Anna Beaudin, and Dr. Juris Grasis for their guidance and support. Each member in their own way has given me the support and encouragement to complete my PhD training.

I also want to thank Dr. Katrina Hoyer and Dr. Kristen Valentine for their support on the work presented in Chapter 2, as well as Dr. David Gravano for years of assistance. I leaned heavily on their expertise as a new graduate student jumping into a tough project.

Everyone (past and present) in the Jensen lab is an exceptional person, particularly Dr. Juan Camilo Sánchez-Arcila, Dr. Angel Kongsomboonvech, Julia Alvarez, Felipe Rodriguez, Sam Splitt, Safuwra Wizzard. I am amazed by the combination of intellect and warmth each of you have and I am grateful for our friendships.

This work was supported by NIH grants R01 AI137126, R15 AI131027, a Hellmann Fellowship and an MCB departmental award to KJ; and by NIH grants U19-AI109962 and R01 AI117890 to NB. The sequencing was carried out at the DNA Technologies and Expression Analysis Cores at the UC Davis Genome Center, supported by NIH Shared Instrumentation Grant 1S10OD010786-01. We would like to thank Dr. David Gravano and the UC Merced Stem Cell Instrumentation Foundry for their assistance utilizing instruments, supported by the DoD Research and Education Program for HBCU/MSI Instrumentation Grant W911NF1910529. Cartoons presented in this thesis were created in Biorender.

## 0.5 Curriculum Vita

Scott Philip Souza  
(805) 795-5396 | ssouza5@ucmerced.edu

### EDUCATION

---

#### University of California, Merced

Degree expected: PhD 2021

Advisor: Dr. Kirk Jensen

Doctoral Thesis: *Nfkbid*-driven antibody responses to *T. gondii*

#### California State University, Channel Islands

Bachelor of Science. Biology 2016

### PUBLICATIONS

---

**Scott P Souza**, Samantha D Splitt, Julia A Alvarez, Safuwra Wizzard, Jessica N Wilson, Zheng Luo, Nicole Baumgarth, Kirk D.C. Jensen. 2020.

*Nfkbid* is required for immunity and antibody responses to *Toxoplasma gondii*  
bioRxiv; DOI: 10.1101/2020.06.26.174151

Samantha D. Splitt\*, **Scott P Souza**\*, Kristen M. Valentine, Brayan E. Castellanos, Andrew B. Curd, Katrina K. Hoyer, and Kirk D. C. Jensen. 2018.

PD-L1, TIM-3, and CTLA-4 Blockade Fails To Promote Resistance to Secondary Infection with Virulent Strains of *Toxoplasma gondii* Infection and Immunity; Spotlight Article DOI: 10.1128/IAI.00459-18

Co-first authors.

### POSTERS AND PRESENTATIONS

---

Talk: 2020, Graduate Visitation Weekend Lightning Talks, QSB recruitment seminar, UC Merced, CA. "Layered Immunity to Parasites"

Talk: 2019, 15th biennial meeting on *Toxoplasma* Biology and Toxoplasmosis, Quindío, Colombia. "Immunity to *Toxoplasma gondii* - *Nfkbid* and the antibody response to the GPI anchor"

Talk: 2019, Woods Hole Immunoparasitology Meeting (WHIP), Woods Hole, MA. "Layers of Immunity to *T. gondii*" (Awarded travel fellowship)

Talk: 2018, Molecular and Cell Biology Seminar, UC Merced, CA. "Layered Immunity to Parasites"

Poster: 2018, Woods Hole Immunoparasitology Meeting (WHIP), Woods Hole,

MA. "Genetic Basis for Immunity to Virulent *T. gondii* Strains implicates *Nfkbid*-Dependent Memory B1 Cell Responses" (Award best poster)

#### **AWARDS**

2020	QSB Dissertation Incentive Award
2018, 2020, 2021	QSB Summer Fellowship
2019	QSB Travel Award
2019	Woods Hole Immuno-Parasitology Travel Fellowship
2018	<b>Young Investigator Award, American Associate of Immunologists</b>
2018	GSA Travel Award, Graduate Student Association
2017, 2018	Graduate Fellowship Incentive Program

#### **TEACHING EXPERIENCE**

---

*University of California, Merced*

Teaching Assistant

*Biology 151 "Molecular Immunology"* Spring 2021

Facilitated remote learning by leading discussions over zoom. Actively engaged students and fostered learning of difficult immunology topics.

Average Student Course Evaluation indicator: 6.5/7 (SD: 0.2)

*Biology 01 "Contemporary Biology"* Fall 2020

Lead remote discussion sections using many active learning techniques. Facilitated team-based learning using breakout rooms.

Average Student Course Evaluation indicator: 6.6/7 (SD: 0.3)

*Biology 151L "Molecular Immunology"* Fall 2018

Set up wet laboratory experiment materials. Instructed students on the fundamental principles and significance of experiments being performed.

Student Course Evaluation indicator: 6/7

*Biology 02 "Introduction to Molecular Biology"* Fall 2016, Spring 2017 & 2018

Utilized group-based learning strategies to engage students in problem solving activities. Developed content and assessments for students.

Average Student Course Evaluation indicator: 6.3/7 (SD: 0.5)

*California State University, Channel Islands*

Lead Tutor

2013-2016

Supplied walk-in tutoring for a Hispanic Serving Institution-STEM grant funded program. Increased awareness for the program by tabling and visiting classrooms.

Responsible for leading training exercises for tutors as well as opening and closing the building.

Learning Assistant 2013-2016

Assisted instructional lab instructors by answering technical and conceptual questions from students. Performed demonstrations of lab techniques.

## **STEM OUTREACH**

---

### **Pre-Health Association**

*President* 2014-2016

Handled club logistics and organized club fundraising. Planned speakers, information seminars, and conference trips. Mentored undergraduates on the expectations of medical school admissions.

### **ACS Student Chapter: Free Radicals Chemistry Club**

*Vice-President* 2014-2016

Filed reports with the American Chemical Society on the status of our club. Set up travel grants for students to attend and present research at conferences. Organized club fundraising efforts and coordinated with chemistry program staff to print and distribute chemistry laboratory manuals to students.

### **Science Carnival STEM Outreach Event**

*Master of Ceremonies* 2013-2016

Planned biology demonstrations for an event attended by 3000+ individuals. Trained volunteers on the execution of science demonstrations. Engaged audience and introduced the experiments for the “Fire Demos” on the main stage.

### **Learning Assistant Science Initiative**

*Founder* 2015-2016

Collaborated with a local Boys and Girls club after-school program to provide hands-on science demonstrations to an underserved community. Maintained communication with the school hosting the club and the volunteers. Fundraised and purchased supplies. Designed and performed the science demonstrations.

## **STUDENT MENTORSHIP**

---

Alex Geronimo (Undergraduate), assisted serological analysis of *T. gondii* infected mice. Transcriptomic analysis of *Igh* isotype expression during infection in various mouse backgrounds.

Summer 2020 - Ongoing

Safuwra Wizzard (Undergraduate), trained in molecular biology techniques: PCR,

ELISA and western blots. Generated a gene KO *T. gondii* strain using CRISPR-CAS9. Summer 2019 – Spring 2020.

Julia Alvarez (Undergraduate), trained in cell culturing techniques: parasite passaging, cell line maintenance, Trained in PCR and primer design. Generated a gene KO *T. gondii* strain using CRISPR-CAS9. Summer 2017- Spring 2018

## 0.6 Abstract

### *Nfkbid*-driven B cell and antibody responses against *T. gondii*

By

Scott P Souza

Doctor of Philosophy, Quantitative and Systems Biology

University of California, Merced, 2021

Advisor: Professor Kirk Jensen

Neglected parasitic diseases, which overlap with known diseases of poverty, cost over 30 million disability-adjusted life years (DALY) and are a massive economic burden for developing countries (Hotez et al., 2014). *Toxoplasma gondii* is the causative agent of toxoplasmosis, termed a "neglected parasitic diseases" and is a major source of foodborne mortality according to the Center for Disease Control and Prevention (CDC). *T. gondii* is a globally distributed parasite that infects 30% of the entire human population and no protective vaccine exists for this pathogen. *T. gondii* has a wide range of virulence; from non-virulent strains endemic to western Europe and North America to highly virulent and genetically diverse strains in South America which are known to evade immunological memory. The overarching goal of my thesis is to find host immunological mechanisms responsible for immunity to virulent *T. gondii* strains.

First, attempts were made to reverse T cell exhaustion that we demonstrated occurs in chronically infected mice given a virulent secondary challenge, but a variety of checkpoint blockade therapies failed to provide immunity to challenge, suggesting alternative immunological mechanisms are required for immunity to secondary infection. We then used an unbiased forward genetic screen to test for survival against virulent secondary infections, and discovered 4 genomic loci associated with immunity. The immunity locus on chromosome 7 encompassed the gene *Nfkbid* which encodes the protein I $\kappa$ BNS, an atypical regulator of NF- $\kappa$ B signaling required for B-1 cell development. We found that mice without *Nfkbid* (*bumble*) could survive primary infection with a low virulent strain, but were susceptible to secondary infections with virulent strains. *T. gondii*-specific T cell responses for both CD4s and CD8s were intact in *bumble* mice. However, antibody responses to *T. gondii* were found to be deficient in *bumble* mice, specifically parasite-specific IgM was completely abrogated and all parasite-specific IgG isotypes were reduced. Using a series of adoptive transfer and mouse chimera strategies, we were able to make two major observations: (1) B-2 cells are responsible for the majority of high avidity *T. gondii*-specific antibody response and (2) B-1 cells are required for

full immunity to *T. gondii* infection. In addition, humoral responses were found to be largely enhanced in resistant mice, with greater activation and class-switch recombination found in both the B-1 and B-2 B cell compartments. Finally, we present further evidence that the GPI-anchor of *T. gondii* may be a favored moiety by antibodies to recognize *T. gondii* parasite antigen. Together, our data suggests that, in addition to T cells, the anti-*T. gondii* immune response must be "layered" by both B-1 and B-2 B cells, to generate protective immunity and that *Nfkbid* is central to the immunological memory responses against *T. gondii*.

# Chapter 1

## Introduction

### 1.1 Toxoplasmosis

*Toxoplasma gondii* is a widespread zoonotic parasite of warm blooded animals. *T. gondii* is estimated to infect over one million people a year and about one third of the human population is seropositive against the parasite indicating infection (Jones & Holland, 2010). Transmission of *T. gondii* occurs through consumption of contaminated water or food. Once an individual is infected, *T. gondii* evades the host's immune system and establishes a life-long chronic infection by differentiating into a slow growing bradyzoite form. Bradyzoites establish tissue cysts within non-replicative cells such as neurons (Remington & Cavanaugh, 1965), where they are both infectious upon consumption and resistant to antibiotics. The feline definitive host, where parasite meiosis occurs, sheds environmentally stable infectious oocysts which are a major source of contamination and infection. Toxoplasmosis, the disease associated with *T. gondii* infection, is a leading cause of foodborne mortality with 24% of deaths from foodborne illness attributed to *T. gondii* infections costing the United States 3 billion dollars annually (Batz et al., 2012). Congenital toxoplasmosis, which is vertically transmitted from infected pregnant mothers to the unborn fetus, is a life-threatening form of toxoplasmosis wherein up to 80% of infected children can manifest serious sequelae in the form of chorioretinitis, blindness, microcephaly, developmental delay, epilepsy, or deafness (Boyer et al., 2011; Torgerson & Mastriacovo, 2013) Moreover, toxoplasmosis is the most common complication associated with acquired immuno-deficiency syndrome (AIDS). Up to 50% of individuals with AIDS are at risk of developing

toxoplasmic encephalitis (Luft et al., 1984, 1993; Basavaraju, 2016), in which *T. gondii* tissue cysts rupture and release parasites that cause brain damage and inflammation.

The severity of symptoms associated with *T. gondii* infection varies by region (Sibley & Boothroyd, 1992; Khan et al., 2007; Boothroyd & Grigg, 2002; Elbez-Rubinstein et al., 2009; Howe & Sibley, 1995). Clonal non-lethal strains of *T. gondii* (type II and type III strains) dominate North America and Europe (Howe & Sibley, 1995; Boothroyd, 2009). In contrast to the non-lethal strains of North America and Europe, high virulence type I strains dominate Asia and the genetically diverse and highly virulent "atypical" strains are endemic to South America (Grigg et al., 2001; Wang et al., 2013). The "atypical" strains have been associated with severe ocular toxoplasmosis, morbidity, and mortality in otherwise healthy adults (Carme et al., 2002; Darde & Pestre-Alexandre, 1992; Demar et al., 2007). The health risks associated with *T. gondii* infection and the potential for mortality necessitate a program to control the parasite, including the creation of a vaccine that delivers robust heterologous protection against genetically diverse atypical strains. However, vaccine development against parasites has been difficult, with only a single vaccine, RTS,S/AS01 against malaria, that has both low efficacy and requires a four dose regimen making it impractical for wide distribution (Sacks, 2014; Dimala et al., 2018). In order to create a better vaccine, one that is fully protective against the highest virulence strains, we must study why vaccines fail to induce protective immunity against parasites such as *T. gondii*.

## **1.2 Host factors mediating immunity to parasites**

The host response to *T. gondii*, an obligate intracellular parasite, requires signaling through the inflammatory cytokine interferon gamma (IFN $\gamma$ ) (Suzuki et al., 1988; Suzuki & Remington, 1990; Gigley et al., 2009a). Upon infection by *T. gondii*, the host detects parasite PAMPS through multiple TLR pathways: Glycosylphosphatidylinositol lipids are detected by Toll-like receptors (TLRs) TLR2 and TLR4, and profilin is detected by both TLR11 and TLR12 (Koblansky et al., 2013; Yarovinsky et al., 2008; Debierre-Grockiego et al., 2007). TLR11/TLR12 engagement in dendritic cells induces production of IL-12, an important driver of Th1 differentiation and IFN $\gamma$  production first by NK and type I ILCs, then critically by T cells during the course of the *T. gondii* infection (Klose et al., 2014; Gazzinelli et al., 1993; Hunter et al., 1994). IFN $\gamma$  initiates the cell autonomous

response to infection by activating Janus kinase (Jak) / signal transducer and activator of transcription 1 (STAT1) signaling pathways to induce expression of immunity-related GTPases (IRGs) to destroy the parasitophorous vacuole which is required for intracellular growth (Howard et al., 2011) (Figure 1.1). In addition, IFN $\gamma$  classically activates (M1) macrophages and induces iNOS to control chronic infection and parasite replication *in vitro* (Dunay et al., 2008; Jensen et al., 2011; Schariton-Kersten et al., 1997; Khan et al., 1997).

Following the innate response, CD8 T cells are primarily responsible for immunity to *T. gondii* reinfection and this immunity is dependent on IFN $\gamma$  (Gigley et al., 2009b; Suzuki & Remington, 1990; Nagasawa et al., 1991; Nishiyama et al., 2020). Of note, the perforin and FAS/FASL-mediated cytolytic function of CD8 T cells provides limited protection against *T. gondii* during acute challenge, and only appears to play a role in controlling the chronic cyst phase of the infection (Denkers et al., 1997; Wang et al., 2004; Suzuki et al., 2010; Jordan et al., 2009). T cell exhaustion has been documented in chronic *T. gondii* infections and checkpoint blockade, neutralization of PD-L1, has been effective at rescuing hypofunctional CD8 T cells from the exhaustion phenotype, thereby preventing reactivation of parasite cysts and hinting at potential means to circumvent parasite-induced immune dysfunction (Bhadra et al., 2011b). Though CD4 T cells play a large role in the production of IFN $\gamma$ , maintaining CD8 T cells (Casciotti et al., 2002), and providing B cell help (Johnson & Sayles, 2002; Stumhofer et al., 2013), only memory CD8 T cells transfer full protective immunity against the type I RH strain in naive mice (Gazzinelli et al., 1991; Gigley et al., 2009a).

Many high virulence *T. gondii* strains evade IFN $\gamma$ -mediated immunity through several layers of secret virulence factors that act at multiple points within the IFN $\gamma$  pathway. The highly virulent strains directly inhibit murine IRGs from attacking the parasitophorous vacuole (PV) membrane by secreting a pseudokinase, ROP5, that binds IRGs and keeps them in a GDP-bound inactive state (Niedelman et al., 2012; Etheridge et al., 2014; Reese et al., 2014), as well as other secreted kinases that phosphorylate IRGs preventing their ability to hydrolyze GTP and destroy the PV. Polymorphisms in these secreted effectors largely explain *T. gondii* strain differences in mouse virulence (Saeij et al., 2006; Taylor et al., 2006; Behnke et al., 2015, 2012; Reese et al., 2011; Melo et al., 2011). In addition, all parasite strains directly inhibit STAT1 dimers making infected cells refractory to both type I and type II IFN signaling (Rosowski & Saeij, 2012; Rosowski et al., 2014; Matta et al., 2019). This inhibition is accomplished by injecting the virulence factor TgIST, which is targeted to the host nucleus and associates with STAT1 dimers to recruit

the repressive Mi-2/NuRD (nucleosome remodeling and deacetylase) complex to inhibit the expression of STAT1-dependent genes including iNOS, chemokines, IRGs, and others, leading to enhanced virulence in mice (Gay et al., 2016; Matta et al., 2019; Olias et al., 2016).

Evasion of host IFN $\gamma$  responses is therefore a major obstacle in eliciting immunity against high virulence strains and calls into question what additional mechanisms are available for the immune system to control *T. gondii* infections. Protective immunity can be generated against some, but not all, IFN $\gamma$ -evading *T. gondii* strains though the mechanism by which that protection occurs is yet unknown (Jensen et al., 2015; Splitt et al., 2018; Niedelman et al., 2012). A protective vaccine against *T. gondii* needs to be robust against the immune evasion strategies characteristic of genetically diverse atypical strains. Hence, more work is needed to discover drivers of heterologous immunity to parasitic infections.

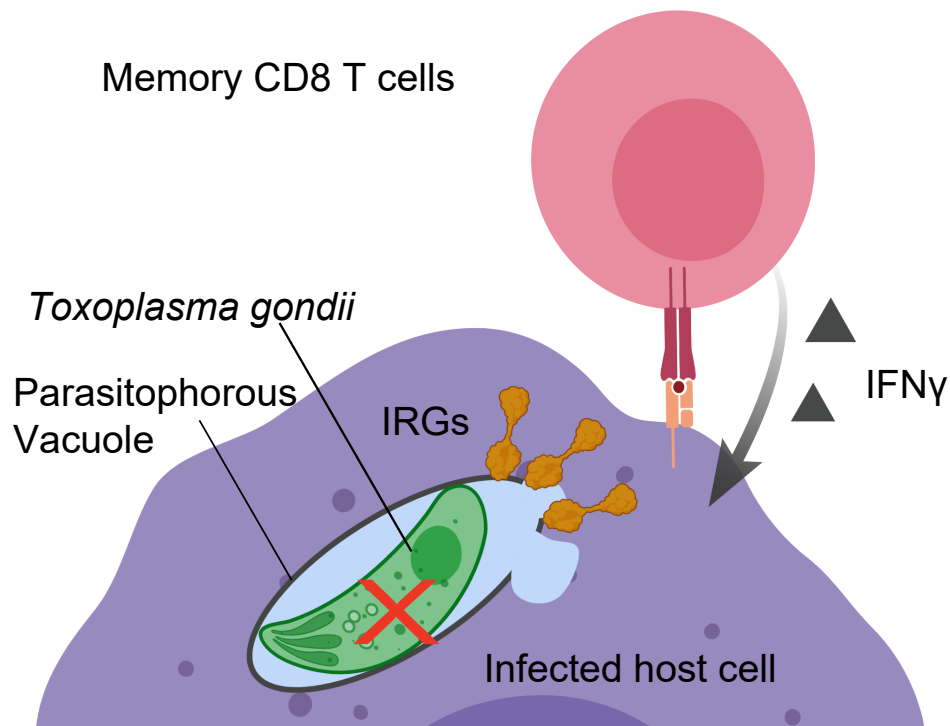


**Figure 1.1: IFN $\gamma$ -mediated immunity to *T. gondii*.** Model of IFN $\gamma$ -mediated immunity to *T. gondii*. CD8 T cells control *T. gondii* infections through IFN $\gamma$ -mediated induction of IRGs which destroy intracellular *T. gondii* by disrupting the parasitophorous vacuole membrane (PVM). This mechanism of immunity is the first and primary means of controlling *T. gondii* infection. However, immunity to IRG-resistant strains is variable and strain-type dependent (Jensen et al., 2015), suggesting alternative mechanisms are needed for protection.

### 1.3 Genetic mapping of correlates of immunity to parasitic infections

One approach to elucidating the requirements of heterologous immunity is the use of mouse genetics. Mouse genetics has a long history of identifying and characterizing host resistance genes (Bailey, 1971). The first evidence of host genetic variation resulting in differential control of *T. gondii* infections were found comparing host susceptibility of several mouse strains to primary infection (Aurajo et al., 1979). Several studies utilized recombinant inbred mice, which are generated

by strategic mating of progeny between two different inbred mouse strains to create a panel of mice that are homozygous for a single parental strain allele at several genomic regions throughout the entire mouse genome (Bailey, 1971; Nesbitt & Skamene, 1984). Recombinant inbred screens of host genes controlling resistance to *T. gondii* identified the H2 locus (McLeod et al., 1989), and eventually MHC I L<sup>d</sup> (Brown et al., 1995), as a major factor of both survival and cyst numbers during chronic infection (Johnson et al., 2002; McLeod et al., 1989; Brown et al., 1995). Genetic mapping of the susceptible B10.Q/J mouse and their first filial generation ('F1') backcrossed progeny identified a singular SNP in Tyk2, an important mediator of IL-12 and type 1 interferon signaling, as responsible for increased susceptibility to *T. gondii* (Shaw et al., 2003), highlighting the efficacy of this approach.

Forward genetic screens focused on the effect of *T. gondii* infection on both murine and human cell lines have been successful at identifying genes integral to the anti-*T. gondii* response. Regulators of STAT1 transcription activity were found using human bone epithelial cell lines and an overexpression cDNA library screen (Beiting et al., 2015). Other genetic and bioinformatic approaches identified the IRG locus as essential to cell autonomous clearance of *T. gondii* strains (Lilue et al., 2013). SNP association studies for human congenital toxoplasmosis led to the identification of the NLRP1 inflammasome as a cell autonomous mediator of immunity (Witola et al., 2011). Rat genetics of primary infection susceptibility similarly identified the rat NLRP1 inflammasome as central to cellular resistance (Cirelli et al., 2014; Gorfou et al., 2014; Cavailles et al., 2014). Though all of these screens have been able to identify essential host resistance factors in the primary response against *T. gondii*, they do not contribute to the understanding of how host genetic variation determines protective immunological memory responses. To that end, genetic mapping of correlates of host heterologous immunity will address an important knowledge gap: how to achieve activation of the host memory responses in the face of a diverse set of immune evasion strategies.

## **1.4 Regulation of NF- $\kappa$ B and its effect on immune development and activation**

A central tenant of host-pathogen studies is that by studying virulence factors, one can decipher the critical host pathways, often novel, that are necessary for pathogen clearance. In addition to the aforementioned *T. gondii* virulence factors

that antagonize the host IFN $\gamma$ -signaling pathway, type II strains of *T. gondii* are known to induce expression of NF- $\kappa$ B in infected cells through the virulence factor GRA15 (Rosowski et al., 2011). That clue coupled with the integral nature of NF- $\kappa$ B in nearly all immunological functions suggests that regulation of NF- $\kappa$ B, the essential transcription factor for development and activation of lymphocytes, is an important tunable host factor for generating protective host responses. Indeed, NF- $\kappa$ B modulators are currently being explored as vaccine additives in combination with selective TLR agonists to elicit specific protective responses (Moser et al., 2020). NF- $\kappa$ B itself is a pleomorphic transcription factor with multiple subunits culminating in 15 potential active forms (Smale, 2012). Pre-lymphocytes have been shown to have significant quantities of nuclear NF- $\kappa$ B, giving survival signals to lymphocytes that have successfully generated a pre-antigen receptor (Grumont et al., 1999). Fully mature B cells require NF- $\kappa$ B for activation either by extensive cross-linking of B cell receptors (BCR) via T-independent antigens or by CD40-CD40L interactions mediated by CD4 T cell help (Ranheim & Kipps, 1993). Strong CD40 signaling, which directly translates to NF- $\kappa$ B activation, has been shown to generate CD80+ memory B cells, a memory subpopulation that preferentially differentiates into plasma cells upon reinfection (Koike et al., 2019; Zuccarino-Catania et al., 2014).

Within the human genome, NF- $\kappa$ B is estimated to have upwards of  $10^6$  binding sites (Antonaki et al., 2011), of which CHIP-seq has found that RelA (one of five NF- $\kappa$ B family proteins) binds to at least 20,000 binding sites (Zhao et al., 2014) controlling expression of over 500 well-characterized genes essential for the immune response (Gilmore, 2017). Regulation of NF- $\kappa$ B is extensive and is intersected at multiple places in its signaling pathway. Specific direct post-translational modifications such as phosphorylation, acetylation, and methylation are made to NF- $\kappa$ B to induce specific transcriptional profiles based on the input signals driving the modifications (Chen & Greene, 2004; Christian et al., 2016; Mankan et al., 2009; Levy et al., 2011). Beyond direct modification, histone modifications can both influence NF- $\kappa$ B transcriptional profiles as well as be subject to further histone modifications due to NF- $\kappa$ B recruitment of HDACs (Saccani et al., 2002; Zhong et al., 2002; Ghosh & Hayden, 2008). NF- $\kappa$ B can also be regulated through protein-protein interactions by nuclear NF- $\kappa$ B regulators (IK $\beta$  family) such as BCL-3, I $\kappa$ B $\zeta$ , and I $\kappa$ BNS. These inducible regulators of NF- $\kappa$ B have complex interactions with NF- $\kappa$ B-controlled transcriptional profiles acting by: stabilizing energetically unfavorable NF- $\kappa$ B dimers, recruitment of histone modifying enzymes, and stabilization of NF- $\kappa$ B dimers on DNA (Ghosh & Hayden,

2008; Schuster et al., 2013). These nuclear NF- $\kappa$ B regulators each uniquely bias the NF- $\kappa$ B transcriptional profiles: I $\kappa$ BNS is known to bind p50 homodimers at the IL-6 promoter and repress transcription (Kuwata et al., 2006), while I $\kappa$ B $\zeta$  binds to the same p50 homodimers at the IL-6 promoter and induces transcription (Yamamoto et al., 2004). Though each of these regulators have been shown to change expression profiles, the full list of genes affected by each regulator, and the context in which they affect those genes, is yet to be known. The rapid induction of NF- $\kappa$ B and its long term effect on the trajectory of immune cell populations makes correct tuning of the NF- $\kappa$ B response essential to combating high virulence pathogens. Fine tuning of the immune response, through modulating NF- $\kappa$ B-dependent transcriptional profiles, will be essential to maximizing the immune response against parasitic pathogens.

## 1.5 The role of B cells in immunity to *T. gondii*

Humoral responses are known to be important in immunity to *T. gondii*, though much less studied than CD8 T cells. Investigations into the requirement of B cells in *T. gondii* responses have largely been performed studying  $\mu$ MT mice, which lack membrane IgM and fail to develop B cells. These B cell deficient  $\mu$ MT mice are susceptible in acute, chronic, and challenge infections (Chen et al., 2003b; Kang et al., 2000; Sayles et al., 2000). Hints of the protective role of B cells in *T. gondii* infections were first found in a study depleting IgM in BALB/c mice, and though all IgM-depleted mice succumbed to the infection unlike control mice (Hooijkaas et al., 1984; Bos et al., 1989), the death kinetic was delayed relative to athymic mice (Frenkel & Taylor, 1982). Surprisingly, adoptive transfer of B-1 cells, innate-like lymphocytes known for constitutive production of natural IgM (Baumgarth et al., 1999), was found to be protective to an intermediate virulence type II strain in  $\mu$ MT mice (Chen et al., 2003b). In this model, protection correlated with increased nitric oxide production suggesting additional roles for the B compartment beyond antibody production (Chen et al., 2003b). *In vitro* studies on the neutralization properties of serum found that *T. gondii*-specific IgM and IgG are capable of preventing parasite invasion (Kang et al., 2000; Couper et al., 2005). The bulk antibody response against *T. gondii* is known to be CD4-dependent, as CD4 depletion results in abrogation of nearly all *T. gondii*-specific antibodies including IgM (Zaretsky et al., 2012). Increased parasite burden and mortality has been correlated with decreased class-switched antibodies in multiple models (Stumhofer et al., 2013; Johnson & Sayles, 2002). Moreover, passive

transfer of immune serum to T cell-sufficient mice has been found to provide partial protection to primary infection (Frenkel & Taylor, 1982; Kang et al., 2000) and prolong survival of vaccinated  $\mu$ MT mice challenged with the lab adapted type I RH strain (Sayles et al., 2000), though these findings must be reconciled with studies that show memory CD8 T cell responses alone are sufficient to control challenge by type I RH (Gigley et al., 2009a; Nagasawa et al., 1991; Gazzinelli et al., 1991). All together, these studies hint at a potential role for B cell-mediated immunity to *T. gondii*, yet more work needs to be done to find models that truly test the requirement of antibody responses at a margin of parasite virulence that surpasses host CD8 and IFN $\gamma$  responses.

## **1.6 Layering immunity to *T. gondii*, roles for CD8 T cells and B cells in protective immunity against *T. gondii***

The goal of the research presented in this dissertation is to elucidate requirements for host immunity to heterologous *T. gondii* infections. Because high virulence strains of *T. gondii* are known to evade host IFN $\gamma$  responses, the major pathway for host control of *T. gondii* infections, we hypothesize that multiple layers of control, including CD8 T cells and antibody responses, are necessary for complete protection against heterologous secondary infections. There are three overarching questions that my research has aimed to answer: 1) Can CD8 T cell activity enhanced through checkpoint blockade promote host survival against high virulence *T. gondii* strains, 2) are B cell responses required for heterologous immunity, and 3) how do *T. gondii* antigens such as the GPI anchor and non-protein associated GPI lipids (GIPLs) influence the antibody response?

To answer these questions we used a secondary infection model to induce a robust anti-*T. gondii* response and to compare resistant versus susceptible mice to identify additional requirements of immunity to heterologous infection. In chapter 2, checkpoint blockade of PD-L1, TIM-3 and CTLA-4 is shown to fail to promote heterologous immunity in susceptible mice, suggesting additional mechanisms beyond CD8 T cells are required for immunity. In chapter 3, we performed an unbiased genetic screen for host factors contributing to heterologous immunity. Importantly, we found a gene, *Nfkbid*, that controls B cell responses against *T. gondii*, furthermore that B cell-mediated protection comes from two

separate and distinct B cell compartments: B-1 and B-2. In chapter 4, we explore how host antibody responses target non-protein *T. gondii* antigens (GIPL) and the requirement of these non-protein structures for antibody recognition of protein antigens. All together our data show that T cell responses, even those enhanced via checkpoint blockade, are insufficient to control the most highly virulent strains of *T. gondii*, and that B cell responses from both the B-1 and B-2 compartment are required for heterologous immunity to *T. gondii*. We propose a model of "layered immunity", where two major points of attack from the host: (1) the CD8 T cell and IFN $\gamma$  response and (2) B cell responses from both the B-1 and B-2 compartment are required for complete protective immunity against *T. gondii* (Figure 1.2).

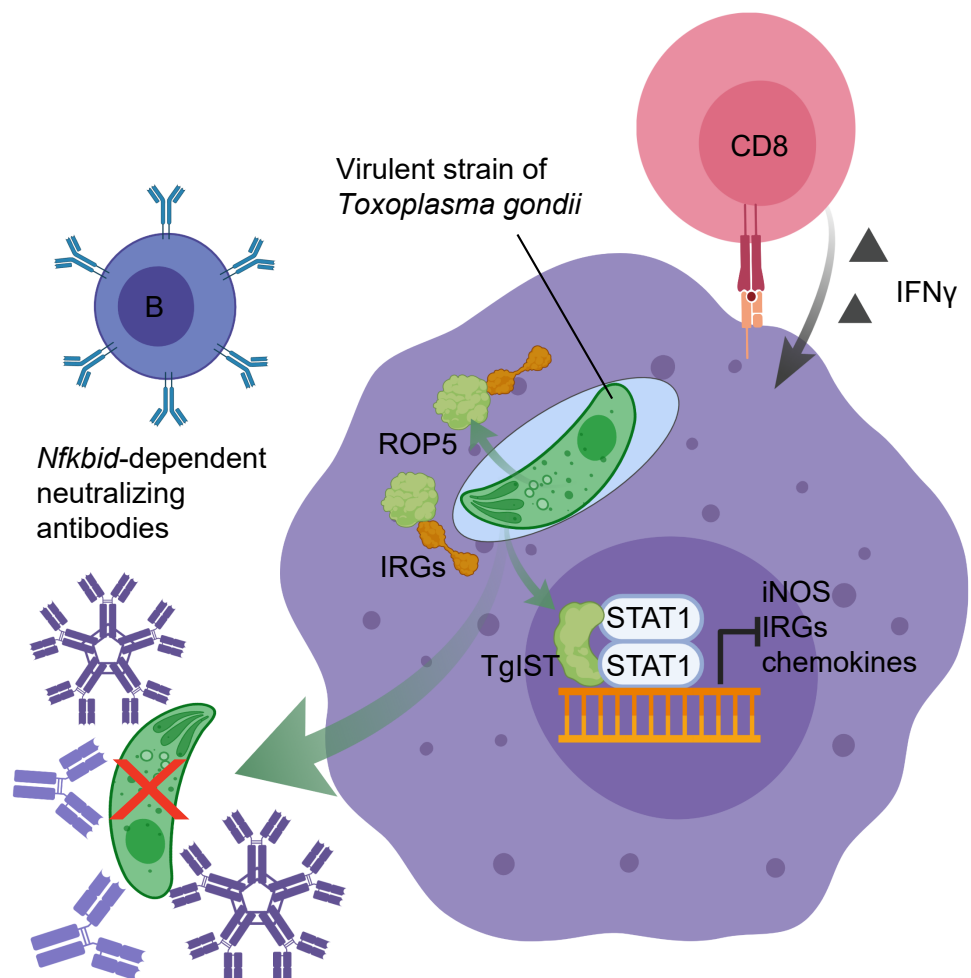


**Figure 1.2: Proposed model of humoral immunity to *T. gondii*.** High virulence *T.*

*gondii* parasite strains that have evaded host CD8 responses and IFN $\gamma$ -induced IRGs are neutralized by antibodies when they are extracellular seeking new cells to invade. The overarching aim of this dissertation is to uncover additional requirements for immunity to *T. gondii*. We hypothesize that B cells assist known CD8 and IFN $\gamma$ -mediated responses to provide another layer of protection to parasitic challenge, which is antibody mediated and *Nfkbid*-dependent.

---

## Chapter 2

# T cell checkpoint therapy does not promote resistance to secondary infection by high virulence strains of *T. gondii*

### 2.1 Introduction

T cell exhaustion is an acquired state of dysfunction that occurs in response to continued antigen stimulation such as chronic infections or inflammation. Exhausted T cells produce fewer cytokines and cytotoxic molecules, lower expression of activating receptors, and increase expression of inhibitory receptors (Wherry, 2011). T cell exhaustion was first characterized in chronic viral infection (LCMV) models (Ahmed et al., 1984), but is now widely studied in cancer (Iwai et al., 2002; Hirano et al., 2005; Sakuishi et al., 2010; Pauken & Wherry, 2015), bacterial infection (Lázár-Molnár et al., 2010; Barber et al., 2011), and parasitic infection models (Joshi et al., 2009; Butler et al., 2012; Bhadra et al., 2011b). This "dysfunction" phenotype is thought to prevent collapse of effector T cell populations during sustained activation (Alfei et al., 2019) as well as limit both immune pathology and autoreactivity. The molecular signature of CD8 and CD4 T cell exhaustion has been thoroughly defined and several markers have been identified to distinguish these hyporesponsive states (Wherry et al., 2007; Doering et al., 2012; Crawford et al., 2014). Several key markers have been identified that label CD8 or CD4 T

cells as exhausted: 1) high expression of the inhibitory receptors PD-1, LAG-3, TIM-3, CTLA-4, 2B4, BTLA, and CD160; 2) lowered expression of the costimulatory receptors 4-1bb, ICOS, and OX40, and 3) differential expression of the transcription factors Tbet, Eomes, BLIMP-1, and others (Wherry & Kurachi, 2015; Pauken et al., 2016; Sen et al., 2016). Exhausted T cells may carry most, or a portion of these markers, and marker expression varies with disease model, progression of disease state, and cell type. Treatment with neutralizing antibodies that target inhibitory receptors, or ‘checkpoint blockade’, has proven effective in reversing disease severity in a variety of mouse models for chronic viral infection and cancer (Barber et al., 2006; Leach et al., 1996). Importantly, these observations have translated to large response rates, tumor regression, and even survival of late stage melanoma patients (Phan et al., 2003; Hodi et al., 2010; Wolchok et al., 2013; Hodi et al., 2016). Therefore, checkpoint blockade is predicted to have a major impact for the treatment of human infectious disease (Attanasio & Wherry, 2016; Rao et al., 2017), but for which category of pathogen (bacterial, fungal, protozoan, helminth, viral), which stage of infection (acute, chronic, secondary), and which checkpoint blockade strategies should be used is less clear.

*Toxoplasma gondii* is a ubiquitous intracellular protozoan parasite that infects nearly all warm-blooded vertebrates, and exhibits a great deal of genetic diversity, especially amongst ‘atypical’ South American strains (Lehmann et al., 2004; Minot et al., 2012; Su et al., 2012; Lorenzi et al., 2016a). *T. gondii* strains differ in virulence in mice, with type I and most atypical strains being virulent, followed by type II and type III strains being relatively less virulent (Howe & Sibley, 1995; Sibley & Boothroyd, 1992; Su et al., 2003; Fux et al., 2007). Using these strains, the immune response to *T. gondii* can be examined under conditions of varied infection intensities, a strategy that is commonly used to study T cell exhaustion in the LCMV system. During the initial phase of infection, host control of *T. gondii* requires both innate and adaptive immune cells that make IFN $\gamma$  (Yarovinsky, 2014). Despite immune pressure, *T. gondii* rapidly disseminates to distal tissues (Konradt et al., 2016) to chronically infect for the lifetime of the host. Both CD4 and CD8 T cells play pivotal roles in preventing reactivation of the chronic form of infection and the prevention of toxoplasmic encephalitis (Suzuki et al., 1989; Gazzinelli et al., 1992b; Kang & Suzuki, 2001; Suzuki et al., 2010; Bhadra et al., 2013). In this context, T cell exhaustion is a critical component of disease progression (Gigley et al., 2011). Chronic infection with the intermediate virulent type II ME49 strain, will cause CD8 T cells to upregulate the inhibitory receptor PD-1 and exhibit diminished effector functions including reduced IFN $\gamma$  and granzyme B (GzmB)

production in genetically susceptible C57BL/6 mice (Bhadra et al., 2012, 2011b). Bhadra et al. rescued exhausted CD8 T cells and parasite recrudescence following antibody blockade of PD-1 ligand (PD-L1) (Bhadra et al., 2011b). They also observed a BLIMP-1-dependent CD4 T cell exhaustion program—with increased inhibitory receptor expression and decreased IFN $\gamma$  production during chronic *T. gondii* infection (Hwang et al., 2016). These results underscore the importance of T cell exhaustion and clinical potential of checkpoint inhibitors to resolve chronic infections, including *T. gondii*.

Can checkpoint blockade therapies be used to treat acute parasitic infections? In early studies on the scope and efficacy of anti-CTLA-4 therapy, it was clearly demonstrated to be beneficial in mouse models for acute visceral leishmaniasis (Murphy et al., 1998) and hook worm infections (McCoy et al., 1997). Furthermore, given the current difficulties in vaccine design for many parasitic pathogens, perhaps immunotherapy could be used as a second option to treat vaccinated individuals that fail to control parasitic infection. By correcting impaired memory T cell responses, immunotherapy could have profound impact in such individuals. Importantly, immunotherapy would be blind to antigen, MHC allele type, and vaccine regimen of the infected individual and could work on antibiotic-resistant parasites. In mouse models of *T. gondii* reinfection (‘secondary infection’ or ‘challenge’), vaccinated (Gazzinelli et al., 1991; Jordan et al., 2009; Gigley et al., 2009a; Fox & Bzik, 2002) or chronically infected mice (Jensen et al., 2015) are not susceptible to secondary infections with the highly virulent type I RH strain. Although naïve mice fail to control infection with as little as one parasite of the type I strain, adoptive transfer of memory CD8 T cells to naïve mice confers protection (Gigley et al., 2009a; Suzuki & Remington, 1988). While primary infection with vaccine or avirulent *T. gondii* strains can induce protective immunity to many virulent *T. gondii* strains, this is not true for most atypical strains (Jensen et al., 2015).

Here we hypothesized that C57BL/6 susceptibility to secondary infection may be due to dysfunctional T cell responses caused by highly virulent *T. gondii* strains. Moreover, we tested whether neutralization of inhibitory receptors that promote T cell dysfunction could induce mouse survival following secondary infection. Although CD8 T cells expressed exhaustion markers and exhibited diminished IFN $\gamma$  responses during secondary infection with virulent *T. gondii* strains, mice were not protected from challenge with the atypical strain MAS or the type I GT1 strain when administered neutralization antibodies to CTLA-4, TIM-3, and/or PD-L1.

## 2.2 Methods

### 2.2.1 Parasite strains and cells.

Human foreskin fibroblast (HFF) monolayers were grown at 37°C with 5% CO<sub>2</sub> in T-25 flasks for parasite passaging in HFF medium (Dulbecco's modified Eagle's medium [DMEM; Life Technologies] supplemented with 2 mM L-glutamine, 10% fetal bovine serum [FBS; Omega Scientific], 1% penicillin-streptomycin [Life Technologies], and 0.2% gentamicin [Life Technologies]). *Toxoplasma gondii* strains were passaged in HFFs in Toxo medium (4.5 g/liter D-glucose and L-glutamine in DMEM supplemented with 1% FBS and 1% penicillin-streptomycin). The following clonal strains were used (clonal types are indicated in parentheses): RH  $\Delta$ *hxgp*rt (type I), RH  $\Delta$ *hxgp*rt  $\Delta$ *ku80* (type I), RH *GFP-cLUC* (1-1) (type I), GT1 (type I), Pru (A7) *GFP-flUC*  $\Delta$ *hxgp*rt::*HXGPRT* (5-8B+) (type II), and CEP *hxgp*rt-(type III). The following atypical strains were used: MAS, MAS *GFP-cLUC* (2C8), and GUY-DOS.

### 2.2.2 Mice and ethics statements.

Six- to seven-week-old female C57BL/6J mice were purchased from Jackson Laboratory. For some experiments, CD45.1 congenic male and female C57BL/6 mice were used. Mouse work was performed in accordance with the National Institutes of Health Guide for the Care and Use of Laboratory Animals. All protocols were reviewed and approved by the UC Merced Institutional Animal Care and Use Committee. UC Merced has an Animal Welfare Assurance filed with OLAW (assurance number A4561-01), is registered with the USDA (registration number 93-R-0518), and the UC Merced Animal Care Program is AAALAC accredited (accreditation number 001318).

### 2.2.3 Primary infection and serotyping.

Parasite injections were prepared by scraping T-25 flasks containing vacuolated HFFs and sequential syringe lysis first through a 25-gauge needle and then a 27-gauge needle. The parasites were spun at 400 rpm for 5 min, and the supernatant was transferred, followed by a spin at 1,700 rpm for 7 min. The parasites were washed with 10mL phosphate-buffered saline (PBS), spun at 1,700 rpm for 7 min, and suspended in PBS. For chronic infections, mice were infected intraperitoneally (i.p.) with 10<sup>4</sup> CEP *hxgp*rt- tachyzoites in 200 $\mu$ l PBS. Parasite viability in the

inoculum was determined by a plaque assay following i.p. infections. A total of 100 or 300 tachyzoites were plated in HFF monolayers grown in a 24-well plate, and 4 to 6 days later, plaques were counted by microscopy (4x objective).

At 30 to 35 days of chronic infection, 50 $\mu$ l of blood was harvested from mice from the tail vein, collected in tubes containing 5 $\mu$ l 0.5 M EDTA, and placed on ice. The blood was pelleted at 10,000 rpm for 5 min, and blood plasma was collected from the supernatant and stored at 80°C. To evaluate the seropositivity of the mice, HFFs were grown on coverslips and infected with green fluorescent protein (GFP)-expressing Pru (A7) or RH (1-1) overnight; 18 hr later, cells were fixed with 3% formaldehyde in PBS, permeabilized with a permeabilization solution (3% bovine serum albumin, 0.2 M Triton X-100, 0.01% sodium azide), incubated with a 1:100 dilution of collected blood plasma for 2 hr at room temperature, washed with PBS, and detected with Alexa Fluor 594-labeled secondary antibodies specific for mouse IgG (Life Technologies). Seropositive parasites were observed by immunofluorescence microscopy.

#### **2.2.4 Secondary infections and bioluminescence imaging.**

Seropositive mice were challenged with 5x10<sup>4</sup> syringe-lysed parasites and euthanized on day 5 for most fluorescence-activated cell sorter (FACS) experiments or weighed every 3 to 4 days for survival experiments. Parasite viability for each strain was determined by a plaque assay following the completion of injections. The viability of the parasites ranged from 20% to 40% of the intended dose. In vivo bioluminescence imaging was performed on mice undergoing secondary infection with luciferase-expressing parasites as described previously (Jensen et al., 2015).

#### **2.2.5 Cell isolation, flow cytometry, and in vitro recall infections.**

To isolate peritoneal exudate cells(PECs) by peritoneal lavage, 4 ml of PBS and 3 ml of air were injected into the peritoneal cavity with a 27-gauge needle. After shaking, the puncture was expanded with scissors, and the PEC wash was poured into a conical tube. PEC washes were filtered through a 70- $\mu$ m cell strainer, pelleted, and washed with FACS buffer (PBS with 1% FBS) before staining. Spleens were dissected, crushed through 70- $\mu$ m cell strainers, pelleted, suspended in ammonium

chloride-potassium (ACK) red blood cell (RBC) lysis buffer for 5 min, quenched with medium containing 10% FBS, and washed with FACS buffer before staining.

For flow cytometry (flow) analysis, cells were further washed in FACS buffer prior to staining. All preparations were done on ice, and cells were blocked in FACS buffer containing Fc block anti-CD16/32 (2.4G2; BD Biosciences), 5% normal hamster serum, and 5% normal rat serum (Jackson ImmunoResearch) prior to staining with fluorophore-conjugated monoclonal antibodies (mAbs). The following mAbs (1:100 staining dilutions) were purchased from eBioscience (Thermo Fisher Scientific) unless otherwise stated: anti-CD4-phycoerythrin (PE)-Cy7 (GK1.5); anti-CD4-fluorescein isothiocyanate (FITC) (clone RM4-5); anti-CD8 $\alpha$ -FITC, -allophycocyanin (APC), or -BV510 (53-6.7); anti-CD3 $\epsilon$ -eFluor 780 (17A2); anti-CD62L-eFluor 450 (MEL-14); anti-KLRG1-FITC (2F1); anti-PD-1-PE or -APC (J43); anti-TIM-3-PE (RMT3-23); and anti-CD19-peridinin chlorophyll protein (PerCP)/Cy5.5 (ebio1D3). All nonfixed samples were stained with propidium iodide (PI) (Sigma) at a final concentration of 1 $\mu$ g/ml. PI-positive (PI+) and CD19+ cells were excluded from the analysis. For cell enumeration, PBS used for peritoneal lavage was spiked with 5x10<sup>4</sup> BD Calibrite APC beads (BD Bioscience). Beads were identified by FACS analysis as side-scatter high (SSCA<sup>hi</sup>), PI negative (PI<sup>neg</sup>), and APC+. The fraction of recovered beads was calculated by taking the count of identified beads and dividing this value by the initial quantity of 5x10<sup>4</sup> beads. Cell enumeration was done by taking the counts of cell populations determined by FACS analysis and dividing them by the fraction of recovered beads per sample.

For the intracellular detection of CTLA-4, cells stained for the surface proteins CD19, CD3 $\epsilon$ , CD62L, KLRG1, CD4, CD8 $\alpha$ , and PD-1 were then fixed with BD Cytfix/Cytoperm and permeabilized with BD Perm/Wash solution (BD Pharmingen) according to the manufacturer's suggestions. Cells were stained with anti-CTLA-4 (CD152)-PE (UC10-4F10-11) (BD Biosciences) in Perm/Wash solution overnight, washed once with BD Perm/Wash solution and once in FACS buffer, and then analyzed by flow analysis. For the detection of FOXP3, cells were stained for surface proteins CD25, CD3 $\epsilon$ , CD4, and CD19 and fixed by using a FoxP3/transcription factor fixation/permeabilization kit (eBioscience) for 45 min at room temperature. Fixed cells were washed and incubated in 1x permeabilization buffer for 10 min prior to intracellular staining with anti-FOXP3-FITC (MF-14; eBioscience) and anti-CTLA-4-PE (UC10-4F10-11) in 1x permeabilization buffer for 45 min, washed once with permeabilization buffer, and washed once with FACS buffer prior to flow analysis.

For in vitro recall experiments, splenocytes and PECs were washed and plated in T cell medium (10% FBS in RPMI 1640 with GlutaMAX, antibiotics, 10 mM HEPES, 1 mM sodium pyruvate (Life Technologies), and 1.75  $\mu\text{L}$   $\beta$ -mercaptoethanol per 500 ml (MP Biomedicals) at a concentration of  $6 \times 10^5$  cells per well (96-well plate). Cells were infected with the type I RH, MAS, or GUY-DOS strain at an MOI (multiplicity of infection) of 0.2 for 18 hr, and 3  $\mu\text{g}/\text{ml}$  brefeldin A (eBioscience) was added for the last 5 hr of infection. Ninety-six-well plates were placed on ice, and cells were harvested by pipetting, washed with FACS buffer, blocked, and stained for the surface markers CD4, CD8 $\alpha$ , CD3 $\epsilon$ , and CD19. Next, cells were fixed with BD Cytotfix/Cytoperm and permeabilized with BD Perm/Wash solution (BD Pharmingen) according to the manufacturer's suggestions. Cells were then stained with anti-IFN- $\gamma$ -PE (XMG1.2), anti-granzyme B-FITC (GB11), and anti-IL-2-APC (JES6-5H4) on ice for 1 hr or overnight for some experiments. Cells were then washed once with BD Perm/Wash solution and once in FACS buffer and analyzed by FACS. All data were acquired on an LSRII flow cytometer and analyzed with FlowJO software (BD).

## 2.2.6 Neutralization and T cell depletion

Mice were injected i.p. with 200  $\mu\text{g}$  of the blocking antibodies anti-PD-L1 (10F.9-G2), anti-TIM-3 (RMT3-23), and anti-CTLA-4 (9H10) or the rat IgG2b anti-keyhole limpet hemocyanin (KLH) (LTF-2) isotype control antibody, all of which were purchased from BioXCell, on days 1, 3, 5, 7, 10, and 13 after challenge with either the MAS or GT1 strain. Antibody injections were prepared in 200  $\mu\text{l}$  of sterile PBS. Mouse survival and weight were monitored for 27 days. For T cell depletions, chronically infected mice were treated with 400  $\mu\text{g}$  i.p. of anti-CD4 (GK1.5) or anti-CD8a (clone 2.43) on days 7 and 3, before challenge, and on days 3, 7, and 11 after challenge. The efficacy of depletion was determined by flow analysis of peripheral blood lymphocytes (PBLs) on days 1 and 8 of challenge. In brief, 15  $\mu\text{l}$  of whole blood was collected and washed, and red blood cells were lysed with ACK lysis buffer, washed with FACS buffer, blocked, and stained with CD4-FITC (clone RM4-5) and CD8a-APC (clone 53.6-7), as described above. CD4 T cell depletion was determined to be 99.9% and 99.3% effective while CD8 T cell depletion was determined to be 99.7% and 99.5% effective on days 1 and 8, respectively (not shown).

## 2.3 Results

### 2.3.1 Cellular responses are required in a mouse model of *T. gondii* secondary infection.

To explore the role of T cell exhaustion during acute secondary infections with *T. gondii*, genetically susceptible C57BL/6 mice were given a primary infection intraperitoneally (i.p.) with the avirulent type III CEP *hxgprt*- strain, which forms a non-lethal chronic infection, and then 35-45 days later, mice were reinfected (secondary infection) with either the atypical strains, MAS and GUY-DOS, or the highly passaged laboratory type I strain, RH (Fig 3.1A). All three *T. gondii* strains cause a lethal primary infection in naive mice (Su et al., 2003; Fux et al., 2007; Jensen et al., 2015); however, chronically infected C57BL/6J mice survive secondary infection with RH, but not MAS or GUY-DOS strains (Jensen et al., 2015). In this model, susceptibility to secondary infection correlates with increased parasite burden, which can be observed by bio-luminescence imaging between days 5 and 12 of secondary infection with luciferase expressing MAS (Fig 3.1B). Consistent with cellular requirements for immunity reported in vaccination studies (Gazzinelli et al., 1991; Jordan et al., 2009; Gigley et al., 2009a), depletion of CD8 but not CD4 T cells after primary infection abrogated protection to RH challenge (Fig 3.1C). Moreover, depletion of CD8 but not CD4 T cells impaired the ability of mice to control chronic infection. Both lineages of T cells are required to prevent reactivation in mice chronically infected with an intermediate virulence type II strain, ME49 (Gazzinelli et al., 1992a; Suzuki et al., 2011), and CD8 T cells are the primary effector T cell responsible for cyst removal in this setting (Ochiai et al., 2016; Suzuki et al., 2010). Overall, our model which uses an avirulent type III strain to generate immunological memory is consistent with the aforementioned models for chronic infection- and vaccine- induced immunity, and position memory CD8 T cells as central players in host resistance to *T. gondii*.

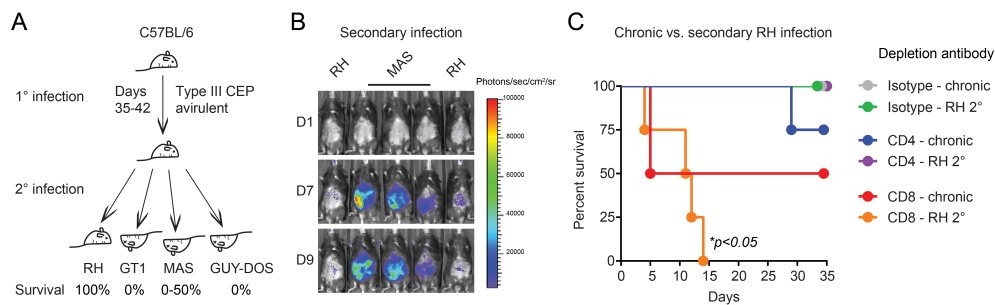


**Figure 2.1: CD8 and CD4 T cells are required for immunity in a mouse model of *T. gondii* secondary infection.** A) Schematic of the model used to assess T cell exhaustion during secondary infection with virulent strains that cause lethal (MAS, GUY-DOS, and GT1) and nonlethal (RH) outcomes. Average percent survivals from previous results (Jensen et al., 2015) are indicated. B) Representative bioluminescence imaging of individual C57BL/6 mice following secondary infection with the RH (1-1) and MAS (2C8) luciferase-expressing strains. Relative parasite burdens are depicted as a heat map, and the maximum and minimum values were set to  $10^5$  and  $3 \times 10^3$  photons/s/cm<sup>2</sup>/sr, respectively. C) Following chronic infection, mice were treated with depletion antibodies to either CD8 or CD4 or given an isotype control antibody for 1 week and then challenged with RH (RH 2°) or not challenged (chronic). The depletion regimen was continued until day 11. Cumulative survival rates from two separate experiments are plotted (n = 4 mice per group); P values were obtained by using the log rank Mantel-Cox test comparing depleted cohorts against similarly infected isotype control-treated groups (n = 2 mice per isotype-treated group). Data from (B) generated by Kirk Jensen.

---

### **2.3.2 Diverse *T. gondii* strains rapidly induce T cell dysfunction within susceptible mice.**

The T cell populations analyzed for exhaustion makers were defined by expression of CD62L and KLRG1. CD62L is expressed on naïve T cells and central memory T cells (T<sub>CM</sub>) (Masopust & Schenkel, 2013). In response to T cell receptor triggering by antigen, T<sub>CM</sub> cells initially produce a very minimal repertoire of cytokines, namely IL-2, but following differentiation into effector T cells, these cells also produce large amounts of cytokines and granzyme (Sallusto et al., 2004). Effector memory T cells (T<sub>EM</sub>) are active, cytokine-producing cells that, like effector T cells (T<sub>E</sub>), do not express CD62L; instead, they express inflammatory chemokine receptors that home these cells to the site of infection. KLRG1 is a transmembrane protein found on lymphocytes that marks highly activated, terminally differentiated T<sub>E</sub> and T<sub>EM</sub> cells following microbial infections, including *T. gondii* (Robbins et al., 2003; Wilson et al., 2010; Chu et al., 2016). CD8 T cells expressing CD62L or KLRG1 have different requirements for IL-12 during differentiation and abilities to make IFN $\gamma$  during *T. gondii* infection (Wilson et al., 2010, 2008). Using this staining approach, we observed an increase in CD62L-KLRG1- and CD62L-KLRG1+ (“KLRG1+”) CD8 T cells isolated from the peritoneal cavity following chronic infection compared to naïve animals (Fig 2.2A). On day 5 of secondary infection with either the type I RH strain, or the atypical strains MAS and GUY-DOS, the relative percentage number of each population remained constant

compared to chronic infection (Fig 2.2A). A similar trend was also observed for CD4 T cell populations in the peritoneum (Fig 2.2A). Changes in splenic T cell responses were found to be minimal in this system (Data not shown). Thus, peritoneal T<sub>E</sub> or T<sub>EM</sub>-like KLRG1+ T cells expand at the site of initial infection and their cellularity remains high following challenge.

Cell surface expression of several inhibitory receptors associated with T cell exhaustion in the LCMV model (Wherry et al., 2007; Crawford et al., 2014): PD-1, TIM-3, and CTLA-4 respectively, was measured on the peritoneal CD62L-KLRG1- and KLRG1+ (T<sub>EM</sub>-like) CD8 T cell populations. Compared to CD8 T cells from mice either chronically infected or given a secondary infection with RH, CD8 T cells from mice given a secondary infection with atypical strains, MAS and GUY-DOS, exhibited increased expression of PD-1, TIM-3 and CTLA-4 (Fig 2.2B). This rapid induction of exhaustion markers relative to the chronic state is largely emblematic of an out-of-control infection, but also signals a potential means to enhance T cell efficacy by using checkpoint blockade.

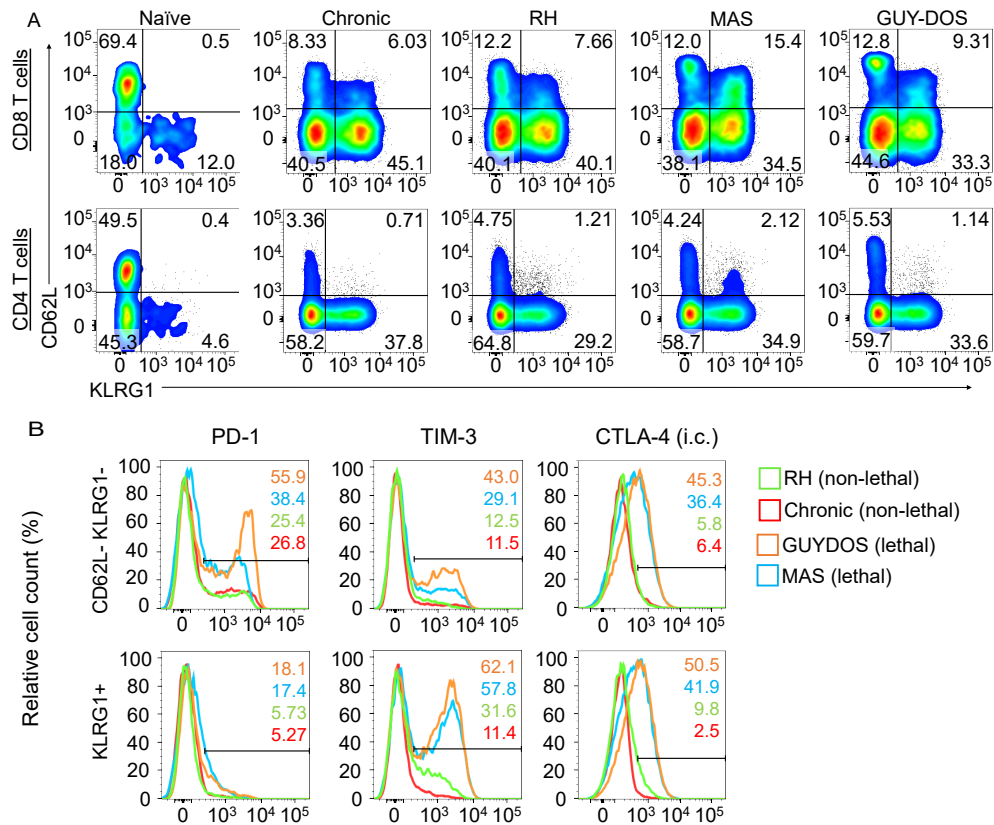


**Figure 2.2: Diverse *T. gondii* strains induce differential T cell responses and levels of exhaustion.** A) Representative flow plots of CD8+ and CD4+ (CD3+CD19-) peritoneal T cells and their expression of CD62L and KLRG1 from naïve C57BL/6J mice, mice that were infected with the type III CEP *hxgprrt*- strain and allowed to progress to chronic infection for 35-45 days (Chronic), or chronically infected mice that were given a secondary infection with the indicated *T. gondii* strains and analyzed on day 5; numbers are the frequency of cells that fall within the indicated gate. Plots are representative of six to eight experiments for CD8 T cells, and three to five experiments for CD4 T cells. B) Representative histogram plots of surface PD-1, TIM-3, or intracellular (i.c.) CTLA-4 expression for peritoneal CD62L-KLRG1- or KLRG1+ CD8+ T cells are shown. Numbers represent the frequency of cells that fall within the indicated gate; numbers and histogram lines are color coded to match the indicated *T. gondii* infection. Results are representative of three to seven experiments for PD-1, TIM-3, and from two experiments for CTLA-4.

---

### 2.3.3 Checkpoint blockade fails to promote survival against atypical *T. gondii* strains

To test whether disease outcome could be reversed following virulent challenge, several neutralizing antibodies were administered to block the pathways of inhibitory receptors most highly expressed on T cells in this system. Both the atypical strain MAS and the type I GT1 strain were used to understand therapeutic efficacy of the various checkpoint blockade strategies. Like MAS and GUY-DOS, the GT1 strain also induces a lethal secondary infection in C57BL/6 mice (Jensen et al., 2015), and induces the expression of PD-1 on CD62L- T<sub>EM</sub>-like CD8 T cells (Fig 2.3E). Although the expression of the PD-1 ligand, PD-L1, was not directly measured, treatment with neutralizing antibodies against PD-L1 is routinely used to block PD-1—PD-L1 signaling (Pauken et al., 2016; Barber et al., 2006). PD-L1 blockade failed to rescue mice following challenge with the atypical strain MAS (Fig 2.3A), which exhibited similar parasite burdens between treated and control cohorts (Fig 2.3B, C), and failed to rescue mice challenged with the GT1 strain (Fig 2.3D). Combining PD-L1 blockade with anti-TIM-3 neutralizing antibodies promotes favorable disease outcomes in chronic LCMV infection (Jin et al., 2010) and in tumor models (Sakuishi et al., 2010). However, neither TIM-3 blockade nor combination therapy with PD-L1 rescued mice following challenge with GT1 (Fig 2.3D). CTLA-4 attenuates T cell proliferation through competition for B7-1/2 ligands with the costimulatory receptor CD28 (Krummel & Allison, 1995, 1996), and by recruitment of the PP2A phosphatase to the TCR-proximal signaling cascade thereby deactivating Akt (Parry et al., 2005). CTLA-4 blockade is known

to increase CD4 T cell IFN $\gamma$  responses in cancer patients (Liakou et al., 2008). Moreover, since CTLA-4 neutralization converts memory CD8 T cells to effector T cells through Treg-CTLA-4 mediated suppression (Kalia et al., 2015), and *ctla4*<sup>-/-</sup> transgenic CD8 T cells demonstrated enhanced secondary but not primary proliferative responses to antigen stimulation (Chambers et al., 1998), the role of CTLA-4 blockade was explored in this system. Yet, neither single CTLA-4 blockade nor combination therapy with PD-L1 altered survival following challenge with either strain (Fig 2.3A, D). The capacity of peritoneal CD4 and CD8 T cells to produce IFN $\gamma$ , IL-2 and GzmB in the context of anti-PD-L1 / anti-CTLA-4 combination therapy was explored. Following MAS challenge, modest but borderline significant (Chi squared, Fig 2.3G; t-tests not shown) increases in the frequency of T cells that produce two or three of the measured immune mediators were observed in the treated compared to control cohorts (Fig 2.3F, G). Resistance to checkpoint blockade is known to be caused by systemic IFN $\gamma$  signaling (Minn & Wherry, 2016; Benci et al., 2016). Since IFN $\gamma$  is highly produced by many cell types and detected in the serum following secondary infection (data not shown), the sustained presence of IFN $\gamma$  may cause the minimal T cell reinvigoration observed in this system. Regardless, these results suggest that blockade of the inhibitory pathways studied here, which are commonly targeted to reverse disease outcomes in mouse models of cancer, LCMV, and chronic *T. gondii* infections, are not suitable to treat acute secondary infections with virulent *T. gondii* strains.

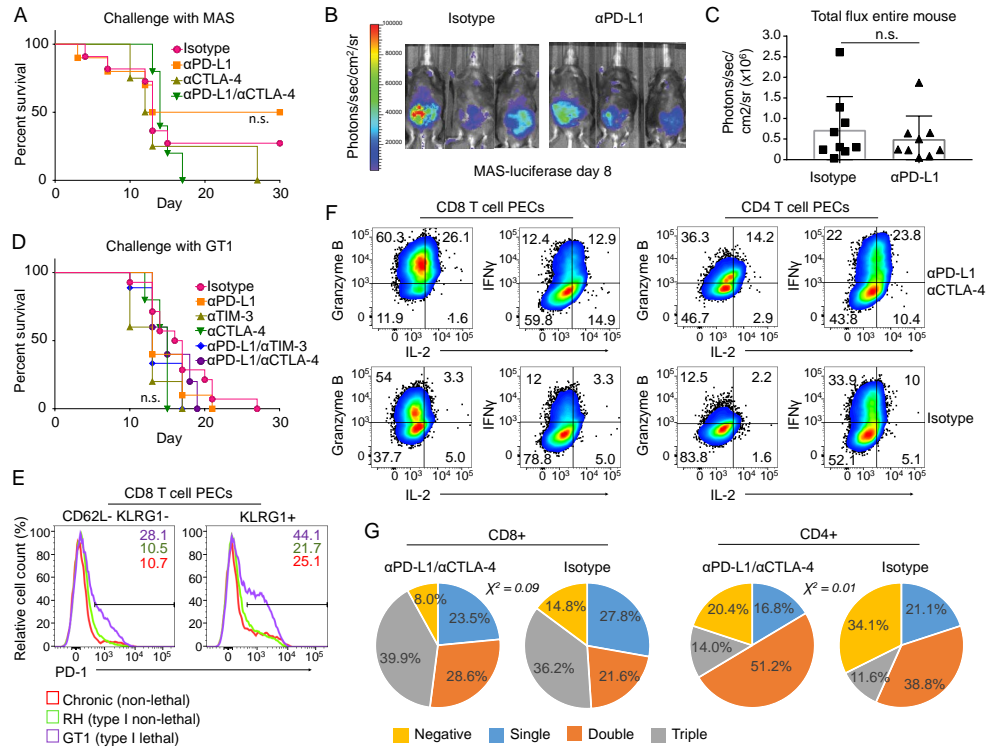


**Figure 2.3: Neutralization with CTLA-4-, TIM-3-, and/or PD-L1-blocking antibodies fails to rescue C57BL/6 mice following challenge with virulent *T. gondii* strains.** A and D) Following secondary infection with either the virulent atypical strain MAS (A) or the type I strain GT1 (D), mice were injected i.p. with 200  $\mu$ g of the following monoclonal antibodies on days 1, 3, 5, 7, 10, and 13 after challenge, and cumulative survival rates from one to two experiments are plotted: rat IgG2b isotype (GT1, n = 9; MAS, n = 11), anti-PD-L1 (GT1, n = 9; MAS, n = 10), anti-TIM-3 (GT1, n = 5), anti-CTLA-4 (GT1, n = 5; MAS, n = 4), anti-PD-L1 plus anti-TIM-3 (GT1, n = 9), and anti-PD-L1 plus anti-CTLA-4 (GT1, n = 5; MAS, n = 5). P values (log rank Mantel-Cox test) were calculated by comparing each therapeutic cohort against the control arm (isotype treated); all P values were > 0.05 and considered not significant (n.s.). (B) Representative bioluminescence images of mice treated with anti-PD-L1 or the rat IgG2b isotype control on day 8 of secondary infection with the MAS-luciferase strain. (C) Same as for panel B, except that the average total body photon emissions (photons per second per square centimeter per steradian)  $\pm$  SD are plotted. Each dot represents the measurement for an individual mouse, and cumulative data from two experiments are shown. The P value was >0.05 (one-way ANOVA), which was not significant. (E) Representative histogram plots from three separate experiments (n = 3 to 5 mice per experiment) of PD-1 expression on CD62L<sup>-</sup> KLRG1<sup>-</sup> or CD62L<sup>-</sup>

KLRG1+ (KLRG1+) CD8+ (CD3+ CD19-) peritoneal T cells during chronic infection or on day 5 of secondary infection with the type I RH or GT1 strain. Numbers represent the frequencies of cells that fall within the indicated gates and are color-coded to match the indicated *T. gondii* infections. (F) Representative flow plots of peritoneal CD8+ and CD4+ (CD3+ CD19) T cells from mice treated with PD-L1 plus anti-CTLA-4 or with the isotype control on day 8 of secondary infection with the MAS strain. Intracellular detection of IFN- $\gamma$ , IL-2, and GzmB was performed after in vitro recall infection; frequencies of cells that fall within each quadrant are shown. (G) Same as for panel F, except that the average frequencies of CD8 or CD4 T cells that express all three (triple), at least two (double), one (single), or none (negative) of the three immune mediators (IFN- $\gamma$ , IL-2, and GzmB), are plotted. Results were obtained from two experiments (n = 3 to 4 mice per experiment), and a chi-squared test was used to compare the therapeutic versus control arms. Data from B generated by Kirk Jensen

---

## 2.4 Discussion

The immune evasion mechanisms used by human parasitic pathogens, including *T. gondii*, have contributed to the difficulty of parasitic disease prevention. Today only one vaccine exists for any human parasitic pathogen, RTS,S/AS01 for *Plasmodium falciparum*, and its efficacy is low and dramatically wanes over time (RTSS Clinical Trials Partnership, 2015). Most vaccines against parasites fail to elicit long-lasting effector T cell responses (Siegrist, 2008) which are required to control the infection (Sacks, 2014; Sher & Coffman, 1992). Given the challenges with parasite vaccination and the estimated three billion people currently infected with parasites (Hotez et al., 2014; Pullan et al., 2014; Torgerson & Mastroiacovo, 2013), an exploration of inhibitory receptor pathways as targets in parasitic disease (Butler et al., 2012), or following vaccination warrants further attention. Since studies in the LCMV model have shown usefulness in combining checkpoint blockade with vaccination to maximize protective immunity (Ha et al., 2008), and because anti-PD-L1 therapy prevents recrudescence during chronic *T. gondii* infection (Bhadra et al., 2011b), we explored whether checkpoint blockade could cure virulent secondary infections with *T. gondii*.

Our data suggest both CD4 and CD8 T cells express receptors associated with T cell exhaustion following challenge with virulent *T. gondii* strains, and that CD8 T cells are hyporesponsive in this context. However, the individual impact of each of these T cell lineages and co-receptors that regulate immunity to reinfection with *T. gondii* is not yet resolved, and has likely contributed to our inability to reverse

disease outcome. CD4 T cell help to activate naïve CD8 T cells conventionally occurs through CD40-CD40L interactions on both APCs (Schoenberger et al., 1998) and on CD40-expressing CD8 T cells (Bourgeois et al., 2002). CD4 T cell help during primary infection is required to generate memory CD8 T cells that protect against *T. gondii* reinfection (Denkers et al., 1996; Casciotti et al., 2002). During prolonged antigen stimulation, memory CD8 T cells are more reliant on CD4 T cell help than naïve cells to control persistent LCMV infections (Aubert et al., 2011) and CD40-CD40L interactions are likely involved (West et al., 2011). Work from the Khan group suggests the CD40-CD40L pathway plays a fundamental role in the rescue of exhausted CD8 T cells during chronic *T. gondii* infection (Bhadra et al., 2011a). For example, following treatment with anti-PD-L1, CD40 was highly expressed on CD8 T cells, and CD8 T-cell-intrinsic CD40-signaling played a major role in reinvigorating CD8 T cells during therapy (Bhadra et al., 2011a). Moreover, deletion of BLIMP-1 from CD4 T cells not only restored CD4 T cell function, but also CD8 T cell function and control of *T. gondii* chronic infection (Hwang et al., 2016). CD4 T cells may also be important in this system. Although CD4 T cells were not impaired in their ability to make IFN $\gamma$ , exhaustion markers were expressed on CD4 T cells following virulent secondary infections. Whether CD4 T cell helper functions fail to be propagated in this model of *T. gondii* reinfection is unknown. Further studies could be conducted to assess the role of CD40-CD40L signaling, other costimulatory pathways, and more generally, CD4 T cell help during secondary challenge with virulent *T. gondii* strains. Costimulatory receptor agonists that mimic helper functions of CD4 T cells might be an avenue for therapeutic intervention in this system.

While PD-1 and TIM-3 were highly expressed on CD4 and CD8 T cells following virulent challenge with *T. gondii*, mice were refractory to therapeutics that target these inhibitory receptors. Whether a therapeutically responsive population of exhausted T cells is present during *T. gondii* reinfection is unknown. Regardless, anti-CTLA-4 treatment, which has broad effects on recently activated T cells as well as memory T cells, did not rescue mice from virulent challenge. Furthermore, anti-PD-L1—anti-CTLA-4 combination therapy, which promotes superior melanoma clearance in mice (Curran et al., 2010) and heightened HCV-specific human CD8 T cell responses *in vitro* (Nakamoto et al., 2009), again failed to rescue mice from secondary infections with virulent strains of *T. gondii*. While we have not explored the therapeutic effect of targeting all known exhaustion markers described in other systems, our data underscores the context-dependent effects of checkpoint blockade strategies in infection models (Attanasio & Wherry, 2016).

For example PD-1—PD-L1 antibody blockade (Brahmamdam et al., 2010; Zhang et al., 2010) prolongs mouse survival during bacterial sepsis, but rapidly exacerbates disease during *Mycobacterial tuberculosis* infection (Lázár-Molnár et al., 2010; Barber et al., 2011). Understanding the tradeoff between enhanced resistance and immune pathology, as well as knowing the pathogen-specific mechanisms required for microbial killing, will be key for predicting success of immunotherapeutic interventions for infectious disease.

Finally, while memory CD8 T cells are necessary for protection and are the only known memory population to adoptively transfer immunity to naïve mice against *T. gondii* strains like RH (Gigley et al., 2009a, 2011), there are likely additional requirements for immunity to more virulent strains like GT1, MAS, and GUY-DOS. It is known that immunity cannot be achieved in B cell deficient mice (Sayles et al., 2000), suggesting a potential role for B cells and/or antibody production in resistance to highly virulent *T. gondii* strains. Intriguingly, T cell exhaustion can also manifest as humoral deficiencies, as PD-L1 and LAG-3 blockade has been shown to boost humoral responses during malaria infections (Butler et al., 2012). In summary, although the exhausted T cell phenotype correlates with increased parasite virulence, this likely represents a secondary effect to an underlying susceptibility factor present in C57BL/6 mice. Identifying this and additional requirements for host immunity to virulent strains of *T. gondii* is the subject of investigation in chapter 3.

## Chapter 3

# ***Nfkbid* is required for immunity and antibody responses to *T. gondii***

### 3.1 Introduction

The goal of vaccination is to induce immunological memory that can protect from natural infection challenge. Depending on the pathogen, effective memory would need to protect also against a wide variety of pathogen strains encountered in nature. Such protection is termed heterologous immunity and is effective against pathogen strains that differ in virulence, immune evasion, or polymorphic antigens. Parasites represent a special challenge to vaccine development as an entirely protective vaccine has yet to be achieved for any human parasite (Sacks, 2014). The apicomplexan parasite *Toxoplasma gondii*, provides an excellent system to explore requirements for heterologous immunity to a parasitic pathogen. *T. gondii* is a globally spread intracellular protozoan parasite of warm-blooded animals that exhibits great genetic diversity (Lorenzi et al., 2016b). *T. gondii* strains differ dramatically in primary infection virulence in laboratory mice (Howe & Sibley, 1995) and in severity of human toxoplasmosis (Grigg et al., 2001; Khan et al., 2006; McLeod et al., 2012). Such infections can be overcome by immunological memory responses elicited by vaccination or natural infection. In particular, memory CD8 T cells and induction of IFN $\gamma$  are primarily responsible for protection against lethal secondary infections with the widely studied type I RH strain, which has a lethal dose of one parasite in naïve mice (Suzuki & Remington, 1990; Gazzinelli et al., 1991; Gigley et al., 2009a). CD4 T cells are required to help the formation of

effector CD8 T cell (Casciotti et al., 2002) and B cell responses (Johnson & Sayles, 2002), but the ability to adoptively transfer vaccine-elicited cellular immunity to naïve recipients against type I RH challenge is unique to memory CD8 T cells (Gazzinelli et al., 1991; Gigley et al., 2009a).

The role of B cells in *T. gondii* infections is less understood. Previous studies showed that B cell deficient mice ( $\mu$ MT) are extremely susceptible to primary (Chen et al., 2003b), chronic (Kang et al., 2000) and secondary infections (Couper et al., 2005), despite unimpaired levels of IFN $\gamma$ . Passive transfer of antibodies from immunized animals into vaccinated  $\mu$ MT mice significantly prolongs their survival after challenge (Johnson & Sayles, 2002; Sayles et al., 2000). IgM seems particularly suited for blocking cellular invasion by *T. gondii* (Couper et al., 2005), while IgG can perform both neutralization (Mineo et al., 1993) and opsonization functions (Joiner et al., 1990). Antibody responses against *T. gondii* are dependent on CD4 T cells (Johnson & Sayles, 2002; Zaretsky et al., 2012), and are regulated by cytokines that modulate T follicular helper cell and germinal center B cell formation in secondary lymphoid organs (Stumhofer et al., 2013), suggesting conventional “B-2” B cell responses provide antibody-mediated immunity to *T. gondii*.

In addition to conventional B-2 cells are “B-1” cells, innate-like lymphocytes that are known for producing self- and pathogen-reactive “natural” IgM (Baumgarth et al., 1999). B-1 cells are the predominant B cell compartment within the body cavities, including the peritoneal and pleural spaces and contribute to antigen-specific responses to many pathogens. In mouse models of secondary bacterial infections, including *Borrelia hermsii*, *Streptococcus pneumoniae* and non-typhoid *Salmonella*, vaccination induces protective memory B-1 cells to T cell-independent bacterial antigens (reviewed in (Smith & Baumgarth, 2019)). This memory is often restricted to the B-1b, or CD5- subset of B-1 cells (Alugupalli et al., 2004), but not in all models (Yang et al., 2012). In the *T. gondii* model, one study suggested that primed CD5+ B-1a cells can rescue B-cell-deficient mice during primary infection with a low virulence strain (Chen et al., 2003b). Memory B cells are also appreciated to secrete pathogen-specific IgM (Pape et al., 2011), and generate somatically mutated IgM to combat blood stage secondary infection with *Plasmodium* (Krishnamurthy et al., 2016). Whether IgM responses to *T. gondii* are B-2 or B-1 derived is unknown. Moreover, the role of B-1 cells in promoting immunity to *T. gondii* during a secondary infection has yet to be determined.

Particularly troubling for vaccine development against *T. gondii* is the lack

of sterilizing immunity achieved following infection (Jensen et al., 2015). Unlike the highly passaged lab type I RH strain, for which most immunological memory studies have been performed, the less passaged type I GT1 strain and atypical strains, many of which are endemic to South America, cause lethal secondary infections in C57BL/6J mice and co-infect (i.e. “superinfect”) the brains of challenged survivors (Jensen et al., 2015). During secondary infection memory CD8 T cells become exhausted, but checkpoint blockade fails to reverse disease outcome (Splitt et al., 2018). The data suggest yet unknown mechanisms are needed to provide heterologous immunity to highly virulent strains of *T. gondii*. Therefore, we set out to address whether additional requirements are necessary for heterologous immunity to *T. gondii*. Through use of forward and reverse genetics, we discovered a previously unidentified essential role for *Nfkbid* in immunity and antibody responses to *T. gondii*, and present evidence that both B-1 and B-2 cells assist resistance to secondary infection with highly virulent parasite strains.

## 3.2 Methods

### 3.2.1 Ethics Statement

Mouse work was performed in accordance with the National Institutes of Health Guide to the Care and Use of Laboratory Animals. Mouse protocols used have been reviewed and approved by UC Merced's Committee on Institutional Animal Care and Use Committee (IACUC). UC Merced has an Animal Welfare Assurance filed with OLAW (A4561-01), is registered with USDA (93-R-0518), and the UC Merced Animal Care Program is AAALAC accredited (001318).

### 3.2.2 Parasite strains and cell lines

Human foreskin fibroblasts (HFFs) monolayers were grown in DMEM (4.5 g/L D-glucose) (Life Technologies) supplemented with 2 mM L-glutamine, 20% fetal bovine serum (FBS) (Omega Scientific), 1% penicillin-streptomycin, and 0.2% gentamycin (Life Technologies). Mouse Embryonic Fibroblasts (MEFs) were grown in DMEM (4.5 g/L D-glucose) (Life Technologies) supplemented with 10% fetal bovine serum (FBS) (Omega Scientific), 20mM HEPES, 1% penicillin-streptomycin, and 0.2% gentamycin (Life Technologies). *Toxoplasma gondii* strains were passaged in HFFs in 'Toxo medium' (4.5 g/L D-glucose, L-glutamine in DMEM supplemented with 1% FBS and 1% penicillin-streptomycin). The following clonal strains were used (clonal types are indicated in parentheses): RH  $\Delta ku80 \Delta hxpprt$  (type I), RH (1-1) *GFP::cLUC* (type I), GT1 (type I), GT1 *GFP::cLUC* (type I), and CEP *hxpprt-* (type III). The following atypical strains were used: MAS, MAS *GFP::cLUC* (2C8) (haplogroup 'HG' HG4), GUY-MAT (HG5), FOU (HG6), GPHT (HG6), TgCATBr5 (HG7), GUY-DOS (HG10), and VAND (HG10). The uracil auxotroph vaccine strain, RH  $\Delta up \Delta ompdc$  (1), was passaged in HFFs in medium containing 250 $\mu$ M uracil. Generation of GFP-expressing GT1 strains GT1 parasites were transfected with linearized plasmids for parasite expression of GFP and click beetle luciferase (*GFP::cLUC*), parasites were grown on HFF monolayers in T-25 flasks in Toxo medium for 2 weeks. Parasites were removed from the flasks by scraping; the parasites were pelleted and washed with PBS and suspended in sterile FACS buffer (2% FBS in PBS). Fluorescent parasites were then sorted via fluorescence-activated cell sorting (FACS) into a 96-well plate with confluent HFF monolayers. To ensure single plaque formation in at least one of the wells, the sort was titrated using the following parasite numbers: 100, 50, 25, 12, 6, 3, 2, and 1 for each well per row of 8.

### 3.2.3 Mice

Female C57BL/6J (H-2b), A/J (H-2a), C57BL/10SnJ (H-2b), B10.A-H2<sup>a</sup> H2-T18<sup>a</sup>/SgSnJ (H-2a), B6AF1/J (A/J x C57BL/6J F1 progeny), B6.129S2-Ighm<sup>tm1Cgn</sup>/J ( $\mu$ MT), B6.SJL-Ptprc<sup>a</sup> Pepc<sup>b</sup>/BoyJ (CD45.1 congenic), B6.Cg-Gpi1<sup>a</sup> Thy1<sup>a</sup> Igh<sup>a</sup>/J (IgH-a triple congenic mice), C57BL/6J-Chr 7<sup>A/J</sup>/NaJ and C57BL/6J-Chr 10<sup>A/J</sup>/NaJ (chromosome 7 and 10 consomic mice), and 26 (AxB;BxA) recombinant inbred (RI) mice derived from A/J and C57BL/6J founders, were purchased from Jackson Laboratories. The *bumble* mouse line used for this research project (Arnold et al., 2012), C57BL/6J-Nfkbid<sup>tm1Btr</sup>/Mmmh, RRID:MMRRC\_036725MU, was obtained from the Mutant Mouse Resource and Research Center (MMRRC) at University of Missouri, an NIH-funded strain repository, and was donated to the MMRRC by Bruce Beutler, M.D., University of Texas Southwestern Medical Center. *Bumble* mice were crossed to C57BL/6J to generate F1 *bumble* heterozygotes (*Nfkbid*<sup>+/-</sup>). Mice were maintained under specific pathogen free conditions at UC Merced.

### 3.2.4 Parasite infections

Parasite injections were prepared by scraping T-25 flasks containing vacuolated HFFs and sequential syringe lysis first through a 25G needle followed by a 27G needle. The parasites were spun at 400 rpm for 5 min to remove debris and the supernatant was transferred, followed by a spin at 1700 rpm washing with PBS. For primary infections, mice were infected intraperitoneally (i.p.) with 10<sup>4</sup> tachyzoites of type III CEP *hxgprt*<sup>-</sup>. For some experiments, mice were vaccinated i.p. with 10<sup>6</sup> tachyzoites of RH  $\Delta$ *up* $\Delta$ *ompdc*. For secondary infections, mice were infected I.P. with 5x10<sup>5</sup> type I parasites (RH or GT1). Parasite viability of the inoculum was determined by plaque assay following i.p. infections. In brief, 100 or 300 tachyzoites were plated in HFF monolayers grown in a 24-well plate and 4-6 days later were counted by microscopy (4X objective).

### 3.2.5 Blood plasma isolation and assessment of seroconversion

All mice were assessed for sero-positivity to *T. gondii* 4-5 weeks post primary infection. 50 $\mu$ L of blood was isolated from mice in tubes containing 5 $\mu$ L of 0.5M EDTA on ice, pelleted and the supernatant containing blood plasma was heat inactivated to denature complement at 56°C for 20 minutes and then stored at -80°C. HFFs were grown on coverslips and infected with GFP-expressing RH

(1-1) overnight, fixed 18 hrs later with 3% formaldehyde (Polysciences) in PBS, washed, permeabilized and blocked with PBS containing 3% bovine serum albumin Fraction V (Sigma), 0.2M Triton X-100, 0.01% sodium azide, incubated with a 1:100 dilution of collected blood plasma for 2 hrs at room temperature, washed with PBS, and detected with Alexa Fluor 594-labeled secondary antibodies specific for mouse IgG (cat# A11032, Life Technologies). Seropositive parasites were observed by immunofluorescence microscopy (Nikon Eclipse Ti-U).

### 3.2.6 Brain superinfection assays

Brains from chronically infected mice (CEP *hxgprt*-) that survived secondary challenge were dissected, rinsed in PBS, passed through a 21G needle several times, pelleted and suspended in 1mL of PBS. For rederivation, 100 $\mu$ L of the brain homogenate was used to inoculate HFF monolayers in Toxo medium. One to two weeks later, infected HFFs were syringe-lysed and plated on new HFF monolayers to encourage parasite growth. Once HFFs were fully vacuolated, parasites were passaged in Toxo medium supplemented with mycophenolic acid (MPA) and xanthine that selects for parasites encoding a functional *HXGPRT* (i.e. the challenging strains) and against the chronically infecting type III *hxgprt*- which lacks a functional *hxgprt* gene. Outgrowth in MPA-xanthine was considered evidence for superinfection.

### 3.2.7 Genetic linkage analysis

Quantitative trait loci (QTL) analysis was performed with the package *r/QTL* in R (version 3.6.1). LOD scores for each marker were calculated using the Haley-Knott regression model with the function 'scanone', or for all possible combination of two markers (i.e. epistatic interactions) using the function 'scantwo'. 1000 permutations were performed to obtain the genome wide LOD threshold for a P value of  $\leq 0.05$ , which was considered statistically significant. Similar results were obtained with a linear mixed regression model. To estimate the effect each QTL had on the overall phenotype, the function 'fitqtl' was first used to fit the data to a multiple-QTL model. Statistical support was found for inclusion of all four QTLs with LOD scores  $> 3$  compared to any lesser combination of three QTLs (ANOVA  $P < 0.02$ ). Individual QTL effects were then calculated under the assumption of the four-QTL model, which collectively accounts for 91% of the observed phenotypic variance.

### 3.2.8 Cell isolation, in vitro recall infections, and FACS analysis

PECs were isolated by peritoneal lavage and splenocytes obtained, as described in (Splitt et al., 2018). In brief, 4mL of FACS buffer (PBS with 1% FBS) and 3mL of air were injected into the peritoneal cavity with a 27G needle. After agitation, the PEC wash was poured into a conical tube. PEC washes were filtered through a 70 $\mu$ m cell strainer, pelleted, and washed with FACS buffer before staining. Spleens were dissected and crushed through 70 $\mu$ m cell strainers, pelleted, incubated in ACK red blood cell RBC lysis buffer (0.15M NH<sub>4</sub>Cl, 10mM KHCO<sub>3</sub>, 0.1mM EDTA) for 5 minutes at room temperature, then washed with FACS buffer. To obtain peripheral blood leukocytes (PBLs), 50 $\mu$ L of blood was isolated from mice in tubes containing 5 $\mu$ L of 0.5 M EDTA on ice, pelleted and incubated in ACK lysis buffer, washed and peripheral blood leukocytes (PBLs) were suspended in FACS buffer.

For FACS analysis, all preparations were done on ice, and cells were blocked in FACS buffer containing Fc Block anti-CD16/32 (2.4G2) (BD Biosciences), 5% normal hamster serum, and 5% normal rat serum (Jackson ImmunoResearch) for 20 minutes prior to staining with fluorophore-conjugated monoclonal antibodies (mAbs). The following mAbs (1:100 staining dilutions) were used: anti-CD1d-BV650 (1B1, BD Bioscience), anti-CD11c-eFlour 450 (N418, eBioscience); anti-CD11c-eFlour 450 (N418, BD Bioscience); anti-CD45.2-eFlour 450 (104, eBioscience); anti-CD4-eFlour 450 (GK1.5, eBioscience), anti-CD4-PECy7 (GK1.5, eBioscience); anti-CD11b-FITC (M1/70, eBioScience), anti-CD11b-BUV395 (M1/70, BD Bioscience), anti-CD11b-BV421 (M1/70, BD Bioscience), anti-CD11b-Pacific Blue (M1/70, BioLegend); anti-IFN $\gamma$ -PE (XMG1.2, BD Bioscience); anti-CD8 $\alpha$ -APC (53-6.7, eBioscience), anti-CD8 $\alpha$ -BV510 (53-6.7, BioLegend), anti-Ly6G-APC (1A8-Ly6g, eBioscience), anti-CD19-PerCP-Cy5.5 (ebio1D3, eBioscience), anti-CD19-PE (6D5, BioLegend), anti-CD19-BV785 (6D5, BioLegend), anti-CD3-eFlour 780 (17A2, BD Biosciences), anti-Ly6C-PECy7 (HK1.4, BioLegend), anti-CD23-Pacific Blue (B3B4, BioLegend), anti-CD23-AF700 (B3B4, BioLegend), anti-CD21/CD35-FITC (7E9, BioLegend), anti-CD21/CD35-PE (7E9, BioLegend), anti-CD5-APC (53-7.3, BioLegend), anti-CD43-BV510 (S7, BD Bioscience), anti-CD43-BUV737 (S7, BD Bioscience), anti-CD5-PerCP-Cy5.5 (53-7.3, BioLegend), anti-CD5- Cy7-APC (53-7.3, BioLegend), anti-CD45R/B220-Cy7-APC (RA3-6B2, anti-CD45R/B220-BUV-661 (RA3-6B2, BD Bioscience), anti-CD73-Cy7-PE (eBioTY/11.9, eBioscience), anti-CD80-BV711 (16-10A1, BioLegend), anti-FCRL5-af88 (polyclonal, R&D systems) anti-

IgM-PECy7 (RMM-1, BioLegend), anti-IgM-BV605 (RMM-1, BioLegend), anti-IgD-FITC (11-26c.2a, BioLegend), anti-IgD-PEDazzle (11-26c.2a, BioLegend), anti-CD138/Syndecan-1-BV510 (281-2, BD Bioscience), anti-CD138/Syndecan-1-BV650 (281-2, BioLegend), anti-mouse-CD267/TACI-AlexaFlour-647 (8F10, BD Biosciences), and anti-CD268/BAFF-R-PE (7H22-E16, BioLegend). Other FACS reagents included the viability dye propidium iodide (Sigma) at a final concentration of  $1\mu\text{g/mL}$ .

For in vitro recall, splenocytes and PerC were isolated from chronic and challenged mice (day 5 or 7 following secondary infection) and  $6 \times 10^5$  cells per well (96-well plate) were plated in T cell medium (RPMI 1640 with GlutaMAX, 20% FBS, 1% Pen/Strep, 1mM NaPyruvate, 10mM HEPES,  $1.75\mu\text{l}$  BME). Cells were infected with a type I strain (RH or GT1) strain at an MOI (multiplicity of infection) of 0.2 for 18 hr;  $3\mu\text{g/mL}$  brefeldin A (eBioscience) was added for the last 5 hr of infection. 96-well plates were placed on ice, cells were harvested by pipetting and washed with FACS buffer, blocked, and stained for surface markers. Cells were fixed with BD Cytofix/Cytoperm and permeabilized with BD Perm/Wash solution (cat# 554714, BD Pharmingen), stained with anti-IFN $\gamma$ -PE (XMG1.2, BD Bioscience), anti-GZB (GB11, BioLegend) and anti-IL-2-APC (JES6-5H4, BioLegend) on ice for 1 hr or overnight. Cells were then washed once with BD Perm/Wash solution, once in FACS buffer, and analyzed by FACS.

For FoxP3 staining, peritoneal lavage was performed on chronic and challenged (day 7 following secondary infection) *bumble* and WT mice. Cells were washed and surface stained. Fixation and permeabilization was performed with the eBioscience Foxp3/Transcription Factor Staining Buffer Set (cat# 00-5523-00) before intracellular staining with anti-Foxp3-PE (MF-14, BioLegend) according to the manufacturer's recommendations. Flow cytometry was performed on a Beckman Coulter Cytoflex LX, LSR II (BD Biosciences), or the Bio-Rad ZE5 and analyzed with FlowJo software.

For serum reactivity analysis, syringe-lysed GFP-expressing strains (RH1-1 and GT1-GFP) were fixed in 3% formaldehyde for 20 minutes, washed twice in PBS, and plated in 96 well micro-titer plates at  $4 \times 10^5$  parasites/well. The parasites were then incubated with serum from chronically infected mice, at serum concentrations ranging from  $10^{-2}$  to  $10^{-6}$  diluted in FACS buffer, for 20 minutes at 37°C. Parasites were then washed with FACS buffer and placed on ice for incubation with anti-isotype detection antibodies depending on application: anti-IgG3-BV421 (R40-82, BD Bioscience), anti-IgM-PE/Cy7 (RMM-1, BioLegend),

anti-IgG1-FITC (RMG1-1, BioLegend), anti-IgG1-APC (RMG1-1, BioLegend), anti-IgG2b-FITC (RMG2b-1, BioLegend), anti-IgG2b-PE (RMG2b-1, BioLegend), anti-IgG2a-FITC (RMG2a-62, BioLegend), anti-IgG2a-PerCP/Cy5.5 (RMG2a-62, BioLegend), anti-IgM-a-PE (DS-1, BD Bioscience), anti-IgM-b-PE (AF6-78, BD Bioscience).

### **3.2.9 Parasite neutralization assay**

Heat-inactivated serum was used to coat live parasites for 20 minutes at 37°C before infecting  $5 \times 10^5$  mouse embryonic fibroblasts/well (MEFs) in 96 well plates. Immediately following addition of parasite to MEF wells, plates were spun at 1200rpm for 3 minutes to synchronize infection. 2 hrs after initiation of infection, cells were placed on ice and harvested by scraping with pipette tips. Cells were washed twice in FACS buffer, suspended in 1:1000 PI in FACS buffer, and then analyzed by flow cytometry. Neutralization was defined as a ratio: the percentage of PI- cells infected with parasites incubated with serum divided by the percentage of PI- cells infected with parasites without serum incubation.

### **3.2.10 SDS-PAGE and immunoblotting for parasite lysate antigen**

To generate parasite lysate antigens *T. gondii* was cultured in HFF and expanded to approximately  $2 \times 10^8$  parasites. Parasites were syringe-lysed, washed with sterile 1X PBS and the parasite pellet was lysed with (1mL) 0.1% TritonX-100 detergent in 1X PBS. Solubilized parasites were centrifuged at 2,000 RCF for 20 minutes to remove large debris. The supernatant was aliquoted and stored at -80°C. Parasite lysate was reduced with  $\beta$ -mercaptoethanol (BME) and separated via SDS-PAGE in 4-20% Mini-PROTEAN TGX pre-cast gels (cat# 4561096, Bio-Rad) before transfer to PVDF membrane using a Trans-Blot Turbo Mini PVDF Transfer Pack (cat# 1704156, Bio-Rad) via Bio-Rad Transblot Turbo (cat# 1704150, Bio-Rad). Membranes were blocked with 10% fortified bovine milk (Raley's) dissolved in Tris-Buffered Saline with 0.1% Tween (TBS-T 0.1%) for 1-2 hrs at room temperature or overnight at 4°C. Blots were then probed with heat-inactivated serum in blocking buffer at either 1:1,000 dilution for serum IgM analysis or 1:5,000 dilution for serum IgG analysis overnight at 4°C. Membranes were washed with TBS-T 0.1% three times for 20 minutes per wash. Blots were then incubated for one hr at room temperature with goat anti-mouse horseradish peroxidase (HRP)-

conjugated antibodies (SouthernBiotec): anti-IgM secondary 1:1000 (cat# 1020-05) and total anti-IgG secondary 1:5000 (cat# 1030-05). Membranes were then washed with TBS-T 0.1% three times and developed with Immobilon® Forte Western HRP Substrate (WBLUF0500). All blots were imaged via chemiluminescence on a ChemiDoc Touch (cat# 12003153, Bio-Rad). Image Lab 6.1 software (Bio-Rad) was used for analysis of bands and total lane signal. Western blots comparing A/J to C57BL/6J were developed simultaneously and the band signal was normalized to A/J.

### **3.2.11 RNA isolation and sequencing**

Peritoneal B-1a (B220<sup>int-neg</sup> CD19<sup>high</sup> CD11b<sup>+</sup> CD5<sup>+</sup> PI-), B-1b (B220<sup>int-neg</sup> CD19<sup>high</sup> CD11b<sup>+</sup> CD5<sup>-</sup> PI-), or B-2 B cells (B220<sup>high</sup> CD19<sup>+</sup> CD11b<sup>-</sup> PI-) were sorted into 500 $\mu$ l RNeasy lysis buffer using a FACS ARIA II cell sorter (BD Biosciences). RNA was purified using the RNeasy mini kit (cat# 74134, Qiagen) according to the manufacturer's protocol. RNA purity was tested by Qubit (ThermoFisher) and Agilent 2100 BioAnalyzer for total RNA with picogram sensitivity. DNA libraries were generated with a Lexogen QuantSeq-UMI FWD 3' mRNA-Seq Library Prep Kit (cat# 015). Samples were sent to UC Davis for QuantSeq 3' mRNA FWD-UMI sequencing.

### **3.2.12 Gene expression analysis and data availability**

Raw reads were trimmed and mapped by the BlueBee genomic pipeline FWD-UMI Mouse (GRCm38) Lexogen Quantseq 2.6.1 (Lexogen). In brief, reads were quality controlled with 'FASTQC', trimmed with 'Bbduk' to remove low quality tails, poly(A)read-through and adapter contaminations, read alignments to the *Mus musculus* genome build GRCm38 were done with 'STAR', and gene reads were quantified with 'HTSeq-count'. Differentially expressed gene (DEG) analysis was performed utilizing limma-voom in R version 3.6.3 in RStudio with Bioconductor suite of packages. Heatmaps were generated with 'gplots'. Pathway and GO term analysis was performed with MouseMine (mousemine.org), and gene set enrichment analysis was performed with GSEA v4.0.3. RNA-sequencing data generated in this dissertation has been deposited in the NCBI Sequence Read Archive (Bioproject accession number PRJNA637442). All other data that support the findings herein are available from the Dr. Kirk Jensen (UC Merced) upon reasonable request.

### 3.2.13 LPS-stimulation of enriched B cells and quantitative PCR

PerC and splenocytes were isolated from naïve 6-8 week-old C57BL/6J and A/J mice and enriched for B cells using the EasySep Mouse Pan B cell Isolation Kit (cat#19844, StemTech). Bead enrichment for splenic samples had the addition of biotinylated anti-CD43 antibodies (clone S7, BD Bioscience) to remove B-1 cells. Enriched samples were plated in a 96-well plate at 400,000 cells per well and stimulated with 25 $\mu$ g/ml of LPS (cat# L4391-1MG, Sigma). After 2 hrs, total RNA was isolated using the Rneasy Mini Kit (cat# 74134) and cDNA was synthesized using High Capacity cDNA Reverse Transcription Kit (ThermoFisher, cat#4368814). Quantitative PCR was performed on synthesized cDNA samples using Thermo Fisher TaqMan Master Mix (cat# 4444556) and TaqMan probes: *Actb* Assay ID:Mm02619580\_g1 (cat# 4331182), and *Nfkbid* - Assay ID: Mm00549082\_m1 (cat# 4331182), according to the manufacturer's protocol. Normalization of *Nfkbid* expression in each sample was calculated in comparison to *Actb* expression levels. Fold change in *Nfkbid* expression of AJ relative to that of C57BL/6J cells was determined through the delta delta CT method ( $2^{-\delta \delta CT}$ ).

### 3.2.14 PerC adoptive transfers and IgH allotype chimeric mouse generation

PerC was harvested by peritoneal lavage of 6-12-week-old C57BL/6J donor mice as described above and  $5 \times 10^6$  total peritoneal exudate cells (total PerC)/60 $\mu$ l PBS dose were transferred i.p. into 2-4 day old *bumble* neonates. Allotype chimeric mouse generation was performed as previously described (Lalor et al., 1989). In brief, 1-day-old C57BL/6J neonates were treated with 0.1mg of anti-IgM-b (clone AF6-78) and twice weekly thereafter treated with 0.2mg of anti-IgM-b for 6 weeks. On day 2 after birth, the neonates were given  $5 \times 10^6$  total PerC from B6.Cg-*Gpi1*<sup>a</sup> *Thy1*<sup>a</sup> *Igh*<sup>a</sup>/J delivered i.p. The mice were then allowed to rest for 6 weeks after the last antibody treatment before infection with *T. gondii*.

### 3.2.15 Bone marrow chimeric mice generation

B6.SJL-*Ptprc*<sup>a</sup> *Peprc*<sup>b</sup>/BoyJ, *bumble*, and C57BL/6J recipient mice were given 2 doses of 500cGy with an X-Rad320 (Precision X-Ray) with a 4 hr interval. Donor BM cells were harvested from  $\mu$ MT, *bumble* and WT C57BL/6J mice, filtered with a 70 $\mu$ m filter, incubated in ACK red blood cell lysis buffer, washed with PBS and

transplanted by retro-orbital injection at a concentration of  $10^7$  cells/200 $\mu$ l PBS dose. For mixed BM chimeras, 1:1 mixtures of  $\mu$ MT and *bumble* or  $\mu$ MT and WT BM cells were created. Recipient mice were then allowed to rest for 8 weeks. Reconstitution was assessed at 8 weeks by FACS analysis of PBL.

### **3.2.16 ELISA**

High-affinity protein binding microplates (Corning) were coated overnight with goat anti-mouse IgM (1mg/ml, Southern Biotech, cat# 1021-01) and blocked with coating buffer containing with 1% BSA (w/v) and 2% goat serum (Omega Scientific) in PBS. Wells were washed with ELISA wash buffer (1X PBS, 0.05% Tween<sup>TM</sup> 20). Mouse serum samples were diluted 1:400 in coating buffer and incubated in the wells for 1 hr. Wells were washed 5 times and secondary goat anti-IgM-HRP (Southern Biotech, cat# 1021-08) at 1:5000 dilution was incubated for 1 hr in the wells. Wells were washed several times and developed with TMB substrate (Invitrogen). Development was stopped after 20 minutes with 1M H<sub>3</sub>PO<sub>4</sub> stop solution. Absorbance was measured at 450nm on a BioTek Epoch microplate spectrophotometer.

### **3.2.17 RNA Structure Prediction**

RNA sequences for *Nfkbid* were taken from the mouse genomes project (Keane et al., 2011). 275 nucleotides (1508-1782) that form the constitutive decay element-containing stem loops were modeled with RNAstructure using default settings (Reuter & Mathews, 2010).

### **3.2.18 Statistics**

Statistical analysis was performed with Graphpad Prism 8 software. Statistical significance was defined as  $P < 0.05$ . P values were calculated using paired or unpaired two-tailed t-tests, 2-way ANOVA with Tukey multiple comparison correction, and multiple t-tests with the Holm-Sidak correction for multiple comparisons. Survival curve significance was calculated using log-rank Mantel-Cox testing. Significance in time to death was calculated using the Gehan-Breslow-Wilcoxon test. Differential gene expression analysis statistics were calculated using the Limma-Voom R package, P values were adjusted with the Benjamini-Hochberg

correction for multiple comparisons. GO term and pathway enrichment analysis statistics were performed at mousemine.org using the Holm-Bonferroni test correction. Statistical methods used for each figure are indicated in the figure legends.

### 3.3 Results

#### 3.3.1 Non-MHC loci control resistance to secondary infection with *Toxoplasma gondii*

To find the requirements for immunity against high virulence strains of *T. gondii* we used a model of natural infections. Mice given a natural infection with a low virulent type III CEP *T. gondii* strain are known to develop protection against secondary infections with the commonly studied lab strain type I RH, a parasite strain that has an LD<sub>100</sub> of 1 parasite in naive mice (Suzuki & Remington, 1990; Gazzinelli et al., 1991; Gigley et al., 2009b). However, this protection is limited as secondary infections with highly virulent "atypical" strains isolated from South America (VAND, GUYDOS, GUYMAT, TgCATBr5) and France (MAS, GPHT, FOU) as well as type I GT1 clonal parasites result in morbidity and mortality in C57BL/6J, at varying frequencies dependent on virulence factors (Jensen et al., 2015). In contrast to the observed susceptibility of C57BL/6J, A/J mice are uniformly resistant to secondary infection with high virulence "atypical" and clonal strains (Figure 3.1A).

A/J mice are known to be resistant to primary infection with type II strains due to polymorphisms at the MHC class I H-2 locus (Mcleod et al., 1989; Brown et al., 1995). To test the contribution of the H-2 locus in susceptibility to high virulence *T. gondii* strains, we performed secondary infections in C57BL/10J (B10; H-2 haplotype: b) and C57BL/10J (B10.A; H-2 haplotype: a) mice. Mice expressing the H-2a haplotype (A/J and B10.A) have overall greater resistance to high virulence strains relative to mice with the H-2b haplotype (C57BL/6J and B10), however that resistance is not uniform, as B10.A mice were susceptible to secondary infection with several strains (VAND, GUY-DOS, GPHT, FOU) (Figure 3.1A). Bioluminescence imaging was used to quantify parasite burden at day 1, 4, and 8 of secondary infection with a luciferase expressing atypical strain, MAS (MAS GFP-cLUC). Mice expressing the H-2a MHC haplotype, but not H-2b mice, showed parasite clearance as early as day 4 of secondary infection (Figure 3.1B).

Together, this data shows that the H-2 locus is a major factor of immunity to secondary infections with *T. gondii*, but there are still yet unknown genetic factors in A/J mice that confer fully protective heterologous immunity to all strains of *T. gondii*.

In order to find evidence of non-MHC loci that confer protection, we turned to a *T. gondii* strain that is not controlled by the H-2 MHC locus. Type I GT1, a high virulence clonal strain, was found to cause lethal secondary infections in B10 and B10.A mice, but not A/J or outcrossed A/J x C57BL/6J mice ('F1') (Figure 3.1C). However, the immunity achieved in resistant A/J or F1 mice was not sterile, as GT1 parasites ("superinfection") were found in the brains of secondary infection survivors (Figure 3.1D). Of note, superinfection was observed to a much greater extent in F1 mice compared to A/J highlighting the non-binary nature of the resistance phenotype. In addition to not being controlled by MHC loci, type I GT1 parasites are known to evade host IFN $\gamma$  responses through multiple virulence factors, and thus is an ideal strain to discover unknown requirements for heterologous immunity.

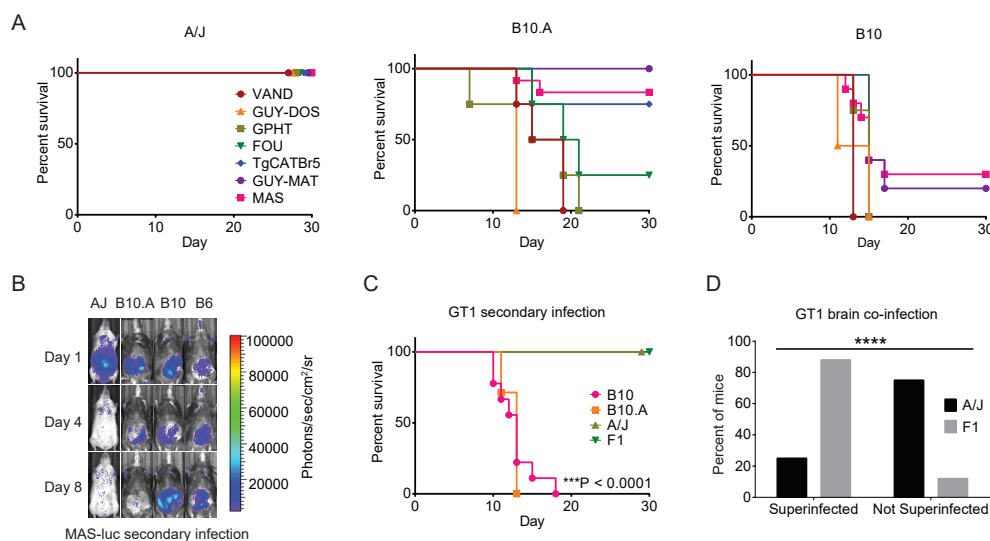


**Figure 3.1: MHC and non-MHC alleles promote immunity to virulent *T. gondii* strains in A/J mice.** All mice were infected with  $10^4$  type III CEP *hxgprrt*- low virulence *T. gondii* parasites and allowed to progress to chronic infection; then, 35 days later, mice were given a secondary infection with  $5 \times 10^4$  of the indicated strains of *T. gondii*. A) Survival of A/J, C57BL/10J (B10), and C57BL/10J.A (B10.A) mice following secondary infection with atypical strains of *T. gondii*. Cumulative results are plotted from 1-2 experiments; n=4 to 12 mice per parasite strain and mouse genetic background. B) Bioluminescence imaging

of individual mice challenged with luciferase expressing MAS strain on days 1, 4 and 8 of secondary infection; parasite burden is shown as a heat map depicting the relative number of photons (photons/sec/cm<sup>2</sup>/sr) detected over a 5-minute exposure. C) Survival of B10 (n=5), B10.A (n=5), A/J (n=12), and F1 (A/J x C57BL/6, n=9) mice following secondary infection with the type I GT1 strain; \*\*\*P<0.0001, Log-rank (Mantel-Cox) compared to A/J mice. Cumulative data from 1 to 2 experiments are plotted. D) Superinfection in surviving A/J (n=12) and F1 (n=9) mice following 35 days of secondary infection with the type I GT1 strain. To evaluate superinfection, brain homogenate was grown in MPA-xanthine selection medium, which selects for GT1 parasites expressing the endogenous *HXGPRT* locus and against the *hxgprrt*- type III CEP strain used to induce chronic infection. Plotted is the fraction of mice for which the presence or absence of the GT1 strain was detected; \*\*\*\*P < 0.0001, Fisher's exact test. Data from B generated by Kirk Jensen. Data from A, C, and D generated by Sam Splitt.

---

### 3.3.2 Genetic mapping reveals four loci that correlate with immunity to *Toxoplasma gondii*

To uncover non-MHC genetic factors that contribute to the heterologous immunity observed in A/J mice we turned to a panel of recombinant inbred mice (AxB:BxA) that are homozygous for either A/J or C57BL/6J alleles randomly distributed throughout the entire mouse genome. The AxB:BxA panel had been used previously to identify host resistance factors for primary infection to type II *T. gondii* strains and differential macrophage responses (McLeod et al., 1989; Hassan et al., 2015). The AxB:BxA panel is of particular use in studying inducible protection against *T. gondii* infections, as more complex panels such as the collaborative cross contain mice with potent IRGs that can independently control high virulence type 1 strain infection (Churchill et al., 2004; Murillo-León et al., 2019; Hassan et al., 2019; Lilue et al., 2013) potentially obfuscating adaptive memory dependent phenotypes. 26 AxB:BxA mice were given a primary infection with type III CEP strain, then a secondary infection with type I GT1 strain to find non-MHC loci correlated with survival. Genetic mapping using Quantitative Trait Loci (QTL) analysis for survival against high virulence secondary infections identified four peaks with logarithm of the odds (LOD) scores greater than 3 on chromosomes 7, 10, 11, and 17 (Figure 3.2A). None of the QTLs bore evidence for epistatic interactions (not shown), and only the chromosome 10 QTL surpassed genome-wide permutation testing (n=1000, P<0.05). Nevertheless, an additive-QTL model including all four QTLs best fit the data compared to any lesser combination of them (P<0.02, ANOVA). Of the loci, only the chromosome 10 QTL passed genome-

wide permutation testing (n=1000, P <0.05). The estimated effect on phenotypic variance associated with each peak was Chr7, 24%; Chr10, 41%; Chr11, 21%; and Chr17, 27%. 100% allelic correlation with either resistance or susceptibility to secondary infection was not observed in any of the major QTL peaks (Figure 3.2B). Consistent with the estimated contributions of each QTL peak to the survival phenotype, chromosomal substitution mice for Chr7 (CSS7) and Chr10 (CSS10) failed to recapitulate the A/J survival phenotype against type I GT1 (Figure 3.2C), again suggesting the requirement of multiple genes to the survival phenotype.

Genes identified within the boundaries of each QTL (Table 3.1; Appendix 6.1) were analyzed for evidence of polymorphisms using the Mouse Genomic Informatics (MGI) SNP database. The majority of SNPs identified in the QTLs were found within introns or within  $2\pm\text{Kb}$  of the various gene candidates, with non-synonymous SNPs representing the least frequent SNP category. Untranslated region (UTR) SNPs were also identified and are known to affect mRNA stability by differential binding of mRNA regulatory elements such as miRNAs or disruption of secondary RNA structures that promote stability resulting in dramatic differences in both transcript and protein expression (Garneau et al., 2007; Skeeles et al., 2013). Within the chromosome (Chr) 7 QTL, the gene with the most non-synonymous and UTR SNPs, as well as encoding multiple intronic and region SNPs, is *Nfkbid*, an atypical regulator of NF- $\kappa$ B. The QTL over Chr11 encompasses *Tspan8*, which is 6-fold more highly expressed in spleens from A/J compared to C57BL/6 mice (immgen.org), perhaps due to the multiple intronic SNPs identified within this gene. *Tspan8* promotes cancer metastasis (Berthier-Vergnes et al., 2011) and can impact leukocyte migration (Zhao et al., 2018), but its role in immunity is largely unknown. The Chr17 QTL identified *St6gal2*, a sialyl-transferase that is widely expressed but is dysregulated in multiple cancer models (Cheng et al., 2020). Interestingly, the QTL analysis identified a survival locus on Chr11 of the C57BL/6J background with two highly polymorphic genes, *Blmh* and *Slc6a4*. *Blmh* is a cysteine protease that is widely expressed in all tissues, though recently has been shown to regulate inflammatory chemokines in atopic dermatitis patients (Riise et al., 2019). *Slc6a4* is a serotonin transporter that has been widely studied in human populations (Murphy et al., 2008). Though of interest, we opted not to investigate Chr11 in favor of investigating A/J's ability to generate heterologous immunity.

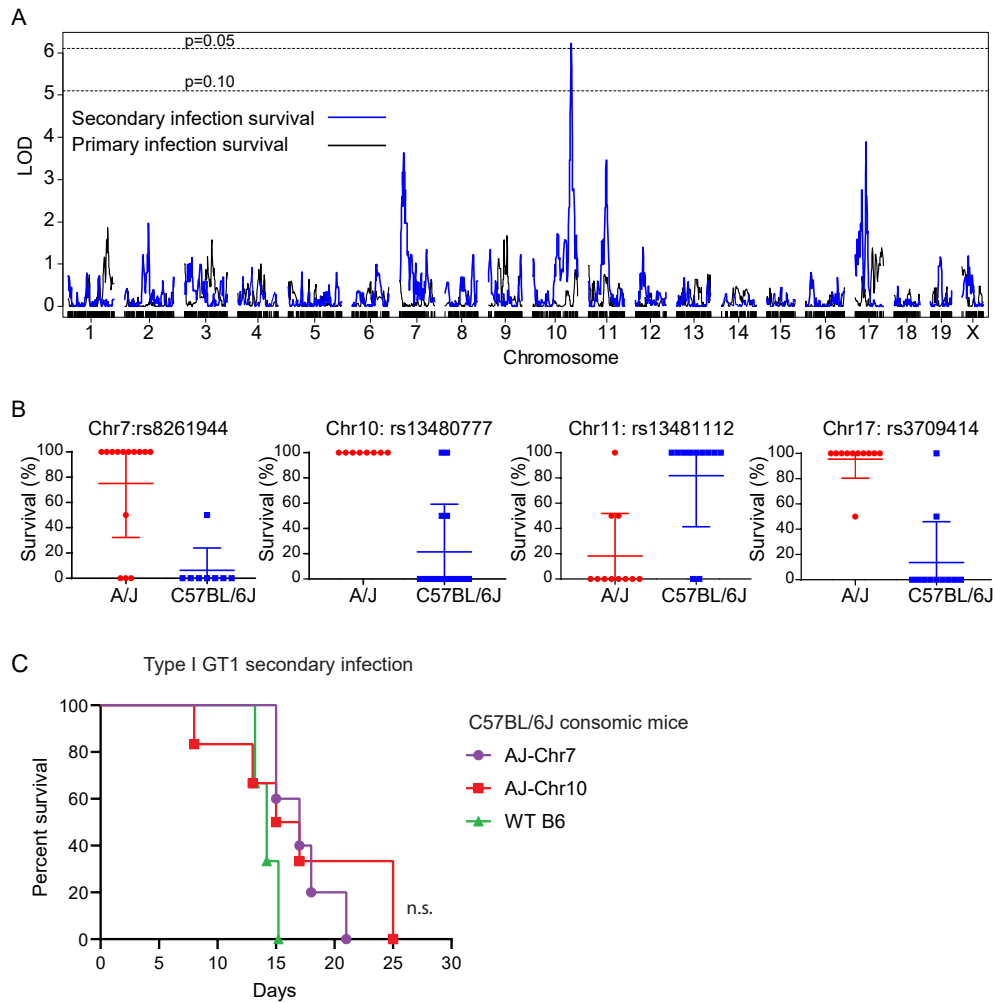


**Figure 3.2: Genetic mapping reveals *Nfkbid* four loci associated with secondary infection immunity.** 26 recombinant inbred (RI) mouse strains from the AxB;BxA panel were primed with  $10^4$  type III *T. gondii* CEP *hxgprt*- parasites; then, 35 days later, mice were challenged with  $5 \times 10^4$  virulent type I GT1 *T. gondii* parasites ( $n=2$  per RI line). A) LOD scores for each marker were calculated using Haley-Knott regression and the running LOD scores of primary (black) and secondary infection survival (blue) for each genetic marker is plotted. 1000 permutations were performed to obtain the genome-wide threshold LOD values;  $P=0.10$  and  $0.05$  thresholds are shown. B) Effect plots for the genetic markers closest to the maximal LOD scores calculated for the chromosome 7, 10, 11 and 17 QTLs are shown. Each dot indicates the percent survival of a unique RI line and whether it encodes an A/J (red) or C57BL/6J (blue) allele at the specified genetic marker. C) Consomic mice of the C57BL/6J background with A/J chromosomal substitutions for chromosome 7

(C57BL/6J-Chr7<sup>A/J</sup>/NaJ) or chromosome 10 (C57BL/6J-Chr10<sup>A/J</sup>/NaJ) were infected with the type III CEP *hxgprt*- strain and allowed to progress to chronic infection. Mice were then given a secondary infection with the type I GT1 strain. Cumulative survival is shown for 2 independent experiments (CSS7 n=5, CSS10 n=6); n.s., Mantel-Cox. AxB and BxA survival studies that were the basis for (A) and (B) performed by Sam Splitt.

Chromosome 7	MGI ID	Feature Type	Symbol	NS-SNP	UTR-SNP	Syn-SNP	Intron SNP	Region SNP	Non-coding Transcript SNP	Sum Mutation	Immune Function
Imputed LOD 3.7	MGI:3041243	protein coding gene	Nfkbid	2	13	2	28	12	0	57	Yes
	MGI:1859637	protein coding gene	Nphs1	0	5	3	48	2	0	58	No
	MGI:1929093	protein coding gene	Prodh2	0	10	5	40	7	0	62	No
LOD = 3.2	MGI:2685928	antisense lncRNA gene	Arhgap33os	0	0	0	23	7	11	41	No
Chromosome 10	MGI ID	Feature Type	Symbol	NS-SNP	UTR-SNP	Syn-SNP	Intron SNP	Region SNP	Non-coding Transcript SNP	Sum Mutation	Immune Function
3.5 < LOD < 5.1	MGI:2384918	protein coding gene	Tspan8	0	1	3	55	4	0	63	Possible
Chromosome 11	MGI ID	Feature Type	Symbol	NS-SNP	UTR-SNP	Syn-SNP	Intron SNP	Region SNP	Non-coding Transcript SNP	Sum Mutation	Immune Function
2.3 < LOD < 3.5	MGI:1858260	protein coding gene	Gosr1	0	6	0	57	0	0	63	No
	MGI:107265	protein coding gene	Cpd	1	11	11	238	0	0	261	Possible
LOD = 3.5	MGI:1345186	protein coding gene	Blmh	1	5	3	159	11	0	179	Possible
	MGI:96285	protein coding gene	Slc6a4	2	1	2	53	5	0	63	No
Chromosome 17	MGI ID	Feature Type	Symbol	NS-SNP	UTR-SNP	Syn-SNP	Intron SNP	Region SNP	Non-coding Transcript SNP	Sum Mutation	Immune Function
LOD = 3.9	MGI:2445190	protein coding gene	St6gal2	0	0	0	0	173	0	173	Possible
	MGI:3761695	protein coding gene	Vmn2r118	0	0	0	0	56	0	56	No
	MGI:1920086	protein coding gene	Pot1b	0	0	0	0	61	0	61	No

**Table 3.1: Polymorphic genes identified by Quantitative Trait Loci analysis.** For each of the four QTLs that define secondary infection immunity to *T. gondii*, a list of all genes that have  $\geq 40$  DNA polymorphisms between A/J and C5BL/6J mice, and are encoded within the QTL boundaries defined by the maximal genetic marker (real or imputed markers

inferred in r/QTL) and the two flanking markers on either side; LOD scores and position are indicated. For each gene, its location and unique identifiers are listed, as well as the number and class of small nucleotide polymorphism (SNP) between A/J and C57BL/6J are shown. Total number of SNPs for each gene were also tallied ('Sum mutation'), and in bold are genes whose SNPs are two standard deviations greater than the average SNP for that class within the QTL region. In these QTL regions, there were also 476 (chr7), 88 (chr10), 40 (chr11) and 375 SNPs (chr17) that did not associate with any gene in the QTL boundaries. UTR, untranslated region; 'Region SNP', SNPs that are +/- 2 kb of the gene boundaries. "Immune function" is a subjective assessment of GO terms and publications associated with each gene for potential involvement in the immune system. Data obtained from Mouse Genome Informatics (MGI). For the entire list of polymorphisms, genes, genetic markers and LOD scores associated with each QTL, see Appendix 1.

---

### **3.3.3 *Nfkbid* on chromosome 7 is required for immunity and the generation of *Toxoplasma gondii*-specific antibodies**

Given the role of *Nfkbid* in several immune functions, degree of polymorphism and central location within the Chr7 QTL, the requirement for *Nfkbid* in immunity to *T. gondii* was further explored. *Nfkbid* is an atypical inhibitor of NF- $\kappa$ B which is differentiated from classical inhibitors by affecting transcriptional profiles via context-dependent induction/repression of genes, rather than broad inhibition of NF- $\kappa$ B activation. Previous work has shown that *Nfkbid* is essential for B-1 cell development and T-independent (TI) type II antigen responses (Touma et al., 2011; Arnold et al., 2012; Pedersen et al., 2016). The protein product of *Nfkbid*, I $\kappa$ BNS, promotes plasmablast differentiation (Khoenkhoen et al., 2019), IgG1 response to T-dependent antigens (Touma et al., 2011; Hosokawa et al., 2017), T cell IL-2 and IFN $\gamma$  production (Touma et al., 2007), stabilization of FOXP3 expression in T regulatory cells (Schuster et al., 2017), suppression of TLR-induced cytokine expression in macrophages (Kuwata et al., 2006), normal marginal zone B cell development (Adori et al., 2017), B cell production of IL-10 (Miura et al., 2016), and T cell differentiation into follicular helper cells (Hosokawa et al., 2017). The extent of *Nfkbid*'s involvement in immune functions, in addition to the numerous polymorphisms between the resistant A/J and susceptible C57BL/6J mice (Table 3.1), made *Nfkbid* our primary candidate for investigation. *Nfkbid*-null (*bumble*) mice on the C57BL/6J background were generated in Bruce Beutler's laboratory (UT Southwestern) by ENU mutagenesis searching for genes essential for T-independent antibody responses (Arnold et al., 2012). Though *bumble* mice are on the susceptible C57BL/6J background, it is unknown if *Nfkbid* is required for

immune responses against *T. gondii*. In our hands, *bumble* mice were found to survive primary infections with the low virulence type III CEP strain at similar frequencies to wild type (WT) C57BL/6J (Figure 3.3A), suggesting *bumble* mice have an intact acute immune response. When given a secondary infection with the type I GT1 strain, *bumble* mice were found to have a faster death kinetic relative to WT (Figure 3.3B). Leveraging the modular virulence of our secondary infection model, we substituted GT1 for the lab adapted type I RH strain, a *T. gondii* strain known to be controlled after vaccination and primary infection in the C57BL6/J background (Suzuki & Remington, 1990; Gazzinelli et al., 1991; Gigley et al., 2009a) and found *bumble* mice were extremely susceptible to type I RH strain secondary infection (Figure 3.3C). Parasite burden in *bumble* mice was significantly higher at day 7 of secondary infection with a GFP-expressing RH strain (RH1-1) relative to WT (Figure 3.3D). The observation of *Nfkbid*-dependent susceptibility only manifesting within secondary, but not primary infection, was encouraging as the forward genetic screen was designed to identify genes that determine secondary infection susceptibility to *T. gondii*, and therefore *Nfkbid* is likely to be the causal gene within the chromosome 7 QTL.

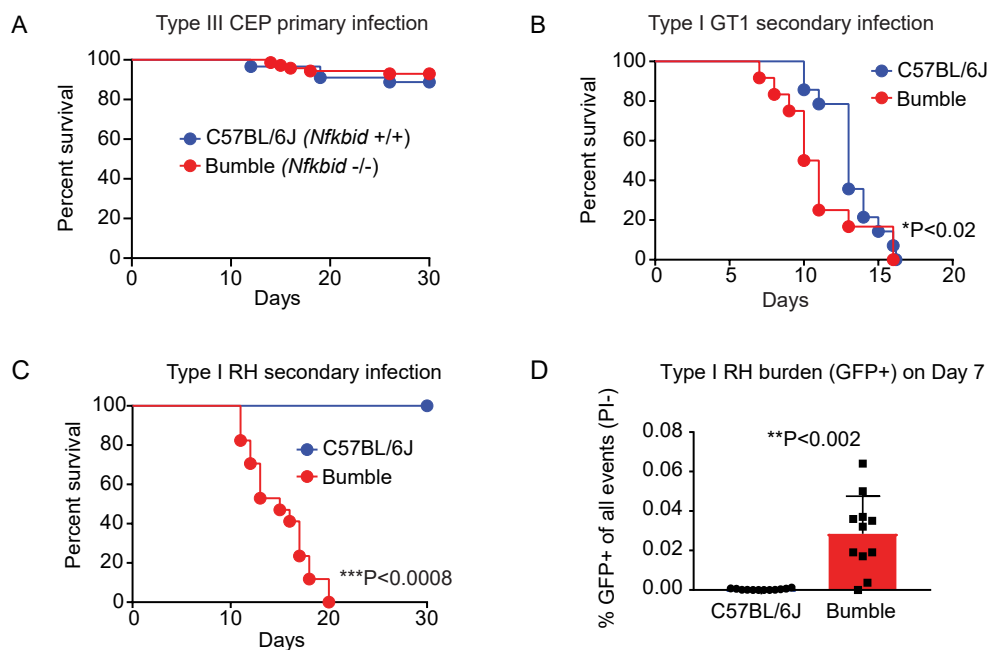


**Figure 3.3: *Nfkbid*-null mice are susceptible to secondary infection but not primary infection.** A) Cumulative survival of *bumble* (*Nfkbid*-/- C57BL/6) (n=71) and wildtype (C57BL/6J) (n=89) naïve mice infected with the avirulent type III CEP strain. B) Survival

of chronically infected *bumble* (n=12) and wildtype (n=8) mice given a secondary infection with the type I GT1 strain. Cumulative survival from 3 separate experiments is shown; \* P<0.05, Gehan-Breslow-Wilcoxon test. C) As in B, but survival to secondary infection with the type I RH strain is shown. Cumulative survival from 3 separate experiments is plotted (*bumble* n=17, C57BL/6J n=4); \*\*\*P<0.001, Mantel-Cox test. D) Frequency of GFP+ events in the peritoneal lavage 7 days post-secondary infection with the GFP-expressing type 1 RH strain (RH 1-1). Each dot represents the result of one mouse, and cumulative results are shown from 3 separate experiments (*bumble* n=13, C57BL/6J n=17); \*\*P<0.01, unpaired two-tailed t-test.

To determine why *bumble* mice are susceptible to secondary infections with high virulence strains, we first looked at known T cell phenotypes of *Nfkbid* deficient mice: lower IFN $\gamma$  and IL-2 production as well as a reduced ability to differentiate into regulatory T cells. *In vitro* stimulation of peritoneal T cells from mice at day 7 of secondary infection showed no significant decrease in IFN- $\gamma$  and IL-2 production (Figure 3.4A). In addition, there was no observed frequency difference in peritoneal T regulatory cells (CD4+ CD25+ FOXP3+) within in *bumble* mice (Figure 3.4B).

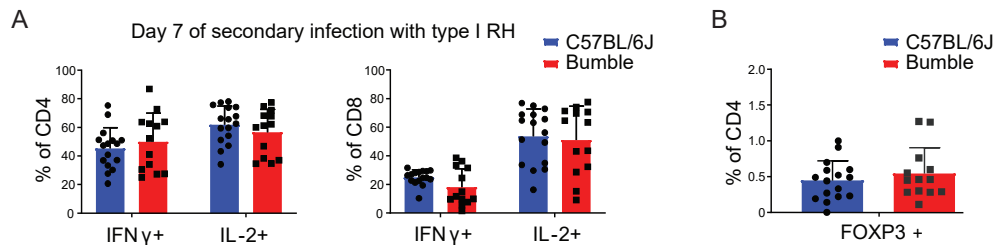


**Figure 3.4: *Bumble* mice have intact T cell responses during secondary infection.** A) Peritoneal CD4 and CD8 T cells from *bumble* and C57BL/6J mice were assessed at day 7 of secondary infection with the type I RH strain by *in vitro* recall assay and assayed for intracellular IFN $\gamma$  and IL-2. In brief, peritoneal cells were harvested and infected with live type I RH parasites for 16 hrs. T cells were assessed for production of IFN $\gamma$  and IL-2 by intracellular staining and FACS. B) Peritoneal T-regulatory cells (CD4+ CD25+ Foxp3+) were quantified at day 7 of secondary infection with type I RH strain. Each dot represents the result from one mouse, and plotted are cumulative averages  $\pm$ SD from 3 experiments; no significant differences were observed between *bumble* and C57BL/6J mice by unpaired t-tests with the Holm-Sidak correction for multiple comparisons.

Serological assays from chronically infected *bumble* mice show an inability

to make parasite-specific IgM (Figure 3.5A), observations which are analogous to previous reports that *Nfkbid*-deficient mice are unable to mount IgM responses to the model antigens 2,4,6-Trinitrophenyl (TNP)-Ficoll (T-dependent) and TNP-Keyhole Limpet Hemocyanin (KLH) (T-independent) (Touma et al., 2011; Arnold et al., 2012). In addition to abrogated parasite-specific IgM, every IgG isotype analyzed was found to be significantly lower in parasite reactivity from chronically infected *bumble* relative to WT mice. The latter observation contrasts to previous reports of class-switched IgG antibodies against model antigens reaching WT levels, though after a 2-week delay (Touma et al., 2011; Arnold et al., 2012). In-line with the lower titer of parasite-specific antibodies in *bumble* mice following infection, *bumble* antibodies were found to be significantly defective at neutralizing *T. gondii* (Figure 3.5B). Antibodies from naïve mice fail to bind *T. gondii*, thus natural antibodies do not recognize *T. gondii*, consistent with previous reports (Couper et al., 2005).

The loss of parasite-specific antibodies prompted us to investigate B cell compartments within *bumble* mice to explain the immune defect against secondary infections. FACS analysis of splenic B cells revealed a developmental block in chronically infected *bumble* compared to WT mice. A stark phenotype observed was the presence of high frequencies of transitional B cells (CD19<sup>+</sup> B220<sup>+</sup> CD21<sup>-</sup> CD23<sup>-</sup>), which were found to be significantly increased at the chronic stage of infection (>28 days) in *bumble* mice (Figure 3.5C), suggesting an inability to replenish the B cell compartment after infection. Within the fully developed B cell compartment, naïve *bumble* mice had reduced frequencies of marginal zone B cells (not shown), consistent with previous reports (Adori et al., 2017). Regarding CD73<sup>+</sup> memory B cells (Parra et al., 2020; Zuccarino-Catania et al., 2014), no difference was observed in the frequencies of this population (not shown), however the frequency of class-switched (IgM<sup>-</sup> IgD<sup>-</sup>) CD73<sup>+</sup> memory B cells was significantly reduced in *bumble* mice (Figure 3.5C). Frequencies of "atypical" memory B cells known to be protective against malaria (FCRL5<sup>+</sup> CD80<sup>+</sup> CD73<sup>+</sup> CD19<sup>+</sup> B220<sup>+</sup>) (Kim et al., 2019) were found to be significantly reduced in *bumble* relative to WT mice (not shown). Together, this data suggests that *Nfkbid* is required for B cell development and class-switching in response to *T. gondii*, and the observed B cell deficiencies in *bumble* mice underlie their immunity defect.

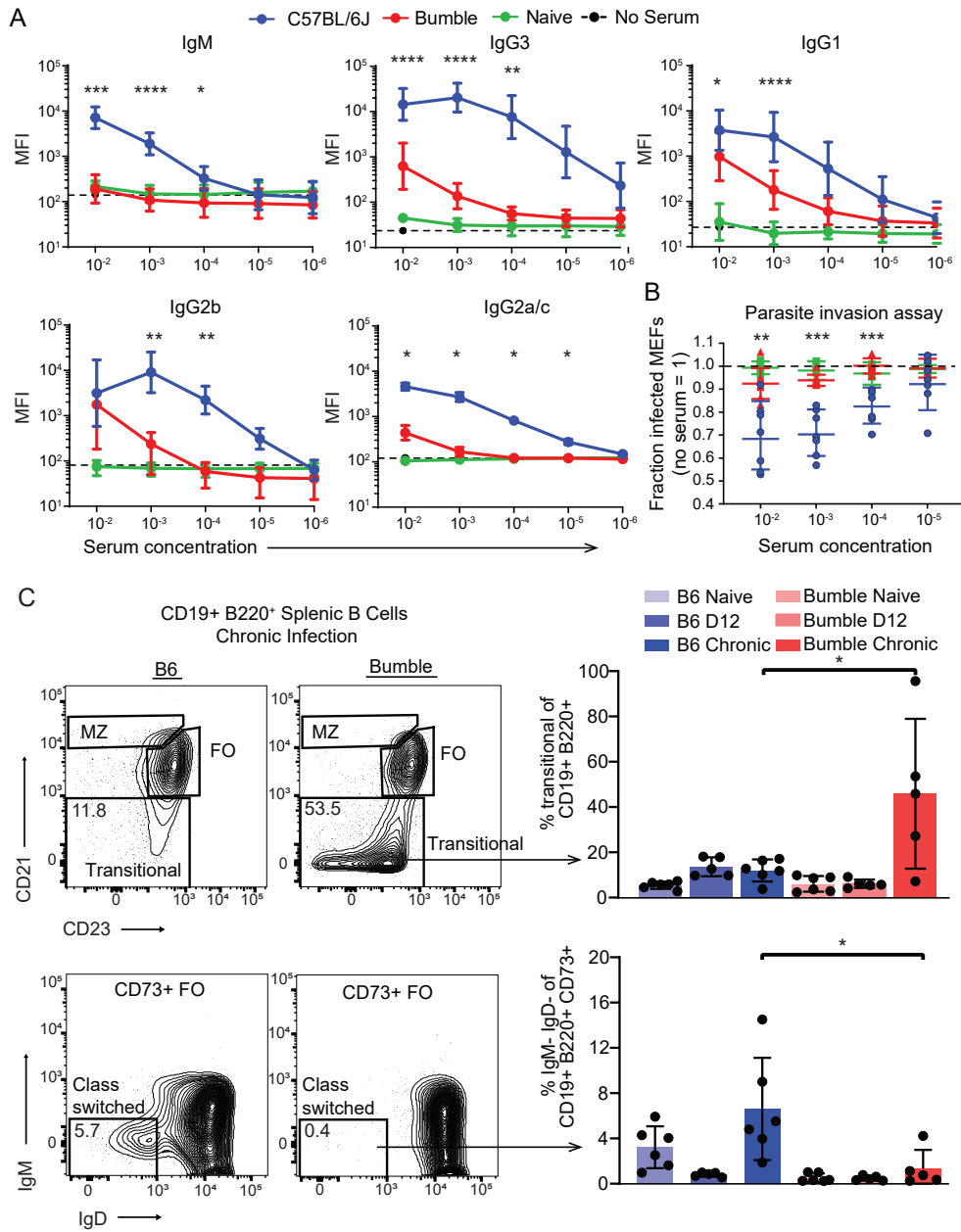


**Figure 3.5: *Nfkbid* is required for humoral responses to *T. gondii*.** A) Whole fixed GFP<sup>+</sup> parasites were incubated with serum from chronically infected mice, stained with fluorescently labeled anti-isotype antibodies and assessed by flow cytometry. Quantification of *T. gondii*-specific antibody isotype binding (IgM, IgG1, IgG2a/c, IgG2b, and IgG3) over

a range of serum concentrations is shown. Background staining in the absence of serum is indicated by the dotted line for each isotype. Plotted is the cumulative average  $\pm$ SD of the geometric mean fluorescence staining intensity (MFI) from 3 separate experiments (*bumble* n=8, C57BL/6J n=11). B) Neutralization of GFP+ parasites coated with serum over a range of concentrations from the indicated chronically infected mice. Parasites were incubated in serum for 20 minutes before infection of mouse embryonic fibroblasts and assessed by FACS 2h later. The fraction of infected host cells (GFP+ cells) is normalized to that of parasite infections without serum. Each dot represents the serum from an individual mouse and cumulative results from 3 separate experiments are shown (*bumble* n=8, C57BL/6J n=7, naïve n=6). For A and B, significance was assessed by unpaired t-tests with Holm-Sidak correction for multiple comparisons; \*\*\* P< 0.001, \*\* P<0.01, \* P<0.01. C) Representative FACS plots and the frequency of splenic transitional B-2 cells and IgM- IgD- conventional memory B cells at naïve, d12 of primary infection, and chronic infection in *bumble* and WT mice. Representative FACS plots of chronically infected *bumble* and B6 mice and scatter plot of the frequency of IgM- IgD- cells of the CD73+ conventional memory B population. Cumulative data from two experiments n=5-6 mice/condition. Each dot represents the results from an individual mouse, and plotted is the average  $\pm$ SD; \* P<0.05 by unpaired two-tailed t-test.

---

### 3.3.4 Defective B-1 and B-2 responses underlie *bumble*'s defect in immunity

The antibody defect observed in *bumble* mice is potentially explained by the observed B-2 maturation and activation defects, however the documented collapse of the B-1 cell compartment in *Nfkb1d*-deficient mice (Touma et al., 2011; Arnold et al., 2012) prompted us to investigate the possibility that the B-1 compartment plays a role in the anti-*T. gondii* antibody response and overall immunity. Previous studies have shown both varieties of B-1 cells (CD5+ B-1a and CD5- B-1b) can respond to infections and create antigen-specific antibodies (Alugupalli et al., 2004; Haas et al., 2005; Yang et al., 2012). To that end, we performed adoptive transfers of total peritoneal exudate cells (PerC) into neonatal *bumble* mice at day 2 of birth (Figure 3.6A), allowing for optimal B-1 cell engraftment (Baumgarth et al., 2000). Reconstitution of the B-1 compartment into *bumble* mice was assessed by IgM ELISA and FACS (Figure 3.9A, B). Mice that received total PerC were allowed to reach age 6-7 weeks then given primary infections with type III CEP and a secondary infection with type I RH strains (Figure 3.6A). Importantly, B-1 transfer into *bumble* mice significantly delayed time to death against type I RH secondary infection (Figure 3.6A). Though mouse serum from adoptively transferred *bumble* mice trended towards higher quantities of parasite-specific antibodies relative to non-transferred controls (Figure 3.6B), robust antibody production was not restored by B-1 transfer suggesting a limited role for the B-1 compartment in producing high-avidity antibodies against *T. gondii*. To further confirm which B cell compartment is producing high-avidity antibodies, IgH-allotype chimeric mice were generated (Figure 3.7A) (Lalor et al., 1989). In this experimental setup, endogenous B cells of the C57BL/6 background (IgH-b allotype) are depleted with allotype specific anti-IgM-b antibodies and replaced with transferred PerC of the IgH-a allotype which are refractory to the depletion antibodies and will engraft for the life of the animal. Following removal of the depleting antibodies, the endogenous B-2 cell population reemerge and are marked with anti-IgM-b antibodies, while the transferred B-1 cell are marked with anti-IgM-a antibodies. Thus we can distinguish which B cell compartment produces parasite-specific antibodies by identifying the allotype (B-1 as IgH-a or B-2 as IgH-b) (as described in detail in the legend to Figure 3.7A). Serology of chimeric mice at day 14 and day 30 of primary infection revealed low levels of B-1 (IgHa) parasite-specific IgM, however the majority of high-avidity antibodies were B-2 derived (Figure 3.7B).

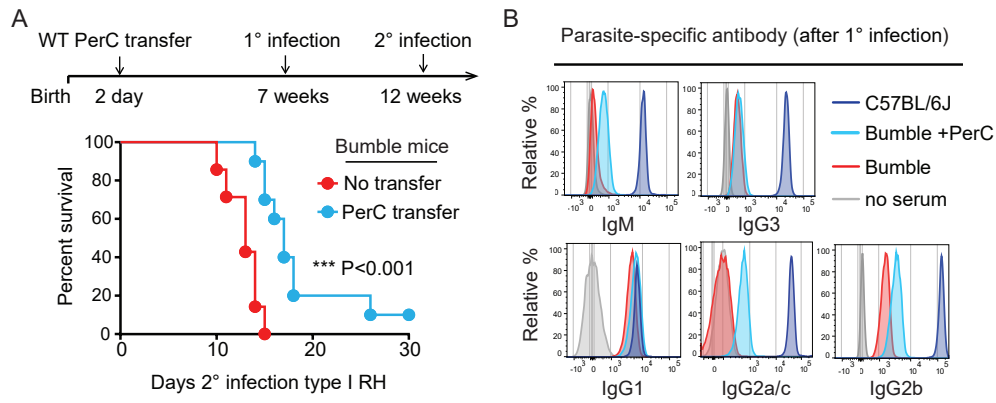


**Figure 3.6: PerC transfer into *Nfkbid*-null mice delays time to death.** A) Schematic of the secondary infection experiment using PerC reconstituted *bumble* mice. 2-4-day-old *bumble* neonates were transferred  $5 \times 10^6$  total PerC and allowed to rest for 7 weeks before primary infection with the type III CEP strain. 5 weeks post-primary infection, mice were given a secondary infection with the type I RH strain. Survival of *bumble* mice given total PerC transfers (n=10) relative to littermate controls (n=12). Cumulative survival is shown from 3 separate experiments; \*\*\* P < 0.001, Mantel-Cox test. B) Representative histograms of anti-isotype staining of parasites coated in serum ( $10^3$  dilution for IgG,  $10^2$  for IgM) from chronically infected *bumble*, *bumble* given PerC transfer, and WT mice. Background staining in the absence of serum is indicated.

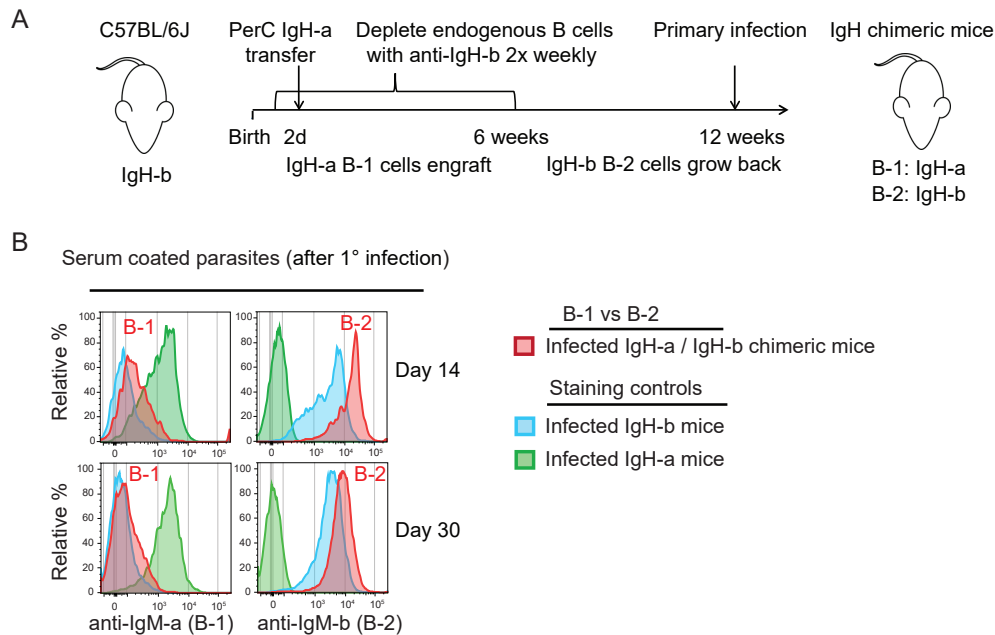


**Figure 3.7: High avidity *T. gondii*-specific antibodies are B-2 derived.** A) Schematic of neonatal allotype chimera generation. C57BL/6J neonates were given anti-IgH-b to deplete endogenous B cells at day 1 post birth and twice weekly after for 6 weeks, thereby depleting the endogenous B-1 pool for the life of the animal due to their restricted fetal/neonatal window of development. Neonates were given  $5 \times 10^6$  total PerC from 6-8-week-old IgH-a congenic C57BL/6 mice donors. These mice then rested for 6 weeks after the last depletion treatment to allow reemergence of the endogenous B-2 IgH-b cells. B) Representative histograms of serum derived anti-IgM-a (B-1 derived) or anti-IgM-b (B-2 derived) staining profiles of type I RH GFP+ parasites taken from the IgH allotype chimeras on day 14 and 30 following primary type III CEP infection. Staining controls with serum from chronically infected C57BL/6J IgH-b littermates, or IgH-a mice are shown.

To decipher the individual contributions of the B-1 and B-2 compartments to survival against *T. gondii*, we attempted adoptive transfers of B-1 and B-2 cells into B cell deficient mice,  $\mu$ MT. However, even though effective B cell reconstitution was observed by IgM ELISA and FACS (Figure 3.8A, D, E),  $\mu$ MT mice were found to be highly susceptible to the low virulence type III CEP strain irrespective of transfer condition (Figure 3.8C). And though this may potentially highlight the importance of B cell responses, other studies have found significant T cell dysfunction within  $\mu$ MT mice (Moulin et al., 2000; Homann et al., 1998; Baumgarth et al., 2000) possibly due to the significant role that B cells have in shaping secondary lymphoid

tissues (Tumanov et al., 2002). Further attempts to unravel the contribution of the individual B-1 and B-2 compartments were performed with a variety of mixed bone marrow (BM) chimera strategies. BM chimeras were generated by lethally irradiating mice and giving bone marrow  $\pm$ PerC as previously described (Kroese et al., 1989; Choi & Baumgarth, 2008). Because B-1 cells do not readily reconstitute from adult HSCs (Kantor et al., 1992), PerC was given to reconstitute the B-1 compartment. However, similar to the  $\mu$ MT adoptive transfer experiments, all irradiated mice given type III CEP primary infections succumbed, irrespective of transfer conditions (Figure 3.9A, B). To mitigate the susceptibility of BM chimeras to live infections, an *in vitro* replication-deficient uracil auxotroph strain (RH  $\Delta up \Delta ompdc$ ) was used to vaccinate the mice (Fox & Bzik, 2010). Though this strategy improved overall survival, mice that received *bumble* BM cells were susceptible to the replication-deficient strain (Figure 3.9C). This was an intriguing result that hints at alternative mechanisms of uracil synthesis or scavenging utilized *in vivo* by this otherwise uracil auxotroph strain. We did not investigate this phenotype further, but the result highlights safety issues using replication deficient pathogens as vaccines in immune compromised individuals (Kew et al., 2004). Mice that survived the replication-deficient strain were challenged with type I RH strain and surprisingly, only *Nfkbid*-sufficient recipients that received WT BM and PerC were fully protected against type I RH challenge (Figure 3.10). From this experiment we made two observations: (1) even though the majority of high avidity anti-*T. gondii* antibodies are B-2 derived as shown in Figure 3.7B, B-1 cells contribute to immunity to *T. gondii* as BM chimeras that received WT BM but not PerC were unable to achieve full protection against challenge, and (2) *Nfkbid* potentially plays a role in non-hematopoietic and/or radio-resistant cells to promote protective immunity, as *bumble* recipients that received WT BM and PerC were still partially susceptible to challenge.

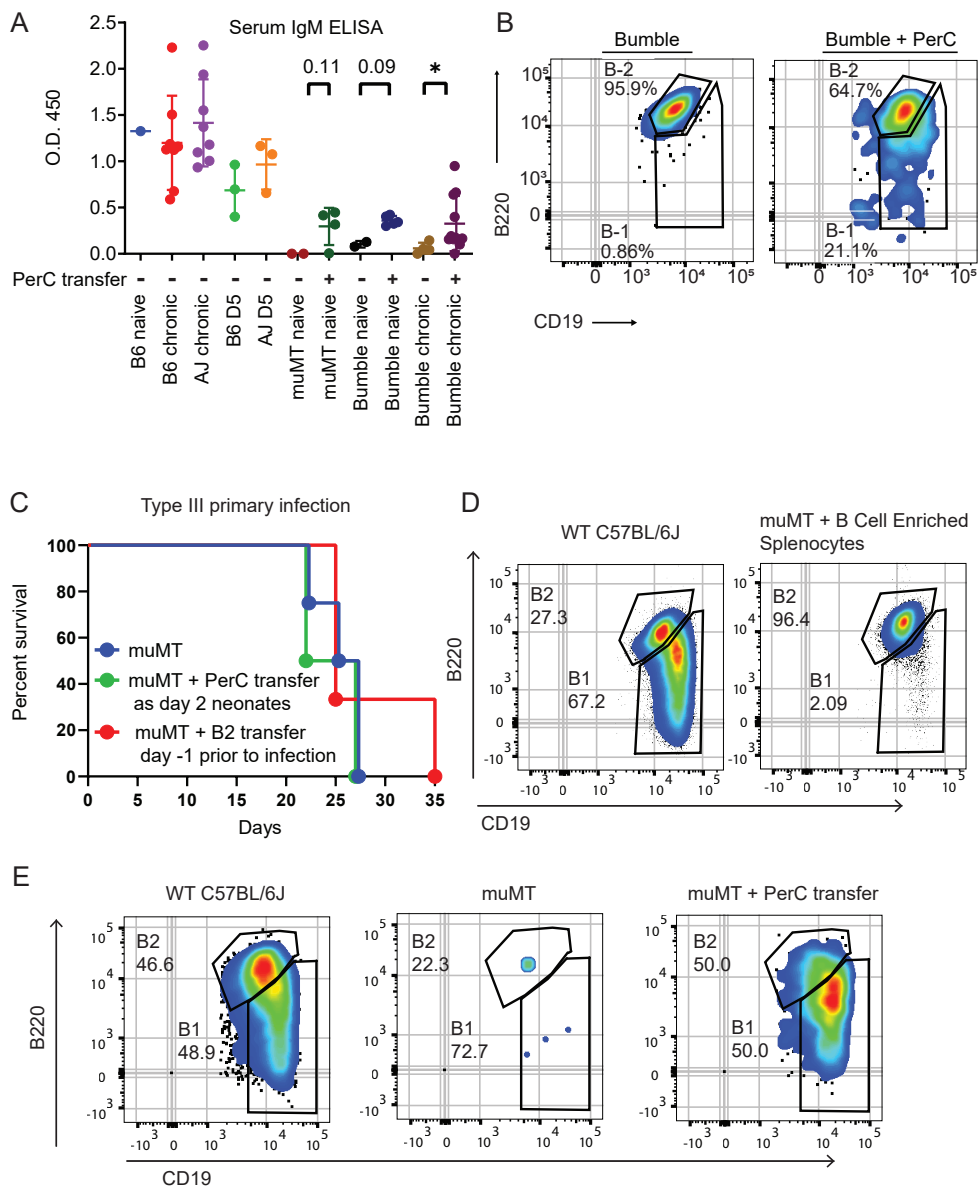


**Figure 3.8: Validating PerC reconstitution by serum IgM ELISAs and flow cytometry, and survival of  $\mu$ MT mice.** A) Serum IgM from C57BL/6J,  $\mu$ MT, *bumble*, and *A/J* mice was measured by ELISA. Serum was harvested from mice either naïve, chronically infected with the type III CEP strain, or on D5 post-secondary infection with the type I GT1

*T. gondii* strain. PerC transfer (+) refers to mice adoptively transferred  $5 \times 10^6$  total PerC cells as a day 2 neonate. Each dot represents the results from an individual mouse, and plotted is the average  $\pm$ SD of the O.D. obtained at 450nm; \*  $P < 0.05$ , unpaired two-tailed t-test. B) *Bumble* reconstitution of the peritoneal B-1 compartment after neonatal PerC adoptive transfer. Representative FACS plots of peritoneal B-2 cells (B220<sup>high</sup> CD19+) and B-1 (B220<sup>int</sup> CD19+) cells from *bumble* mice with or without PerC adoptive transfer. Shown are mice on day 20 of primary infection with the type III CEP strain. C) B cell deficient  $\mu$ MT mice (n=3),  $\mu$ MT given WT PerC adoptive transfers as 2-day neonates then allowed to reconstitute for 6-7 weeks into adulthood (n=2), and  $\mu$ MT given B cell enriched splenocytes (n=3) 1 day prior to infection with the type III CEP strain were assessed for survival. D)  $\mu$ MT reconstitution of B-2 cell compartment, WT and  $\mu$ MT with B cell enriched splenocytes (EasySep™ Mouse Pan-B Cell Isolation Kit, cat# 19844) adoptively transferred 24 hrs earlier. E)  $\mu$ MT reconstitution of peritoneal B cell compartment after neonatal adoptive transfer. Representative FACS plots of peritoneal B-2 cells (B220<sup>high</sup> CD19+) and B-1 B cells (B220<sup>int</sup> CD19+) from WT, and  $\mu$ MT mice or  $\mu$ MT mice with neonatal PerC adoptive transfer. For D and E, uninfected mice are 6-8 weeks of age and numbers indicate the percent of cells that fall within the depicted gate.

---

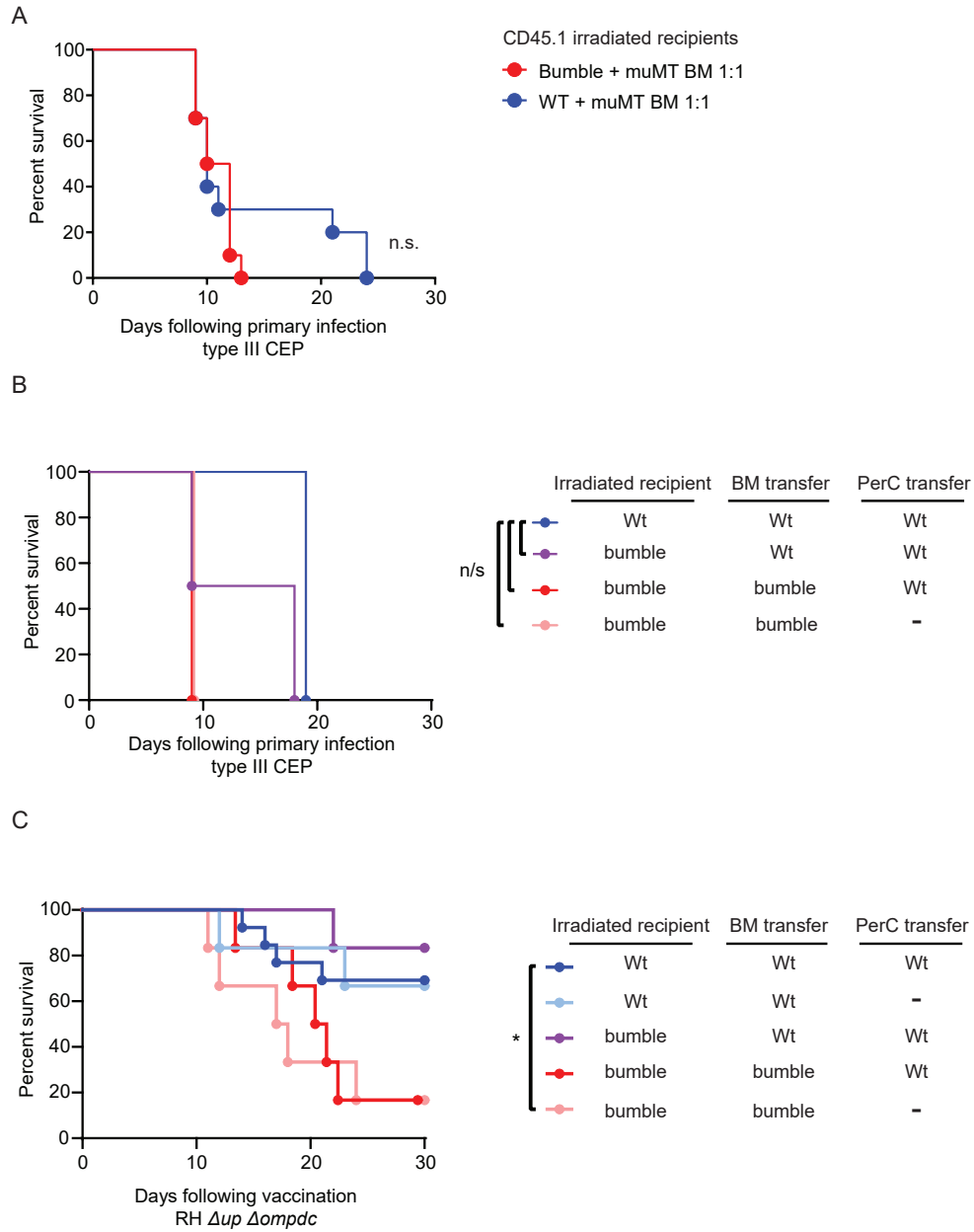


**Figure 3.9: Susceptibility of irradiated mice to type III primary infections and vaccination.** A) Survival of 45.1 BM chimeras given 1:1 mixtures of  $\mu mt$  + WT or  $\mu mt$  + *bumble* bone marrow. Results are cumulative from 2 experiments (n=10 per condition). B) Survival of the indicated bone marrow (BM) chimeras infected with the type III CEP *T.*

*gondii* strain are plotted from a single experiment (n=2 for *bumble* recipients per condition; n=1 for C57BL/6J recipients); n.s., Mantel-Cox. C) Survival of the indicated BM chimeras vaccinated (10<sup>6</sup> i.p.) with the replication deficient type I strain, RH  $\Delta up \Delta ompdc$ . Results are cumulative from 2-3 separate experiments (n=4-9 mice per condition).

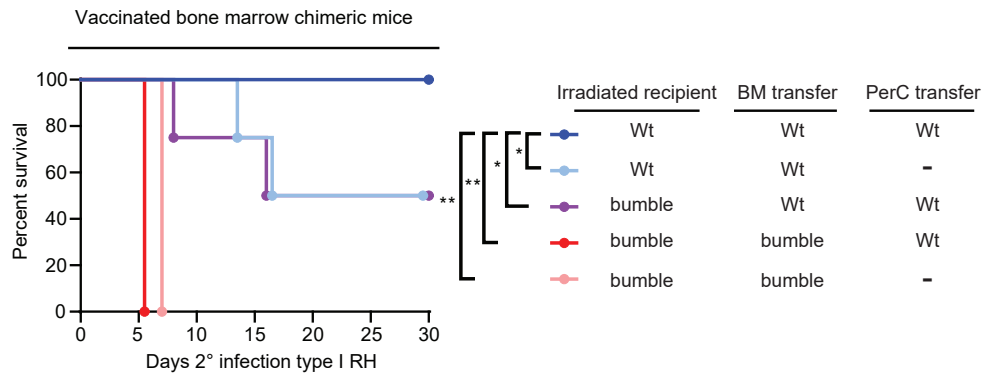


**Figure 3.10: Bone marrow chimeras reveal B-1 cells are required for complete immunity after vaccination.** Irradiated *bumble* and WT recipients (45.1 or 45.2) were given WT or *bumble* bone marrow (BM) with or without total WT PerC (45.2). Mice were vaccinated with type I strain (RH  $\Delta up \Delta ompdc$ ) and 30d later challenged with type I RH. Cumulative survival is shown from 2-3 experiments (n=4-9 mice per condition); \* P<0.05 by Mantel-Cox test.

### 3.3.5 Evidence for enhanced B-1 and B-2 cell activation in resistant A/J mice

*Nfkbid* has a profound effect on maturation and activation of multiple B cell populations within the C57BL/6J background, and thus we hypothesized that resistant A/J mice, with their polymorphic *Nfkbid* allele, may have enhanced B cell activation and a greater humoral response. To investigate this possibility, we tested serum from A/J and C57BL/6J mice at chronic and day 5 of secondary infection time points. Western blot analysis of antibody reactivity against *T. gondii* lysate found that A/J have greater quantities of parasite-specific IgG relative to C57BL/6J (Figure 3.11A). FACS analysis of splenic B cell populations at multiple time points revealed that A/J and C67BL/6J mice have similar frequencies of CD73+ memory and CD73+ FCRL5+ CD80+ memory B cells (not shown). Of note, within those memory populations A/J mice exhibited greater frequencies of class-switched (IgM- and IgD-) cells at chronic and day 5 of secondary infection (Figure 3.11B),

indicative of a robust B cell response within the resistant background.

Enhanced B cell responses were also observed within the B-1 compartment of A/J mice. Within the peritoneal B-1 compartment (CD19<sup>+</sup> B220<sup>int</sup> CD11b<sup>+</sup>) A/J mice showed an increase in the ratio of CD5<sup>-</sup> B-1b cells to CD5<sup>+</sup> B-1a cells during secondary infection (Figure 3.12A, B), suggesting expansion of the B-1b population possibly due to down-regulation of CD5 in response to infection (Savage et al., 2019). In addition to the increased frequency, the B-1b cells also were found to be IgM<sup>low</sup>, indicative of down-regulation of the BCR as well as potential evidence of class-switch recombination within the B-1 compartment (Figure 3.12B). Because B-1 cells are known to migrate to secondary lymphoid tissues to produce antibodies (Waffarn et al., 2015; Ha et al., 2006; Yang et al., 2007), we investigated the splenic B-1 compartment for markers of enhanced activation. Within the splenic B-1 compartment (CD19<sup>+</sup> B220<sup>int</sup> CD43<sup>+</sup>) of A/J mice, a similar trend of increased B-1b to B-1a ratios were observed during secondary infection (Figure 3.12C). Because *Nfkbid* is known to regulate activation markers BAFFR and TACI, and the plasmablast differentiation marker CD138 (Khoenkhoen et al., 2019), we looked for differential expression of these markers on B-1 cells both in the spleen and PerC. CD138 was found to be highly expressed on A/J B-1 cells within the spleen but not the peritoneal cavity, indicating robust differentiation into antibody secreting cells upon entry into the spleen (Figure 3.12C, D). The activation markers BAFFR and TACI were found to decrease during *T. gondii* infection within C57BL/6J mice, but remained high in A/J mice suggesting sustained activation potential within these B cell populations. In addition, A/J B-1 cells bore evidence for enhanced class-switch recombination potential in both the splenic and peritoneal compartments as larger proportions of IgM-IgD<sup>-</sup> cells were observed in A/J compared to C57BL/6J mice, providing further evidence of engagement of this cell population.

Beyond the observed increased humoral response, A/J peritoneal T cell production of IFN $\gamma$  was greater than C57BL/6J after *in vitro* recall (Figure 3.13A), indicative of a robust cellular response at the site of infection, but not reaching significance within the spleen. Altogether, this data shows A/J B cells have greater expression of activation and differentiation markers as well as overall activation within the B-1 cell population, phenotypes previously described as *Nfkbid*-dependent. The enhanced humoral response, driven by these potentially *Nfkbid*-dependent phenotypes, is also layered by enhanced cell-mediated responses in the resistant mice.

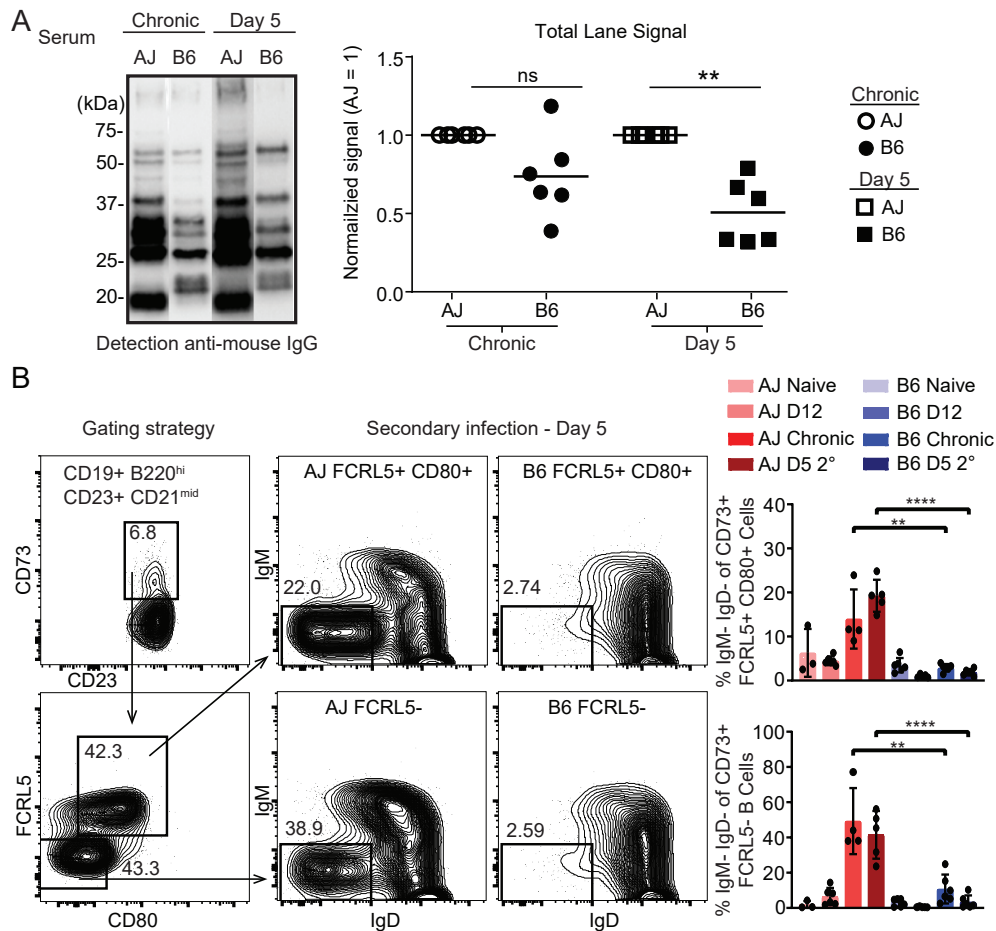


**Figure 3.11: Immunity in A/J mice correlates with enhanced class-switching in memory B-2 cells and increased serum reactivity to parasite lysate antigen.** A) Serum obtained from A/J and C57BL/6J mice chronically infected (CEP) or at D5 of secondary infection (GT1) were used to probe GT1 parasite lysate antigen separated by SDS-PAGE; western blots were detected with anti-mouse IgG. “Total Lane Signal” is the signal obtained from the entire lane of C57BL/6J compared to that of A/J (=1); western blots were developed in tandem and analyzed by Image Lab. Results are from 6 individual experiments; \*\* P < 0.01, \* P < 0.05; unpaired two-tailed t-tests. B) Gating strategies for identifying memory B cells. Memory B cells are identified as CD19+ B220+ CD23+ CD21<sup>mid</sup> CD73+. Conventional memory B cells are FCRL5- CD80- while atypical memory B cells are identified as FCRL5+, CD80+. Representative FACS plots of memory compartments in A/J and C57BL/6J mice on day 5 of secondary infection with the type I GT1 strain are shown. The frequency of class-switched (IgM- IgD-) memory cells at the indicated infection states were analyzed. Each dot represents the results from an individual

mouse and the cumulative averages  $\pm$ SD from 2 experiments are plotted. N=3-6 mice per infection state. Significance was assessed with an unpaired two-tailed t-test; \*\*\* P<0.0001, \*\* P<0.01. Data from (A) generated by Jessica Wilson.

---

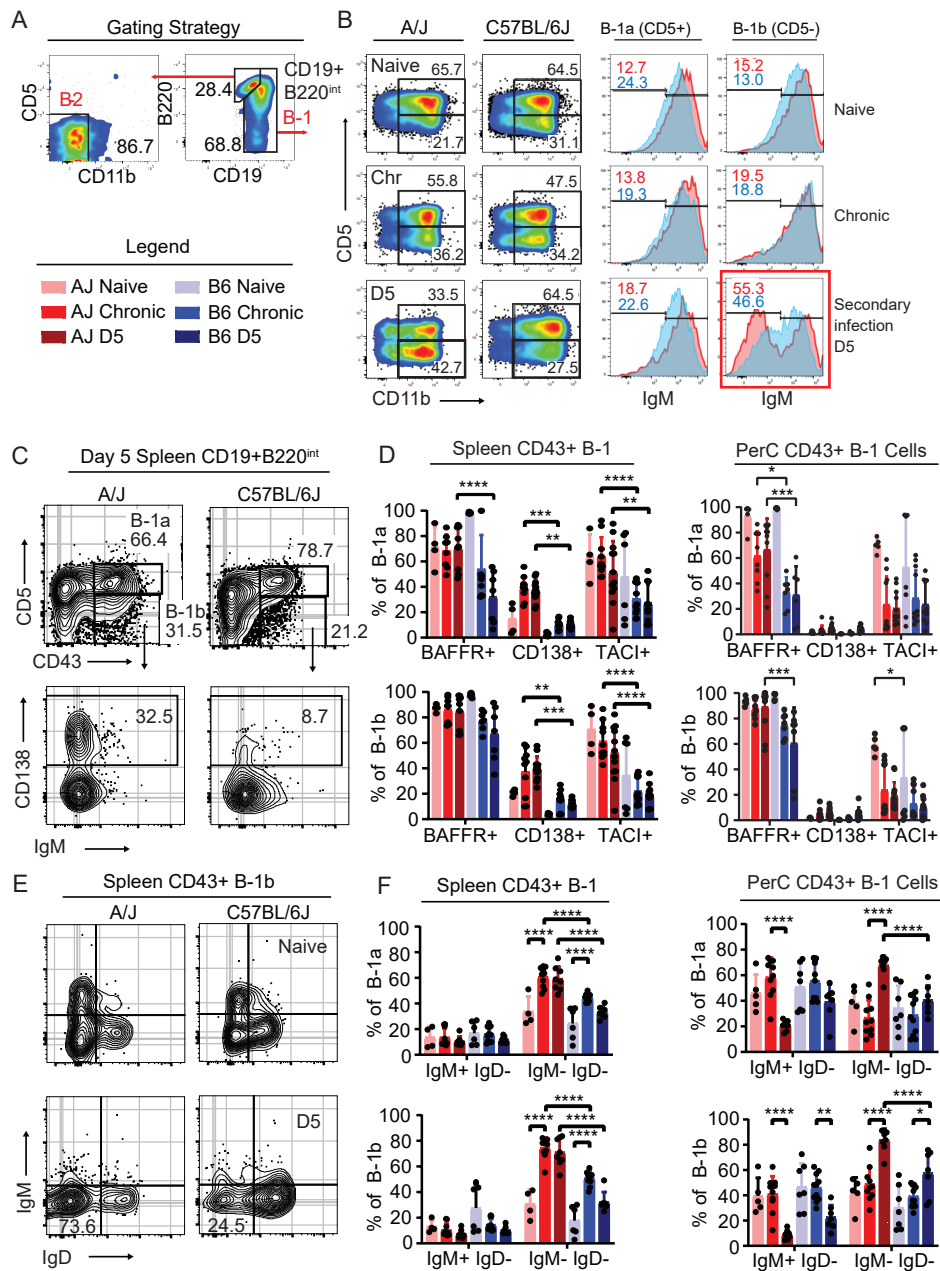


**Figure 3.12: Evidence for enhanced B-1 cell activation in resistant A/J mice.** A) Gating strategies for identifying B-1 (CD19+ B220<sup>int</sup>) and B-2 (CD19+ B220<sup>hi</sup>) B cells. The legend applies to panels D and F. B) Representative FACS plots of the CD11b+ peritoneal B-1 B cell compartment in A/J and C57BL/6J (B6) mice at naïve, chronic (Chr), and 5 days

(D5) post-secondary infection with the GT1 strain. Numbers indicate the percent of cells that fall within the indicated gate. Representative histograms of IgM surface expression and percent of cells that fall within the IgM<sup>low</sup> gate of CD5+ B-1a and CD5- B-1b cells from A/J (red) and C57BL/6J (blue) at the indicated time points. C) Representative FACS plots of splenic CD19+ B220<sup>int</sup> B cells stained for CD43 and CD5 in A/J and C57BL/6J mice at D5 of secondary infection. Representative CD138 expression on CD5- CD43+ B-1b cells. D) Frequencies of CD43+ splenic and peritoneal B-1a and B-1b cells from A/J and C57BL/6J mice that express BAFFR+, TACI+, or CD138+ at the indicated infection states. E) Representative IgM and IgD expression of CD5- CD43+ B-1b cells at naive and Day 5 secondary infection. F) Frequencies of splenic CD43+ B-1a (CD5+) or B-1b (CD5-) that are IgM+IgD- or IgM-IgD- in A/J and C57BL/6J mice at the indicated infection states. For D and F, the cumulative average  $\pm$ SD from 2-4 experiments is plotted and each dot represents the result from an individual mouse; P values calculated by 2-way ANOVA with Tukey correction; \*\*\*\* P<0.0001, \*\*\* P<0.001, \*\* P<0.01, \* P<0.05. Data from (A) and (B) were generated by Sam Splitt.

---

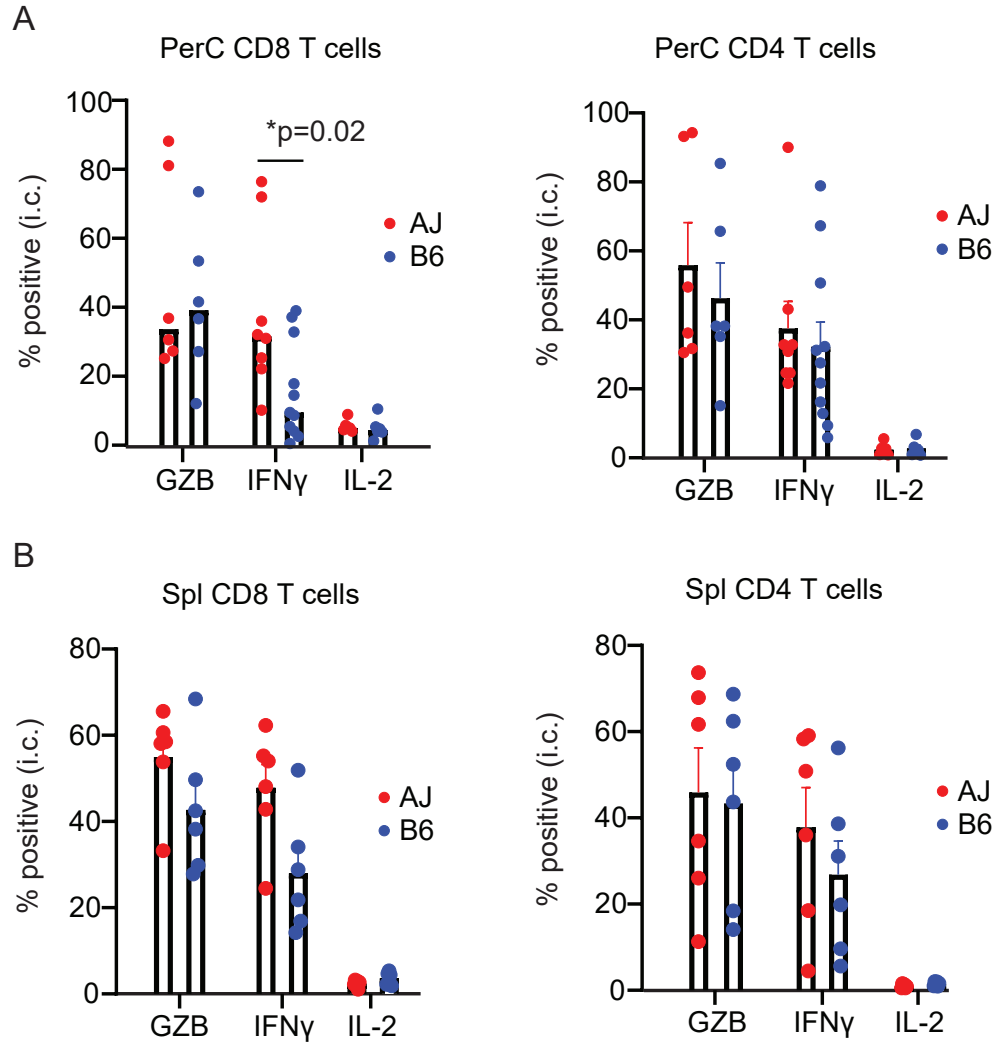


**Figure 3.13: CD8 T cell IFN $\gamma$  frequencies are increased in resistant A/J mice.** A) Peritoneal and B) splenic cells were harvested from A/J and C57BL6/J mice chronically infected with type III CEP *T. gondii* strain, and infected with live type I parasites for 16 hrs. T cells were assessed for production of granzyme B (GZB), IFN $\gamma$ , and IL-2 by intracellular staining and FACS. The average frequency  $\pm$ SD of positive staining CD4+ or CD8+ T cells (CD3+ CD19-) and cumulative results from 2-3 experiments (AJ n=8, C57BL6/J n=11) are shown; \* P<0.05, unpaired two-tailed t-test.

### 3.3.6 B-1 cells in resistant A/J mice have enhanced germline transcription of *Ighg* constant regions, class-switch recombination and different activation profiles

The diminished antibody responses within *bumble* mice combined with the B cell phenotypic differences observed in A/J mice prompted us to investigate how *Nfkbid* may be regulating the B cell compartment of both A/J and C57BL/6J B cells. A transcriptomic approach was taken to define gene expression profiles in peritoneal B-1a, B-1b, and B-2 cells throughout the course of a *T. gondii* infection and secondary infection (Dataset found here: (Souza et al., 2020) and NCBI SRA Bioproject PRJNA637442). Consistent with the conversion to IgM<sup>low</sup> previously observed, germline transcription of *Ighg1*, *Ighg2a/c*, *Ighg2b*, and *Ighg3* was greatly enhanced within A/J's CD5- B-1b cells during secondary infection (Figure 3.14A). This finding prompted us to look for intra-cellular IgG heavy and light chain (H+L) within the B-1 compartment to find direct evidence of class-switch recombination in the B-1 compartment. Consistent with our previous experiments, during secondary infection a large portion of B-1 cells become IgM- in the A/J background, however robust expression of class-switched IgG(H+L) was only observed within the spleen (Figure 3.14B), similar to the observed B-1 migration and antibody production in the spleen after LPS stimulation (Ha et al., 2006; Yang et al., 2007) infection. Moreover, the IgG isotype class-switch recombination was greatly enhanced within A/J in both the CD5+ B-1a and CD5- B-1b populations, indicating the engagement of this cell type within the resistant background (Figure 3.14C).

Pathway and GO term analysis focused on genes uniquely induced during secondary infection within A/J B-1b cells found evidence of overall enhanced activation, as expected given acute reinfection (Figure 3.15A). GO terms that were enriched in the resistant genetic background suggests this activation appeared to be induced by type I and II interferon signaling. Within the A/J B-1b transcriptomic profile we found TLR-signaling, complement activation and somatic recombination pathways were significantly enhanced, as well as gene expression of *Tbx21* (T-bet) which has been shown to increase antibody affinity maturation in malaria infections (Ly et al., 2019; Obeng-Adjei et al., 2017) and differentiation into antibody-secreting cells (Stone et al., 2019). Comparing genes with over fourfold upregulation in A/J B-1b cells compared to C57BL/6J B-1b cells during secondary infection found several interesting genes: *Scimp*, an adapter protein for TLR4 signaling (Luo et al., 2017); *Semaphorin7* (Suzuki et al., 2007), an inducer of inflammatory cytokines, alarmins *S100a8* and *S100a9*, as well as genes asso-

ciated with tissue tolerance *Retnlg* and *Slpi* (Figure 3.15B). Gene set enrichment analysis (GSEA) of transcriptional variation between A/J and C57BL/6J B-1b cells during secondary infection found correlation with gene sets distinguishing B cells stimulated with different TLR adjuvants (GSE25677: Sorted B cells from mice treated with MPL and/or R837), MPL which triggers TLR2 and R848 which triggers TLR7/8 (Figure 3.15C). Altogether, this data shows robust activation and class-switching occurs within the B-1 compartment of resistant A/J, compared to C57BL/6J mice, and that this is potentially driven by *Nfkbid*-modulated TLR signaling (Kuwata et al., 2006).

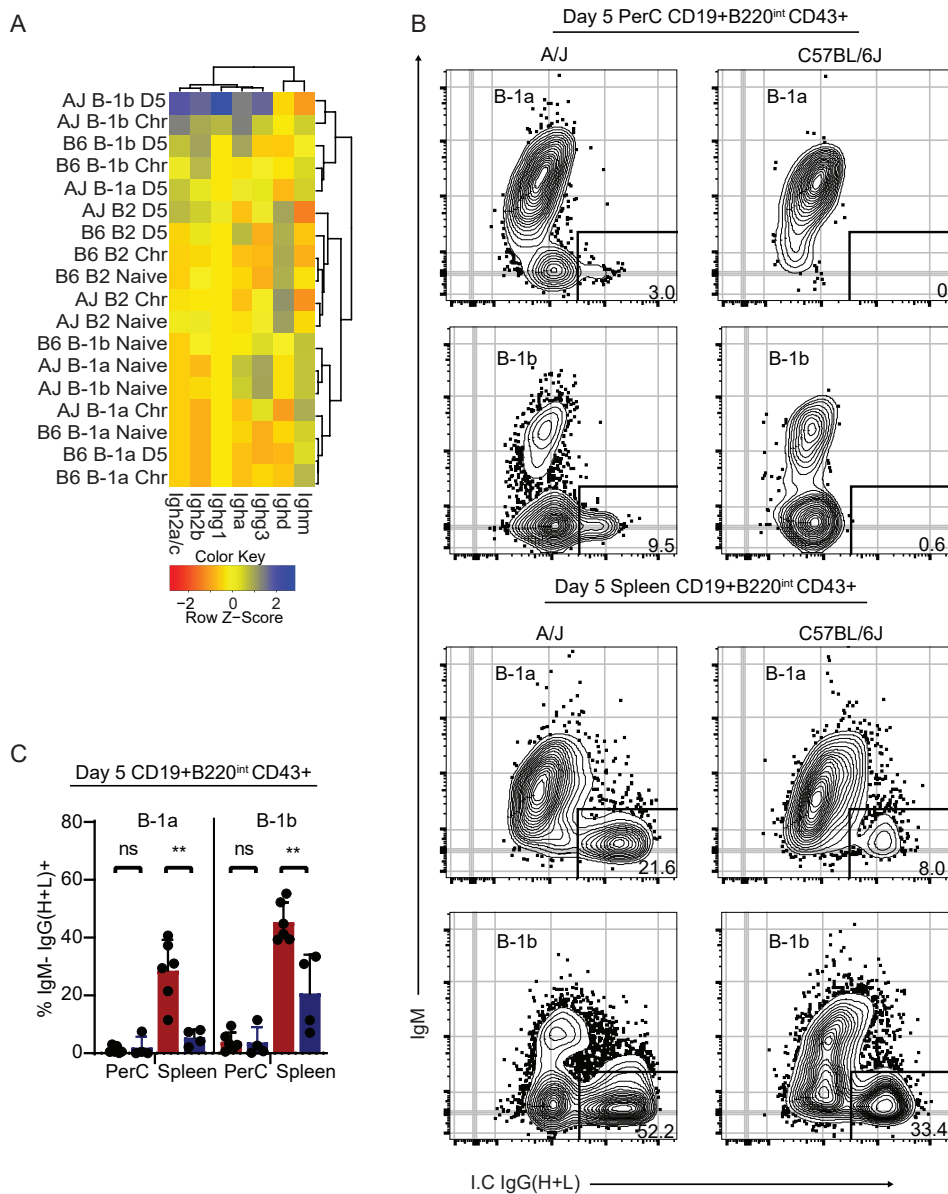


**Figure 3.14: B-1 cells express *Ighg* transcripts in the peritoneal cavity but only express IgG antibody protein in the spleen during *T. gondii* infection.** A) Heatmap depicting the relative expression of all *Ighg* transcripts from the indicated B cell population, mouse strain and infection state. B) Representative FACS plots of intracellular IgG (H+L) of both

peritoneal and splenic CD43<sup>+</sup> B220<sup>mid-lo</sup> CD19<sup>+</sup> (CD5<sup>+</sup>) B-1a and (CD5<sup>-</sup>) B-1b cells. C)  
Frequency of peritoneal and splenic B-1a and B-1b cells of A/J and C57BL/6J mice at day  
5 of secondary infection. P values calculated by unpaired t-tests; \*\* P<0.01.

---

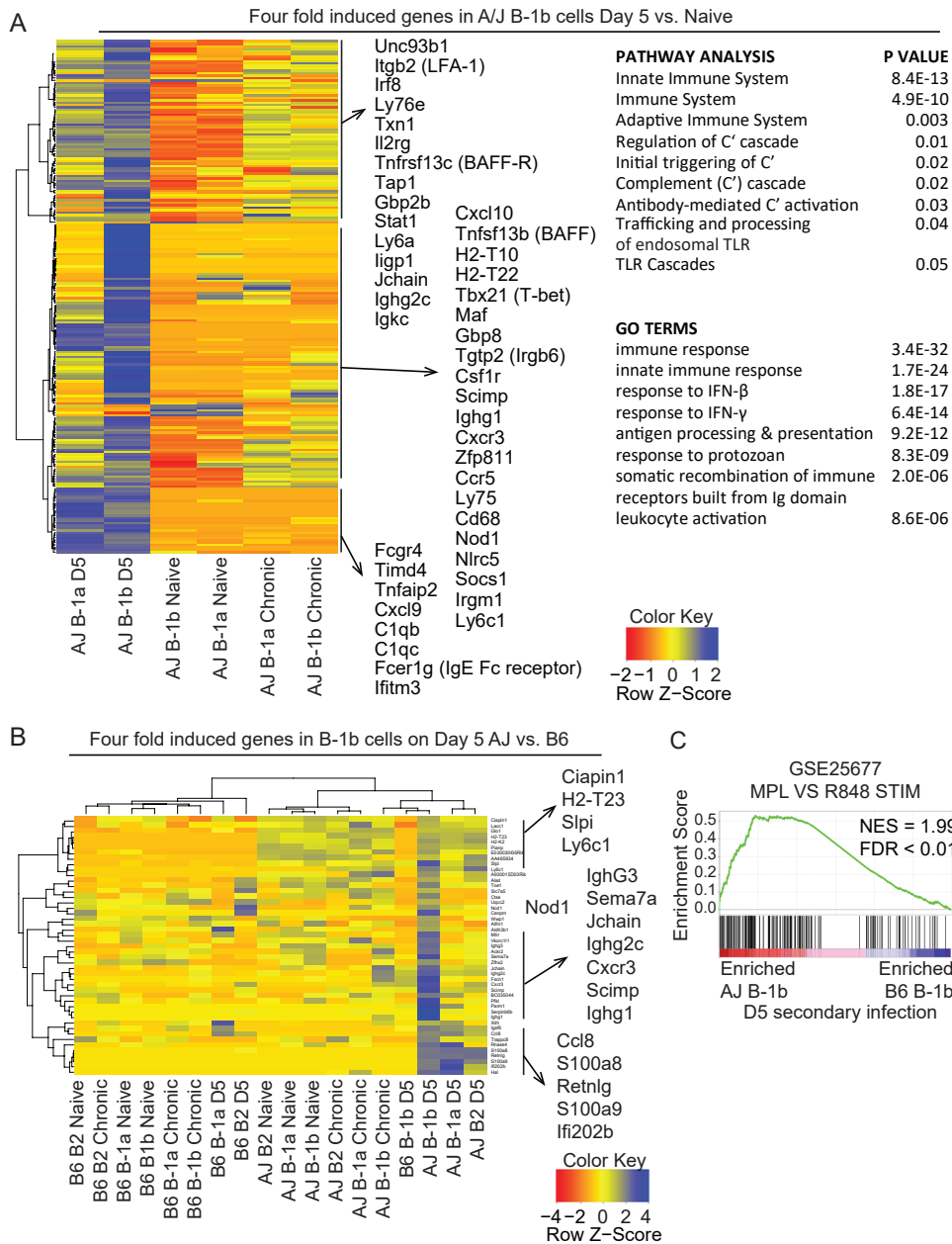


**Figure 3.15: Genes uniquely induced in B-1b cells on day 5 of secondary infection in resistant A/J mice.** Transcriptomic analysis of peritoneal B-1a (CD19<sup>+</sup> B220<sup>int</sup> CD11b<sup>+</sup> CD5<sup>+</sup>), B-1b (CD19<sup>+</sup> B220<sup>int</sup> CD11b<sup>+</sup> CD5<sup>-</sup>) and B-2 (CD19<sup>+</sup> B220<sup>hi</sup> CD11b<sup>-</sup> CD5<sup>-</sup>) B cells from A/J and C57BL/6J mice was performed using 3'-Tag RNA sequencing. A) Genes

that were differentially upregulated in B-1b cells on day 5 of secondary infection compared to naïve mice in the A/J genetic background. P values of differentially expressed genes were calculated using the Benjamini-Hochberg adjustment for false discovery rate, and only those genes that survived significance were included in the heatmap. For comparison, all B-1 compartments in A/J mice are shown for this gene set. A/J B-1 Pathway and GO term enrichment were assessed on the genes presented in the heatmap in A. P values for enrichment analysis were adjusted with the Holm-Bonferroni correction. B) A cluster of genes found to be differentially induced in B-1b cells in A/J compared to C57BL/6J mice on day 5 of secondary infection are plotted as a heat map. C) Gene set enrichment analysis of the rank-ordered list of differentially expressed genes between A/J and C57BL/6J B-1b cells at D5 of secondary infection. Gene set depicted was in the top 10 gene sets ranked by false discovery rate (FDR) within MSigDB C7: immunologic signatures collection. Enrichment score is the degree of overrepresentation of a gene set at the top or bottom of a ranked list. NES is the enrichment score after normalizing for gene set size.

---

### **3.3.7 Gene dosage of *Nfkbid* impacts parasite-specific IgG1 and plasmablast differentiation**

A/J's *Nfkbid* polymorphisms are largely found within non-coding regions of the mRNA (Table 3.1). This led us to hypothesize that the B cell differences observed in our system could be due to differences in *Nfkbid* transcript expression. To investigate this possibility, we quantified *Nfkbid* expression within our transcriptomic dataset and verified it by qPCR. Overall, B cells from C57BL/6J mice had greater expression levels of *Nfkbid* relative to A/J, particularly at the chronic infection timepoint (Figure 3.16A). To rule out the effect of parasite burden on *Nfkbid* transcript expression, as the susceptible C57BL/6J B-1 cells could have greater stimulation from the increased parasite load, we stimulated peritoneal and splenic B cells from A/J and C57BL/6J mice with LPS and quantified *Nfkbid* expression. B cells from C57BL/6J on average had 1.5-2 fold greater induction of *Nfkbid*, though this only reached significance within splenic B cells (Figure 3.16B). This led us to hypothesize that A/J *Nfkbid* polymorphisms are destabilizing the mRNA transcripts. *Nfkbid* in mice is unique as it is the only described gene that produces mRNA with two distinct constitutive decay element (CDE) stem-loop motifs through which it is tightly bound by the RNA-degradation factor Roquin (Leppek et al., 2013). Therefore, we used 2D RNA structure modeling (Reuter & Mathews, 2010) to compare the ability of A/J and C57BL/6J *Nfkbid* transcripts to form the CDE stem-loop motif. We found an A/J polymorphism that abrogates the P1-L1 loop shortening the first of the tandem CDE stem-loops (Figure 3.16C). Disruption of

these stem-loop motifs has been previously shown to modulate TNF mRNA decay through differential binding to Roquin (Leppek et al., 2013; Codutti et al., 2015), which potentially explains the *Nfkbid* transcript expression differences between the resistant and susceptible genetic backgrounds.

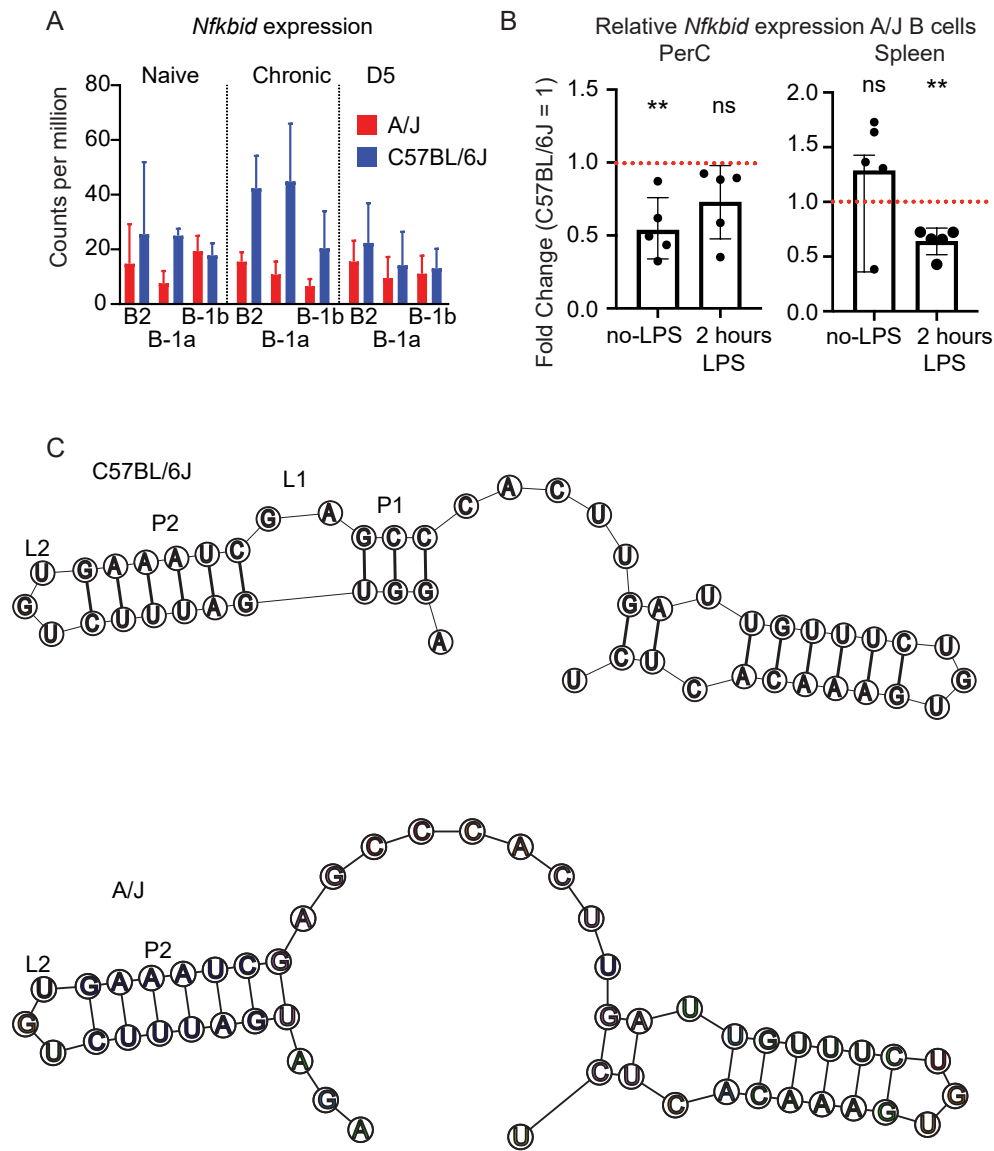


**Figure 3.16: Resistance to *T. gondii* is correlated with reduced mRNA transcript levels of *Nfkbid*.** A) *Nfkbid* expression in CPM (Counts per million) of 3'-Tag RNA-seq reads of the indicated B cell populations obtained from A/J and C57BL/6J mice that were either naïve, chronically infected, or on D5 of secondary infection with the type I GT1 strain. B) Enriched B cells from the PerC and spleen were stimulated with LPS for 2 hrs and *Nfkbid* transcripts were quantified by qPCR. Plotted is the fold change of A/J *Nfkbid* transcripts

levels relative to C57BL/6J expression in the same condition. P values were calculated with a paired t-test, \*\* P < 0.01. C) RNA structures of *Nfkbid* 3' UTR CDE-stem loops from C57BL/6J (top) and A/J (bottom). qPCR data from (B) generated by Julia Alvarez.

---

Because *Nfkbid* transcript levels in A/J B cells are about half that of C57BL/6J's, possibly due to the disrupted CDE stem-loop motif, we investigated *bumble* F1 back cross (*Nfkbid*<sup>+/-</sup>) to find phenotypes associated with reduced *Nfkbid* expression. To that end, we analyzed serum from chronically infected A/J, C57BL/6J and *Nfkbid*<sup>+/-</sup> mice for parasite-specific antibody isotypes. IgM and IgG3, the major known B-1 antibody isotypes, were not observed to be different between mouse strains. However, parasite-specific IgG1 was significantly enhanced in resistant A/J and *Nfkbid*<sup>+/-</sup> mice compared to C57BL/6J, consistent with previous reports of *Nfkbid* controlling IgG1 class-switching (Hosokawa et al., 2017). Of note, parasite-specific IgG2b was significantly enhanced in C57BL/6J and *Nfkbid*<sup>+/-</sup> compared to A/J but this does not appear to be an *Nfkbid*-controlled isotype as IgG2b does not differ within the C57BL/6J background. Phenotypic analysis of splenocytes during secondary infection found a significant increase in CD138<sup>+</sup> plasmablasts in *Nfkbid*<sup>+/-</sup> relative to the C57BL/6J background (Figure 3.17C, D), consistent with previous studies demonstrating that *Nfkbid* modulates plasmablast differentiation (Khoenkhoen et al., 2019). No other major B cell phenotype difference was observed when looking at proportions of marginal zone (MZ) (CD21<sup>high</sup>), germinal center (GL7<sup>+</sup>), CD73<sup>+</sup> memory, CD80<sup>+</sup> FCRL5<sup>+</sup> "atypical" memory, or B-1 and B-2 class-switching (IgM- IgD-) (Figure 3.17E). Finally, the increased IgG1 class-switching and plasmablast differentiation did not confer a survival advantage against type I GT1 secondary infection, as *Nfkbid*<sup>+/-</sup> were found to have a similar death kinetic as C57BL/6J (Figure 3.18). Though this may have been expected given the low phenotypic penetrance calculated for the Chr7 QTL within our screen, the susceptibility of Chr7 CSS mice (Figure 3.2C), as well as the potential need for additional protective genes found on chromosome 10 and 17. Nevertheless, *Nfkbid* is required for antibody responses against *T. gondii*, and gene dosage of *Nfkbid* appears to modulate IgG1 class-switching and plasmablast development during infection.

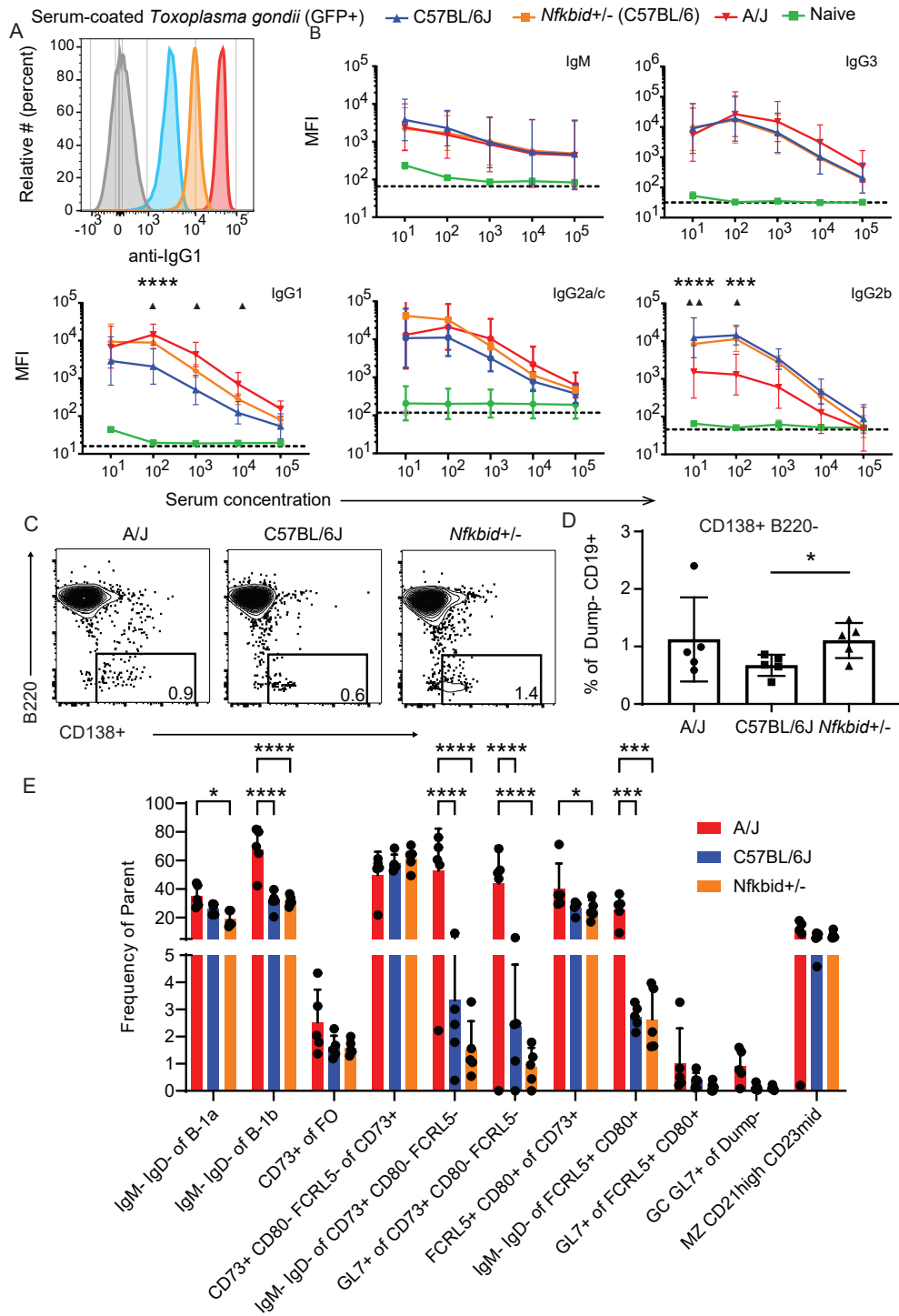


**Figure 3.17: Gene dosage of *Nfkbid* influences class-switching to IgG1 and plasmablast differentiation.** A) Representative histograms display the detection of parasite-specific IgG1 bound to formaldehyde fixed GFP+ type I GT1 parasites; diluted serums ( $10^3$ ) from C57BL/6J, *Nfkbid*<sup>+/-</sup> (C57BL/6J x *bumble* F1), and A/J mice chronically infected with the type III CEP strain were assayed. Anti-mouse IgG1 background staining in the absence of serum is shown. B) As in A, but quantification of the parasite-specific antibody isotypes binding over a range of serum concentrations is shown. Plotted is the cumulative average  $\pm$ SD of the MFI from 2-3 separate experiments (C57BL/6J n=8; *Nfkbid*<sup>+/-</sup> n=7; A/J n=8); significance was assessed by unpaired t-tests and Holm-Sidak corrections comparing A/J vs C57BL/6J (\*) or *Nfkbid*<sup>+/-</sup> vs C57BL/6J ( $\blacktriangle$ ); \*\*\*\* P<0.0001,  $\blacktriangle\blacktriangle$  P<0.01,  $\blacktriangle$  P<0.05. IgG1 staining was not significantly different between A/J and *Nfkbid*<sup>+/-</sup> serums. C) Representative FACS plots of the dump- CD19+ CD138+ plasmablast populations within A/J, C57BL/6J and *Nfkbid*<sup>+/-</sup> mice at day 5 of secondary infection with type I GT1 parasites. D) Frequency of B220- CD138+ plasmablasts of total live dump- CD19+ cells. Plotted is the cumulative average  $\pm$ SD of 2 separate experiments (n=5 per mouse strain); significance was assessed by unpaired t-tests; \* P< 0.05. E) Frequency of B cell phenotypes screen in A/J, C57BL/6J and *Nfkbid*<sup>+/-</sup> mice at day 5 of secondary infection with type I GT1 parasites. Plotted is the cumulative average  $\pm$ SD of 2 separate experiments (n=5 per mouse strain); significance was assessed by 2-way ANOVA with Tukey correction; \* P< 0.05.

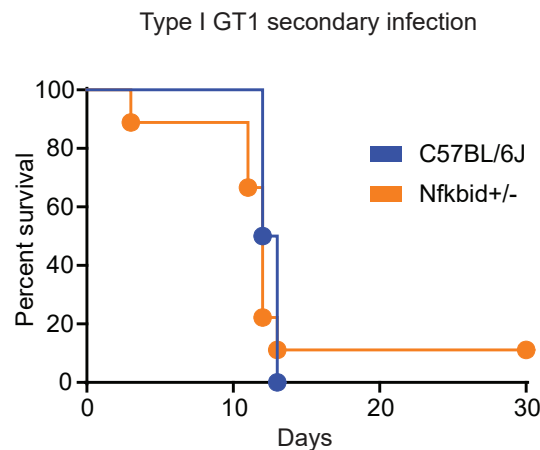


**Figure 3.18: *Nfkbid*<sup>+/-</sup> mice do not have a survival advantage against *T. gondii*.** Survival curve of *Nfkbid*<sup>+/-</sup> and C57BL/6J against type I GT1 secondary infection. Plotted is the cumulative survival of 2 separate experiments (C57BL/6J n=4, *Nfkbid*<sup>+/-</sup> n=6).

### 3.4 Discussion

The findings of this study underscore the utility of using inbred mouse panels to uncover novel determinants of immunity to parasites. An unbiased genetic screen identified *Nfkbid*, a tunable regulator of humoral responses to parasites. Within the C57BL/6J background, *Nfkbid* is required for maturation and class-switching of B-2 cells during chronic *T. gondii* infection. While B-2 responses dominate the antibody response in this background, the lack of B-1 cells appear partially responsible for the immunity defect observed in *bumble* and are required for immunity in bone marrow chimeric mice. In contrast, survival against *T. gondii* infection in resistant mice correlates with a strong layered humoral response: enhanced activation and class-switching in both B-1 and B-2 cells. In this context, B-1 cells may assist the B-2 response to provide full immunity to challenge. The ability of B-1 cells to make parasite-specific antibodies, though of lower affinity, potentially amplifies B-2 immune responses to *T. gondii* through internalization of B-1 cell-derived antigen-antibody complexes (Nguyen et al., 2017), thereby assisting MHCII antigen presentation for CD4 T cell help (Blandino & Baumgarth, 2019). Moreover, the effect of B cell-mediated immunity to *T. gondii* and other pathogens is likely underestimated in murine models using the C57BL/6 background, as enhanced B-1 and B-2 responses were primarily observed in A/J mice.

Though the exact pathway remains to be investigated, *Nfkbid* is downstream of TLR signaling in B cells (Touma et al., 2011; Arnold et al., 2012; Khoenkhoen et al., 2019), which in B-1a cells causes them to downregulate CD5 and facilitate differentiation into antibody secreting cells (Kreuk et al., 2019; Savage et al., 2019). CD5 is a potent negative regulator of antigen receptor signaling that renders B-1a cells unresponsive to B cell receptor (BCR)-triggering. This inhibition is overcome by TLR-stimulation which causes CD5 to dissociate with the BCR, thereby releasing repression of BCR-mediated signaling and antibody secretion (Savage et al., 2019) against foreign- and self-antigen (Kreuk et al., 2019). These data suggest CD5- B-1b cells may represent an activated state of B-1 cells, and calls into question a strict division of labor between these two subsets. This supposition would fit several of the observations made in our system, including evidence for enhanced class-switch recombination and TLR-gene signatures observed in the CD5- B-1 cells of the resistant background. In addition, BAFFR and TACI are known inducers of class-switch recombination (Castigli et al., 2005), and increased expression of these receptors may further lower the threshold of activation and differentiation into CD138+ plasmablasts/plasma cells, all of which are regulated

by *Nfkbid* (Khoenkhoen et al., 2019) and occurring with greater magnitude in B-1 cells of genetically resistant A/J mice. Although class-switch recombination occurs with much greater frequency in B-2 cells of A/J mice, we found no evidence for enhanced expression of BAFFR and TACI in this compartment following *T. gondii* infection.

*Nfkbid* appears to regulate transitional development in B-2 cells, which is analogous to previous findings in B-1 cells (Pedersen et al., 2014), but only evident following *T. gondii* infection. As immature B cells migrate out of the bone marrow to the spleen, there are several checkpoints which are controlled by NF- $\kappa$ B such as BCR- or BAFF-mediated signaling (Rowland et al., 2010), both of which are regulated by *Nfkbid* (Khoenkhoen et al., 2019). Our observation of an accumulation of transitional B cells during *T. gondii* infection in *bumble* mice suggest *Nfkbid* plays a role in stabilizing advancement out of these developmental checkpoints. *Nfkbid* could act as a negative regulator of BCR signaling, enabling pathogen-reactive B-2 cells to develop beyond negative selection that would otherwise occur as antigen accumulates in secondary lymphoid organs over time. Alternatively, *Nfkbid* could be a positive regulator of NF- $\kappa$ B signaling, increasing the strength of BCR signaling to enable transitional B cells to become mature B cells. In both cases, a developmental defect likely restricts the pool of *T. gondii*-reactive mature B cells, preventing replenishment of antibody secreting cells during infection, culminating in the low parasite-specific antibody titers observed in *bumble* mice.

Though *Nfkbid* has a large effect on humoral responses, our study does not address whether this is due to a B cell intrinsic effect or a T follicular helper cell phenotype. Previous studies using model T-dependent antigens, such as 2,4,6-Trinitrophenyl (TNP)-KLH and 4-hydroxy-3-nitrophenylacetyl (NP)-ovalbumin (OVA), have demonstrated the *Nfkbid*-dependent IgM response is B cell intrinsic, but the IgG1 response was not and required *Nfkbid*-dependent CD4 T cell help. Moreover, C57BL/6J mice undergo T cell exhaustion during chronic infection with *T. gondii* (Bhadra et al., 2011b; Splitt et al., 2018) and during *Plasmodium* infection, PD-L1 and LAG3 blockade improves germinal center and plasma cell responses via an enhanced T follicular help (Butler et al., 2012). T cell exhaustion may serve as an explanation for why C57BL/6J have both reduced humoral responses and IFN $\gamma$ + CD8 T cells relative to A/J mice. However, whether the humoral or IFN $\gamma$  differences were due to a T cell intrinsic phenotype regulated by *Nfkbid* or overall T cell dysfunction mediated by extrinsic factors in the C57BL/6J background was not explored in our system. Further investigation of pathways upstream of *Nfkbid* and the major cell types driving humoral responses has the potential to elucidate

key requirements for *T. gondii* immunity.

It is important to emphasize that multiple polymorphisms determine the complex phenotype of secondary infection immunity to *T. gondii*. Our genetic screen revealed at least 4 loci that each account for 20-40% of the overall heterologous immunity to *T. gondii*, and that the H-2 locus can be an important modifier of resistance against certain parasite strains. Perhaps not surprising, the *Nfkbid* polymorphism in a stand-alone fashion did not fully restore immunity, as inferred from chromosome 7 consomic mice and by our attempts to mimic the lower gene expression observed in resistant mice through heterozygous expression. Whereas polymorphic *Nfkbid* contributes 21% to this phenotype, perhaps by regulating plasma cell differentiation, this smaller effect QTL was instrumental in identifying *Nfkbid*, where a more drastic gene inactivation revealed its role in multiple compartments in *bumble* mice, notwithstanding its requirement for humoral immunity.

In summary, heterologous immunity to a parasitic pathogen should, at a minimum, prevent disease against a wide variety of strains that differ in virulence or polymorphic antigens. An ideal parasite vaccine would entirely protect against re-infection and induce sterile immunity, thought possible since re-infection studies were first performed in mice (Nussenzweig et al., 1967) and humans immunized with irradiated sporozoites and Plasmodium sp. challenge (Hoffmann et al., 2002). Yet, only one partially protective vaccine is in use for any human parasitic pathogen, RTS,S/AS01, which has low efficacy for malaria prevention (RTSS Clinical Trials Partnership, 2015). Our findings highlight the role of both innate-like and conventional B cells in humoral immunity to *T. gondii*, introducing B-1 cells as a potential vaccine target along with B-2 cells to maximize immunity to parasitic infections. Moreover, we present a modulator of antibody responses against parasitic infections, *Nfkbid*, a transcriptional regulator that can tune B cell responses to provide an overall effective class-switched antibody response against parasites.

# Chapter 4

## GPI reactivity from anti-*T. gondii* antibodies

### 4.1 Introduction

The surface of *T. gondii* is dominated by proteins linked by glycosylphosphatidylinositol (GPI) anchors (Manger et al., 1998; Nagel & Boothroyd, 1989). GPI anchors are post-translational modifications that "anchor" proteins to the outer leaflet of the cell membrane (Paulick & Bertozzi, 2008). GPI anchors are largely conserved molecules (Fontaine et al., 2003; Homans et al., 1988; Low, 1987; Naik et al., 2000; Nosjean et al., 1997), with its structure first elucidated by parasitologists studying variant surface glycoproteins (VSG) of trypanosomes (Ferguson et al., 1985). The core structure of GPI anchors include a phosphatidylinositol, a glucosamine, three mannoses, and an ethanolamine phosphate that is covalently linked to proteins, with variations manifesting along side-chains connected to the mannose backbone. Two saturated fatty acid tails emanate from the inositol via a phosphate linkage embedding the GPI and its linked protein into the membrane (Ferguson, 1999). Production of GPI precursors and linkage to proteins occur within the ER, where they are then transported to the cell surface (Brown & Rose, 1992).

*T. gondii* has been found to create six GPI precursor isoforms, each consisting of different combinations of side chains and/or ethanolamine attached to the core structure (Striepen et al., 1997). GPIs also exist on the surface membrane without protein attachment (GPI lipids or 'GIPLs'). These non-protein associated

precursors (GIPLs) are transported to the cell membrane along with GPI anchored proteins via the Golgi where they act as immunogenic molecules (Striepen et al., 1997). Both protein associated GPI and GIPL consist of two glycoforms that differ in their sugar composition (Striepen et al., 1997; Zinecker et al., 2001). These two GPI glycoforms are defined by a side chain addition of  $\beta$ -GalNAc to the mannose with or without a terminal glucose (Figure 4.1) (Striepen et al., 1997) and importantly, can be distinguished from higher eukaryotes by the lack of a phosphoethanolamine (Paulick & Bertozzi, 2008). The most immunogenic portions of the *T. gondii* anchor in humans are thought to be the glucose addition to the  $\beta$ -GalNAc side chain which is unique to *T. gondii* (Striepen et al., 1997; Götze et al., 2015). GPI anchors isolated from parasites have been shown to play a role in the activation of NF- $\kappa$ B through TLR2 and TLR4, contributing to the induction of TNF $\alpha$  in macrophages (Debierre-Grockiego et al., 2007; Campos et al., 2001). Studies of *T. gondii*-infected human sera have found that not only is free GIPL targeted by human antibodies, but that it is preferentially bound by IgM, suggesting an extrafollicular/T-independent response (Giraldo et al., 2000).

Our work described in chapter 3 has shown B-1 cells can be enhanced in certain genetic backgrounds. Given that B-1 cells produce 80% of serum IgM (Baumgarth et al., 1999) and are major contributors to T-independent humoral responses (Martin et al., 2001) with known reactivity against GPI-anchored self-antigens (Hayakawa et al., 1999), we wanted to investigate the role of the GPI anchor and non-protein associated GIPLs as potential antigens. Beyond purely investigating the GIPL as an epitope, previous studies also have shown that GPI anchors are integral to protein conformation as antibody recognition of Thy-1, a GPI anchored protein, is ablated after treatment with phosphatidylinositol-specific phospholipase C (PI-PLC) (Barboni et al., 1995). Thus we asked two major questions: (1) Do resistant A/J mice, with their enhanced B-1 responses, target the non-protein antigens on *T. gondii*? and (2) are intact GPI anchors required for antibody recognition of *T. gondii* antigens? Our work herein has uncovered that antibody reactivity against the non-protein-*T. gondii* antigens is greater in the resistant A/J background, correlating with enhanced B-1 responses, and that intact GPI-anchors are fundamentally required for antibody recognition of major *T. gondii* surface antigens.

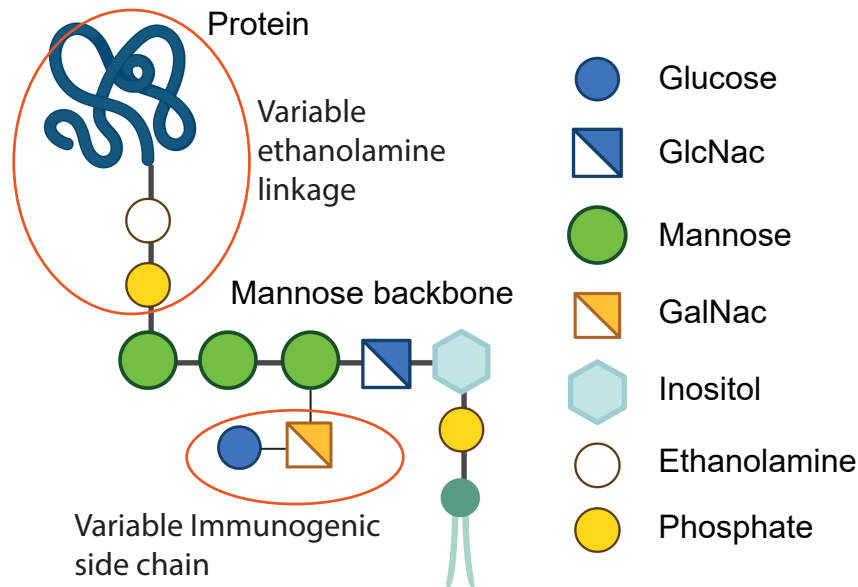


**Figure 4.1: Model of GPI anchors, a widely conserved structure and immunogenic target.** Schematic of the structure of the GPI anchor. The core structure of *T. gondii* GPI anchors consist of a phosphatidylinositol, a glucosamine, three mannoses, and an ethanolamine phosphate. Circled in red are the variable and unique regions of *T. gondii* GPIs.

## 4.2 Methods

### 4.2.1 Ethics Statement

Mouse work was performed in accordance with the National Institutes of Health Guide to the Care and Use of Laboratory Animals. Mouse protocols used have been reviewed and approved by UC Merced's Committee on Institutional Animal Care and Use Committee (IACUC). UC Merced has an Animal Welfare Assurance filed with OLAW (A4561-01), is registered with USDA (93-R-0518), and the UC Merced Animal Care Program is AAALAC accredited (001318).

## 4.2.2 Parasite strains and cell lines

Human foreskin fibroblasts (HFFs) monolayers were grown in DMEM (4.5 g/L D-glucose) (Life Technologies) supplemented with 2 mM L-glutamine, 20% fetal bovine serum (FBS) (Omega Scientific), 1% penicillin-streptomycin, and 0.2% gentamycin (Life Technologies). Mouse Embryonic Fibroblasts (MEFs) were grown in DMEM (4.5 g/L D-glucose) (Life Technologies) supplemented with 10% fetal bovine serum (FBS) (Omega Scientific), 20mM HEPES, 1% penicillin-streptomycin, and 0.2% gentamycin (Life Technologies). *Toxoplasma gondii* strains were passaged in HFFs in 'Toxo medium' (4.5 g/L D-glucose, L-glutamine in DMEM supplemented with 1% FBS and 1% penicillin-streptomycin). The following clonal strains were used (clonal types are indicated in parentheses): RH  $\Delta ku80 \Delta hxp1$  (type I), RH (1-1) *GFP::cLUC* (type I), GT1 (type I) and CEP *hxp1-* (type III).

## 4.2.3 Mice

Female C57BL/6J (H-2b) and A/J (H-2a) were purchased from Jackson Laboratories. Mice were maintained under specific pathogen free conditions at UC Merced.

## 4.2.4 Parasite infections

Parasite injections were prepared by scraping T-25 flasks containing vacuolated HFFs and sequential syringe lysis first through a 25G needle followed by a 27G needle. The parasites were spun at 400 rpm for 5 min to remove debris and the supernatant was transferred, followed by a spin at 1700 rpm washing with PBS. For primary infections, mice were infected intraperitoneally (i.p.) with  $10^4$  tachyzoites of type III CEP *hxp1-*. Parasite viability of the inoculum was determined by plaque assay following i.p. infections. In brief, 100 or 300 tachyzoites were plated in HFF monolayers grown in a 24-well plate and 4-6 days later were counted by microscopy (4x objective).

## 4.2.5 Blood plasma isolation and assessment of seroconversion

All mice were assessed for sero-positivity to *T. gondii* 4-5 weeks post primary infection. 50 $\mu$ L of blood was isolated from mice in tubes containing 5 $\mu$ L of 0.5M EDTA on ice, pelleted and the supernatant containing blood plasma was

heat inactivated to denature complement at 56°C for 20 minutes and then stored at -80°C. HFFs were grown on coverslips and infected with GFP-expressing RH (1-1) overnight, fixed 18 hrs later with 3% formaldehyde (Polysciences) in PBS, washed, permeabilized and blocked with PBS containing 3% bovine serum albumin Fraction V (Sigma), 0.2M Triton X-100, 0.01% sodium azide, incubated with a 1:100 dilution of collected blood plasma for 2 hrs at room temperature, washed with PBS, and detected with Alexa Fluor 594-labeled secondary antibodies specific for mouse IgG (cat# A11032, Life Technologies). Seropositive parasites were observed by immunofluorescence microscopy (Nikon Eclipse Ti-U).

#### **4.2.6 Generation of *T. gondii* lysate and PI-PLC cleavage of *T. gondii* lysate**

To generate parasite lysate antigens *Toxoplasma gondii* was cultured in HFF and expanded to approximately  $2 \times 10^8$  parasites. Parasites were syringe-lysed, washed with sterile 1X PBS and the parasite pellet was lysed with (1mL) 0.1% Triton X-100 detergent in 1X PBS. Solubilized parasites were centrifuged at 2,000 relative centrifugal force (RCF) for 20 minutes to remove large debris. The supernatant was aliquoted and stored at -80°C. 50  $\mu$ L parasite lysate was thawed on ice then incubated at 37°C for 1 hour with 0.5 units of phosphatidylinositol-specific phospholipase C (PI-PLC), isolated from *B. cereus* [P6466, Life Technologies], at a V:V ratio of 10:1 (lysate:PI-PLC), respectively, in the presence of a protease inhibitor cocktail [4693116001, Roche] used at 1X of reaction volume. Mock treated parasite lysate was incubated with equivalent volumes of PBS in place of PI-PLC under identical conditions. Lysates were then denatured at 95°C for 5 minutes in 2:1 Laemmli loading buffer (125mM Tris HCL pH6.8, 10% glycerol, 2% SDS 0.2% Bromophenol Blue, 5%  $\beta$ -Mercaptoethanol) to sample.

#### **4.2.7 SDS-PAGE and immunoblotting for parasite lysate antigen**

Parasite lysate was reduced with  $\beta$ -mercaptoethanol (BME) and separated via SDS-PAGE in 4-20% Mini-PROTEAN TGX pre-cast gels (cat# 4561096, Bio-Rad or 4-20% hand-poured acrylamide gels (from a 30% acrylamide/bis solution 29:1, Bio-Rad cat# 1610156) before transfer to PVDF membrane with a 20% W/V methanol transfer buffer (150mM TRIS, 20mM glycine) via a Bio-Rad Transblot Turbo machine using the "low molecular weight" settings (cat# 1704150, Bio-Rad),

or using a Trans-Blot Turbo Mini PVDF Transfer Pack (cat# 1704156, Bio-Rad) via a Bio-Rad Transblot Turbo using the "2 minigels" settings (cat# 1704150, Bio-Rad). Detection of GIPL antigens required 20% methanol transfer buffer. Membranes were blocked with 10% fortified bovine milk (Railey's) dissolved in Tris-Buffered Saline with 0.1% Tween (TBS-T 0.1%) for 1-2 hrs at room temperature or overnight at 4°C. Blots were then probed with heat-inactivated serum in block at either 1:1,000 dilution for serum IgM analysis or 1:5,000 dilution for serum IgG analysis overnight at 4°C. For probing with monoclonal antibodies to *T. gondii* surface antigens anti-SAG1 (clone T4 1E5, BEI cat#NR-50255), anti-P35 (SRS29C) (clone T4 3F12, BEI cat#NR-50259), anti-SAG3 (clone T4 1F12, BEI cat#NR-50257), the GalNAc glycoform-specific anti-GPIL antibody (clone T3 3F12, BEI cat#: NR-50253), or anti-GRA3 (clone T6 2H11, BEI cat#NR-50269); 1:7500 dilution information here. Membranes were washed with TBS-T 0.1% three times for 20 minutes per wash. Blots were then incubated for one hr at room temperature with goat anti-mouse horseradish peroxidase (HRP)-conjugated antibodies (SouthernBiotec): anti-IgM secondary 1:1000 (cat# 1020-05) and total anti-IgG secondary 1:5000 (cat# 1030-05). Membranes were then washed with TBS-T 0.1% three times and developed with Immobilon® Forte Western HRP Substrate (WBLUF0500). All blots were imaged via chemiluminescence on a ChemiDoc Touch (cat# 12003153, Bio-Rad). Image Lab 6.1 software (Bio-Rad) was used for analysis of bands and total lane signal. Western blots comparing A/J to C57BL/6J were developed simultaneously and the band signal was normalized to A/J.

## 4.3 Results

### 4.3.1 Non-protein antigens (GIPL) are targets of durable B cell populations

Glycoinositolphospholipids (GIPLs) are known to be actively targeted by the acute antibody response in both mice and humans by IgM secreting B cells (Couvreur et al., 1988; Giraldo et al., 2000; Garg et al., 2019), suggesting a rapid T-independent response against a non-protein antigen. In our secondary infection model of resistant (A/J) and susceptible mice (C57BL/6J), we have observed enhanced activation of the A/J B-1 compartment, innate-like B cells known to rapidly respond to T-independent antigens (reviewed in (Baumgarth, 2017)). Therefore, we investigated the potential IgM binding of serum from *T. gondii* infected A/J

and C57BL/6J mice to GIPL antigen. To accomplish this, western blot analysis of serum was used to probe type I GT1 *T. gondii* lysate to find evidence of durable antibody recognition of GIPL (Figure 4.2A, B) from chronically infected mice. Serum from chronically infected mice was found to have GIPL-specific IgM antibodies 35 days after primary infection, which given the short 2 day serum half-life of IgM (Vieira & Rajewsky, 1988) suggests this IgM-secreting B cell population is maintained at least throughout chronic infection (Figure 4.2C). Interestingly, antibodies from both mouse strains did not have GIPL reactivity to the lab adapted type I RH lysate, similar to observations made in the West laboratory (University of Georgia)(Gas-Pascual et al., 2019). Consistent with our previous findings, serum from A/J mice had 2 fold greater band intensity for GIPL antigen (Figure 4.2D), again signaling the robust humoral response of the resistant mouse.

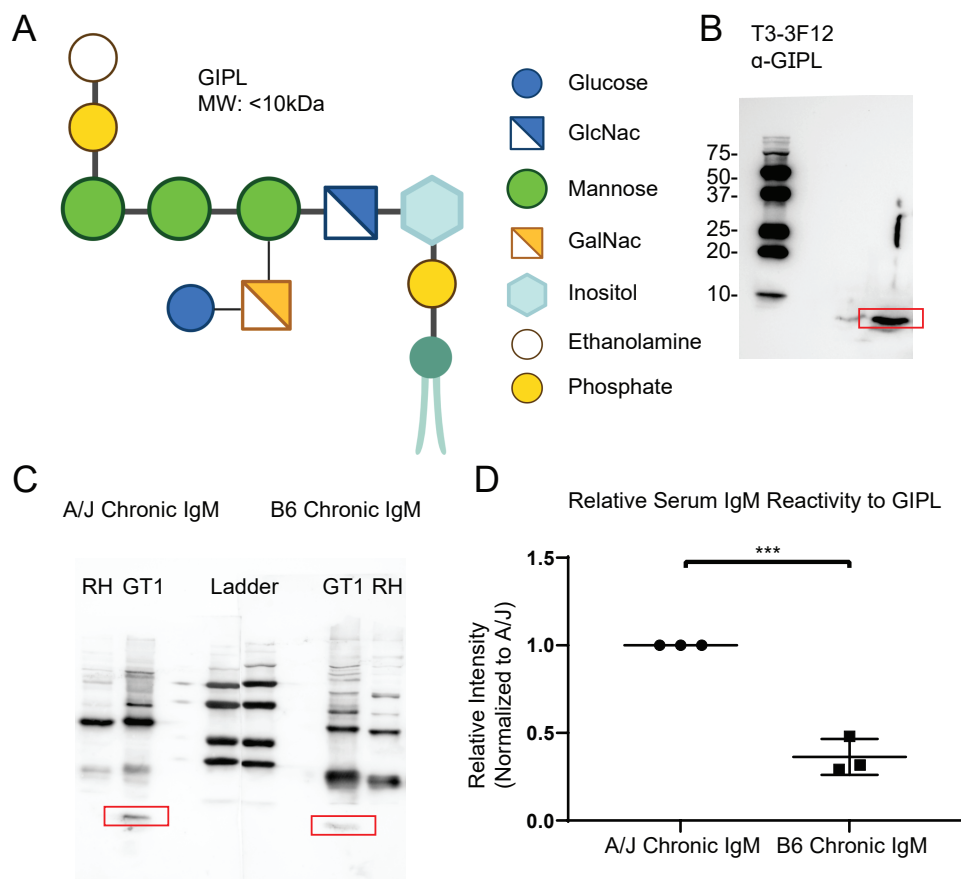


**Figure 4.2: Immunity to *T. gondii* is correlated with antibody responses to GIPL.** A) Structure model of the non-protein associated GIPL. B) Representative western blot of

monoclonal antibody binding (Clone: T3 3F12) to the low molecular weight (<10kDa) GIPL antigen boxed in red. C) Representative western blot of type I GT1 and RH parasite lysate probed with A/J or C57BL/6J serum after 35 days of chronic infection with the type III CEP strain, and detected with anti-mouse IgM. The red box denotes the location of GIPL. Western blots were developed in tandem. D) As in C, but GIPL band intensity detected by anti-mouse IgM was quantified by Image Lab. C57BL/6J GIPL band intensity was normalized to that of A/J's. Each dot represents the result from an individual mouse from 3 separate experiments. Significance was assessed with an unpaired two-tailed t-test; \*\*\* P<0.0001.

---

### 4.3.2 Intact GPI anchors are required for antibody recognition of *T. gondii* GPI-anchored surface antigens

Cleavage of the GPI lipid moiety by phosphatidylinositol-specific phospholipase C  $\gamma$  (PI-PLC $\gamma$ ) (modeled in Figure 4.3) has been shown to abrogate antibody recognition of GPI-anchored Thy1 without inducing proteolysis (Barboni et al., 1995), though the mechanism of recognition loss is unknown. Because *T. gondii* expresses its own PI-PLC that localizes to the cell membrane (Fang et al., 2006), we were curious if PI-PLC $\gamma$  disrupts antibody recognition of *T. gondii* antigens. To test this hypothesis, we assessed monoclonal antibody binding to GPI-anchored surface antigen glycoproteins (SAGs) of *T. gondii* (SAG1, P35, SAG3 which represent three of five immunodominant *T. gondii* surface antigens (Couvreur et al., 1988)) and a non-anchored secretory protein GRA3 with and without enzymatic cleavage of the lipid moiety by PI-PLC $\gamma$ . Signal loss in western blot bands was only observed in GPI-anchored proteins treated with PI-PLC $\gamma$  (Figure 4.4A), indicating PI-PLC $\gamma$  disrupts monoclonal antibody recognition specifically on GPI-anchored *T. gondii* proteins. Extending this analysis to the total serum IgG antibody repertoire of chronically infected A/J and C57BL/6J mice, we saw an 80% reduction in total lane signal from *T. gondii* lysate treated with PI-PLC $\gamma$  relative to untreated lysate (Figure 4.4B,C). Signal loss is observed at molecular weights consistent with *T. gondii* GPI-anchored SAGs (20-45 kDa). Similar results were observed when assaying for IgM reactivity to *T. gondii* lysate antigen (not shown). Importantly, both A/J and C57BL/6J mice equally lost antibody recognition to *T. gondii* antigens after PI-PLC $\gamma$  treatment, suggesting a fundamental requirement for an intact GPI-anchor to maintain antibody reactivity rather than a difference in the repertoire between resistant and susceptible mice.

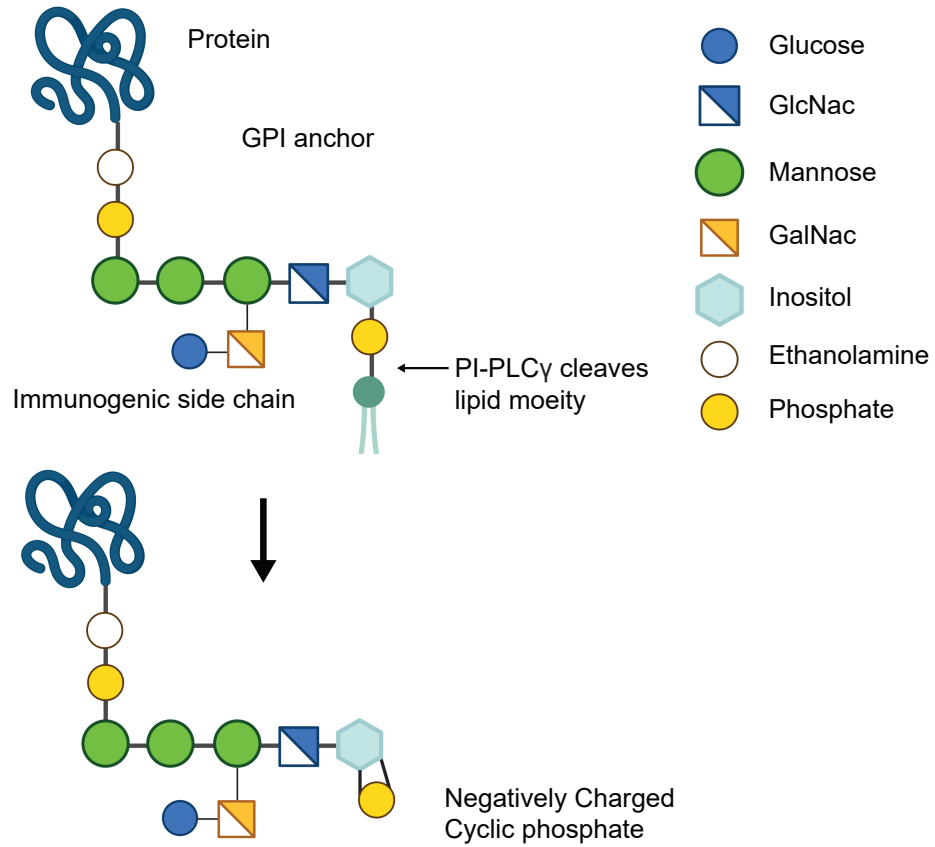


**Figure 4.3: Mode of action for the cleavage of GPI-anchored proteins by PI-PLC $\gamma$ .** Many *T. gondii* surface antigens are anchored to the cell membrane via GPI anchors which contain immunogenic side chain epitopes. PI-PLC $\gamma$  enzymatic cleavage of GPI-anchors occurs above the lipid tail leaving a negatively charged cyclic phosphate on the inositol sugar group.

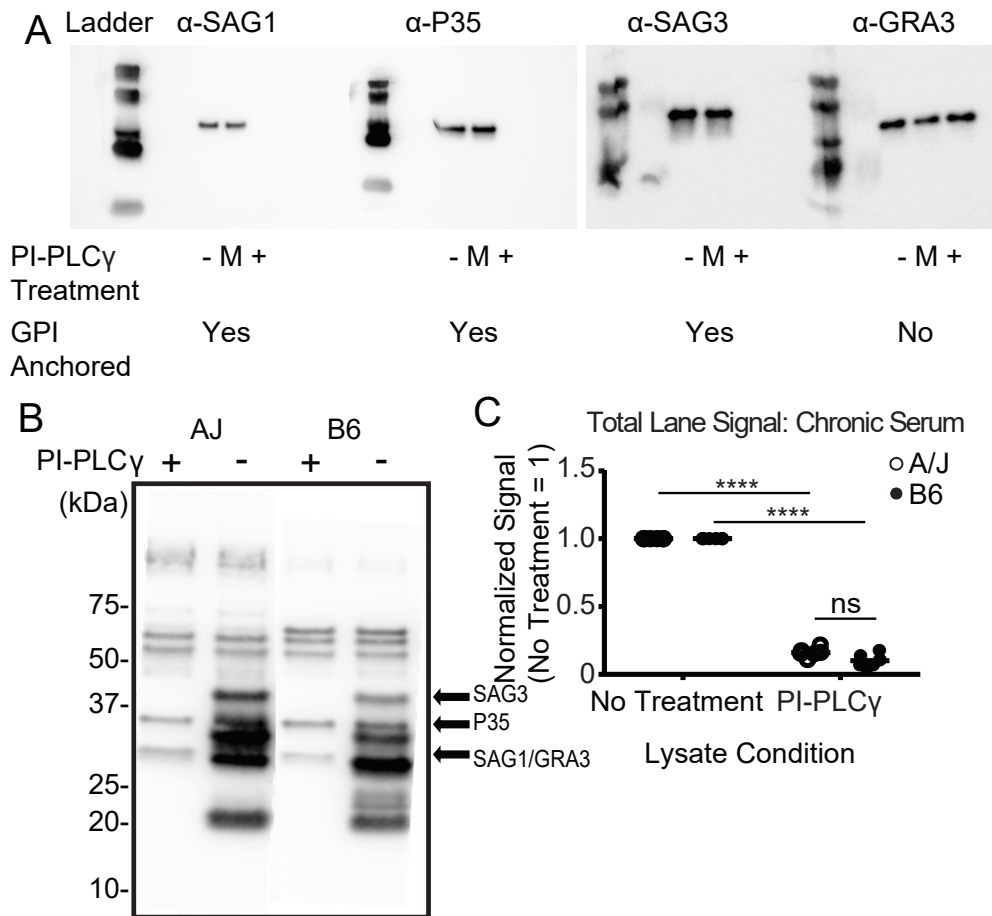


**Figure 4.4: Intact GPI moieties are required for antibody reactivity to GPI-linked proteins.** A) Representative western blots of type I GT1 parasite lysate treated with PI-PLC $\gamma$  (+), mock treated (M), or untreated (-) and probed with monoclonal antibodies against major *T. gondii* surface antigens SAG1, SAG3, P35, and GRA3. SAG1, SAG3, and P35 are GPI-anchored proteins while GRA3 is not GPI-anchored. B) Representative western blots of type I GT1 parasite lysate treated with PI-PLC $\gamma$  (+) and untreated (-) and probed with serum from chronically infected A/J and C57BL/6J. C) Total lane signal from PI-PLC $\gamma$  treated and untreated parasite lysate quantified from (B). Lane signal from PI-PLC $\gamma$  lanes were normalized to untreated lanes. Each dot represents the results from one mouse (n=6-7) obtained from three separate experiments. Significance was assessed by student's t-test comparing normalized PI-PLC treated to non-treated within the same strain (P<0.0001). B and C are data generated by Jessica Wilson.

## 4.4 Discussion

Our previous studies described in chapter 3 found an important role for B-1 cells in generating complete immunity to secondary infection with highly virulent strains. However, our analysis of antibody binding to whole parasite found that the entirety of the high avidity anti-*T. gondii* antibodies were generated by the B-2 compartment within the susceptible genetic background. Though B-1 cells were not found to make high avidity anti-*T. gondii* antibodies, they still have the potential to make low avidity T-independent responses which could be protective in the early acute phase before a B-2 response has fully formed (Herzenberg & Herzenberg, 1989). To identify potential B-1 targets, we investigated putative T-independent antigens, *T. gondii* GIPL, and defined differences in antibody reactivity within our resistant and susceptible mouse model. Mirroring our earlier results illustrating the robust humoral immunity in the resistant background, A/J mice generated greater quantities of anti-GIPL antibodies than C57BL/6J. This increased recognition correlates with a robust B-1 response. A previous study found that SAG1 antibodies transition from IgM to being dominated by IgG antibody populations during the course of infection, whereas antibodies reactive to GIPL remain IgM (Garg et al., 2019), suggesting a persistent, potentially B-1 derived, IgM-secreting memory population (Savage et al., 2017). It is also possible the persistent IgM is generated in an extrafollicular response, as IgM+ memory B cells have been shown to rapidly respond to malaria challenge in both a T-dependent and T-independent manner (Krishnamurthy et al., 2016).

Regarding GPI-anchored proteins, the mechanism explaining the loss of antibody recognition to GPI-anchored proteins after PI-PLC $\gamma$  cleavage is yet unknown. Previous studies have postulated that conformational shifts occur after phospholipid cleavage (Barboni et al., 1995), and that antibodies generated against the cleaved phospholipid form of the protein have lower recognition of the intact GPI form and vice versa (Butikofer et al., 2001). However, our specific observation is of linearized proteins, via reduction SDS page, and the loss of antibody recognition after lipid cleavage suggests conformational shifts play a limited role. Phospholipid cleavage by PLC $\gamma$  leaves a negatively charged cyclic phosphate (Ferguson, 1999) that could potentially disrupt antigen transfer to blotting membrane or directly hinder antibody recognition. The loss of transfer to blotting membrane hypothesis is unlikely, as there is a long history of detecting the cyclic phosphate by PLC $\gamma$  cleavage (termed the common reactive determinant or CRD) via western blot to determine if a protein is GPI-anchored (Zamze et al., 1988; Nagel & Boothroyd,

1989; Ferguson, 1999). It is important to note that neither monoclonal (Figure 4.3B) nor polyclonal (Meek et al., 2001) antibodies targeting GIPL cross-react with GPI anchored proteins, nor do monoclonal antibodies raised against *T. gondii* SAGs cross-react with GIPL (Figure 4.4A). Therefore it is possible that the majority of antibody epitopes found on SAGs are conformationally dependent and on the protein itself rather than binding on the GPI anchor. Such predictions await experimental validation.

Altogether, this data demonstrates an interesting phenomenon with potentially large impact on research into vaccine development. The majority of *T. gondii* surface antigens are GPI-anchored (Manger et al., 1998) and are the major candidates for vaccine subunits. Importantly, recombinantly expressing GPI-anchored proteins in bacterial systems creates proteins without GPI anchors attached (Diep et al., 1998). This could lead to systemic underestimation of the efficacy of vaccine subunit candidates lacking the GPI anchor, as it would induce an antibody response with lower reactivity against the natural conformation of GPI-anchored proteins (Butikofer et al., 2001) and potentially miss a necessary epitope required for pathogen neutralization. Including carbohydrate antigens targeting B-1 cells, beyond simple TLR stimulating adjuvants, may be an important addition to vaccines to promote full immunity. Additionally, induction of B-1 responses to produce low avidity T-independent antibodies could play an important immunoregulatory role during the challenge event by clearing out immunogenic carbohydrates before they induce excessive inflammation and/or cytokine storms (Shaw et al., 2000; Chou et al., 2009; Schofield et al., 2002). Finally, the only vaccine against eukaryotic pathogens, RTS,AS01 vaccine against malaria, has been shown to have 27% efficacy after 4 doses with a marked loss of humoral immunity within months of the final dose (White et al., 2015). The RTS vaccine uses the GPI-anchored circumsporozoite protein (CSP) expressed without a GPI anchor, which potentially explains the low efficacy. Though the exact mechanism of GPI-mediated immunity is yet unknown, possibly by inducing anti-carbohydrate antibodies or preserving conformational dependent epitopes on antigens, it is likely that including GPI within vaccine antigen formulations is better than foregoing GPI.

## Chapter 5

# Conclusion: Layered cellular and humoral responses are required for maximal immunity to *T. gondii*

### 5.0.1 Contributions to the field

The goal of the research presented in this dissertation was to elucidate requirements for host immunity to high virulence *T. gondii* infections by addressing three overarching questions: 1) Can CD8 T cell activity enhanced through checkpoint blockade promote host survival against high virulence *T. gondii* strains, 2) are B cell responses required for heterologous immunity, and 3) how do *T. gondii* antigens such as the GPI anchor and non-protein associated, putative T-independent, GPI lipid (GIPL) antigen influence the antibody response? In our attempts to answer these questions we made a number of noted observations: We saw checkpoint blockade does not protect against atypical *T. gondii* strains, which helps define the context in which these potent therapies are effective. We used a forward genetic screen to probe questions about immunological memory and our very first gene candidate was found not to be required for primary infection but absolutely required for secondary infection with *T. gondii*, highlighting the efficacy of our approach. And though cursory, we have uncovered a compelling phenomenon wherein delipidating GPI-anchored *T. gondii* antigens abrogates the reactivity of antibodies derived from a natural *T. gondii* infection, which may inform parasite vaccine design as the majority of parasite surface antigens are GPI-anchored.

## **Checkpoint blockade is ineffective at protecting against atypical *T. gondii* strains**

The use of checkpoint blockade therapies has been wildly successful at treating cancer, potently inducing large response rates, tumor regression, and survival of late-stage melanoma patients (Phan et al., 2003; Hodi et al., 2010; Wolchok et al., 2013; Hodi et al., 2016). These therapies act by targeting inhibitory receptors on T cells with neutralizing antibodies to reverse disease severity in chronic viral infections and cancer (Barber et al., 2006; Leach et al., 1996), diseases associated with T cell dysfunction or "exhaustion" (Ahmed et al., 1984; Iwai et al., 2002; Hirano et al., 2005; Sakuishi et al., 2010; Pauken & Wherry, 2015). The success of these therapies, combined with observations of T cell exhaustion occurring in chronic *T. gondii* infection (Bhadra et al., 2011b, 2012), spurred us to investigate the use of checkpoint blockade in preventing mortality to infection by high virulence atypical strains of *T. gondii*. We used a secondary infection with high virulence atypical strains approach (Jensen et al., 2015) to model a scenario that likely occurs in endemic regions with high frequencies of atypical strains such as South America. We found this approach consistent with other models of chronic *T. gondii* infection that require CD8 T cells for control of *T. gondii* (Bhadra et al., 2011b) in that atypical *T. gondii* strains potently induce T cell exhaustion markers after challenge (Splitt et al., 2018). In contrast, we found our attempts to ameliorate T cell exhaustion via checkpoint blockade was unsuccessful at promoting immunity to secondary infection with atypical strains. Thus, though checkpoint blockade was not able to promote survival during acute secondary infection, our work contributed to the overall context to which checkpoint blockades are effective.

## **Experimental model for resistance against high virulence *T. gondii* strains**

A major goal for our research was to establish a new model for screening adaptive memory response phenotypes that are protective against high virulence *T. gondii* infections. Studies on atypical strains largely focuses on cell autonomous immunity through IRGs, as wild-derived mouse strains have been reported to contain polymorphic IRG loci that are well adapted to handling even primary infections by high virulence type I and some atypical strains (Lilue et al., 2013; Murillo-León et al., 2019; Hassan et al., 2019). Our A/J versus C57BL/6J *in vivo* model sits in a space between the more complex mouse panels such as the collaborative cross (Churchill et al., 2004), which was created with parental mouse strains that have the aforementioned protective polymorphic IRG loci (Lilue et al., 2013), and

reverse genetics solely using the C57BL/6J background which we have shown to not be representative of a robust anti-*T. gondii* response. Thus, we can study resistance against atypical *T. gondii* strains without potent, but confounding, IRG loci promoting survival, while simultaneously exploring new immune phenotypes that emerge due to genetic diversity.

### **Unbiased genetic screen identified loci correlated with immunity to secondary infections**

The overarching question that shaped the experiments shown within this dissertation was: How do we achieve protective immunity against the highest virulence *T. gondii* strains? To that end we utilized a 40-year-old recombinant inbred mouse panel (Nesbitt & Skamene, 1984) to answer that important question. While this particular recombinant inbred panel had been previously used within the *T. gondii* field to answer questions regarding primary infection (McLeod et al., 1989; Brown et al., 1995), our work presented here is the first to extend the model to find novel host factors for protective immunological memory responses. Using a forward genetic approach, we identified four loci correlated with survival against secondary infection over chromosomes 7, 10, 11, and 17. Investigation of our first gene candidate, *Nfkbid*, found a host factor that was not required for survival against primary infection but was absolutely required for survival against secondary infection, highlighting the efficacy of both our screen and the A/J versus C57BL/6J model.

### ***Nfkbid* is required for antibody responses against *T. gondii***

*Nfkbid* has been shown to influence a plethora of phenotypes such as T cell cytokine production (Touma et al., 2007), plasmablast differentiation (Khoenkhoen et al., 2019), and B-1 cell development (Touma et al., 2011; Arnold et al., 2012). Using a forward genetic screen we were able to identify *Nfkbid* as a requirement for secondary infection to *T. gondii*. Notably within the *T. gondii* secondary infection model, no differences were observed within known *Nfkbid*-regulated T cell phenotypes. However, a significant humoral defect was observed as infected *bumble* mice completely lacked parasite-specific IgM and had dramatically reduced levels of parasite-specific class-switched IgG isotypes. We found an accumulation of transitional B cells within the spleen 35 days after primary infection, signaling the requirement of *Nfkbid* in timely replenishment of the B cell compartment after infection. This observation is analogous to other studies showing delayed development of other B cell compartments in the steady state, such as marginal

zone B cells (Adori et al., 2017) and a complete developmental block of B-1a cells (Pedersen et al., 2014). Of note, Touma et al. found *Nfkbid*<sup>-/-</sup> mice can reach IgG antibody titers to the T-dependent antigen TNP-KLH on par with WT mice, albeit with a 2-week delay (Touma et al., 2011). In contrast, *bumble* mice in our system were unable to generate WT levels of *T. gondii*-specific antibodies out to day 35 of chronic infection, and we hypothesize this is due to the inability to generate enough B cells to sustain multiple waves of GC output (Inamine et al., 2005; Zhang et al., 2018).

### **B-1 cells are required for full immunity to *T. gondii* within the C57BL/6J background and are enhanced in resistant mice**

A consistent observation within multiple models described in chapter 3 is the protective influence of B-1 cells even in the susceptible background (Figure 3.6a, 3.10). The entirety of literature focused on B-1 mediated immunity to *T. gondii* exists in three publications generated by a single lab (Chen et al., 2000, 2003b,a), and though they show transfer of B-1 cells from C57BL/6 mice into B cell deficient  $\mu$ MT mice provides some level of protection against an intermediate virulence type II *T. gondii* strain, the transfer method described (transfer of B-1 cells 1 week prior to infection) is potentially at odds with known host-graft rejection of transferred peripheral B cell populations into adult  $\mu$ MT mice (Baumgarth et al., 2000). A potential explanation for the lack of studies focused on B-1 immunity to *T. gondii* is the small B-1 response observed in the commonly used C57BL/6J background compared to the resistant A/J background. Thus, our work exploring B-1 phenotypes in resistant A/J mice identifies a systemic underestimation of B-1 mediated immunity to *T. gondii* in studies utilizing the C57BL/6J background.

### **GPI anchors are required for antibody reactivity against *T. gondii* surface antigens**

B-1 cells are known to have specific reactivities to non-protein antigens such as PtC (Micolino et al., 1988) and carbohydrate epitopes (Hayakawa et al., 1990). Our investigation into potential B-1 epitopes focused on GPI-anchored proteins and glycoinositolphospholipids, carbohydrate molecules that are found extensively on the surface of *T. gondii* (Manger et al., 1998; Nagel & Boothroyd, 1989). Our data shows mice generate a durable IgM anti-GIPL-specific B cell response as IgM reactivity was found in serum 35 days after primary infection. In addition, we showed delipidation of *T. gondii* antigens destroys monoclonal recognition of major

*T. gondii* surface antigens, in-line with previous reports of other GPI-anchored proteins (Barboni et al., 1995; Butikofer et al., 2001). We extended this observation to bulk serum antibody repertoires and found an 80% loss in total lane signal to parasite lysate treated with PI-PLC $\gamma$ , suggesting that intact GPI anchors are fundamentally required for antibody recognition of *T. gondii* surface antigens.

## 5.0.2 Future Directions

### The role of *Nfkbid* outside of B cell intrinsic studies

Within this study we largely focused on B cell phenotypes that contributed to the humoral response, with an emphasis on observing B-1 populations, which are known to respond to T-independent antigens. However, most high-avidity *T. gondii*-specific antibodies are B-2 derived. Thus, the next logical progression of this system is to look for potential *Nfkbid*-driven T-dependent phenotypes by investigating T follicular helper cells (Tfh) and their contribution to the humoral responses found within *bumble* and resistant mice. Currently only one study has investigated *Nfkbid* phenotypes in T follicular helper cells (Hosokawa et al., 2017), and they found overexpression of *Nfkbid* increased functional Tfh populations and that Tfh differentiation from *Nfkbid*<sup>-/-</sup> T cells is significantly reduced. Because of the integral role Tfh cells have in generating humoral responses (Crotty, 2019), studying potential Tfh phenotypes within both *bumble* and resistant A/J mice during secondary infection will likely lead to fruitful future studies.

An interesting observation made within our bone marrow chimera experiments is the presence of a protective non-hematopoietic or radio-resistant population that requires *Nfkbid*, as only *Nfkbid*-sufficient recipients were able to achieve full protection against type I RH strain challenge. Similar observations have been made in *T. gondii* models for the IFN $\gamma$  and TNF $\alpha$  receptors, which are both required in non-hematopoietic cells for protection against type II strains (Yap & Sher, 1999). However, while the requirement of the IFN $\gamma$  receptor in non-hematopoietic cells is logical, due to the induction of IFN $\gamma$ -induced IRGs for cell autonomous parasite clearance, the role of *Nfkbid* in non-hematopoietic cells is less clear. The identification of these non-hematopoietic cells and the entire role *Nfkbid* has in promoting immunity to *T. gondii* remains to be explored.

### ***Nfkbid* polymorphisms**

We made note of predicted RNA structure differences of a conserved stem loop motif, the constitutive decay element (CDE), found on the 3'UTR of *Nfkbid* mRNA, and how A/J polymorphisms abrogates the P1->L1 structure (Figure 3.16c) thereby shortening the stem loop which serves as the binding site for Roquin, an mRNA degradation factor (Leppek et al., 2013). Shortening these loops leads to lower mRNA degradation due to reduced Roquin binding, and degradation is restored by overexpression of Roquin (Codutti et al., 2015). By this model of molecular action, one would hypothesize that A/J *Nfkbid* mRNA would be resistant to Roquin-mediated degradation due to the abrogation of the stem loop and subsequent reduced Roquin binding, but we in fact found *Nfkbid* transcript levels to be lower in A/J B cells. This is potentially explained by a trait unique to *Nfkbid* mRNA within the entirety of the mouse genome: *Nfkbid* mRNA has two CDE stem loops and therefore may have a different mechanism of regulation not adequately described by single CDE experiments. One possible mechanism is an inhibitory function for the first CDE stem loop, preventing Roquin binding to the second stem loop. Exactly how A/J's *Nfkbid* polymorphism may influence Roquin binding and mRNA degradation remains an open question and an intriguing avenue of research.

### **Protective functions of B-1 cells in *T. gondii* infections**

The exact protective function of B-1 cells remains unknown within the *T. gondii* infection model. The only report of B-1 mediated *T. gondii* immunity linked increased nitric oxide and splenic cytokine levels following transfer of primed B-1 cells into B cell deficient  $\mu$ MT mice (Chen et al., 2003b). In our own experiments, we observed an increase in survival within bone marrow chimeras that received B-1 cells, as well as a delay in time to death of *bumble* mice adoptively transferred B-1 cells. Our data suggests the B-1 mechanism of immunity is through antibody generation, as transcriptomic analysis and intracellular IgG staining show robust class-switch recombination within the A/J B-1 population. However, there are known antibody-independent mechanisms for B-1 cells such as immunomodulation via B-1 derived IL-10 (Lino et al., 2018) or GM-CSF (Hilgendorf et al., 2014), both of which are labeled as CD19+ CD138+ CD43+ plasmablast phenotypes. While we identify large frequencies of these markers within the A/J B-1 compartment, it is difficult to distinguish whether these cells are cytokine and/or antibody producing populations with our current dataset. A more thorough examination of these

CD138+ B-1 populations to identify the mechanism of B-1 mediated immunity to *T. gondii* is necessary.

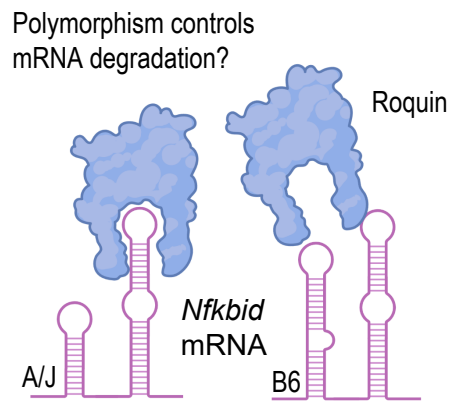
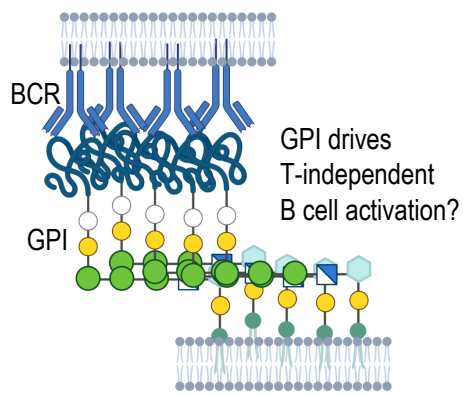
### **GPI-mediated antibody responses**

*T. gondii* GIPL-specific monoclonal antibodies T5 4E10 and T3 3F12 are IgM and IgG3 isotypes, respectively (Tomavo et al., 1994), and though circumstantial, these are two antibody isotypes preferentially generated by B-1 cells (Hayakawa et al., 1985; Savage et al., 2017). We found GIPL-reactive serum IgM antibodies in A/J and C57BL/6J mice 35 days after primary infection, suggesting a durable IgM secreting memory population is continuously secreting GIPL-specific antibodies. IgM memory populations are known to be generated by extrafollicular responses, though there is burgeoning evidence of germinal center reactions also producing affinity matured IgM memory cells (Pape et al., 2011, 2018), and either IgM memory population can arise independent of the other (Papillion et al., 2017). Whether this IgM memory population is a B-1 or B-2 derived memory population is unknown. GPI anchors induces oligomerization of surface antigens (Seong et al., 2013), which may promote T-Independent extrafollicular responses via robust BCR signaling. Testing this hypothesis with a live infection model is likely to be unfeasible, due to dramatic loss in fitness and invasion potential by removing enzymes of the core GPI biosynthesis pathway (Sidik et al., 2016) and hence, GPI-anchored motif from *T. gondii* surface antigens (Seeber et al., 1998). Therefore, testing the ability of GPI anchors to oligomerize multiple surface antigens in lipid nanoparticles then observing any subsequent effect on extrafollicular responses may be informative for vaccine development

### **5.0.3 Summary**

High virulence atypical strains of *T. gondii* are masters of evading the host immune system through a variety of potent virulence factors. The host IFN $\gamma$  response is the primary driver of immunity to *T. gondii*. Atypical strains, however, are capable of evading IFN $\gamma$  induced factors and are lethal in the commonly studied C57BL/6J mouse background. Thus, there is an open question - what is required for protective immunity against high virulence *T. gondii* strains? The aim of the experiments described in this dissertation was to elucidate novel requirements for immunity to high virulence strains of *T. gondii* with an earnest goal of contributing to the creation of an effective vaccine against parasites. We first tested the ability of potent checkpoint blockade therapies to promote survival against atypical strains

of *T. gondii* and found checkpoint blockade was unable to induce control of the infection. We demonstrated that induction of protective immunity against high virulence strains of *T. gondii* is possible, and that this immunological memory is genetically controlled. Genetic mapping of loci that correlated with survival identified *Nfkbid*, an atypical regulator of NF- $\kappa$ B, and a novel host resistance factor that works specifically against *T. gondii* secondary infections. Through investigation of *Nfkbid*, we further find an underappreciated B-1 cell population that is required for full protective immunity against high virulence secondary infections. We also present evidence that this B-1 cell population is heavily activated in resistant, but not susceptible, mouse backgrounds. Within the resistant background, we also show increased reactivity to non-protein *T. gondii* antigens (GPI and GIPL), which represent a potential target for this B-1 population. Altogether, we hypothesize that immunity to the highest virulence strains of *T. gondii* requires that CD8 T cell IFN $\gamma$  responses must be layered with *Nfkbid*-dependent neutralizing antibodies needed to block invasion and subsequent parasite dissemination during infection (Figure 5.1).



*Nfkbid*-dependent Tfh populations?

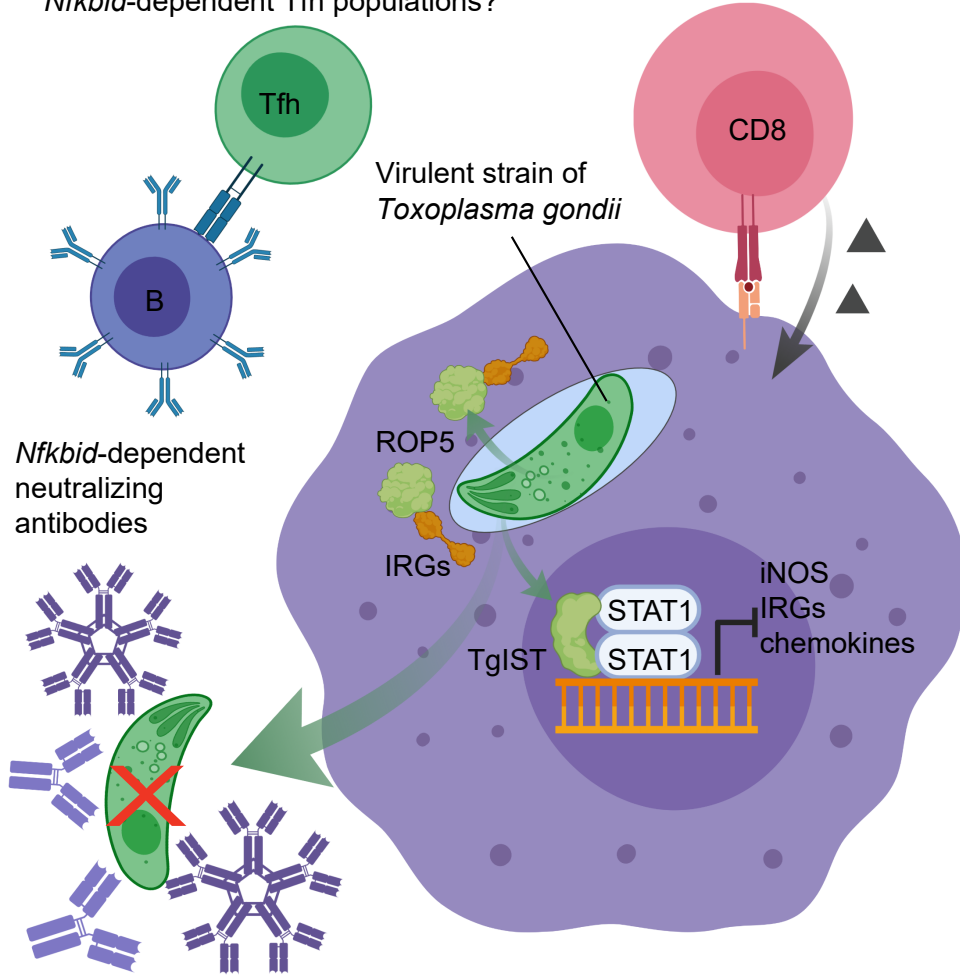


**Figure 5.1: *Nfkbid*-driven immunity to *T. gondii* - current understanding and outstanding questions.** High virulence *T. gondii* parasites that have evaded host CD8 responses and IFN $\gamma$ -induced IRGs are neutralized by antibodies when they are extracellular seeking new cells to infect. We hypothesize that B cells assist known CD8 and IFN $\gamma$ -mediated responses to provide another layer of protection to parasitic challenge, which is antibody mediated and *Nfkbid*-dependent. *Nfkbid* may be differentially regulated by mRNA degradation via Roquin, and that difference may be due to polymorphisms in a conserved stem loop motif in its 3' UTR. GPI anchored proteins may drive T-independent activation of B cells. *Nfkbid* programming of T follicular helper cells may be required for maximal humoral responses.

---

# **Chapter 6**

## **Appendix tables**

**Table 6.1 Genes identified by QTL analysis**

Chromosome 7	MGI ID	Feature Type	Symbol	Name	NS-SNP	UTR-SNP	Syn-SNP	Intron SNP	Region SNP	Non-coding Transcript SNP	Sum Mutation
<b>D7Mit246 = LOD 3.2</b>											
<b>LOD 3.2</b>	MGI:2442512	protein coding gene	Lrnf3	leucine rich repeat and fibronectin type III domain containing 3	0	0	2	6	0	0	8
	MGI:5591188	lncRNA gene	Gm32029	predicted gene, 32029	0	0	0	6	5	0	11
	MGI:1277211	protein coding gene	Tyrobp	TYRO protein tyrosine kinase binding protein	0	0	0	10	6	0	16
	MGI:1344360	protein coding gene	Hcst	hematopoietic cell signal transducer	0	0	1	8	7	0	16
<b>r8261820 = LOD 3.2</b>											
<b>Imputed LOD 3.7</b>	MGI:5683874	CpG island	Cpg18799	CpG island 18799	0	0	0	0	7	0	7
	MGI:3041243	protein coding gene	Nfkbid	nuclear factor of kappa light polypeptide gene enhancer in B cells inhibitor, delta	2	13	2	28	12	0	57
	MGI:5683875	CpG island	Cpg18800	CpG island 18800	0	0	0	0	2	0	2
	MGI:80046	protein coding gene	Apo1	amyloid beta (A4) precursor-like protein 1	0	0	3	35	2	0	40
<b>r8261944 = LOD 3.2</b>											
<b>LOD 3.2</b>	MGI:5683877	CpG island	Cpg18801	CpG island 18801	0	0	0	0	1	0	1
	MGI:5683877	CpG island	Cpg18802	CpG island 18802	0	0	0	0	3	0	3
	MGI:2442334	protein coding gene	Kirrel2	kin of IRRE like 2 (Drosophila)	1	1	0	7	3	0	12
	MGI:5683879	CpG island	Cpg18804	CpG island 18804	0	0	0	0	1	0	1
	MGI:1859637	protein coding gene	Nphs1	nephrosis 1, nephrin	0	5	3	48	2	0	58
	MGI:2675468	antisense lncRNA gene	Nphs1os	nephrosis 1 homolog, nephrin, opposite strand	0	0	0	6	7	5	18
	MGI:5683880	CpG island	Cpg18805	CpG island 18805	0	0	0	0	8	0	3
	MGI:1929093	protein coding gene	Prodh2	proline dehydrogenase (oxidase) 2	0	10	5	40	7	0	62
	MGI:2685928	antisense lncRNA gene	Arhgap33os	Rho GTPase activating protein 33, opposite strand	0	0	0	23	7	11	41
	MGI:2673998	protein coding gene	Arhgap33	Rho GTPase activating protein 33	0	0	0	1	0	0	1
	MGI:2681861	protein coding gene	Proser3	proline and serine rich 3	0	0	0	3	1	0	4
	MGI:2685325	protein coding gene	Hspb6	heat shock protein, alpha-crystallin-related, B6	0	2	0	0	1	0	3
	MGI:1922910	protein coding gene	Lin37	lin-37 homolog (C. elegans)	0	0	0	1	2	0	3
	MGI:1913590	protein coding gene	Psenen	presenilin enhancer gamma secretase subunit	0	0	0	3	0	0	3
	MGI:2678374	protein coding gene	U2af114	U2 small nuclear RNA auxiliary factor 1-like 4	0	0	0	0	3	0	3
	MGI:3655979	protein coding gene	Igf1r1	IGF-like family receptor 1	0	0	0	1	0	0	1
	MGI:6121629	protein coding gene	Gm49396	predicted gene, 49396	0	0	0	0	1	0	1
	MGI:109565	protein coding gene	Kmt2b	lysine (K)-specific methyltransferase 2B	5	0	3	13	1	0	22
	MGI:1891838	protein coding gene	Zbtb32	zinc finger and BTB domain containing 32	2	0	6	14	0	0	22
	MGI:5591241	lncRNA gene	Gm32082	predicted gene, 32082	0	0	0	1	1	0	2
	MGI:98911	protein coding gene	Upk1a	uroplakin 1A	0	0	0	2	2	0	4
	MGI:107460	protein coding gene	Cox6b1	cytochrome c oxidase, subunit 6B1	0	0	0	4	0	0	4
	MGI:99253	protein coding gene	Etv2	ets variant 2	0	0	0	0	2	0	2
	MGI:1924278	lncRNA gene	4921520E09Rik	RIKEN cDNA 4921520E09 gene	0	0	0	0	2	0	2
	MGI:1915285	protein coding gene	Rbm42	RNA binding motif protein 42	0	1	2	14	2	0	19
	MGI:5439451	lncRNA gene	Gm21982	predicted gene 21982	0	0	0	0	39	0	39
	MGI:5683893	CpG island	Cpg18818	CpG island 18818	0	0	0	0	2	0	2
	MGI:5477104	lncRNA gene	Gm26610	predicted gene, 26610	0	0	0	0	2	0	2
	MGI:1919159	protein coding gene	Haus5	HAUS augmin-like complex, subunit 5	1	0	1	15	4	0	21
	MGI:5683894	CpG island	Cpg18819	CpG island 18819	0	0	0	0	1	0	1
	MGI:1916397	protein coding gene	Z200002124Rik	RIKEN cDNA Z200002124 gene	1	0	0	18	3	0	22
	MGI:88113	protein coding gene	Atp4a	ATPase, H+/K+ exchanging, gastric, alpha polypeptide	0	0	0	19	1	0	20
	MGI:1915011	protein coding gene	Tmem147	transmembrane protein 147	0	0	0	0	1	0	1
	MGI:95653	protein coding gene	Gapdh3	glyceraldehyde-3-phosphate dehydrogenase, spermatogenic	0	1	0	20	3	0	24
	MGI:3642392	antisense lncRNA gene	Tmem147os	transmembrane protein 147, opposite strand	0	0	0	7	14	3	24
	MGI:5504050	lncRNA gene	Gm26935	predicted gene, 26935	0	0	0	13	0	0	13

	MGI:2446326	protein coding gene	Sbsn	suprabasin	0	4	0	1	2	0	7
	MGI:1920962	protein coding gene	Dmkn	dermokine	0	0	0	5	0	0	5
	MGI:2441731	protein coding gene	Ffar2	free fatty acid receptor 2	0	1	0	0	2	0	3
	MGI:5591395	lncRNA gene	Gm32236	predicted gene, 32236	0	0	0	1	4	0	5
	MGI:2685324	protein coding gene	Ffar3	free fatty acid receptor 3	0	1	0	0	0	0	1
	MGI:88322	protein coding gene	Cd22	CD22 antigen	0	0	1	2	0	0	3
	MGI:96912	protein coding gene	Mag	myelin-associated glycoprotein	0	0	0	1	0	0	1
	MGI:1923665	protein coding gene	Fam187b	family with sequence similarity 187, member B	0	0	0	4	0	1	5
	MGI:1927471	protein coding gene	Lsr	lipolysis stimulated lipoprotein receptor	0	0	0	0	1	0	1
	MGI:5683905	CpG island	Cpg18830	CpG island 18830	0	0	0	0	1	0	1
	MGI:1201785	protein coding gene	Fxyd5	FXID domain-containing ion transport regulator 5	0	0	0	1	0	0	1
	MGI:1889006	protein coding gene	Fxyd7	FXID domain-containing ion transport regulator 7	0	0	0	1	2	0	3
	MGI:5621869	lncRNA gene	Gm38984	predicted gene, 38984	0	0	0	0	4	0	4
	MGI:1889273	protein coding gene	Fxyd1	FXID domain-containing ion transport regulator 1	0	1	0	2	0	0	3
	MGI:2180197	protein coding gene	Lgi4	leucine-rich repeat LGI family, member 4	1	0	1	1	1	0	4
	MGI:107497	protein coding gene	Fxyd3	FXID domain-containing ion transport regulator 3	0	0	0	3	5	0	8
	MGI:1196620	protein coding gene	Hpn	hepsin	0	0	0	7	1	0	8
	MGI:98247	protein coding gene	Scn1b	sodium channel, voltage-gated, type I, beta	0	0	0	15	6	0	21
	MGI:5683911	CpG island	Cpg18836	CpG island 18836	0	0	0	0	1	0	1
	MGI:5683912	CpG island	Cpg18837	CpG island 18837	0	0	0	0	1	0	1
	MGI:105490	protein coding gene	Gramd1a	GRAM domain containing 1A	1	1	0	10	0	0	12
	MGI:3045288	lncRNA gene	G63003009Rik	RIKEN cDNA G63003009 gene	0	0	0	0	2	0	2
	MGI:5683914	CpG island	Cpg18839	CpG island 18839	0	0	0	0	2	0	2
	MGI:1930867	protein coding gene	Scgb1b2	secretoglobin, family 28, member 2	0	0	0	0	2	0	2
	MGI:3042579	protein coding gene	Scgb2b2	secretoglobin, family 28, member 2	1	0	0	2	6	0	9
	MGI:3782547	protein coding gene	Scgb2b3	secretoglobin, family 28, member 3	1	0	0	0	2	0	3
	MGI:5578756	pseudogene	Scgb2b4-ps	secretoglobin, family 28, member 4, pseudogene	0	0	0	2	0	0	2
	MGI:3782864	protein coding gene	Scgb2b7	secretoglobin, family 28, member 7	0	0	0	1	0	0	1
	MGI:3646832	protein coding gene	Scgb2b30	secretoglobin, family 28, member 30	0	0	0	0	2	0	2

D7Mh224 = LOD 3.2

Chromosome 10	MGI ID	Feature Type	Symbol	Name	NS-SNP	UTR-SNP	Syn-SNP	Intron SNP	Region SNP	Non-coding Transcript SNP	Sum Mutation
rs13480775 = LOD 3.5											
3.5 < LOD < 5.1	MGI:1921893	lncRNA gene	493042222rik	RIKEN cDNA 493042222 gene	0	0	0	0	18	0	18
	MGI:2384918	protein coding gene	Tspan8	tetraspanin 8	0	1	3	55	4	0	63
rs13480776 = LOD 5.1											
Imputed LOD = 6.2	MGI:109559	protein coding gene	Ptpr	protein tyrosine phosphatase, receptor type, R	0	0	0	2	0	0	2
rs13480777 = LOD 5.5											
3.9 < LOD < 5.5	MGI:1919318	protein coding gene	Cno2	CCR4-NOT transcription complex, subunit 2	0	0	0	1	0	0	1
	MGI:3026931	lncRNA gene	5330438012rik	RIKEN cDNA 5330438012 gene	0	0	0	0	1	0	1
	MGI:1100860	protein coding gene	Frs2	fibroblast growth factor receptor substrate 2	0	0	0	2	0	0	2
	MGI:5667359	CpG island	Cpg2230	CpG island 2230	0	0	0	0	1	0	1
	MGI:6098673	lncRNA gene	Gm48903	predicted gene, 48903	0	0	0	0	4	0	4
	MGI:1913948	protein coding gene	Cpsf6	cleavage and polyadenylation specific factor 6	0	3	0	19	1	0	23
	MGI:5667358	CpG island	Cpg2229	CpG island 2229	0	0	0	0	1	0	1
MGI:5621351	lncRNA gene	Gm38466	predicted gene, 38466	0	0	0	0	3	1	4	
rs3670118 = LOD 3.9											

Chromosome 11	MGI ID	Feature Type	Symbol	Name	NS-SNP	UTR-SNP	Syn-SNP	Intron SNP	Region SNP	Non-coding Transcript SNP	Sum Mutation
<b>rs13481109 = LOD 2.3</b>											
<b>2.3 &lt; LOD &lt; 3.5</b>	MGI:107771	protein coding gene	Abr	active BCR-related gene	0	0	0	0	37	0	37
	MGI:5477274	lncRNA gene	Gm26780	predicted gene, 26780	0	0	0	0	6	0	6
	MGI:5825925	lncRNA gene	Gm46288	predicted gene, 46288	0	0	0	0	2	0	2
	MGI:3029307	protein coding gene	Trarg1	trafficking regulator of GLUT4 (SLC24A4) 1	0	2	0	1	0	0	3
	MGI:1858260	protein coding gene	Gosr1	golgi SNAP receptor complex member 1	0	6	0	57	0	0	63
	MGI:107265	protein coding gene	Cpd	carboxypeptidase D	1	11	11	238	0	0	261
MGI:1913851	protein coding gene	Tmigd1	transmembrane and immunoglobulin domain containing 1	0	0	0	20	6	0	26	
<b>D11MIT116 = LOD 3.5</b>											
<b>LOD = 3.5</b>	MGI:1345186	protein coding gene	Blimh	bleomycin hydrolase	1	5	3	159	11	0	179
	MGI:5668402	CpG island	Cpg3299	CpG island 3299	0	0	0	0	7	0	7
	MGI:96285	protein coding gene	Slc6a4	solute carrier family 6 (neurotransmitter transporter,)	2	1	2	53	5	0	63
	MGI:5668404	CpG island	Cpg3301	CpG island 3301	0	0	0	0	1	0	1
	MGI:3649817	lncRNA gene	Gm12343	predicted gene 12343	0	0	0	4	10	1	15
<b>rs13481111 = LOD 3.5</b>											
<b>LOD = 3.5</b>	MGI:2442440	protein coding gene	Efcab5	EF-hand calcium binding domain 5	0	0	0	3	0	0	3
	MGI:2679255	protein coding gene	Suh2	slingshot protein phosphatase 2	0	0	0	2	0	0	2
	MGI:2144501	protein coding gene	Ankr13b	ankyrin repeat domain 13b	2	0	2	1	0	0	5
	MGI:5668412	CpG island	Cpg3309	CpG island 3309	0	0	0	0	2	0	2
	MGI:1927140	protein coding gene	Git1	GIT ArfGAP 1	0	0	0	1	0	0	1
MGI:1914490	protein coding gene	Taok1	TAO kinase 1	0	3	0	1	0	0	4	
<b>rs13481112 = LOD 3.5</b>											
<b>2.4 &lt; LOD &lt; 3.5</b>	MGI:267185	protein coding gene	Myo18a	myosin XVIIIa	0	0	0	2	0	0	2
	MGI:1915814	protein coding gene	Nufip2	nuclear fragile X mental retardation protein interacting protein 2	0	0	0	1	0	0	1
	MGI:5589138	lncRNA gene	Gm29979	predicted gene, 29979	0	0	0	1	0	0	1
	MGI:1924057	protein coding gene	Phf12	PHD finger protein 12	0	0	0	1	0	0	1
	MGI:103309	protein coding gene	Flot2	flotilin 2	0	1	0	2	0	0	3
	MGI:5296816	complex/cluster/region	Mirc12	microRNA cluster 12, including Mir144 through Mir451a	0	0	0	0	1	0	1
	MGI:1202880	protein coding gene	Traf4	TNF receptor associated factor 4	0	0	0	1	0	0	1
	MGI:107726	protein coding gene	Supf6	SPT6, histone chaperone and transcription elongation factor	0	6	1	0	2	0	9
	MGI:108019	protein coding gene	Sdf2	stromal cell derived factor 2	0	1	1	3	0	0	5
	MGI:2136419	protein coding gene	Sarm1	sterile alpha and HEAT/Armadillo motif containing 1	0	12	0	0	2	0	14
	MGI:5668454	CpG island	Cpg3351	CpG island 3351	0	0	0	0	2	0	2
	MGI:98940	protein coding gene	Vtn	vitronectin	3	0	2	3	2	0	10
	MGI:5668455	CpG island	Cpg3352	CpG island 3352	0	0	0	0	8	0	8
	MGI:108012	protein coding gene	Sebox	SEBOX homeobox	0	0	0	0	9	0	9
	MGI:1201387	protein coding gene	Nlk	niemo like kinase	0	0	0	7	0	0	7
	MGI:105051	protein coding gene	Ksr1	kinase suppressor of ras 1	0	0	0	8	0	0	8
	MGI:1926139	protein coding gene	Wsb1	WD repeat and SOCS box-containing 1	0	0	0	1	0	0	1
<b>rs13481117 = LOD 2.4</b>											

Chromosome 17	MGI ID	Feature Type	Symbol	Name	NS-SNP	UTR-SNP	Syn-SNP	Intron SNP	Region SNP	Non-coding Transcript SNP	Sum Mutation
n3714226 = LOD 1.8											
n3714819 = LOD 3.9											
LOD = 3.9	MGI:5674411	CpG island	Cpg9322	CpG island 9322	0	0	0	0	9	0	9
	MGI:2445190	protein coding gene	St6gal2	beta galactoside alpha 2,6 sialyltransferase 2	0	0	0	0	173	0	173
	MGI:5477041	lncRNA gene	Gm26547	predicted gene, 26547	0	0	0	0	11	0	11
	MGI:3761695	protein coding gene	Vmn2r118	vomeronasal 2, receptor 118	0	0	0	0	56	0	56
MGI:1920086	protein coding gene	Pot1b	protection of telomeres 1b	0	0	0	0	61	0	61	
n3709414 = LOD 3.9											
2.6 < LOD < 3.9	MGI:5010833	pseudogene	Gm18648	predicted gene, 18648	0	0	0	0	5	0	5
	MGI:1196464	protein coding gene	Adgr4	adhesion G protein-coupled receptor 64	0	0	0	1	0	0	1
	MGI:1345189	protein coding gene	Zfp119a	zinc finger protein 119a	0	0	0	1	0	0	1
	MGI:2385058	protein coding gene	Zfp959	zinc finger protein 959	0	0	0	1	0	0	1
	MGI:2285323	protein coding gene	Zfp119b	zinc finger protein 119b	0	0	0	0	2	0	2
	MGI:1354171	protein coding gene	Ebi3	Eprotein-Barr virus induced gene 3	0	0	0	1	0	0	1
	MGI:2442355	protein coding gene	Kdm4b	lysine (K)-specific demethylase 4b	0	0	0	1	0	0	1
	MGI:2146808	protein coding gene	Safb2	scaffold attachment factor B2	1	0	0	0	0	1	2
	MGI:2147030	protein coding gene	Catsperd	cation channel sperm associated auxiliary subunit delta	0	0	0	2	2	0	4
	MGI:104647	pseudogene	Fu4-ps1	fucosyltransferase 4, pseudogene 1	0	0	0	0	0	1	1
	MGI:106583	protein coding gene	Rfx2	regulatory factor X, 2 (influences HLA class II expression)	0	0	0	1	0	0	1
	MGI:107848	protein coding gene	Tubb4a	tubulin, beta 4A class IVA	0	0	0	8	0	0	8
	MGI:5674483	CpG island	Cpg9394	CpG island 9394	0	0	0	0	2	0	2
	MGI:3779362	lncRNA gene	Gm11110	predicted gene 11110	0	0	0	11	0	0	11
	MGI:5826226	lncRNA gene	Gm46589	predicted gene, 46589	0	0	0	0	1	0	1
	MGI:1101058	protein coding gene	Tnf9	tumor necrosis factor (ligand) superfamily, member 9	1	0	1	0	0	0	2
	MGI:5674485	CpG island	Cpg9396	CpG island 9396	0	0	0	0	2	0	2
	MGI:1355317	protein coding gene	Tnf14	tumor necrosis factor (ligand) superfamily, member 14	0	0	0	0	1	0	1
	MGI:88227	protein coding gene	C3	complement component 3	0	0	0	4	0	0	4
	MGI:5531240	miRNA gene	Mir6978	microRNA 6978	0	0	0	0	1	0	1
D17Mt20 = LOD 2.6											
											0

**Table 6.1: Genes identified by QTL analysis** For each of the four QTLs that define secondary infection immunity to *T. gondii*, a list of all genes that have  $\geq 1$  DNA polymorphisms between A/J and C5BL/6J mice, and are encoded within the QTL boundaries defined by the maximal genetic marker (real or imputed markers inferred in r/QTL) and

the two flanking markers on either side; LOD scores and position are indicated. For each gene, its location and unique identifiers are listed, as well as the number and class of small nucleotide polymorphism (SNP) between A/J and C57BL/6J are shown. Total number of SNPs for each gene were also tallied ('Sum mutation'), and in bold are genes who's SNPs are two standard deviations greater than the average SNP for that class within the QTL region. In these QTL regions, there were also 476 (chr7), 88 (chr10), 40 (chr11) and 375 SNPs (chr17) that did not associate with any gene in the QTL boundaries. UTR, untranslated region; 'Region SNP', SNPs that are +/- 2 kb of the gene boundaries. Data obtained from Mouse Genome Informatics (MGI).

---

**Table 6.2: List of bone marrow chimeras generated in this paper**

Bone Marrow Chimeras		
Recipient Mouse	Donor BM	Donor PerC
CD45.1	C57BL/6J	C57BL/6J
CD45.1	C57BL/6J	None
CD45.1	<i>bumble</i>	C57BL/6J
CD45.1	<i>bumble</i>	None
CD45.1	1:1 muMT C57BL/6J	C57BL/6J
CD45.1	1:1 muMT  <i>bumble</i>	None
C57BL/6J	C57BL/6J	C57BL/6J
<i>bumble</i>	C57BL/6J	C57BL/6J
<i>bumble</i>	<i>bumble</i>	C57BL/6J
<i>bumble</i>	<i>bumble</i>	None

**Table 6.3: Antibodies**

Antibodies used			
Antibodies	Source	Identifier	Clone
CD11b BUV395	BDBioscience	Cat# 563553	M1/70
CD11b BV421	BDBioscience	Cat# 562605	M1/70
CD11b FITC	eBioscience	Cat# 11-0112-81	M1/70
CD11b Pacific Blue	BioLegend	Cat# 101224	M1/70
CD11c eFlour450	eBioscience	Cat# 48-0114-82	N418
CD138/Syndecan-1 BV510	BDBioscience	Cat# 558626	281-2
CD138/Syndecan-1 BV650	BioLegend	Cat# 142518	281-2
CD19 BV785	BioLegend	Cat# 115543	6D5
CD19 PE	BioLegend	Cat# 115508	6D5
CD19 PerCPCy5.5	eBioscience	Cat# 45-0193-82	ebio1D3
CD21/CD35-(CR2/CR1) FITC	BioLegend	Cat# 123407	7E9
CD21/CD35-PE	BioLegend	Cat# 123409	7E9
CD23 AF-700	BioLegend	Cat# 101631	B3B4
CD23 Pacific Blue	BioLegend	Cat# 101615	B3B4
CD25 APC	Invitrogen	Cat# 50-112-9564	PC61.5
CD267/TACI AF-647	BDBiosciences	Cat# 558410	8F10
CD268 (BAFF-R) PE	BioLegend	Cat# 134103	7H22-E16
CD3 APC-eFluor780	eBioscience	Cat# 47-0032-82	17A2
CD38 BUV395	BDBiosciences	Cat# 740245	90/CD38

CD4 eFlour450	eBioscience	Cat# 48-0041-82	GK1.5
CD4 PE-Cy7	BioLegend	Cat# 100422	GK1.5
CD43 Biotin	BDBioscience	Cat# 553269	S7
CD43 BUV737	BDBioscience	Cat# 612840	S7
CD43 BV510	BDBioscience	Cat# 563206	S7
CD45.2 eFlour450	eBioscience	Cat# 48-0454-82	104
CD45R/B220 APC-Cy7	BDBioscience	Cat# 561102	RA3-6B2
CD45R/B220 APC-Cy7	BioLegend	Cat# 103224	RA3-6B2
CD45R/B220 BUV-661	BDBioscience	Cat# 612972	RA3-6B2
CD45R/B220 BV421	BDBiosciences	Cat# 562922	RA3-6B2
CD5 APC	BioLegend	Cat# 100626	53-7.3
CD5 APC-Cy7	BioLegend	Cat# 100649	53-7.3
CD5 PerCP-Cy5.5	BioLegend	Cat# 100623	53-7.3
CD73 PE-Cy7	eBioscience	Cat# 25-0731-82	eBioTY/11.9
CD80 BUV563	BDBiosciences	Cat# 741272	16-10A1
CD80 BV711	BioLegend	Cat# 104743	16-10A1
CD8 $\alpha$ APC	eBioscience	Cat# 17-0081-83	53-6.7
CD8 $\alpha$ BV510	BioLegend	Cat# 100752	53-6.7
FCRL5 af488	R&D Systems	Cat# FAB6757G	Polyclonal
Foxp3 PE	BioLegend	Cat# 126403	MF-14
Goat anti-mouse IgG HRP	SouthernBiotech	Cat# 1030-05	Polyclonal
Goat anti-mouse IgM HRP	SouthernBiotech	Cat# 1020-05	Polyclonal
Goat anti-mouse IgM BIOT	SouthernBiotech	Cat# 1021-08	Polyclonal
Goat anti-mouse IgM UNLB	SouthernBiotech	Cat# 1021-01	Polyclonal
Granzyme-B FITC	BioLegend	Cat# 515403	GB11
IFN $\gamma$ PE	eBioscience	Cat# 12-7311-82	XMG1.2
IgD FITC	BioLegend	Cat# 405703	11-26c.2a
IgD PE-Dazzle594	BioLegend	Cat# 405741	11-26c.2a
IgG1 APC	BioLegend	Cat# 406610	RMG1-1
IgG1 FITC	BioLegend	Cat# 406605	RMG1-1
IgG2a FITC	BioLegend	Cat# 407105	RMG2a-62
IgG2a PerCP-Cy5.5	BioLegend	Cat# 407112	RMG2a-62
IgG2b FITC	BioLegend	Cat# 406705	RMG2b-1
IgG2b PE	BioLegend	Cat# 406708	RMG2b-1
IgG3 BV421	BDBioscience	Cat# BDB565808	R40-82
IgM BV605	BioLegend	Cat# 406523	RMM-1

IgM PE-Cy7	BioLegend	Cat# 406514	RMM-1
IgM[a] PE	BDBioscience	Cat# 553517	DS-1
IgM[b] PE	BDBioscience	Cat# 553521	AF6-78
IL-2 APC	BioLegend	Cat# 503809	JES6-5H4
Ly-6C PE-Cy7	eBioscience	Cat# 25-5932-80	HK1.4
Ly-6G (Gr 1) APC	eBioscience	Cat# 17-9668-80	1A8-Ly6G
Mouse IgM	SouthernBiotech	Cat# 0101-01	11E10
NK-1.1 FITC	eBioscience	Cat# 11-5941-81	PK136
Streptavidin APC	BDBioscience	Cat# 554067	
CD4 PerCP/Cy5.5	Biolegend	Cat# 100434	GK1.5
F4/80 PerCP/Cy5.5	Biolegend	Cat# 123127	BM8
NK-1.1 PerCP/Cy5.5	Biolegend	Cat# 45-5941-80	PK136
CD8 $\alpha$ PerCP/Cy5.5	Biolegend	Cat# 100733	53-6.7
Gr-1 PerCP/Cy5.5	Biolegend	Cat# 108427	RB6-8C5
Mouse IgG af594	Invitrogen	Cat# A-11032	Polyclonal
IgG(H+L) af350	Invitrogen	Cat# A11045	Polyclonal
SAG1 unconjugated	BEI	Cat# NR-50255	T4 1E5
P35 unconjugated	BEI	Cat# NR-50259	T4 3F12
SAG3 unconjugated	BEI	Cat# NR-50257	T4 1F12
GPI unconjugated	BEI	Cat# NR-50253	T3 3F12
GRA3 unconjugated	BEI	Cat# NR-50269	T6 2H11

**Table 6.4: Blocking Reagents**

Blocking reagents	Source	Identifier
Normal Mouse Serum	Jackson Immunoresearch	Cat# 015-000-120
Normal Syrian Hamster Serum	Jackson Immunoresearch	Cat# 007-000-120
CD16/CD32 Mouse BD Fc Block	BDBioscience	Cat# 553142

**Table 6.5: Commercial Products**

Commercial Products	Source	Identifier
BD Cytofix/Cytoperm Solution Kit	BDBioscience	Cat# 554714
Foxp3 / Transcription Factor Staining Buffer Set	eBioscience	Cat# 50-112-8857
4-20% Mini-PROTEAN Precast Protein Gels	Bio-Rad	Cat# 4561096
Trans-Blot Turbo Mini PVDF Transfer Pack	Bio-Rad	Cat# 1704156
RNeasy Plus Mini Kit	Qiagen	Cat# 74134
High-Capacity cDNA Reverse Transcription Kit	Applied Biosystems	Cat# 4368814
EasySep Pan-B cell Isolation kits	Stem Cell Technologies	Cat# 19844

**Table 6.6: qPCR probes and reagents**

qPCR probes and reagents	Source	Identifier
TaqMan probes: <i>Nfkbid</i> - Assay ID: Mm00549082_m1	ThermoFisher	Cat# 4331182
TaqMan probes: <i>Actb</i> - Assay ID: Mm02619580_g1	ThermoFisher	Cat# 4331182
TaqMan™ Fast Advanced Master Mix - 1mL	ThermoFisher	Cat# 4444556

**Table 6.7: Chemicals and reagents**

Chemicals and reagents	Source	Identifier
Mycophenolic Acid	Millipore Sigma	Cat# 80058-446
Xanthine	Alfa Aesar	Cat# AAA11077-22
Fetal Bovine Serum	Omega Scientific	Cat# FB-03
Tween-20	VWR	Cat# 97062-332
Fortified Dehydrated Milk	Raleys	
Western HRP Substrate	Millipore Sigma	Cat# WBLUF0500
TMB Substrate	Invitrogen	Cat# 501129758
Normal Goat Serum	Omega Scientific	Cat# NG-11
TritonX-100	Millipore Sigma	Cat# TX1568
$\beta$ -Mercaptoethanol	Fisher	Cat# 21985-023
Bovine Serum Albumin	Millipore Sigma	Cat# EM-2930
DMEM	Gibco	Cat# 10566024
RPMI	Gibco	Cat# 61870127
PBS	Gibco	Cat# 10010049
Brefeldin A	eBioscience	Cat# 00-4506-51
Formaldehyde	Polysciences	Cat# NC9864402
LPS	Millipore Sigma	Cat# L4391-1MG
D-luciferin	Gold Biotechnology	Cat# LUCK-100
30% Acrylamide/Bis Solution	Bio-Rad	Cat# 1610156
TEMED	Invitrogen	Cat# 15524010

**Table 6.8: Experimental Models: Parasite strains**

Experimental Models: Parasite strains	Source
RH $\Delta ku80 \Delta hxgprt$ (type I)	Huyn and Carruthers, 2007
RH (1-1) <i>GFP::cLUC</i> (type I)	Boyle, 2007
RH $\Delta up \Delta ompdc$ (type I)	Fox and Bzik, 2010
GT1 (type I)	Dubey, 1980
GT1 <i>GFP::cLuc</i> (type I)	This Paper

CEP <i>hxgprt</i> - (type III)	Pfefferkorn and Colby 1977
MAS	Darde, 1992
MAS <i>GFP::cLuc</i> (2C8) (HG4)	Jensen, 2015
GUY-MAT (HG5)	Carme, 2002
FOU (HG6)	Darde, 1992
GPHT (HG6)	Darde, 1996
TgCATBr5 (HG7)	Dubey, 2004
GUY-DOS (HG10)	Carme, 2002
VAND (HG10)	Bossi, 1998

**Table 6.9: Experimental Models: Plasmid**

Experimental Models: Plasmid	Source
GFP::cLUC	Saeij, 2005

**Table 6.10: Experimental Models: Cell Lines**

Experimental Models: Cell Lines	Source
HFFs	Boothroyd lab
Mouse Fibroblasts	Sinai Lab

**Table 6.11: Experimental Models: Organisms/strains**

Experimental Models: organisms/strains	Source	Identifier
C57BL/6J	Jackson Laboratory	000664
A/J	Jackson Laboratory	000646
B6.SJL-Ptprca Pepcb/BoyJ	Jackson Laboratory	002014
B10.A-H2a H2- T18a/SgSnJ	Jackson Laboratory	000469
B6AF1/J (A/J x C57BL/6J F1 progeny)	Jackson Laboratory	100002

B6.129S2- Ighmtm1Cgn/J (muMT)	Jackson Laboratory	002288
C57BL/6J- Chr7A/J/NaJ	Jackson Laboratory	004385
C57BL/6J- Chr10A/J/NaJ	Jackson Laboratory	004388
C57BL/6J- Nfkbidm1Btlr/Mmmh	MMRRC	RRID:MMRRC_036725 -MU

**Table 6.12: Experimental Models: Recombinant Inbred Panel**

Experimental Models: Recombinant Inbred Panel	Source	Identifier
Strain	Source	Identifier
AXB1	Jackson Laboratory	001673
AXB2	Jackson Laboratory	001674
AXB4	Jackson Laboratory	001676
AXB5	Jackson Laboratory	001677
AXB6	Jackson Laboratory	001678
AXB8	Jackson Laboratory	001679
AXB10	Jackson Laboratory	001681
AXB12	Jackson Laboratory	001683
AXB13	Jackson Laboratory	001826
AXB15	Jackson Laboratory	001685
AXB19	Jackson Laboratory	001687
AXB23	Jackson Laboratory	001690
AXB24	Jackson Laboratory	001691
BXA1	Jackson Laboratory	001692
BXA2	Jackson Laboratory	001693
BXA4	Jackson Laboratory	001694
BXA7	Jackson Laboratory	001696
BXA8	Jackson Laboratory	001697
BXA11	Jackson Laboratory	001699
BXA12	Jackson Laboratory	001700
BXA13	Jackson Laboratory	001701

BXA14	Jackson Laboratory	001702
BXA16	Jackson Laboratory	001703
BXA24	Jackson Laboratory	001710
BXA25	Jackson Laboratory	001711
BXA26	Jackson Laboratory	001999

**Table 6.13: Deposited Data**

Deposited Data	Source	Identifier
Raw sequence data	NCBI SRA	Bioproject PR-JNA637442

**Table 6.14: Software**

Software	Source	Identifier
Graphpad Prism 9	Graphpad	graphpad.com/scientific-software/prism/
r v3.6.3	r	r-project.org/
R/qtl	1.44-9	rqtl.org/
Bioconductor	Bioconductor	bioconductor.org/
Mousemine	Mousemine	mousemine.org
GSEA v4.0.3	GSEA	gsea-msigdb.org/gsea/index.jsp
Bluebee Genomics Platform	Lexogen	bluebee.com/lexogen/
Excel	Microsoft	microsoft.com/en-us/microsoft-365/excel
Flowjo v 10.7.1	BDBioscience	flowjo.com/
Image Lab v 6.1	Bio-Rad	bio-rad.com/en-us/product/image-lab-software

**Table 6.15: Instruments**

Instruments	Source	Identifier
Nikon Eclipse Ti-U	Nikon	n/a
LSR II Flow Cytometer	BDBioscience	n/a
Aria II Cell Sorter	BDBioscience	n/a
ZE5 Cell Analyzer	Bio-Rad	n/a
X-RAD 320	Precision X-Ray	n/a
IVIS Spectrum	Xenogen	n/a
Gene Pulser Xcell Electroporation System	Bio-Rad	n/a
Mx3000P qPCR System	Agilent	n/a
Epoch Microplate Spectrophotometer	Biotek	n/a

# Bibliography

- Adori, M., Pedersen, G. K., Adori, C., Erikson, E., Khoenkhoen, S., Stark, J. M., Choi, J. H., Dosenovic, P., Karlsson, M. C. I., Beutler, B., & Karlsson Hedestam, G. B. (2017). Altered Marginal Zone B Cell Selection in the Absence of I $\kappa$ BNS. *The Journal of Immunology*, *200*(2), ji1700791.
- Ahmed, R., Salmi, A., Butler, L., Chiller, J., & Oldstone, M. B. (1984). Selection of genetic variants of lymphocytic choriomeningitis virus in spleens of persistently infected mice. Role in suppression of cytotoxic T lymphocyte response and viral persistence. *The Journal of experimental medicine*, *160*(2), 521–540.
- Alfei, F., Kanev, K., Hofmann, M., Wu, M., Ghoneim, H. E., Roelli, P., Utzschneider, D. T., von Hoesslin, M., Cullen, J. G., Fan, Y., Eisenberg, V., Wohlleber, D., Steiger, K., Merkler, D., Delorenzi, M., Knolle, P. A., Cohen, C. J., Thimme, R., Youngblood, B., & Zehn, D. (2019). TOX reinforces the phenotype and longevity of exhausted T cells in chronic viral infection. *Nature*, *571*(7764), 265–269.  
URL <http://dx.doi.org/10.1038/s41586-019-1326-9>
- Alugupalli, K. R., Leong, J. M., Woodland, R. T., Muramatsu, M., Honjo, T., & Gerstein, R. M. (2004). B1b lymphocytes confer T cell-independent long-lasting immunity. *Immunity*, *21*(3), 379–390.
- Antonaki, A., Demetriades, C., Polyzos, A., Banos, A., Vatsellas, G., Lavigne, M. D., Apostolou, E., Mantouvalou, E., Papadopoulou, D., Mosialos, G., & Thanos, D. (2011). Genomic analysis reveals a novel nuclear factor- $\kappa$ B (NF- $\kappa$ B)-binding site in Alu-repetitive elements. *Journal of Biological Chemistry*, *286*(44), 38768–38782.  
URL <http://dx.doi.org/10.1074/jbc.M111.234161>
- Arnold, C. N., Pirie, E., Dosenovic, P., McInerney, G. M., Xia, Y., Wang, N., Li,

- X., Siggs, O. M., Karlsson Hedestam, G. B., & Beutler, B. (2012). A forward genetic screen reveals roles for Nfkbid, Zeb1, and Ruvbl2 in humoral immunity. *Proceedings of the National Academy of Sciences*, *109*(31), 12286–12293.
- Attanasio, J., & Wherry, E. J. (2016). Costimulatory and coinhibitory receptor pathways in infectious disease. *Immunity*, *44*(5), 1052–1068.
- Aubert, R. D., Kamphorst, A. O., Sarkar, S., Vezys, V., Ha, S.-J., Barber, D. L., Ye, L., Sharpe, A. H., Freeman, G. J., & Ahmed, R. (2011). Antigen-specific CD4 T-cell help rescues exhausted CD8 T cells during chronic viral infection. *Proceedings of the National Academy of Sciences*, *108*(52), 21182–21187.
- Aurajo, F., Williams, D., Grumet, F. C., & Remington, J. (1979). Strain-dependent differences in murine susceptibility to coccidia. *Infection and Immunity*, *26*(3), 1111–1115.
- Bailey, D. W. (1971). Recombinant-inbred strains. An aid to finding identity, linkage, and function of histocompatibility and other genes. *Transplantation*, *11*(3), 325–327.
- Barber, D. L., Mayer-Barber, K. D., Feng, C. G., Sharpe, A. H., & Sher, A. (2011). CD4 T cells promote rather than control tuberculosis in the absence of PD-1–mediated inhibition. *The Journal of Immunology*, *186*(3), 1598–1607.
- Barber, D. L., Wherry, E. J., Masopust, D., Zhu, B., Allison, J. P., Sharpe, A. H., Freeman, G. J., & Ahmed, R. (2006). Restoring function in exhausted CD8 T cells during chronic viral infection. *Nature*, *439*(7077), 682–687.
- Barboni, E., Pliego Rivero, B., George, A. J., Martin, S. R., Renouf, D. V., Hounsell, E. F., Barber, P. C., & Morris, R. J. (1995). The glycoposphatidylinositol anchor affects the conformation of Thy-1 protein. *Journal of Cell Science*, *108*(2), 487–497.
- Basavaraju, A. (2016). Toxoplasmosis in HIV infection: An overview. *Tropical Parasitology*, *6*(2), 129–135.
- Batz, M. B., Hoffman, S., MORRIS, J. G., HOFFMANN, S., & MORRIS, J. G. (2012). Ranking the Disease Burden of 14 Pathogens in Food Sources in the United States Using Attribution Data from Outbreak Investigations and Expert Elicitation. *Journal of Food Protection*, *75*(7), 1278–1291.

- Baumgarth, N. (2017). A Hard(y) Look at B-1 Cell Development and Function. *The Journal of Immunology*, 199(10), 3387–3394.
- Baumgarth, N., Herman, O. C., Jager, G. C., Brown, L., Herzenberg, L. A. L. A., & Herzenberg, L. A. L. A. (1999). Innate and acquired humoral immunities to influenza virus are mediated by distinct arms of the immune system. *Immunology*, 96(March), 2250–2255.
- Baumgarth, N., Jager, G. C., Herman, O. C., & Herzenberg, L. a. (2000). CD4+ T cells derived from B cell-deficient mice inhibit the establishment of peripheral B cell pools. *Proceedings of the National Academy of Sciences of the United States of America*, 97(9), 4766–4771.
- Behnke, M. S., Fentress, S. J., Mashayekhi, M., Li, L. X., Taylor, G. A., & Sibley, L. D. (2012). The polymorphic pseudokinase ROP5 controls virulence in *Toxoplasma gondii* by regulating the active kinase ROP18. *PLoS Pathog*, 8(11), e1002992.
- Behnke, M. S., Khan, A., Lauron, E. J., Jimah, J. R., Wang, Q., Tolia, N. H., & Sibley, L. D. (2015). Rhoptry proteins ROP5 and ROP18 are major murine virulence factors in genetically divergent South American strains of *Toxoplasma gondii*. *PLoS Genet*, 11(8), e1005434.
- Beiting, D. P., Hidano, S., Baggs, J. E., Geskes, J. M., Fang, Q., Wherry, E. J., Hunter, C. A., Roos, D. S., & Cherry, S. (2015). The orphan nuclear receptor TLX is an enhancer of STAT1-mediated transcription and immunity to *Toxoplasma gondii*. *PLoS Biology*, 13(7), 1–23.
- Benci, J. L., Xu, B., Qiu, Y., Wu, T. J., Dada, H., Twyman-Saint Victor, C., Cucolo, L., Lee, D. S. M., Pauken, K. E., & Huang, A. C. (2016). Tumor interferon signaling regulates a multigenic resistance program to immune checkpoint blockade. *Cell*, 167(6), 1540–1554.
- Berthier-Vergnes, O., El Kharbili, M., de la Fouchardière, A., Pointecouteau, T., Verrando, P., Wierinckx, A., Lachuer, J., Le Naour, F., & Lamartine, J. (2011). Gene expression profiles of human melanoma cells with different invasive potential reveal TSPAN8 as a novel mediator of invasion. *British journal of cancer*, 104(1), 155–165.

- Bhadra, R., Cobb, D. A., & Khan, I. A. (2013). Donor CD8+ T cells prevent *Toxoplasma gondii* de-encystation but fail to rescue the exhausted endogenous CD8+ T cell population. *Infection and immunity*, *81*(9), 3414–3425.
- Bhadra, R., Gigley, J. P., & Khan, I. A. (2011a). Cutting Edge: CD40–CD40 Ligand Pathway Plays a Critical CD8-Intrinsic and -Extrinsic Role during Rescue of Exhausted CD8 T Cells. *The Journal of Immunology*, *187*(9), 4421 LP – 4425. URL <http://www.jimmunol.org/content/187/9/4421.abstract>
- Bhadra, R., Gigley, J. P., & Khan, I. A. (2012). PD-1–mediated attrition of polyfunctional memory CD8+ T cells in chronic *Toxoplasma* infection. *The Journal of infectious diseases*, *206*(1), 125–134.
- Bhadra, R., Gigley, J. P., Weiss, L. M., & Khan, I. A. (2011b). Control of *Toxoplasma* reactivation by rescue of dysfunctional CD8 + T-cell response via PD-1-PDL-1 blockade. *Proceedings of the National Academy of Sciences of the United States of America*, *108*(22), 9196–9201.
- Blandino, R., & Baumgarth, N. (2019). Secreted IgM: New tricks for an old molecule. *Journal of leukocyte biology*, *106*(5), 1021–1034.
- Boothroyd, J. C. (2009). Expansion of host range as a driving force in the evolution of *Toxoplasma*. *Memorias do Instituto Oswaldo Cruz*, *104*(2), 179–184.
- Boothroyd, J. C., & Grigg, M. E. (2002). Population biology of *Toxoplasma gondii* and its relevance to human infection: do different strains cause different disease? *Current Opinion in Microbiology*, *5*(4), 438–442.
- Bos, N. A., Kimura, H., Meeuwse, C. G., Visser, H. D., Hazenberg, M. P., Westmann, B. S., Pleasants, J. R., Benner, R., & Marcus, D. M. (1989). Serum immunoglobulin levels and naturally occurring antibodies against carbohydrate antigens in germ-free BALB/c mice fed chemically defined ultrafiltered diet. *European journal of immunology*, *19*(12), 2335–2339.
- Bourgeois, C., Rocha, B., & Tanchot, C. (2002). A role for CD40 expression on CD8+ T cells in the generation of CD8+ T cell memory. *Science*, *297*(5589), 2060–2063.
- Boyer, K., Hill, D., Mui, E., Wroblewski, K., Karrison, T., Dubey, J. P., Sautter, M., Noble, A. G., Withers, S., Swisher, C., Heydemann, P., Hosten, T., Babiarz, J., Lee, D., Meier, P., & McLeod, R. (2011). Unrecognized ingestion of *Toxoplasma*

- gondii oocysts leads to congenital toxoplasmosis and causes epidemics in North America. *Clinical Infectious Diseases*, 53(11), 1081–1089.
- Brahmamdam, P., Inoue, S., Unsinger, J., Chang, K. C., McDunn, J. E., & Hotchkiss, R. S. (2010). Delayed administration of anti-PD-1 antibody reverses immune dysfunction and improves survival during sepsis. *Journal of Leukocyte Biology*, 88(2), 233–240.  
URL <https://doi.org/10.1189/jlb.0110037>
- Brown, C. R., Hunter, C. A., Estes, R. G., Beckmann, E., Forman, J., David, C., Remington, J. S., & McLeod, R. (1995). Definitive identification of a gene that confers resistance against *Toxoplasma* cyst burden and encephalitis. *Immunology*, 85(3), 419–28.
- Brown, D. A., & Rose, J. K. (1992). Sorting of GPI-anchored proteins to glycolipid-enriched membrane subdomains during transport to the apical cell surface. *Cell*, 68(3), 533–544.
- Butikofer, P., Malherbe, T., Boschung, M., & Roditi, I. (2001). GPI-anchored proteins: now you see'em, now you don't. *The FASEB journal*, 15(2), 545–548.
- Butler, N. S., Moebius, J., Pewe, L. L., Traore, B., Doumbo, O. K., Tygrett, L. T., Waldschmidt, T. J., Crompton, P. D., & Harty, J. T. (2012). Therapeutic blockade of PD-L1 and LAG-3 rapidly clears established blood-stage *Plasmodium* infection. *Nature immunology*, 13(2), 188–195.
- Campos, M. A. S., Almeida, I. C., Takeuchi, O., Akira, S., Valente, E. P., Procópio, D. O., Travassos, L. R., Smith, J. A., Golenbock, D. T., & Gazzinelli, R. T. (2001). Activation of Toll-Like Receptor-2 by Glycosylphosphatidylinositol Anchors from a Protozoan Parasite. *The Journal of Immunology*, 167(1), 416–423.
- Carme, B., Bissuel, F., Ajzenberg, D., Bouyne, R., Aznar, C., Demar, M., Bichat, S., Louvel, D., Bourbigot, A. M., Peneau, C., Neron, P., & Dardé, M. L. (2002). Severe acquired toxoplasmosis in immunocompetent adult patients in French Guiana. *Journal of Clinical Microbiology*, 40(11), 4037–4044.
- Casciotti, L., Ely, K. H., Williams, M. E., & Khan, I. A. (2002). CD8<sup>+</sup>-T-cell immunity against *Toxoplasma gondii* can be induced but not maintained in mice lacking conventional CD4<sup>+</sup> T cells. *Infection and Immunity*, 70(2), 434–443.

- Castigli, E., Wilson, S. A., Scott, S., Dedeoglu, F., Xu, S., Lam, K.-P., Bram, R. J., Jabara, H., & Geha, R. S. (2005). TACI and BAFF-R mediate isotype switching in B cells. *The Journal of experimental medicine*, 201(1), 35–39.
- Cavaillès, P., Flori, P., Papapietro, O., Bisanz, C., Lagrange, D., Pilloux, L., Massera, C., Cristinelli, S., Jublot, D., Bastien, O., Loeuillet, C., Aldebert, D., Touquet, B., Fournié, G. J., & Cesbron-Delauw, M. F. (2014). A Highly Conserved Toxo1 Haplotype Directs Resistance to Toxoplasmosis and Its Associated Caspase-1 Dependent Killing of Parasite and Host Macrophage. *PLOS Pathogens*, 10(4), e1004005.  
URL <https://doi.org/10.1371/journal.ppat.1004005>
- Chambers, C. A., Sullivan, T. J., Truong, T., & Allison, J. P. (1998). Secondary but not primary T cell responses are enhanced in CTLA-4-deficient CD8+ T cells. *European journal of immunology*, 28(10), 3137–3143.
- Chen, L. F., & Greene, W. C. (2004). Shaping the nuclear action of NF- $\kappa$ B. *Nature Reviews Molecular Cell Biology*, 5(5), 392–401.
- Chen, M., Aosai, F., Mun, H. S., Norose, K., Hata, H., & Yano, A. (2000). Anti-HSP70 autoantibody formation by B-1 cells in *Toxoplasma gondii*-infected mice. *Infection and Immunity*, 68(9), 4893–4899.
- Chen, M., Aosai, F., Norose, K., Mun, H., & Yano, A. (2003a). The role of anti-HSP70 autoantibody-forming VH1–JH1 B-1 cells in *Toxoplasma gondii*-infected mice. *International immunology*, 15(1), 39–47.
- Chen, M., Mun, H. S., Piao, L. X., Aosai, F., Norose, K., Mohamed, R. M., Belal, U. S., Fang, H., Ahmed, A. K., Kang, H. K., Matsuzaki, G., Kitamura, D., & Yano, A. (2003b). Induction of Protective Immunity by Primed B-1 Cells in *Toxoplasma gondii*-Infected B Cell-Deficient Mice. *Microbiology and Immunology*, 47(12), 997–1003.
- Cheng, J., Wang, R., Zhong, G., Chen, X., Cheng, Y., Li, W., & Yang, Y. (2020). ST6GAL2 downregulation inhibits cell adhesion and invasion and is associated with improved patient survival in breast cancer. *OncoTargets and therapy*, 13, 903.
- Choi, Y. S., & Baumgarth, N. (2008). Dual role for B-1a cells in immunity to influenza virus infection. *Journal of Experimental Medicine*, 205(13), 3053–3064.

- Chou, M. Y., Fogelstrand, L., Hartvigsen, K., Hansen, L. F., Woelkers, D., Shaw, P. X., Choi, J., Perkmann, T., Bäckhed, F., Miller, Y. I., Hörkkö, S., Corr, M., Witztum, J. L., & Binder, C. J. (2009). Oxidation-specific epitopes are dominant targets of innate natural antibodies in mice and humans. *Journal of Clinical Investigation*, *119*(5), 1335–1349.
- Christian, F., Smith, E., & Carmody, R. (2016). The Regulation of NF- $\kappa$ B Subunits by Phosphorylation. *Cells*, *5*(1), 12.
- Chu, H. H., Chan, S.-W., Gosling, J. P., Blanchard, N., Tsitsiklis, A., Lythe, G., Shastri, N., Molina-París, C., & Robey, E. A. (2016). Continuous effector CD8<sup>+</sup> T cell production in a controlled persistent infection is sustained by a proliferative intermediate population. *Immunity*, *45*(1), 159–171.
- Churchill, G. A., Airey, D. C., Allayee, H., Angel, J. M., Attie, A. D., Beatty, J., Beavis, W. D., Belknap, J. K., Bennett, B., Berrettini, W., Bleich, A., Bogue, M., Broman, K. W., Buck, K. J., Buckler, E., Burmeister, M., Chesler, E. J., Cheverud, J. M., Clapcote, S., Cook, M. N., Cox, R. D., Crabbe, J. C., Crusio, W. E., Darvasi, A., Deschepper, C. F., Doerge, R. W., Farber, C. R., Forejt, J., Gaile, D., Garlow, S. J., Geiger, H., Gershenfeld, H., Gordon, T., Gu, J., Gu, W., de Haan, G., Hayes, N. L., Heller, C., Himmelbauer, H., Hitzemann, R., Hunter, K., Hsu, H.-C., Iraqi, F. A., Ivandic, B., Jacob, H. J., Jansen, R. C., Jepsen, K. J., Johnson, D. K., Johnson, T. E., Kempermann, G., Kendzioriski, C., Kotb, M., Kooy, R. F., Llamas, B., Lammert, F., Lassalle, J.-M., Lowenstein, P. R., Lu, L., Luskis, A., Manly, K. F., Marcucio, R., Matthews, D., Medrano, J. F., Miller, D. R., Mittleman, G., Mock, B. A., Mogil, J. S., Montagutelli, X., Morahan, G., Morris, D. G., Mott, R., Nadeau, J. (2004). The Collaborative Cross, a community resource for the genetic analysis of complex traits. *Nature Genetics*, *36*(11), 1133–1137.  
URL <https://doi.org/10.1038/ng1104-1133>
- Cirelli, K. M., Gorfou, G., Hassan, M. A., Printz, M., Crown, D., Leppla, S. H., Grigg, M. E., Saeij, J. P. J., & Moayeri, M. (2014). Inflammasome sensor NLRP1 controls rat macrophage susceptibility to *Toxoplasma gondii*. *PLoS Pathog*, *10*(3), e1003927.
- Codutti, L., Leppek, K., Zálešák, J., Windeisen, V., Masiewicz, P., Stoecklin, G., & Carlomagno, T. (2015). A Distinct, Sequence-Induced Conformation Is Required for Recognition of the Constitutive Decay Element RNA by Roquin. *Structure*, *23*(8), 1437–1447.

- Couper, K. N., Roberts, C. W., Brombacher, F., Alexander, J., & Johnson, L. L. (2005). Immunoglobulin M Limits Parasite Dissemination by Preventing Host Cell Invasion *Toxoplasma gondii* -Specific Immunoglobulin M Limits Parasite Dissemination by Preventing Host Cell Invasion. *Infection and Immunity*, 73(12), 8060–8068.
- Couvreur, G., Sadak, A., Fortier, B., & Dubremetz, J. F. (1988). Surface antigens of *Toxoplasma gondii*. *Parasitology*, 97(1), 1–10.
- Crawford, A., Angelosanto, J. M., Kao, C., Doering, T. A., Odorizzi, P. M., Barnett, B. E., & Wherry, E. J. (2014). Molecular and transcriptional basis of CD4+ T cell dysfunction during chronic infection. *Immunity*, 40(2), 289–302.
- Crotty, S. (2019). T Follicular Helper Cell Biology: A Decade of Discovery and Diseases. *Immunity*, 50(5), 1132–1148.  
URL <https://doi.org/10.1016/j.immuni.2019.04.011>
- Curran, M. A., Montalvo, W., Yagita, H., & Allison, J. P. (2010). PD-1 and CTLA-4 combination blockade expands infiltrating T cells and reduces regulatory T and myeloid cells within B16 melanoma tumors. *Proceedings of the National Academy of Sciences*, 107(9), 4275 LP – 4280.  
URL <http://www.pnas.org/content/107/9/4275.abstract>
- Darde, M. L., & Pestre-Alexandre, B. . B. (1992). Isoenzyme Analysis of 35 *Toxoplasma gondii* Isolates and the Biological and Epidemiological Implications. *The Journal of Parasitology*, 78(5), 786–794.
- Debierre-Grockiego, F., Campos, M. A., Azzouz, N., Schmidt, J., Bieker, U., Resende, M. G., Mansur, D. S., Weingart, R., Schmidt, R. R., Golenbock, D. T., Gazzinelli, R. T., & Schwarz, R. T. (2007). Activation of TLR2 and TLR4 by Glycosylphosphatidylinositols Derived from *Toxoplasma gondii* . *The Journal of Immunology*, 179(2), 1129–1137.
- Demar, M., Ajzenberg, D., Maubon, D., Djossou, F., Panchoe, D., Punwasi, W., Valery, N., Peneau, C., Daigre, J. L., Aznar, C., Cottrelle, B., Terzan, L., Dardé, M. L., & Carme, B. (2007). Fatal outbreak of human toxoplasmosis along the Maroni River: Epidemiological, clinical, and parasitological aspects. *Clinical Infectious Diseases*, 45(7).
- Denkers, E. Y., Scharton-Kersten, T., Barbieri, S., Caspar, P., & Sher, A. (1996). A role for CD4+NK1.1+ T lymphocytes as major histocompatibility complex class

II independent helper cells in the generation of CD8+ effector function against intracellular infection. *Journal of Experimental Medicine*, 184(1), 131–139.

Denkers, E. Y., Yap, G., Scharon-Kersten, T., Charest, H., Butcher, B. A., Caspar, P., Heiny, S., & Sher, A. (1997). Perforin-mediated cytolysis plays a limited role in host resistance to *Toxoplasma gondii*. *Journal of immunology (Baltimore, Md. : 1950)*, 159(4), 1903–8.

URL <http://www.ncbi.nlm.nih.gov/pubmed/9257855>

Diep, D. B., Nelson, K. L., Raja, S. M., Pleshak, E. N., & Buckley, J. T. (1998). Glycosylphosphatidylinositol anchors of membrane glycoproteins are binding determinants for the channel-forming toxin aerolysin. *Journal of Biological Chemistry*, 273(4), 2355–2360.

URL <http://dx.doi.org/10.1074/jbc.273.4.2355>

Dimala, C. A., Kika, B. T., Kadia, B. M., & Blencowe, H. (2018). Current challenges and proposed solutions to the effective implementation of the RTS, S/ AS01 Malaria Vaccine Program in sub-Saharan Africa: A systematic review. *PLoS ONE*, 13(12), 1–11.

Doering, T. A., Crawford, A., Angelosanto, J. M., Paley, M. A., Ziegler, C. G., & Wherry, E. J. (2012). Network analysis reveals centrally connected genes and pathways involved in CD8+ T cell exhaustion versus memory. *Immunity*, 37(6), 1130–1144.

Dunay, I. R., DaMatta, R. A., Fux, B., Presti, R., Greco, S., Colonna, M., & Sibley, L. D. (2008). Gr1+ Inflammatory Monocytes Are Required for Mucosal Resistance to the Pathogen *Toxoplasma gondii*. *Immunity*, 29(2), 306–317.

Elbez-Rubinstein, A., Ajzenberg, D., Dardé, M.-L., Cohen, R., Dumètre, A., Yera, H., Gondon, E., Janaud, J.-C., & Thulliez, P. (2009). Congenital Toxoplasmosis and Reinfection during Pregnancy: Case Report, Strain Characterization, Experimental Model of Reinfection, and Review. *The Journal of Infectious Diseases*, 199(2), 280–285.

URL <https://doi.org/10.1086/595793>

Etheridge, R. D., Alaganan, A., Tang, K., Lou, H. J., Turk, B. E., & Sibley, L. D. (2014). The *Toxoplasma* pseudokinase ROP5 forms complexes with ROP18 and ROP17 kinases that synergize to control acute virulence in mice. *Cell Host and*

- Microbe*, 15(5), 537–550.  
URL <http://dx.doi.org/10.1016/j.chom.2014.04.002>
- Fang, J., Marchesini, N., & Moreno, S. (2006). A *Toxoplasma gondii* phosphoinositide phospholipase C (TgPI-PLC) with high affinity for phosphatidylinositol. *Biochemical Journal*, 394(2), 417–425.  
URL <https://doi.org/10.1042/BJ20051393>
- Ferguson, M. A. (1999). The structure, biosynthesis and functions of glycosylphosphatidylinositol anchors, and the contributions of trypanosome research. *Journal of Cell Science*, 112(17), 2799–2809.
- Ferguson, M. A. J., Haldar, K., & Cross, A. M. (1985). Trypanosoma brucei Variant Surface Glycoprotein Has a sn- 1 , 2- Dimyristyl Glycerol Membrane Anchor at Its COOH Terminus. *Journal of Biological Chemistry*, 260(8), 4963–4968.  
URL [http://dx.doi.org/10.1016/S0021-9258\(18\)89166-9](http://dx.doi.org/10.1016/S0021-9258(18)89166-9)
- Fontaine, T., Magnin, T., Melhert, A., Lamont, D., Latgé, J.-P., & Ferguson, M. A. J. (2003). Structures of the glycosylphosphatidylinositol membrane anchors from *Aspergillus fumigatus* membrane proteins. *Glycobiology*, 13(3), 169–177.
- Fox, B. A., & Bzik, D. J. (2002). De novo pyrimidine biosynthesis is required for virulence of *Toxoplasma gondii*. *Nature*, 415(6874), 926–929.  
URL <http://www.nature.com/doi/finder/10.1038/415926a>
- Fox, B. A., & Bzik, D. J. (2010). Avirulent uracil auxotrophs based on disruption of orotidine-5'-monophosphate decarboxylase elicit protective immunity to *Toxoplasma gondii*. *Infection and Immunity*, 78(9), 3744–3752.
- Frenkel, J. K., & Taylor, D. W. (1982). Toxoplasmosis in immunoglobulin M-suppressed mice. *Infection and Immunity*, 38(1), 360–367.
- Fux, B., Nawas, J., Khan, A., Gill, D. B., Su, C., & Sibley, L. D. (2007). *Toxoplasma gondii* strains defective in oral transmission are also defective in developmental stage differentiation. *Infection and immunity*, 75(5), 2580–2590.
- Garg, M., Stern, D., Groß, U., Seeberger, P. H., Seeber, F., & Varón Silva, D. (2019). Detection of Anti- *Toxoplasma gondii* Antibodies in Human Sera Using Synthetic Glycosylphosphatidylinositol Glycans on a Bead-Based Multiplex Assay. *Analytical Chemistry*, 91(17), 11215–11222.

- Garneau, N. L., Wilusz, J., & Wilusz, C. J. (2007). The highways and byways of mRNA decay. *Nature Reviews Molecular Cell Biology*, 8(2), 113–126.
- Gas-Pascual, E., Ichikawa, H. T., Sheikh, M. O., Serji, M. I., Deng, B., Mandalasi, M., Bandini, G., Samuelson, J., Wells, L., & West, C. M. (2019). CRISPR/Cas9 and glycomics tools for *Toxoplasma* glycobiology. *The Journal of biological chemistry*, 294(4), 1104–1125.  
 URL <https://pubmed.ncbi.nlm.nih.gov/30463938>  
<https://www.ncbi.nlm.nih.gov/pmc/articles/PMC6349120/>
- Gay, G., Braun, L., Brenier-Pinchart, M. P., Vollaire, J., Josserand, V., Bertini, R. L., Varesano, A., Touquet, B., De Bock, P. J., Coute, Y., Tardieux, I., Bougdour, A., & Hakimi, M. A. (2016). *Toxoplasma gondii* TgIST co-opts host chromatin repressors dampening STAT1-dependent gene regulation and IFN- $\gamma$ -mediated host defenses. *Journal of Experimental Medicine*, 213(9), 1779–1798.
- Gazzinelli, R., Xu, Y., Hieny, S., Cheever, A., & Sher, A. (1992a). Simultaneous depletion of CD4+ and CD8+ T lymphocytes is required to reactivate chronic infection with *Toxoplasma gondii*. *The Journal of Immunology*, 149(1), 175–180.
- Gazzinelli, R. T., Hakim, F. T., Hieny, S., Shearer, G. M., Sher, A., Gazzinelli, S. R. T., Hakim, F. T., Hieny, S., & Shearer, G. M. (1991). Synergistic role of CD4+ and CD8+ T lymphocytes in IFN-gamma production and protective immunity induced by an attenuated *Toxoplasma gondii* vaccine. *Journal of immunology (Baltimore, Md. : 1950)*, 146(1), 286–92.
- Gazzinelli, R. T., Hieny, S., Wynn, T. A., Wolf, S., & Sher, A. (1993). Interleukin 12 is required for the T-lymphocyte-independent induction of interferon  $\gamma$  by an intracellular parasite and induces resistance in T-cell- deficient hosts. *Proceedings of the National Academy of Sciences of the United States of America*, 90(13), 6115–6119.
- Gazzinelli, R. T., Oswald, I. P., James, S. L., Sher, A., Macrophages, I., Gazzinelli, R. T., Oswald, P., & James, S. L. (1992b). IL-10 inhibits parasite killing and nitrogen oxide production by IFN-gamma-activated Information about subscribing to The Journal of Immunology is online at : IL-10 INHIBITS PARASITE KILLING AND NITROGEN OXIDE PRODUCTION BY. *The Journal of Immunology*.
- Ghosh, S., & Hayden, M. S. (2008). New regulators of NF- $\kappa$ B in inflammation. *Nature Reviews Immunology*, 8(11), 837–848.

- Gigley, J. P., Bhadra, R., & Khan, I. A. (2011). CD8 T cells and toxoplasma gondii: A new paradigm. *Journal of Parasitology Research*, 2011.
- Gigley, J. P., Fox, B. A., & Bzik, D. J. (2009a). Cell-Mediated Immunity to Toxoplasma gondii Develops Primarily by Local Th1 Host Immune Responses in the Absence of Parasite Replication. *The Journal of Immunology*, 182(2), 1069–1078.
- Gigley, J. P., Fox, B. A., & Bzik, D. J. (2009b). Long-term immunity to lethal acute or chronic type II Toxoplasma gondii infection is effectively induced in genetically susceptible C57BL/6 mice by immunization with an attenuated type I vaccine strain. *Infection and Immunity*, 77(12), 5380–5388.
- Gilmore, T. (2017). NF-κB Target Genes » NF-κB Transcription Factors | Boston University.  
URL <http://www.bu.edu/nf-kb/gene-resources/target-genes/>
- Giraldo, M., Cannizzaro, H., Ferguson, M. A. J., Almeida, I. C., & Gazzinelli, R. T. (2000). Fractionation of membrane components from tachyzoite forms of Toxoplasma gondii: Differential recognition by immunoglobulin M (IgM) and IgG present in sera from patients with acute or chronic toxoplasmosis. *Journal of Clinical Microbiology*, 38(4), 1453–1460.
- Gorfu, G., Cirelli, K. M., Melo, M. B., Mayer-Barber, K., Crown, D., Koller, B. H., Masters, S., Sher, A., Leppla, S. H., & Moayeri, M. (2014). Dual role for inflammasome sensors NLRP1 and NLRP3 in murine resistance to Toxoplasma gondii. *MBio*, 5(1), e01117–13.
- Götze, S., Reinhardt, A., Geissner, A., Azzouz, N., Tsai, Y.-H., Kurucz, R., Varón Silva, D., & Seeberger, P. H. (2015). Investigation of the protective properties of glycosylphosphatidylinositol-based vaccine candidates in a Toxoplasma gondii mouse challenge model. *Glycobiology*, 25(9), 984–991.  
URL <https://doi.org/10.1093/glycob/cwv040>
- Grigg, M. E., Ganatra, J., Boothroyd, J. C., & Margolis, T. P. (2001). Unusual Abundance of Atypical Strains Associated with Human Ocular Toxoplasmosis. *The Journal of Infectious Diseases*, 184(5), 633–639.
- Grumont, R. J., Rourke, I. J., & Gerondakis, S. (1999). Rel-dependent induction of A1 transcription is required to protect B cells from antigen receptor ligation-induced apoptosis. *J*, 400–411.

- Ha, S.-a., Tsuji, M., Suzuki, K., Meek, B., Yasuda, N., Kaisho, T., & Fagarasan, S. (2006). Regulation of B1 cell migration by signals through Toll-like receptors. *The Journal of Experimental Medicine*, 203(11), 2541–2550.  
URL <http://www.jem.org/lookup/doi/10.1084/jem.20061041>
- Ha, S. J., Mueller, S. N., Wherry, E. J., Barber, D. L., Aubert, R. D., Sharpe, A. H., Freeman, G. J., & Ahmed, R. (2008). Enhancing therapeutic vaccination by blocking PD-1-mediated inhibitory signals during chronic infection. *Journal of Experimental Medicine*, 205(3), 543–555.
- Haas, K. M., Poe, J. C., Steeber, D. A., & Tedder, T. F. (2005). B-1a and B-1b cells exhibit distinct developmental requirements and have unique functional roles in innate and adaptive immunity to *S. pneumoniae*. *Immunity*, 23(1), 7–18.
- Hassan, M. A., Jensen, K. D., Butty, V., Hu, K., Boedec, E., Prins, P., & Saeij, J. P. (2015). Transcriptional and Linkage Analyses Identify Loci that Mediate the Differential Macrophage Response to Inflammatory Stimuli and Infection. *PLoS Genetics*, 11(10), 1–25.
- Hassan, M. A., Olijnik, A.-A., Frickel, E.-M., & Saeij, J. P. (2019). Clonal and atypical *Toxoplasma* strain differences in virulence vary with mouse sub-species. *International Journal for Parasitology*, 49(1), 63–70.
- Hayakawa, K., Asano, M., Shinton, S. A., Gui, M., Allman, D., Stewart, C. L., Silver, J., & Hardy, R. R. (1999). Positive selection of natural autoreactive B cells. *Science*, 285(5424), 113–116.
- Hayakawa, K., Carmack, C. E., Hyman, R., & Hardy, R. R. (1990). Natural autoantibodies to thymocytes: origin, VH genes, fine specificities, and the role of Thy-1 glycoprotein. *Journal of Experimental Medicine*, 172(3), 869–878.  
URL <https://doi.org/10.1084/jem.172.3.869>
- Hayakawa, K., Hardy, R. R., Herzenberg, L. A., & Herzenberg, L. A. (1985). Progenitors for Ly-1 B cells are distinct from progenitors for other B cells. *J Exp Med*, 161(6), 1554–1568.
- Herzenberg, L. A. L. A., & Herzenberg, L. A. L. A. (1989). Toward a layered immune system. *Cell*, 59(6), 953–954.
- Hilgendorf, I., Theurl, I., Gerhardt, L. M. S., Robbins, C. S., Weber, G. F., Gonen, A., Iwamoto, Y., Degousee, N., Holderried, T. A. W., Winter, C., Zirlik, A.,

- Lin, H. Y., Sukhova, G. K., Butany, J., Rubin, B. B., Witztum, J. L., Libby, P., Nahrendorf, M., Weissleder, R., & Swirski, F. K. (2014). Innate Response Activator B Cells Aggravate Atherosclerosis by Stimulating T Helper-1 Adaptive Immunity. *Circulation*, *129*(16), 1677–1687.  
URL <https://doi.org/10.1161/CIRCULATIONAHA.113.006381>
- Hirano, F., Kaneko, K., Tamura, H., Dong, H., Wang, S., Ichikawa, M., Rietz, C., Flies, D. B., Lau, J. S., & Zhu, G. (2005). Blockade of B7-H1 and PD-1 by monoclonal antibodies potentiates cancer therapeutic immunity. *Cancer research*, *65*(3), 1089–1096.
- Hodi, F. S., Chesney, J., Pavlick, A. C., Robert, C., Grossmann, K. F., McDermott, D. F., Linette, G. P., Meyer, N., Giguere, J. K., & Agarwala, S. S. (2016). Combined nivolumab and ipilimumab versus ipilimumab alone in patients with advanced melanoma: 2-year overall survival outcomes in a multicentre, randomised, controlled, phase 2 trial. *The Lancet Oncology*, *17*(11), 1558–1568.
- Hodi, F. S., O'Day, S. J., McDermott, D. F., Weber, R. W., Sosman, J. A., Haanen, J. B., Gonzalez, R., Robert, C., Schadendorf, D., Hassel, J. C., Akerley, W., van den Eertwegh, A. J., Lutzky, J., Lorigan, P., Vaubel, J. M., Linette, G. P., Hogg, D., Ottensmeier, C. H., Lebbé, C., Peschel, C., Quirt, I., Clark, J. I., Wolchok, J. D., Weber, J. S., Tian, J., Yellin, M. J., Nichol, G. M., Hoos, A., & Urba, W. J. (2010). Improved survival with ipilimumab in patients with metastatic melanoma. *New England Journal of Medicine*, *363*(8), 711–723.
- Hoffmann, A., Levchenko, A., & Scott, M. L. (2002). The I $\kappa$ B – NF- $\kappa$ B Signaling Module : Temporal Control and Selective Gene Activation. *298*(November), 1241–1245.
- Homann, D., Tishon, A., Berger, D. P., Weigle, W. O., von Herrath, M. G., & Oldstone, M. B. A. (1998). Evidence for an Underlying CD4 Helper and CD8 T-Cell Defect in B-Cell-Deficient Mice: Failure To Clear Persistent Virus Infection after Adoptive Immunotherapy with Virus-Specific Memory Cells from  $\mu$ MT/ $\mu$ MT Mice. *Journal of Virology*, *72*(11), 9208–9216.  
URL <https://journals.asm.org/jvi>  
<https://doi.org/10.1128/JVI.72.11.9208-9216.1998>
- Homans, S. W., Ferguson, M. A. J., Dwek, R. A., Rademacher, T. W., Anand, R., & Williams, A. F. (1988). Complete structure of the glycosyl phosphatidylinositol membrane anchor of rat brain Thy-1 glycoprotein. *Nature*, *333*(6170), 269–272.

- Hooijkaas, H., Benner, R., Pleasants, J. R., & Wostmann, B. S. (1984). Isotypes and specificities of immunoglobulins produced by germ-free mice fed chemically defined ultrafiltered “antigen-free” diet. *European journal of immunology*, *14*(12), 1127–1130.
- Hosokawa, J., Suzuki, K., Meguro, K., Tanaka, S., Maezawa, Y., Suto, A., Fujimura, L., Sakamoto, A., Clevers, H., Ohara, O., & Nakajima, H. (2017). I $\kappa$ BNS enhances follicular helper T-cell differentiation and function downstream of ASC12. *Journal of Allergy and Clinical Immunology*, *140*(1), 288–291.e8.
- Hotez, P., Boussinesq, M., Brooker, S. J., Brown, A. S., Buckle, G., Budke, C. M., King, C. H., Lozano, R., Jasrasaria, R., Johns, N. E., Keiser, J., Pion, D. S., Pullan, R. L., & Ramaiah, K. D. (2014). The Global Burden of Disease Study 2010 : Interpretation and Implications for the Neglected Tropical Diseases. *PLoS Neglected Tropical Diseases*, *8*(7).
- Howard, J. C., Hunn, J. P., & Steinfeldt, T. (2011). The IRG protein-based resistance mechanism in mice and its relation to virulence in *Toxoplasma gondii*. *Current opinion in microbiology*, *14*(4), 414–421.
- Howe, D. K., & Sibley, L. D. (1995). *Toxoplasma gondii* Comprises Three Clonal Lineages: Correlation of Parasite Genotype with Human Disease. *The Journal of Infectious Diseases*, *172*(6), 1561–1566.  
URL <https://doi.org/10.1093/infdis/172.6.1561>
- Hunter, C. A., Subauste, C. S., Van Cleave, V. H., & Remington, J. S. (1994). Production of gamma interferon by natural killer cells from *Toxoplasma gondii*-infected SCID mice: Regulation by interleukin-10, interleukin-12, and tumor necrosis factor alpha. *Infection and Immunity*, *62*(7), 2818–2824.
- Hwang, S., Cobb, D. A., Bhadra, R., Youngblood, B., & Khan, I. A. (2016). Blimp-1-mediated CD4 T cell exhaustion causes CD8 T cell dysfunction during chronic toxoplasmosis. *Journal of Experimental Medicine*, *213*(9), 1799–1818.
- Inamine, A., Takahashi, Y., Baba, N., Miyake, K., Tokuhisa, T., Takemori, T., & Abe, R. (2005). Two waves of memory B-cell generation in the primary immune response. *International immunology*, *17*(5), 581–589.
- Iwai, Y., Ishida, M., Tanaka, Y., Okazaki, T., Honjo, T., & Minato, N. (2002). Involvement of PD-L1 on tumor cells in the escape from host immune system

- and tumor immunotherapy by PD-L1 blockade. *Proceedings of the National Academy of Sciences*, 99(19), 12293–12297.
- Jensen, K. D., Camejo, A., Melo, M. B., Cordeiro, C., Julien, L., Grotenbreg, G. M., Frickel, E. M., Ploegh, H. L., Young, L., & Saeij, J. P. (2015). Toxoplasma gondii superinfection and virulence during secondary infection correlate with the exact ROP5/ROP18 allelic combination. *mBio*, 6(2), 1–15.
- Jensen, K. D., Wang, Y., Wojno, E. D. T., Shastri, A. J., Hu, K., Cornel, L., Boedec, E., Ong, Y.-C., Chien, Y.-h., Hunter, C. A., Boothroyd, J. C., & Saeij, J. P. (2011). Toxoplasma Polymorphic Effectors Determine Macrophage Polarization and Intestinal Inflammation. *Cell Host & Microbe*, 9(6), 472–483.
- Jin, H.-T., Anderson, A. C., Tan, W. G., West, E. E., Ha, S.-J., Araki, K., Freeman, G. J., Kuchroo, V. K., & Ahmed, R. (2010). Cooperation of Tim-3 and PD-1 in CD8 T-cell exhaustion during chronic viral infection. *Proceedings of the National Academy of Sciences*, 107(33), 14733–14738.
- Johnson, J., Suzuki, Y., Mack, D., Mui, E., Estes, R., David, C., Skamene, E., Forman, J., & McLeod, R. (2002). Genetic analysis of influences on survival following Toxoplasma gondii infection. *International Journal for Parasitology*, 32(2), 179–185.
- Johnson, L. L., & Sayles, P. C. (2002). Deficient humoral responses underlie susceptibility to Toxoplasma gondii in CD4-deficient mice. *Infection and Immunity*, 70(1), 185–191.
- Joiner, K. A., Fuhrman, S. A., Miettinen, H. M., Kasper, L. H., & Mellman, I. (1990). Toxoplasma gondii: fusion competence of parasitophorous vacuoles in Fc receptor-transfected fibroblasts. *Science*, 249(4969), 641 LP – 646.
- Jones, J. L., & Holland, G. N. (2010). Short report: Annual burden of ocular toxoplasmosis in the United States. *American Journal of Tropical Medicine and Hygiene*, 82(3), 464–465.
- Jordan, K. A., Wilson, E. H., Tait, E. D., Fox, B. A., Roos, D. S., Bzik, D. J., Dzierszynski, F., & Hunter, C. A. (2009). Kinetics and phenotype of vaccine-induced CD8+ T-cell responses to Toxoplasma gondii. *Infection and Immunity*, 77(9), 3894–3901.

- Joshi, T., Rodriguez, S., Perovic, V., Cockburn, I. A., & Stäger, S. (2009). B7-H1 blockade increases survival of dysfunctional CD8+ T cells and confers protection against *Leishmania donovani* infections. *PLoS Pathog*, 5(5), e1000431.
- Kalia, V., Penny, L. A., Yuzefpolskiy, Y., Baumann, F. M., & Sarkar, S. (2015). Quiescence of memory CD8+ T cells is mediated by regulatory T cells through inhibitory receptor CTLA-4. *Immunity*, 42(6), 1116–1129.
- Kang, H., Remington, J. S., & Suzuki, Y. (2000). Decreased Resistance of B Cell-Deficient Mice to Infection with *Toxoplasma gondii* Despite Unimpaired Expression of IFN- $\gamma$ , TNF- $\alpha$ , and Inducible Nitric Oxide Synthase. *The Journal of Immunology*, 164(5), 2629–2634.  
URL <http://www.jimmunol.org/cgi/doi/10.4049/jimmunol.164.5.2629>
- Kang, H., & Suzuki, Y. (2001). Requirement of non-T cells that produce gamma interferon for prevention of reactivation of *Toxoplasma gondii* infection in the brain. *Infection and immunity*, 69(5), 2920–2927.
- Kantor, A. B., Stall, A. M., Adams, S., Herzenberg, L. A., & Herzenberg, L. A. (1992). Differential development of progenitor activity for three B-cell lineages. *Proceedings of the National Academy of Sciences*, 89(8), 3320–3324.
- Keane, T. M., Goodstadt, L., Danecek, P., White, M. A., Wong, K., Yalcin, B., Heger, A., Agam, A., Slater, G., Goodson, M., Furlotte, N. A., Eskin, E., Nellåker, C., Whitley, H., Cleak, J., Janowitz, D., Hernandez-Pliego, P., Edwards, A., Belgard, T. G., Oliver, P. L., McIntyre, R. E., Bhomra, A., Nicod, J., Gan, X., Yuan, W., Van Der Weyden, L., Steward, C. A., Bala, S., Stalker, J., Mott, R., Durbin, R., Jackson, I. J., Czechanski, A., Guerra-Assunção, J., Donahue, L. R., Reinholdt, L. G., Payseur, B. A., Ponting, C. P., Birney, E., Flint, J., & Adams, D. J. (2011). Mouse genomic variation and its effect on phenotypes and gene regulation. *Nature*, 477(7364), 289–294.
- Kew, O. M., Wright, P. F., Agol, V. I., Delpeyroux, F., Shimizu, H., Nathanson, N., & Pallansch, M. A. (2004). Circulating vaccine-derived polioviruses : current state of knowledge. *006320(03)*, 16–23.
- Khan, A., Fux, B., Su, C., Dubey, J. P., Darde, M. L., Ajioka, J. W., Rosenthal, B. M., & Sibley, L. D. (2007). Recent transcontinental sweep of *Toxoplasma gondii* driven by a single monomorphic chromosome. *Proceedings of*

*the National Academy of Sciences of the United States of America*, 104(37), 14872–14877.

- Khan, A., Jordan, C., Muccioli, C., Vallochi, A. L., Rizzo, L. V., Belfort, R., Vitor, R. W., Silveira, C., & Sibley, L. D. (2006). Genetic divergence of *Toxoplasma gondii* strains associated with ocular toxoplasmosis, Brazil. *Emerging Infectious Diseases*, 12(6), 942–949.
- Khan, I. A., Schwartzman, J. D., Matsuura, T., & Kasper, L. H. (1997). A dichotomous role for nitric oxide during acute *Toxoplasma gondii* infection in mice. *Proceedings of the National Academy of Sciences of the United States of America*, 94(25), 13955–13960.
- Khoenkhoe, S., Erikson, E., Ádori, M., Stark, J. M., Scholz, J. L., Cancro, M. P., Pedersen, G. K., & Karlsson Hedestam, G. B. (2019). TACI expression and plasma cell differentiation are impaired in the absence of functional I $\kappa$ BNS. *Immunology and Cell Biology*, 97(5), 485–497.
- Kim, C. C., Baccarella, A. M., Bayat, A., Pepper, M., & Fontana, M. F. (2019). FCRL5 + Memory B Cells Exhibit Robust Recall Responses. *Cell Reports*, 27(5), 1446–1460.e4.  
URL <https://doi.org/10.1016/j.celrep.2019.04.019>
- Klose, C. S., Flach, M., Möhle, L., Rogell, L., Hoyler, T., Ebert, K., Fabiunke, C., Pfeifer, D., Sexl, V., Fonseca-Pereira, D., Domingues, R. G., Veiga-Fernandes, H., Arnold, S. J., Busslinger, M., Dunay, I. R., Tanriver, Y., & Diefenbach, A. (2014). Differentiation of type 1 ILCs from a common progenitor to all helper-like innate lymphoid cell lineages. *Cell*, 157(2), 340–356.
- Koblansky, A. A., Jankovic, D., Oh, H., Hieny, S., Sungnak, W., Mathur, R., Hayden, M. S., Akira, S., Sher, A., & Ghosh, S. (2013). Recognition of Profilin by Toll-like Receptor 12 Is Critical for Host Resistance to *Toxoplasma gondii*. *Immunity*, 38(1), 119–130.  
URL <http://dx.doi.org/10.1016/j.immuni.2012.09.016>
- Koike, T., Harada, K., Horiuchi, S., & Kitamura, D. (2019). The quantity of CD40 signaling determines the differentiation of B cells into functionally distinct memory cell subsets. *eLife*, 8, 1–25.
- Konradt, C., Ueno, N., Christian, D. A., Delong, J. H., Pritchard, G. H., Herz, J., Bzik, D. J., Koshy, A. A., McGavern, D. B., & Lodoen, M. B. (2016). Endothelial

cells are a replicative niche for entry of *Toxoplasma gondii* to the central nervous system. *Nat Microbiol* 1: 16001.

- Kreuk, L. S. M., Koch, M. A., Slayden, L. C., Lind, N. A., Chu, S., Savage, H. P., Kantor, A. B., Baumgarth, N., & Barton, G. M. (2019). B cell receptor and Toll-like receptor signaling coordinate to control distinct B-1 responses to both self and the microbiota. *Elife*, 8, e47015.
- Krishnamurthy, A. T., Thouvenel, C. D., Portugal, S., Keitany, G. J., Kim, K. S., Holder, A., Crompton, P. D., Rawlings, D. J., & Pepper, M. (2016). Somatically Hypermutated Plasmodium-Specific IgM+ Memory B Cells Are Rapid, Plastic, Early Responders upon Malaria Rechallenge. *Immunity*, 45(2), 402–414.  
URL <http://dx.doi.org/10.1016/j.immuni.2016.06.014>
- Kroese, F. G., Butcher, E. C., Stall, A. M., & Herzenberg, L. A. (1989). A major peritoneal Reservoir of precursors for intestinal iga plasma cells. *Immunological Investigations*, 18(1-4), 47–58.
- Krummel, M. F., & Allison, J. P. (1995). CD28 and CTLA-4 have opposing effects on the response of T cells to stimulation. *The Journal of experimental medicine*, 182(2), 459–465.
- Krummel, M. F., & Allison, J. P. (1996). CTLA-4 engagement inhibits IL-2 accumulation and cell cycle progression upon activation of resting T cells. *The Journal of experimental medicine*, 183(6), 2533–2540.
- Kuwata, H., Matsumoto, M., Atarashi, K., Morishita, H., Hirotani, T., Koga, R., & Takeda, K. (2006). I $\kappa$ BNS inhibits induction of a subset of toll-like receptor-dependent genes and limits inflammation. *Immunity*, 24(1), 41–51.
- Lalor, P. A., Herzenberg, L. A., Adams, S., & Stall, A. M. (1989). Feedback regulation of murine Ly-1 B cell development. *European journal of immunology*, 19(3), 507–513.
- Lázár-Molnár, E., Chen, B., Sweeney, K. A., Wang, E. J., Liu, W., Lin, J., Porcelli, S. A., Almo, S. C., Nathenson, S. G., & Jacobs, W. R. (2010). Programmed death-1 (PD-1)-deficient mice are extraordinarily sensitive to tuberculosis. *Proceedings of the National Academy of Sciences*, 107(30), 13402–13407.
- Leach, D. R., Krummel, M. F., & Allison, J. P. (1996). Enhancement of antitumor immunity by CTLA-4 blockade. *Science*, 271(5256), 1734–1736.

- Lehmann, T., Graham, D. H., Dahl, E. R., Bahia-Oliveira, L. M. G., Gennari, S. M., & Dubey, J. P. (2004). Variation in the structure of *Toxoplasma gondii* and the roles of selfing, drift, and epistatic selection in maintaining linkage disequilibria. *Infection, Genetics and Evolution*, 4(2), 107–114.
- Leppek, K., Schott, J., Reitter, S., Poetz, F., Hammond, M. C., & Stoecklin, G. (2013). Roquin promotes constitutive mrna decay via a conserved class of stem-loop recognition motifs. *Cell*, 153(4), 869–881.
- Levy, D., Kuo, A. J., Chang, Y., Schaefer, U., Kitson, C., Cheung, P., Espejo, A., Zee, B. M., Liu, C. L., Tangsombatvisit, S., Tennen, R. I., Kuo, A. Y., Tanjing, S., Cheung, R., Chua, K. F., Utz, P. J., Shi, X., Prinjha, R. K., Lee, K., Garcia, B. A., Bedford, M. T., Tarakhovsky, A., Cheng, X., & Gozani, O. (2011). Lysine methylation of the NF- $\kappa$  B subunit RelA by SETD6 couples activity of the histone methyltransferase GLP at chromatin to tonic repression of NF- $\kappa$  B signaling. *Nature Immunology*, 12(1), 29–36.
- Liakou, C. I., Kamat, A., Tang, D. N., Chen, H., Sun, J., Troncoso, P., Logothetis, C., & Sharma, P. (2008). CTLA-4 blockade increases IFN $\gamma$ -producing CD4+ ICOS<sup>hi</sup> cells to shift the ratio of effector to regulatory T cells in cancer patients. *Proceedings of the National Academy of Sciences*, 105(39), 14987–14992.
- Lilue, J., Müller, U. B., Steinfeldt, T., & Howard, J. C. (2013). Reciprocal virulence and resistance polymorphism in the relationship between *Toxoplasma gondii* and the house mouse. *eLife*, 2, 1–21.
- Lino, A. C., Dang, V. D., Lampropoulou, V., Welle, A., Joedicke, J., Pohar, J., Simon, Q., Thalmensi, J., Baures, A., Flühler, V., Sakwa, I., Stervbo, U., Ries, S., Jouneau, L., Boudinot, P., Tsubata, T., Adachi, T., Hutloff, A., Dörner, T., Zimmer-Strobl, U., de Vos, A. F., Dahlke, K., Loh, G., Korniotis, S., Goosmann, C., Weill, J.-C., Reynaud, C.-A., Kaufmann, S. H. E., Walter, J., & Fillatreau, S. (2018). LAG-3 Inhibitory Receptor Expression Identifies Immunosuppressive Natural Regulatory Plasma Cells. *Immunity*, 49(1), 120–133.e9.
- Lorenzi, H., Khan, A., Behnke, M. S., Namasivayam, S., Swapna, L. S., Hadjithomas, M., Karamycheva, S., Pinney, D., Brunk, B. P., & Ajioka, J. W. (2016a). Local admixture of amplified and diversified secreted pathogenesis determinants shapes mosaic *Toxoplasma gondii* genomes. *Nat Commun* 7: 10147.

- Lorenzi, H., Khan, A., Behnke, M. S., Namasivayam, S., Swapna, L. S., Hadjithomas, M., Karamycheva, S., Pinney, D., Brunk, B. P., Ajioka, J. W., Ajzenberg, D., Boothroyd, J. C., Boyle, J. P., Dardé, M. L., Diaz-Miranda, M. A., Dubey, J. P., Fritz, H. M., Gennari, S. M., Gregory, B. D., Kim, K., Saeij, J. P. J., Su, C., White, M. W., Zhu, X.-Q., Howe, D. K., Rosenthal, B. M., Grigg, M. E., Parkinson, J., Liu, L., Kissinger, J. C., Roos, D. S., & David Sibley, L. (2016b). Local admixture of amplified and diversified secreted pathogenesis determinants shapes mosaic *Toxoplasma gondii* genomes. *Nature Communications*, 7, 10147. URL <http://www.nature.com/doi/10.1038/ncomms10147>
- Low, M. G. (1987). Biochemistry of the glycosyl-phosphatidylinositol membrane protein anchors. *Biochemical Journal*, 244(1), 1.
- Luft, B. J., Brooks, R. G., Conley, F. K., McCabe, R. E., & Remington, J. S. (1984). Toxoplasmic Encephalitis in Patients With Acquired Immune Deficiency Syndrome. *JAMA*, 252(7), 913–917. URL <https://doi.org/10.1001/jama.1984.03350070031018>
- Luft, B. J., Hafner, R., Korzun, A. H., Leport, C., Antoniskis, D., Bosler, E. M., Bourland, D. D., Uttamchandani, R., Fuhrer, J., Jacobson, J., Morlat, P., Vilde, J.-L., & Remington, J. S. (1993). Toxoplasmic Encephalitis in Patients with the Acquired Immunodeficiency Syndrome. *New England Journal of Medicine*, 329(14), 995–1000.
- Luo, L., Bokil, N. J., Wall, A. A., Kapetanovic, R., Lansdaal, N. M., Marceline, F., Burgess, B. J., Tong, S. J., Guo, Z., & Alexandrov, K. (2017). SCIMP is a transmembrane non-TIR TLR adaptor that promotes proinflammatory cytokine production from macrophages. *Nature communications*, 8(1), 1–14.
- Ly, A., Liao, Y., Pietrzak, H., Ioannidis, L. J., Sidwell, T., Gloury, R., Doerflinger, M., Triglia, T., Qin, R. Z., Groom, J. R., Belz, G. T., Good-Jacobson, K. L., Shi, W., Kallies, A., & Hansen, D. S. (2019). Transcription Factor T-bet in B Cells Modulates Germinal Center Polarization and Antibody Affinity Maturation in Response to Malaria. *Cell Reports*, 29(8), 2257–2269.e6. URL <https://doi.org/10.1016/j.celrep.2019.10.087>
- Manger, I., Hehl, A., & Boothroyd, J. (1998). The Surface of *Toxoplasma* Tachyzoites Is Dominated by a Family of Glycosylphosphatidylinositol-Anchored Antigens Related to SAG1. *Infection and Immunity*, 66(5), 2237–2244. URL <https://doi.org/10.1128/IAI.66.5.2237-2244.1998>

- Mankan, A. K., Lawless, M. W., Gray, S. G., Kelleher, D., & McManus, R. (2009). NF- $\kappa$ B regulation: The nuclear response. *Journal of Cellular and Molecular Medicine*, 13(4), 631–643.
- Martin, F., Oliver, A. M., & Kearney, J. F. (2001). Marginal zone and B1 B cells unite in the early response against T-independent blood-borne particulate antigens. *Immunity*, 14(5), 617–629.
- Masopust, D., & Schenkel, J. M. (2013). The integration of T cell migration, differentiation and function. *Nature Reviews Immunology*, 13(5), 309–320.
- Matta, S. K., Olias, P., Huang, Z., Wang, Q., Park, E., Yokoyama, W. M., & Sibley, L. D. (2019). Toxoplasma gondii effector TgIST blocks type I interferon signaling to promote infection. *Proceedings of the National Academy of Sciences*, 116(35), 17480–17491.
- McCoy, K., Camberis, M., & Gros, G. L. (1997). Protective immunity to nematode infection is induced by CTLA-4 blockade. *The Journal of experimental medicine*, 186(2), 183–187.
- McLeod, R., Boyer, K. M., Lee, D., Mui, E., Wroblewski, K., Karrison, T., Noble, A. G., Withers, S., Swisher, C. N., Heydemann, P. T., Sautter, M., Babiarz, J., Rabiah, P., Meier, P., Grigg, M. E., & Group, t. T. S. (2012). Prematurity and Severity Are Associated With Toxoplasma gondii Alleles (NCCCTS, 1981–2009). *Clinical Infectious Diseases*, 54(11), 1595–1605.  
URL <https://doi.org/10.1093/cid/cis258>
- McLeod, R., Skamene, E., Brown, C. R., Mack, D. G., & Eisenhauer, B. (1989). Genetic regulation of early survival and cyst number after peroral Toxoplasma gondii infection of A x B / B x A recombinant inbred and B10 congenic mice. *Journal of Immunology*.
- Meek, B., van Gool, T., Gilis, H., & Peek, R. (2001). Dissecting the IgM antibody response during the acute and latent phase of toxoplasmosis. *Diagnostic microbiology and infectious disease*, 41 3, 131–137.
- Melo, M. B., Jensen, K. D., & Saeij, J. P. (2011). Toxoplasma gondii effectors are master regulators of the inflammatory response. *Trends Parasitol.*
- Mercolino, T. J., Arnold, L. W., Hawkins, L. A., & Houghton, G. (1988). Normal mouse peritoneum contains a large population of Ly-1+(CD5) B cells that

- recognize phosphatidyl choline. Relationship to cells that secrete hemolytic antibody specific for autologous erythrocytes. *The Journal of experimental medicine*, 168(2), 687–698.
- Mineo, J. R., McLeod, R., Mack, D., Smith, J., Khan, I. A., Ely, K. H., & Kasper, L. H. (1993). Antibodies to *Toxoplasma gondii* major surface protein (SAG-1, P30) inhibit infection of host cells and are produced in murine intestine after peroral infection. *The Journal of Immunology*, 150(9), 3951 LP – 3964.  
URL <http://www.jimmunol.org/content/150/9/3951.abstract>
- Minn, A. J., & Wherry, E. J. (2016). Combination cancer therapies with immune checkpoint blockade: convergence on interferon signaling. *Cell*, 165(2), 272–275.
- Minot, S., Melo, M. B., Li, F., Lu, D., Niedelman, W., Levine, S. S., & Saeij, J. P. J. (2012). Admixture and recombination among *Toxoplasma gondii* lineages explain global genome diversity. *Proceedings of the National Academy of Sciences*, 109(33), 13458–13463.  
URL [www.pnas.org/cgi/doi/10.1073/pnas.1117047109](http://www.pnas.org/cgi/doi/10.1073/pnas.1117047109)
- Miura, M., Hasegawa, N., Noguchi, M., Sugimoto, K., & Touma, M. (2016). The atypical I $\kappa$ B protein I $\kappa$ BNSis important for Toll-like receptor-induced interleukin-10 production in B cells. *Immunology*, 147(4), 453–463.
- Moser, B. A., Steinhardt, R. C., Escalante-Buendia, Y., Boltz, D. A., Barker, K. M., Cassaidy, B. J., Rosenberger, M. G., Yoo, S., McGonnigal, B. G., & Esser-Kahn, A. P. (2020). Increased vaccine tolerability and protection via NF- $\kappa$ B modulation. *Science Advances*, 6(37).
- Moulin, V., Andris, F., Thielemans, K., Maliszewski, C., Urbain, J., & Moser, M. (2000). B lymphocytes regulate dendritic cell (DC) function in vivo: Increased interleukin 12 production by DCs from B cell-deficient mice results in T helper cell type 1 deviation. *Journal of Experimental Medicine*, 192(4), 475–482.
- Murillo-León, M., Müller, U. B., Zimmermann, I., Singh, S., Widdershooven, P., Campos, C., Alvarez, C., Könen-Waisman, S., Lukes, N., Ruzsics, Z., Howard, J. C., Schwemmler, M., & Steinfeldt, T. (2019). Molecular mechanism for the control of virulent *Toxoplasma gondii* infections in wild-derived mice. *Nature Communications*, 10(1).  
URL <http://dx.doi.org/10.1038/s41467-019-09200-2>

- Murphy, D. L., Fox, M. A., Timpano, K. R., Moya, P. R., Ren-Patterson, R., Andrews, A. M., Holmes, A., Lesch, K. P., & Wendland, J. R. (2008). How the serotonin story is being rewritten by new gene-based discoveries principally related to SLC6A4, the serotonin transporter gene, which functions to influence all cellular serotonin systems. *Neuropharmacology*, *55*(6), 932–960.  
URL <http://dx.doi.org/10.1016/j.neuropharm.2008.08.034>
- Murphy, M. L., Cotterell, S. E. J., Gorak, P. M. A., Engwerda, C. R., & Kaye, P. M. (1998). Blockade of CTLA-4 enhances host resistance to the intracellular pathogen, *Leishmania donovani*. *The Journal of Immunology*, *161*(8), 4153–4160.
- Nagasawa, H., Manabe, T., Maekawa, Y., Himeno, K., & Oka, M. (1991). Role of L3T4+ and Lyt-2+ T Cell Subsets in Protective Immune Responses of Mice against Infection with a Low or High Virulent Strain of *Toxoplasma gondii*. *Microbiology and Immunology*, *35*(3), 215–222.
- Nagel, S. D., & Boothroyd, J. C. (1989). The Major Surface Antigen, P30, of *Toxoplasma gondii* Is Anchored by a Glycolipid. *Journal of Biological Chemistry*, *264*(10), 5569–5574.
- Naik, R. S., Branch, O. H., Woods, A. S., Vijaykumar, M., Perkins, D. J., Nahlen, B. L., Lal, A. A., Cotter, R. J., Costello, C. E., & Ockenhouse, C. F. (2000). Glycosylphosphatidylinositol anchors of *Plasmodium falciparum*: molecular characterization and naturally elicited antibody response that may provide immunity to malaria pathogenesis. *The Journal of experimental medicine*, *192*(11), 1563–1576.
- Nakamoto, N., Cho, H., Shaked, A., Olthoff, K., Valiga, M. E., Kaminski, M., Gostick, E., Price, D. A., Freeman, G. J., Wherry, E. J., & Chang, K.-M. (2009). Synergistic Reversal of Intrahepatic HCV-Specific CD8 T Cell Exhaustion by Combined PD-1/CTLA-4 Blockade. *PLOS Pathogens*, *5*(2), e1000313.  
URL <https://doi.org/10.1371/journal.ppat.1000313>
- Nesbitt, M. N., & Skamene, E. (1984). Recombinant inbred mouse strains derived from A/J and C57BL/6J: a tool for the study of genetic mechanisms in host resistance to infection and malignancy. *Journal of leukocyte biology*, *36*(3), 357–64.  
URL <http://www.ncbi.nlm.nih.gov/pubmed/6592283>

- Nguyen, T. T. T., Kläsener, K., Zürn, C., Castillo, P. A., Brust-Mascher, I., Imai, D. M., Bevins, C. L., Reardon, C., Reth, M., & Baumgarth, N. (2017). The IgM receptor Fc $\mu$ R limits tonic BCR signaling by regulating expression of the IgM BCR. *Nature immunology*, *18*(3), 321–333.
- Niedelman, W., Gold, D. A., Rosowski, E. E., Sprokholt, J. K., Lim, D., Arenas, A. F., Melo, M. B., Spooner, E., Yaffe, M. B., & Saeij, J. P. (2012). The rhoptry proteins ROP18 and ROP5 mediate *Toxoplasma gondii* evasion of the murine, but not the human, interferon-gamma response. *PLoS Pathogens*, *8*(6).
- Nishiyama, S., Pradipta, A., Ma, J. S., Sasai, M., & Yamamoto, M. (2020). T cell-derived interferon- $\gamma$  is required for host defense to *Toxoplasma gondii*. *Parasitology International*, *75*, 102049.
- Nosjean, O., Briolay, A., & Roux, B. (1997). Mammalian GPI proteins: sorting, membrane residence and functions. *Biochimica et biophysica acta*, *1331*(2), 153–186.
- Nussenzweig, R. S., Vanderberg, J., Most, H., & Orton, C. (1967). Protective immunity produced by the injection of x-irradiated sporozoites of *Plasmodium berghei*. *Nature*, *216*(5111), 160–162.
- Obeng-Adjei, N., Portugal, S., Holla, P., Li, S., Sohn, H., Ambegaonkar, A., Skinner, J., Bowyer, G., Doumbo, O. K., Traore, B., Pierce, S. K., & Crompton, P. D. (2017). Malaria-induced interferon- $\gamma$  drives the expansion of Tbethiatypical memory B cells. *PLoS Pathogens*, *13*(9), 1–30.
- Ochiai, E., Sa, Q., Perkins, S., Grigg, M. E., & Suzuki, Y. (2016). CD8+ T cells remove cysts of *Toxoplasma gondii* from the brain mostly by recognizing epitopes commonly expressed by or cross-reactive between type II and type III strains of the parasite. *Microbes and Infection*, *18*(7), 517–522.
- Olias, P., Etheridge, R. D., Zhang, Y., Holtzman, M. J., & Sibley, L. D. (2016). *Toxoplasma* effector recruits the Mi-2/NuRD complex to repress STAT1 transcription and block IFN- $\gamma$ -dependent gene expression. *Cell host & microbe*, *20*(1), 72–82.
- Pape, K. A., Maul, R. W., Dileepan, T., Paustian, A. S., Gearhart, P. J., & Jenkins, M. K. (2018). Naive B Cells with High-Avidity Germline-Encoded Antigen Receptors Produce Persistent IgM+ and Transient IgG+ Memory B Cells. *Immunity*,

- 48(6), 1135–1143.e4.  
URL <https://doi.org/10.1016/j.immuni.2018.04.019>
- Pape, K. A., Taylor, J. J., Maul, R. W., Gearhart, P. J., & Jenkins, M. K. (2011). Different B Cell Populations Mediate Early and Late Memory During an Endogenous Immune Response. *Science*, *331*(6021), 1203 LP – 1207.  
URL <http://science.sciencemag.org/content/331/6021/1203.abstract>
- Papillion, A. M., Kenderes, K. J., Yates, J. L., & Winslow, G. M. (2017). Early derivation of IgM memory cells and bone marrow plasmablasts. *PLOS ONE*, *12*(6), e0178853.  
URL <https://doi.org/10.1371/journal.pone.0178853>
- Parra, M., Weitner, M., Yang, A., Akue, A., Liu, X., Schmidt, T., Allman, W. R., Akkoyunlu, M., & Derrick, S. C. (2020). Memory CD73+IgM+ B cells protect against Plasmodium yoelii infection and express Granzyme B. *PLoS ONE*, *15*(9 september), 1–19.  
URL <http://dx.doi.org/10.1371/journal.pone.0238493>
- Parry, R. V., Chemnitz, J. M., Frauwirth, K. A., Lanfranco, A. R., Braunstein, I., Kobayashi, S. V., Linsley, P. S., Thompson, C. B., & Riley, J. L. (2005). CTLA-4 and PD-1 receptors inhibit T-cell activation by distinct mechanisms. *Molecular and cellular biology*, *25*(21), 9543–9553.
- Pauken, K. E., Sammons, M. A., Odorizzi, P. M., Manne, S., Godec, J., Khan, O., Drake, A. M., Chen, Z., Sen, D., Kurachi, M., Barnitz, R. A., Bartman, C., Bengsch, B., Huang, A. C., Schenkel, J. M., Vahedi, G., Haining, W. N., Berger, S. L., & Wherry, E. J. (2016). Epigenetic stability of exhausted T cells limits durability of reinvigoration by PD-1 blockade. *Science (New York, N.Y.)*, *354*(6316), 1160–1165.
- Pauken, K. E., & Wherry, E. J. (2015). SnapShot: T Cell Exhaustion. *Cell*, *163*(4), 1038–1038e1.  
URL <http://dx.doi.org/10.1016/j.cell.2015.10.054>
- Paulick, M. G., & Bertozzi, C. R. (2008). The glycosylphosphatidylinositol anchor: A complex membrane-anchoring structure for proteins. *Biochemistry*, *47*(27), 6991–7000.  
URL <https://pubs.acs.org/sharingguidelines>

- Pedersen, G. K., Ádor, M., Star, J. M., Khoenkho, S., Arnold, C., Beutler, B., & Karlsson Hedestam, G. B. (2016). Heterozygous mutation in IκBNS leads to reduced levels of natural IgM antibodies and impaired responses to T-independent type 2 antigens. *Frontiers in Immunology*, 7(MAR), 1–9.
- Pedersen, G. K., Àdori, M., Khoenkhoen, S., Dosenovic, P., Beutler, B., & Karlsson Hedestam, G. B. (2014). B-1a transitional cells are phenotypically distinct and are lacking in mice deficient in IκBNS. *Proceedings of the National Academy of Sciences*, 111(39), E4119–E4126.  
URL <http://www.pnas.org/lookup/doi/10.1073/pnas.1415866111>
- Phan, G. Q., Yang, J. C., Sherry, R. M., Hwu, P., Topalian, S. L., Schwartzentruber, D. J., Restifo, N. P., Haworth, L. R., Seipp, C. A., & Freezer, L. J. (2003). Cancer regression and autoimmunity induced by cytotoxic T lymphocyte-associated antigen 4 blockade in patients with metastatic melanoma. *Proceedings of the National Academy of Sciences*, 100(14), 8372–8377.
- Pullan, R. L., Smith, J. L., Jasrasaria, R., & Brooker, S. J. (2014). Global numbers of infection and disease burden of soil transmitted helminth infections in 2010. *Parasites & vectors*, 7(1), 1–19.
- Ranheim, E. A., & Kipps, T. J. (1993). Activated t cells induce expression of B7/BB1 on normal or leukemic B cells through a CD40-dependent signal. *Journal of Experimental Medicine*, 177(4), 925–935.
- Rao, M., Valentini, D., Dodoo, E., Zumla, A., & Maeurer, M. (2017). Anti-PD-1/PD-L1 therapy for infectious diseases: learning from the cancer paradigm. *International Journal of Infectious Diseases*, 56, 221–228.
- Reese, M. L., Shah, N., & Boothroyd, J. C. (2014). The Toxoplasma pseudokinase ROP5 is an allosteric inhibitor of the immunity-related GTPases. *Journal of Biological Chemistry*, 289(40), 27849–27858.
- Reese, M. L., Zeiner, G. M., Saeij, J. P. J., Boothroyd, J. C., & Boyle, J. P. (2011). Polymorphic family of injected pseudokinases is paramount in Toxoplasma virulence. *Proceedings of the National Academy of Sciences*, 108(23), 9625–9630.
- Remington, J. S., & Cavanaugh, E. N. (1965). Isolation of the encysted form of Toxoplasma gondii from human skeletal muscle and brain. *New England Journal of Medicine*, 273(24), 1308–1310.

- Reuter, J. S., & Mathews, D. H. (2010). RNAstructure: Software for RNA secondary structure prediction and analysis. *BMC Bioinformatics*, *11*.
- Riise, R., Odqvist, L., Mattsson, J., Monkley, S., Abdillahi, S. M., Tyrchan, C., Muthas, D., & Yrlid, L. F. (2019). Bleomycin hydrolase regulates the release of chemokines important for inflammation and wound healing by keratinocytes. *Scientific Reports*, *9*(1), 1–10.
- Robbins, S. H., Terrizzi, S. C., Sydora, B. C., Mikayama, T., & Brossay, L. (2003). Differential regulation of killer cell lectin-like receptor G1 expression on T cells. *The Journal of Immunology*, *170*(12), 5876–5885.
- Rosowski, E. E., Lu, D., Julien, L., Rodda, L., Gaiser, R. A., Jensen, K. D., & Saeij, J. P. (2011). Strain-specific activation of the NF- $\kappa$ B pathway by GRA15, a novel *Toxoplasma gondii* dense granule protein. *Journal of Experimental Medicine*, *208*(1), 195–212.
- Rosowski, E. E., Nguyen, Q. P., Camejo, A., Spooner, E., & Saeij, J. P. J. (2014). *Toxoplasma gondii* inhibits gamma interferon (IFN- $\gamma$ )-and IFN- $\beta$ -induced host cell STAT1 transcriptional activity by increasing the association of STAT1 with DNA. *Infection and immunity*, *82*(2), 706–719.
- Rosowski, E. E., & Saeij, J. P. J. (2012). *Toxoplasma gondii* Clonal Strains All Inhibit STAT1 Transcriptional Activity but Polymorphic Effectors Differentially Modulate IFN $\gamma$  Induced Gene Expression and STAT1 Phosphorylation. *PLOS ONE*, *7*(12), e51448.  
URL <https://doi.org/10.1371/journal.pone.0051448>
- Rowland, S. L., Leahy, K. F., Halverson, R., Torres, R. M., & Pelanda, R. (2010). BAFF receptor signaling aids the differentiation of immature B cells into transitional B cells following tonic BCR signaling. *The Journal of Immunology*, *185*(8), 4570–4581.
- RTSS Clinical Trials Partnership (2015). Vaccines: A step change in malaria prevention? *The Lancet*, *385*(9978), 1591.  
URL [http://dx.doi.org/10.1016/S0140-6736\(15\)60721-8](http://dx.doi.org/10.1016/S0140-6736(15)60721-8)
- Saccani, S., Pantano, S., & Natoli, G. (2002). p38-dependent marking of inflammatory genes for increased NF- $\kappa$ B recruitment. *Nature Immunology*, *3*(1), 69–75.

- Sacks, D. L. (2014). Answer To a Persisting Problem. *Nature Immunology*, *15*(5), 403–405.
- Saeij, J. P. J., Boyle, J. P., Collier, S., Taylor, S., Sibley, L. D., Brooke-Powell, E. T., Ajioka, J. W., & Boothroyd, J. C. (2006). Polymorphic secreted kinases are key virulence factors in toxoplasmosis. *Science*, *314*(5806), 1780–1783.
- Sakuishi, K., Apetoh, L., Sullivan, J. M., Blazar, B. R., Kuchroo, V. K., & Anderson, A. C. (2010). Targeting Tim-3 and PD-1 pathways to reverse T cell exhaustion and restore anti-tumor immunity. *Journal of Experimental Medicine*, *207*(10), 2187–2194.
- Sallusto, F., Geginat, J., & Lanzavecchia, A. (2004). Central memory and effector memory T cell subsets: function, generation, and maintenance. *Annu. Rev. Immunol.*, *22*, 745–763.
- Savage, H. P., Klasener, K., Smith, F. L., Luo, Z., Reth, M., & Baumgarth, N. (2019). TLR induces reorganization of the IgM-BCR complex regulating murine B-1 cell responses to infections. *eLife*, *8*, 1–26.
- Savage, H. P., Yenson, V. M., Sawhney, S. S., Mousseau, B. J., Lund, F. E., & Baumgarth, N. (2017). Blimp-1-dependent and -independent natural antibody production by B-1 and B-1-derived plasma cells. *The Journal of experimental medicine*, (pp. 1–18).
- Sayles, P. C., Gibson, G. W., Lawrence, L., & Johnson, L. L. (2000). B Cells Are Essential for Vaccination-Induced Resistance to Virulent *Toxoplasma gondii* B Cells Are Essential for Vaccination-Induced Resistance to Virulent *Toxoplasma gondii*. *Infection and Immunity*, *68*(3), 1026–1033.
- Scharton-Kersten, T. M., Yap, G., Magram, J., & Sher, A. (1997). Inducible nitric oxide is essential for host control of persistent but not acute infection with the intracellular pathogen *Toxoplasma gondii*. *Journal of Experimental Medicine*, *185*(7), 1261–1273.
- Schoenberger, S. P., Toes, R. E. M., Van Der Voort, E. I. H., Offringa, R., & Melief, C. J. M. (1998). T-cell help for cytotoxic T lymphocytes is mediated by CD40–CD40L interactions. *Nature*, *393*(6684), 480–483.
- Schofield, L., Hewitt, M. C., Evans, K., Siomos, M.-A., & Seeberger, P. H. (2002). Synthetic GPI as a candidate anti-toxic vaccine in a model of malaria. *Nature*,

418(6899), 785–789.

URL <https://doi.org/10.1038/nature00937>

Schuster, M., Annemann, M., Plaza-sirvent, C., & Schmitz, I. (2013). Atypical I $\kappa$ B proteins – nuclear modulators of NF- $\kappa$ B signaling. *Cell Communication & Signaling*, 11(23), 1–11.

Schuster, M., Plaza-Sirvent, C., Matthies, A.-M., Heise, U., Jeron, A., Bruder, D., Visekruna, A., Huehn, J., & Schmitz, I. (2017). c-REL and I $\kappa$ BNS Govern Common and Independent Steps of Regulatory T Cell Development from Novel CD122-Expressing Pre-Precursors. *Journal of immunology (Baltimore, Md. : 1950)*, 199(3), 920–930.

URL <http://www.ncbi.nlm.nih.gov/pubmed/28652399>

Seeber, F., Dubremetz, J. F., & Boothroyd, J. C. (1998). Analysis of *Toxoplasma gondii* stably transfected with a transmembrane variant of its major surface protein, SAG1. *Journal of Cell Science*, 111(1), 23–29.

URL <https://doi.org/10.1242/jcs.111.1.23>

Sen, D. R., Kaminski, J., Barnitz, R. A., Kurachi, M., Gerdemann, U., Yates, K. B., Tsao, H.-W., Godec, J., LaFleur, M. W., & Brown, F. D. (2016). The epigenetic landscape of T cell exhaustion. *Science*, 354(6316), 1165–1169.

Seong, J., Wang, Y., Kinoshita, T., & Maeda, Y. (2013). Implications of lipid moiety in oligomerization and immunoreactivities of GPI-Anchored proteins. *Journal of Lipid Research*, 54(4), 1077–1091.

URL <http://www.jlr.org>

Shaw, M. H., Boyartchuk, V., Wong, S., Karaghiosoff, M., Ragimbeau, J., Pellegrini, S., Muller, M., Dietrich, W. F., & Yap, G. S. (2003). A natural mutation in the Tyk2 pseudokinase domain underlies altered susceptibility of B10.Q/J mice to infection and autoimmunity. *Proceedings of the National Academy of Sciences of the United States of America*, 100(20), 11594–11599.

Shaw, P. X., Hörkkö, S., Chang, M. K., Curtiss, L. K., Palinski, W., Silverman, G. J., & Witztum, J. L. (2000). Natural antibodies with the T15 idiotype may act in atherosclerosis, apoptotic clearance, and protective immunity. *Journal of Clinical Investigation*, 105(12), 1731–1740.

- Sher, A., & Coffman, R. L. (1992). Regulation of Immunity to Parasites by T Cells and T Cell-Derived Cytokines. *Annual Review of Immunology*, *10*(1), 385–409.  
URL <https://doi.org/10.1146/annurev.iy.10.040192.002125>
- Sibley, L. D., & Boothroyd, J. C. (1992). Virulent strains of *Toxoplasma gondii* comprise a single clonal lineage. *Nature*, *359*(6390), 82–5.
- Sidik, S. M., Huet, D., Ganesan, S. M., Huynh, M. H., Wang, T., Nasamu, A. S., Thiru, P., Saeij, J. P., Carruthers, V. B., Niles, J. C., & Lourido, S. (2016). A Genome-wide CRISPR Screen in *Toxoplasma* Identifies Essential Apicomplexan Genes. *Cell*, *166*(6), 1423–1435.e12.  
URL <http://dx.doi.org/10.1016/j.cell.2016.08.019>
- Siegrist, C.-A. (2008). Vaccine immunology. *Vaccines*, *5*(1), 17–36.
- Skeeles, L. E., Fleming, J. L., Mahler, K. L., & Toland, A. E. (2013). The Impact of 3 UTR Variants on Differential Expression of Candidate Cancer Susceptibility Genes. *PLoS ONE*, *8*(3).
- Smale, S. T. (2012). Dimer-specific regulatory mechanisms within the NF-kappa B family of transcription factors. *Immunological Reviews*, *246*, 193–204.
- Smith, F. L., & Baumgarth, N. (2019). B-1 cell responses to infections. *Current Opinion in Immunology*, *57*, 23–31.  
URL <https://doi.org/10.1016/j.coi.2018.12.001>
- Souza, S. P., Splitt, S. D., Alvarez, J. A., Wizzard, S., Wilson, J. N., Luo, Z., Baumgarth, N., & Jensen, K. D. C. (2020). Nfkbid is required for immunity and antibody responses to *Toxoplasma gondii*. *bioRxiv*, (p. 2020.06.26.174151).
- Splitt, S. D., Souza, S. P., Valentine, K. M., Castellanos, B. E., Curd, A. B., Hoyer, K. K., & Jensen, K. D. C. (2018). PD-L1, TIM-3, and CTLA-4 blockade fail to promote resistance to secondary infection with virulent strains of *Toxoplasma gondii*. *Infection and immunity*, *86*(July), IAI.00459–18.  
URL <http://www.ncbi.nlm.nih.gov/pubmed/29967089>
- Stone, S. L., Peel, J. N., Scharer, C. D., Risley, C. A., Chisolm, D. A., Schultz, M. D., Yu, B., Ballesteros-Tato, A., Wojciechowski, W., & Mousseau, B. (2019). T-bet transcription factor promotes antibody-secreting cell differentiation by limiting the inflammatory effects of IFN- $\gamma$  on B cells. *Immunity*, *50*(5), 1172–1187.

- Striepen, B., Zinecker, C. F., Damm, J. B., Melgers, P. A., Gerwig, G. J., Koolen, M., Vliegthart, J. F., Dubremetz, J. F., & Schwarz, R. T. (1997). Molecular structure of the 'low molecular weight antigen' of *Toxoplasma gondii*: A glucose  $\alpha$ 1-4 N-acetylgalactosamine makes free glycosyl-phosphatidylinositols highly immunogenic. *Journal of Molecular Biology*, 266(4), 797–813.
- Stumhofer, J. S., Silver, J. S., & Hunter, C. A. (2013). IL-21 Is Required for Optimal Antibody Production and T Cell Responses during Chronic *Toxoplasma gondii* Infection. *PLoS ONE*, 8(5), 1–10.
- Su, C., Evans, D., Cole, R. H., Kissinger, J. C., Ajioka, J. W., & Sibley, L. D. (2003). Recent expansion of *Toxoplasma* through enhanced oral transmission. *Science*, 299(5605), 414–416.
- Su, C., Khan, A., Zhou, P., Majumdar, D., Ajzenberg, D., Dardé, M.-L., Zhu, X.-Q., Ajioka, J. W., Rosenthal, B. M., & Dubey, J. P. (2012). Globally diverse *Toxoplasma gondii* isolates comprise six major clades originating from a small number of distinct ancestral lineages. *Proceedings of the National Academy of Sciences*, 109(15), 5844–5849.
- Suzuki, K., Okuno, T., Yamamoto, M., Pasterkamp, R. J., Takegahara, N., Takamatsu, H., Kitao, T., Takagi, J., Rennert, P. D., & Kolodkin, A. L. (2007). Semaphorin 7A initiates T-cell-mediated inflammatory responses through  $\alpha$ 1 $\beta$ 1 integrin. *Nature*, 446(7136), 680–684.
- Suzuki, Y., Conley, F. K., & Remington, J. S. (1989). Importance of endogenous IFN-gamma for prevention of toxoplasmic encephalitis in mice. *The Journal of Immunology*, 143(6), 2045–2050.
- Suzuki, Y., Orellana, M. A., Schreiber, R. D., & Remington, J. S. (1988). Interferon- $\gamma$ : The major mediator of resistance against *Toxoplasma gondii*. *Science*, 240(4851), 516–518.
- Suzuki, Y., & Remington, J. S. (1988). Dual regulation of resistance against *Toxoplasma gondii* infection by Lyt-2+ and Lyt-1+, L3T4+ T cells in mice. *The Journal of Immunology*, 140(11), 3943–3946.
- Suzuki, Y., & Remington, J. S. (1990). The effect of anti-IFN-gamma antibody on the protective effect of Lyt-2 + immune T cells against toxoplasmosis in mice. *Journal of Immunology*, (pp. 2–5).

- Suzuki, Y., Sa, Q., Gehman, M., & Ochiai, E. (2011). Interferon-gamma- and perforin-mediated immune responses for resistance against *Toxoplasma gondii* in the brain. *Expert reviews in molecular medicine*, *13*, e31–e31.  
 URL <https://pubmed.ncbi.nlm.nih.gov/22005272>  
<https://www.ncbi.nlm.nih.gov/pmc/articles/PMC3372998/>
- Suzuki, Y., Wang, X., Jortner, B. S., Payne, L., Ni, Y., Michie, S. A., Xu, B., Kudo, T., & Perkins, S. (2010). Removal of *Toxoplasma gondii* cysts from the brain by perforin-mediated activity of CD8+ T cells. *American Journal of Pathology*, *176*(4), 1607–1613.  
 URL <http://dx.doi.org/10.2353/ajpath.2010.090825>
- Taylor, S., Barragan, A., Su, C., Fux, B., Fentress, S. J., Tang, K., Beatty, W. L., El Hajj, H., Jerome, M., & Behnke, M. S. (2006). A secreted serine-threonine kinase determines virulence in the eukaryotic pathogen *Toxoplasma gondii*. *Science*, *314*(5806), 1776–1780.
- Tomavo, S., Couvreur, G., Leriche, M. A., Sadak, A., Achbarou, A., Fortier, B., & Dubremetz, F. (1994). Immunolocalization and characterization of the low molecular weight antigen (4–5 kDa) of *Toxoplasma gondii* that elicits an early IgM response upon primary infection. *Parasitology*, *108*(2), 139–145.
- Torgerson, P. R., & Mastroiacovo, P. (2013). The global burden of congenital toxoplasmosis: a systematic review. *Bulletin of the World Health Organization*, *91*, 501–508.
- Touma, M., Antonini, V., Kumar, M., Osborn, S. L., Bobenchik, A. M., Keskin, D. B., Connolly, J. E., Grusby, M. J., Reinherz, E. L., & Clayton, L. K. (2007). Functional Role for I BNS in T Cell Cytokine Regulation As Revealed by Targeted Gene Disruption. *The Journal of Immunology*, *179*(3), 1681–1692.  
 URL <http://www.jimmunol.org/cgi/doi/10.4049/jimmunol.179.3.1681>
- Touma, M., Keskin, D. B., Shiroki, F., Saito, I., Koyasu, S., Reinherz, E. L., & Clayton, L. K. (2011). Impaired B Cell Development and Function in the Absence of IκBNS. *The Journal of Immunology*, *187*(8), 3942–3952.  
 URL <http://www.jimmunol.org/lookup/doi/10.4049/jimmunol.1002109>
- Tumanov, A. V., Kuprash, D. V., Lagarkova, M. A., Grivennikov, S. I., Abe, K., Shakhov, A. N., Drutskaya, L. N., Stewart, C. L., Chervonsky, A. V., & Nedospasov, S. A. (2002). Distinct role of surface lymphotoxin expressed by

- B cells in the organization of secondary lymphoid tissues. *Immunity*, 17(3), 239–250.
- Vieira, P., & Rajewsky, K. (1988). The half-lives of serum immunoglobulins in adult mice. *European journal of immunology*, 18(2), 313–316.
- Waffarn, E. E., Hasteley, C. J., Dixit, N., Soo Choi, Y., Cherry, S., Kalinke, U., Simon, S. I., & Baumgarth, N. (2015). Infection-induced type I interferons activate CD11b on B-1 cells for subsequent lymph node accumulation. *Nature Communications*, 6, 8991.  
URL <http://dx.doi.org/10.1038/ncomms9991>  
<http://www.nature.com/doifinder/10.1038/ncomms9991>
- Wang, L., Chen, H., Liu, D., Huo, X., Gao, J., Song, X., Xu, X., Huang, K., Liu, W., Wang, Y., Lu, F., Lun, Z. R., Luo, Q., Wang, X., & Shen, J. (2013). Genotypes and Mouse Virulence of *Toxoplasma gondii* Isolates from Animals and Humans in China. *PLoS ONE*, 8(1).
- Wang, X., Kang, H., Kikuchi, T., & Suzuki, Y. (2004). Gamma interferon production, but not perforin-mediated cytolytic activity, of T cells is required for prevention of toxoplasmic encephalitis in BALB/c mice genetically resistant to the disease. *Infection and Immunity*, 72(8), 4432–4438.
- West, E., Youngblood, B., Tan, W., Jin, H.-T., Araki, K., Alexe, G., Konieczny, B., Calpe, S., Freeman, G., Terhorst, C., Haining, W., & Ahmed, R. (2011). Tight Regulation of Memory CD8<sup>+</sup> T Cells Limits Their Effectiveness during Sustained High Viral Load. *Immunity*, 35(2), 285–298.  
URL <https://doi.org/10.1016/j.immuni.2011.05.017>
- Wherry, E. J. (2011). T cell exhaustion. *Nature immunology*, 12(6), 492–499.
- Wherry, E. J., Ha, S.-J., Kaech, S. M., Haining, W. N., Sarkar, S., Kalia, V., Subramaniam, S., Blattman, J. N., Barber, D. L., & Ahmed, R. (2007). Molecular signature of CD8<sup>+</sup> T cell exhaustion during chronic viral infection. *Immunity*, 27(4), 670–684.
- Wherry, E. J., & Kurachi, M. (2015). Molecular and cellular insights into T cell exhaustion. *Nature Reviews Immunology*, 15(8), 486–499.
- White, M. T., Verity, R., Griffin, J. T., Asante, K. P., Owusu-Agyei, S., Greenwood, B., Drakeley, C., Gesase, S., Lusingu, J., & Ansong, D. (2015). Immunogenicity

of the RTS, S/AS01 malaria vaccine and implications for duration of vaccine efficacy: secondary analysis of data from a phase 3 randomised controlled trial. *The Lancet infectious diseases*, 15(12), 1450–1458.

- Wilson, D. C., Grotenbreg, G. M., Liu, K., Zhao, Y., Frickel, E.-M., Gubbels, M.-J., Ploegh, H. L., & Yap, G. S. (2010). Differential regulation of effector-and central-memory responses to *Toxoplasma gondii* Infection by IL-12 revealed by tracking of Tgd057-specific CD8+ T cells. *PLoS Pathog*, 6(3), e1000815.
- Wilson, D. C., Matthews, S., & Yap, G. S. (2008). IL-12 signaling drives CD8+ T cell IFN- $\gamma$  production and differentiation of KLRG1+ effector subpopulations during *Toxoplasma gondii* infection. *The Journal of Immunology*, 180(9), 5935–5945.
- Witola, W. H., Mui, E., Hargrave, A., Liu, S., Hypolite, M., Montpetit, A., Cavailles, P., Bisanz, C., Cesbron-Delauw, M.-F., & Fournié, G. J. (2011). NALP1 influences susceptibility to human congenital toxoplasmosis, proinflammatory cytokine response, and fate of *Toxoplasma gondii*-infected monocytic cells. *Infection and immunity*, 79(2), 756–766.
- Wolchok, J. D., Kluger, H., Callahan, M. K., Postow, M. A., Rizvi, N. A., Lesokhin, A. M., Segal, N. H., Ariyan, C. E., Gordon, R.-A., Reed, K., Burke, M. M., Caldwell, A., Kronenberg, S. A., Agunwamba, B. U., Zhang, X., Lowy, I., Inzunza, H. D., Feely, W., Horak, C. E., Hong, Q., Korman, A. J., Wigginton, J. M., Gupta, A., & Sznol, M. (2013). Nivolumab plus ipilimumab in advanced melanoma. *N Engl J Med*, 369(2), 122–133.
- Yamamoto, M., Yamazaki, S., Uematsu, S., Sato, S., Hemmi, H., Hoshino, K., Kaisho, T., Kuwata, H., Takeuchi, O., Takeshige, K., Saitoh, T., Yamaoka, S., Yamamoto, N., Yamamoto, S., Muta, T., Takeda, K., & Akira, S. (2004). Regulation of Toll/IL-1-receptor-mediated gene expression by the inducible nuclear protein I $\kappa$ B $\zeta$ . *Nature*, 430(6996), 218–222.  
URL <https://doi.org/10.1038/nature02738>
- Yang, Y., Ghosn, E. E. B., Cole, L. E., Obukhanych, T. V., Sadate-Ngatchou, P., Vogel, S. N., Herzenberg, L. A., & Herzenberg, L. A. (2012). Antigen-specific memory in B-1a and its relationship to natural immunity. *Proceedings of the National Academy of Sciences of the United States of America*, 109(14), 5388–5393.

- Yang, Y., Tung, J. W., Ghosn, E. E., Herzenberg, L. A., & Herzenberg, L. A. (2007). Division and differentiation of natural antibody-producing cells in mouse spleen. *Proceedings of the National Academy of Sciences of the United States of America*, *104*(11), 4542–4546.
- Yap, G. S., & Sher, A. (1999). Effector Cells of Both Nonhemopoietic and Hemopoietic Origin Are Required for Interferon (IFN)- $\gamma$ - and Tumor Necrosis Factor (TNF)- $\alpha$ -dependent Host Resistance to the Intracellular Pathogen, *Toxoplasma gondii*. *Journal of Experimental Medicine*, *189*(7), 1083–1092.  
URL <https://doi.org/10.1084/jem.189.7.1083>
- Yarovinsky, F. (2014). Innate immunity to *Toxoplasma gondii* infection. *Nature Reviews Immunology*, *14*(2), 109–121.
- Yarovinsky, F., Hieny, S., & Sher, A. (2008). Recognition of *Toxoplasma gondii* by TLR11 Prevents Parasite-Induced Immunopathology. *The Journal of Immunology*, *181*(12), 8478–8484.
- Zamze, S. E., Ferguson, M. A., Collins, R., Dwek, R. A., & Rademacher, T. W. (1988). Characterization of the cross-reacting determinant (CRD) of the glycosylphosphatidylinositol membrane anchor of *Trypanosoma brucei* variant surface glycoprotein. *European Journal of Biochemistry*, *176*(3), 527–534.
- Zaretsky, A. G., Silver, J. S., Siwicki, M., Durham, A., Ware, C. F., & Hunter, C. A. (2012). Infection with *Toxoplasma gondii* alters lymphotoxin expression associated with changes in splenic architecture. *Infection and Immunity*, *80*(10), 3602–3610.
- Zhang, Y., Tech, L., George, L. A., Acs, A., Durrett, R. E., Hess, H., Walker, L. S. K., Tarlinton, D. M., Fletcher, A. L., & Hauser, A. E. (2018). Plasma cell output from germinal centers is regulated by signals from Tfh and stromal cells. *Journal of Experimental Medicine*, *215*(4), 1227–1243.
- Zhang, Y., Zhou, Y., Lou, J., Li, J., Bo, L., Zhu, K., Wan, X., Deng, X., & Cai, Z. (2010). PD-L1 blockade improves survival in experimental sepsis by inhibiting lymphocyte apoptosis and reversing monocyte dysfunction. *Critical Care*, *14*(6), R220.  
URL <https://doi.org/10.1186/cc9354>
- Zhao, B., Barrera, L. A., Ersing, I., Willox, B., Schmidt, S. C., Greenfeld, H., Zhou, H., Mollo, S. B., Shi, T. T., Takasaki, K., Jiang, S., Cahir-McFarland, E., Kellis,

- M., Bulyk, M. L., Kieff, E., & Gewurz, B. E. (2014). The NF- $\kappa$ B Genomic Landscape in Lymphoblastoid B Cells. *Cell Reports*, 8(5), 1595–1606.
- Zhao, K., Wang, Z., Hackert, T., Pitzer, C., & Zöller, M. (2018). Tspan8 and Tspan8/CD151 knockout mice unravel the contribution of tumor and host exosomes to tumor progression. *Journal of Experimental & Clinical Cancer Research*, 37(1), 1–23.
- Zhong, H., May, M. J., Jimi, E., & Ghosh, S. (2002). The phosphorylation status of nuclear NF- $\kappa$ B determines its association with CBP/p300 or HDAC-1. *Molecular Cell*, 9(3), 625–636.  
URL [http://dx.doi.org/10.1016/S1097-2765\(02\)00477-X](http://dx.doi.org/10.1016/S1097-2765(02)00477-X)
- Zinecker, C. F., Striepen, B., Geyer, H., Geyer, R., Dubremetz, J. F., & Schwarz, R. T. (2001). Two glycoforms are present in the GPI-membrane anchor of the surface antigen 1 (P30) of *Toxoplasma gondii*. *Molecular and Biochemical Parasitology*, 116(2), 127–135.
- Zuccarino-Catania, G. V., Sadanand, S., Weisel, F. J., Tomayko, M. M., Meng, H., Kleinstein, S. H., Good-Jacobson, K. L., & Shlomchik, M. J. (2014). CD80 and PD-L2 define functionally distinct memory B cell subsets that are independent of antibody isotype. *Nature Immunology*, 15(7), 631–637.